UNIVERSITY OF Southampton

University of Southampton Research Repository
ePrints Soton

Copyright © and Moral Rights for this thesis are retained by the author and/or other copyright owners. A copy can be downloaded for personal non-commercial research or study, without prior permission or charge. This thesis cannot be reproduced or quoted extensively from without first obtaining permission in writing from the copyright holder/s. The content must not be changed in any way or sold commercially in any format or medium without the formal permission of the copyright holders.

When referring to this work, full bibliographic details including the author, title, awarding institution and date of the thesis must be given e.g.

AUTHOR (year of submission) "Full thesis title", University of Southampton, name of the University School or Department, PhD Thesis, pagination

http://eprints.soton.ac.uk

UNIVERSITY OF SOUTHAMPTON

Mathematical studies of conservation and extinction in inhomogeneous environments

by

Vasthi Alonso Chávez

Supervised by

T. J. Sluckin, G. Richardson and C. P. Doncaster

A thesis submitted in partial fulfillment for the
degree of Doctor of Philosophy

in the
Faculty of Social and Human Sciences
School of Mathematics

October 14, 2011

UNIVERSITY OF SOUTHAMPTON

ABSTRACT

FACULTY OF SOCIAL AND HUMAN SCIENCES

SCHOOL OF MATHEMATICS

Doctor of Philosophy

MATHEMATICAL STUDIES OF CONSERVATION AND EXTINCTION IN INHOMOGENEOUS ENVIRONMENTS

by Vasthi Alonso Chávez

Supervised by

T. J. Sluckin, G. Richardson and C. P. Doncaster

A fragmented ecosystem contains communities of organisms that live in fragmented habitats. Understanding the way biological processes such as reproduction and dispersal over the fragmented habitats take place constitutes a major challenge in spatial ecology. In this thesis we discuss a number of mathematical models of density-dependent populations in inhomogeneous environments presenting growth, decay and diffusion amongst woodland patches of variable potential for reproductive success. These models include one- and two-dimensional analyses of single population systems in fragmented environments. We investigate and compute effective properties for single patch systems in one dimension, linking ecological features with landscape structure and size. A mathematical analysis of potential impacts on spread rates due to the behaviour of individuals in the population is then developed. For the analysis of the population dispersal between areas of plentiful resources and areas of scarce resources, we introduce a novel development that models individuals hazard sensitivity when outside plentiful regions. This sensitivity is modelled by introducing a term called dendrotaxis that generates a dispersal gradient, resulting in realistically low migration between regions of plentiful resources. Numerical methods and semi-analytic results yield maximum patch separations for one and two dimensional systems and show that the velocity of spread depends on inter-patch distances and patch geometries. By introducing Allee effects (*i.e.*, inverse density-dependent responses to the difficulty of finding mates at low density) over the population growth function, we find that dispersal is slowed down when combined with hazard sensitivity. In the final Chapter we sumarise the results of the previous chapters, concluding that the work performed in this thesis complements and enriches the current mathematical models of movement behaviour.

Contents

List of Figures

DECLARATION OF AUTHORSHIP

I, **Vasthi Alonso Chávez**, declare that the thesis entitled **Mathematical Studies of conservation and extinction in inhomogeneous environments** and the work presented in the thesis are both my own, and have been generated by me as the result of my own research. I confirm that:

- this work was done wholly or mainly while in candidature for a research degree at this University;
- if any part if this thesis has previously been submitted for a degree or any other qualification at this University or any other institution, this has been clearly stated;
- where I have consulted the published work of others, this is always clearly attributed;
- where I have quoted from the work of others, the source is always given. With the exception of such quotations this thesis entirely my own work;
- I have acknowledged all main sources of help;
- where the thesis is based on work done by myself jointly with others, I have made clear exactly what was done by others and what I have contributed myself;
- none of this work have been published before submission.

Signed:

Date: *October 14, 2011*

Acknowledgements

To God, who is always by my side and has given me the ability, strength and will to finish this journey.
To my supervisors Giles, Tim and Patrick, for their constant enthusiasm, encouragement, guidance and motivation along these years. Your advice and support not only in the academic matters, but also in the personal ones had given me the strength to continue until now.
A mis papás, por su amor y apoyo incondicional, su motivación y oraciones. Su fuerza, ejemplo y persistencia infalible han sido clave para que yo este aquí, ahora.
A mi hermano Israel y a Yeni por su cariño y eterna disposición a ayudarme.
To my husband Mac, for all the emotional support in the last years. Cocuyito, you have been my light and strength these last months. Thank you for coping with my moaning and ever-changing moods, always replying to me with nice and loving words.
A toda mi familia por el amor y apoyo recibido durante estos años.
Dziękuję również mojej wspaniałej nowej polskiej rodzinie, która cały czas wspierała mnie duchowo.
To my most beloved UK family, Alinne, Eri and Renato. You have made of this journey, one of the most enjoyable experiences of my life.
To all my friends that I do not mention by name, just in case I manage to forget someone. You have spiced up my life by making it bright and joyful. Your presence in my life make me feel immensely grateful and lucky.
To all my office-mates and colleagues that make the life inside a rather dull and ugly building, so pleasant. A special thanks to Jamie, Ila and Chris for the technical support and help, either by proof-reading my scripts, or by discussing mathematical matters that later developed into solutions and interpretations to my models.
To my sponsor CONACyT for the 4 years of funding provided for my Ph.D. studies and living expenses.
To my people in México. From elementary school until now, you have given me the possibility to continue my studies by paying your taxes. I hope to never become a waste of money, but a real investment for the development of our country.

A mis papás Francisco y Vasthi
siempre presentes en mi mente y en mi corazón

Chapter 1

Introduction

1.1 Motivation

An ecosystem can be defined as a spatial region which includes all the organisms which interact with the physical environment. In these systems the flow of energy leads to the exchange of materials between living structures and non-living factors such as water, soil and air [1].

The study of how ecosystem dynamics change with their environment has become more important in recent years. Many branches of science such as mathematics, biology, statistics, engineering and physics have been used to investigate this area. The relevance of studying ecosystems interactions with their environment becomes greater with the increase and spread of environmental changes such as fragmentation of ecosystems. However, accurate measurements of the factors determining the impact of environmental changes on ecosystem dynamics, are difficult to obtain due to the number of elements involved in these measurements. Mathematical models can provide a general panorama of the dynamics of a particular system.

Studies of ecosystems usually focus on the fluxes of individuals, energy and matter inside the ecosystem. The understanding and measurement of biological parameters, through mathematical techniques, are the principal objectives of this thesis, concentrating in particular on single population systems where individuals interact with each other and

with their environment, which we take to be fragmented. In order to illustrate such systems we consider the Asiatic red-bellied beautiful squirrel *Callosciurus erythraeus* as our biological system of reference along this thesis. This is a species introduced into the Argentinian pampas in 1974 that lives and disperses over a very fragmented habitat, where patches of woodland constitute their habitat, while grassland areas are hazardous regions for the species.

The basis for modelling ecosystems in this thesis are reaction-diffusion population models, a standard continuum approach to study population ecology. These types of models are later extended to include some terms that aim to explain characteristics of fragmented ecosystems and populations not widely considered in population models.

Some of the ecosystem dynamic features in which we would like to focus throughout this thesis are essential to understand populations behaviour and have been studied by different authors throughout the years [2–15]. In this thesis we recreate some of these results including methods and solutions which are developed in literature alike to gather deeper understanding of these type of systems and their constraints. The study of the constraints of these types of systems leads us to develop alternative and novel models for animals moving through heterogeneous landscapes. These reveal new results and provide new interpretations, analyses and methodologies to the standard results found in literature. Finally, alternative, novel models and results needed to explain the dynamics and constraints of these types of systems are investigated. These models and results provide a novel insight to some properties found in individual populations constrained to ecosystems presenting fragmentation, *i.e.*, ecosystems that due to different factors have been broken in two or more patches starting from a single homogeneous region initially, increasing the alternatives to approach and understand these type of systems.

The results found in this thesis involve an extensive study of individual fluxes in one and two-dimensional systems, and the study of individuals diffusing in fragmented or broken environments. We analyse the population individuals movement between regions of plentiful resources and regions with scarce-resources, as well as intrinsic biological factors for populations inhabiting one and two-dimensional regions. We develop our models on the basis of biological examples. For example, the analysis in Chapters 4

and 5 is carried out with reference to the behaviour of the Asiatic red-bellied beautiful squirrel *Callosciurus erythraeus* introduced in the Argentinian pampas.

1.2 Objectives

The objectives of this thesis are: *a*) To give a short introduction to population ecology, explaining the basic conceptual ideas related to different types of ecosystems and in particular, of fragmented ecosystems from both, a biological perspective and a mathematical one. *b*) To describe a set of concepts and quantities associated with populations living in this type of habitat. *c*) To study one and two-dimensional models for fragmented ecosystems. In doing so we find expressions that explain relevant biological quantities such as carrying capacity, diffusion rates and gap crossing time, in one and two-dimensional fragmented ecosystems. *d*) To provide a summary of the research achieved in this thesis and analysed in related literature, determining the emerging problems and limitations of the methods used to investigate the dynamics of these systems.

1.3 Biological context

1.3.1 Ecology and ecosystems

The word ecology originates from the Greek words $o\iota\kappa o\varsigma$, (oikos=household), and $\lambda o\gamma o\varsigma$ (logos=study) and is usually seen as a branch of biology. The term ecology was coined in 1866 by the biologist Ernst Haeckel who defined it as the science that studies the relationship of living organisms to the environment. In this context *relationships* include interactions with the physical world as well as with members of the same and other species [16]. The *environment* of an organism is everything that affects the organism during its lifetime. The *habitat* of an organism is the space that the organism lives in [17].

Individuals interact with the environment in the context of the ecosystem: *eco-* refers to the environment, whilst *-system* refers to the interactions among all the parts of the

ecosystem. Therefore, the region including all of the organisms which interact with the physical environment, such that a flow of energy leads to the exchange of materials between *biotic* or living and *abiotic* or non-living factors, is an *ecosystem* [1].

The different types of organisms that inhabit an ecosystem constitute the populations. A *population* is a group of individuals of the same species that occupy a given area. Generally speaking, the populations of an ecosystem interact with each other in diverse ways. The set of populations of different species living and interacting within an ecosystem can be referred as a *community* [16].

Ecosystems, consisting of the *biotic* or pertaining to life, and *abiotic* or characterized by the absence of life factors have many levels. These levels are shown schematically in figure 1.1. At the most basic level individuals interact with the environment. These individuals form populations. Populations start interacting with each other to form communities. Communities can be seen in a larger perspective which is called a landscape. A *landscape* is an area of land or water composed of a patchwork of communities and ecosystems.

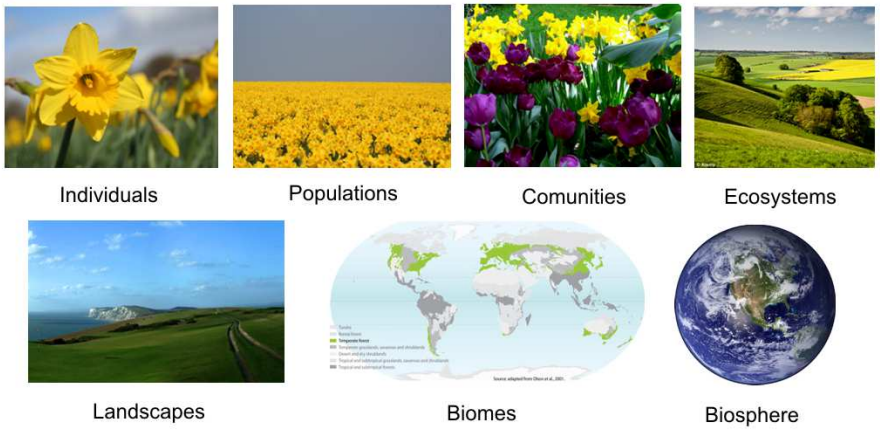

FIGURE 1.1: The hierarchy of ecological systems. Ecosystems show different levels according to their structure. Sources: bywynyrardd.net, webshot.com, mintytrips.co.uk, hebig.org and dailymail.co.uk

Beyond landscapes, biomes are encountered. A *biome* is a region dominated by the same kind of ecosystems and climatic conditions (e.g. tundra, taiga, rainforest) [16].

A *realm* is the largest scale of biogeographic division of the earth's surface. It represents large areas where plants and animals develop in relative isolation. Over long periods of time, they are then separated from one another by geological features, such as oceans,

broad deserts, or high mountain ranges [18].

Finally, the largest and only complete ecosystem is the *biosphere*, which can be defined as the layer about the Earth that sustains all of life. The interdependence of all ecosystems makes it the largest ecosystem on Earth.

1.3.2 Fragmented ecosystems

A *patchy* or *fragmented ecosystem* is an ecological community constituted by those organisms who have a fragmented living habitat. By *fragmentation* we mean that a homogeneous habitat breaks up into several *patches* of habitat. This fragmentation is exemplified in figure 1.2 where the original ecosystem established by the Pampas was re-shaped into a fragmented arboreous area constituted by grassland areas and forested regions.

There are a number of reasons why an ecosystem might be fragmented. Possible reasons include: habitat invasion due to intrusion of foreign species, natural fragmentation due to limited food, resources or geological processes and human activity such as land conversion. Fragmented ecosystems differ from continuous ecosystems, given that population

FIGURE 1.2: Satellite image of Argentinian pampas at 34,43'S 59,10'W. The image shows ecosystem fragmentation by land conversion (roads and forestation). Source: Google Earth, February 7, 2011

dynamics change, due to the amount of available resources. In a fragmented ecosystem

each patch has, more or less, independent dynamics depending on the amount of interaction between populations. This kind of dynamics leads to different behaviours, which can have a positive or negative impact on the ecosystem.

In principle, fragmentation can be a natural phenomenon to which species have adapted. However, in practice, human population growth and the ability of humans to change their environment are the main causes of habitat fragmentation. This can affect biodiversity in many ways. For example, it reduces the amount of available resources within a habitat for plants and animals. As a consequence, the anhilation of some species and the retreat of others into the habitat patches is generated. This process leads to an increase in competition for the remaining resources. Fragmentation can also partition out problems. For example, it can slow the spread of a disease inside an ecosystem. However, it can also accommodate local extinction. In this case, whenever any fluctuation in the population size is introduced, the population becomes more prone to extinction than it would be in a homogeneous ecosystem.

1.3.3 Ecological concepts

Here we introduce a series of ecological concepts related to fragmented ecosystems, that we take into account for the modelling interpretation and explanation of population dynamics in the following chapters.

Patches are relatively homogeneous areas which have different structure and species composition from their surroundings. Their variance in terms of size, composition, shape and type can also affect the population dynamics. Shape, geometry and orientation can determine the movement of the species inside the patch and level of connectivity between them as shown in figure 1.3. They are usually confined to a lager complex system of patches, which are generally separated by distinct boundaries. These varying features affect patch dynamics and determine patch suitability as a habitat for plants and animals. They also influence many ecological properties such as, wind flow, dispersal and movement of animals [16].

Sensitivity to fragmentation changes from species to species, leaving the open question

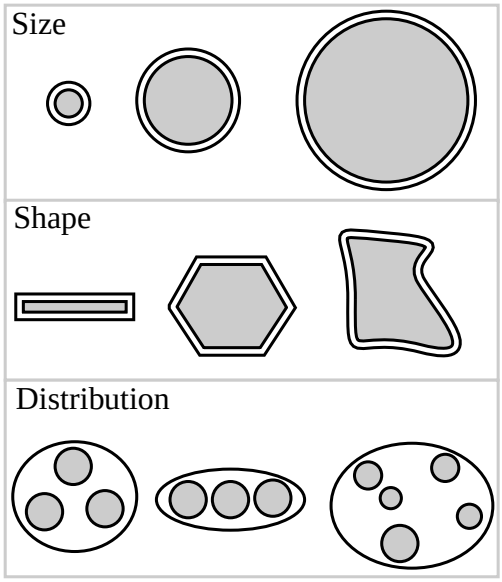

FIGURE 1.3: Patches vary in distribution, shape and size. These features determine patch dynamics.

of species conservation: "How small a fragment can each species occupy successfully?". This question leads us to the definition of another concept: the *critical patch size* [19].

The *critical patch size* (CPS) is the minimum habitat size required for population persistence. A population inhabiting a patch with size larger than that of the CPS will persist and expand into the unoccupied habitat. However, if the fragment size is smaller than the CPS, the population will die out [20]. This concept applies for all the species within a patch. The CPS is influenced by many factors. For example, the CPS needed to conserve populations of a species increases with isolation. This is because immigration is restrained to the patch. Populations in more isolated areas must be larger to prevent extinction before migration from these isolated areas to other patches can rescue the population [18].

The *carrying capacity* of an ecosystem is the maximum population size of the species of a population that an ecosystem can support as a sustainable community with the available resources inside it, such as food, water and other necessities. As an example, figure 1.4 shows how the environmental factors limit the population size inside it, and this determines its carrying capacity [17].

When the population size is smaller than the carrying capacity, the *population growth*

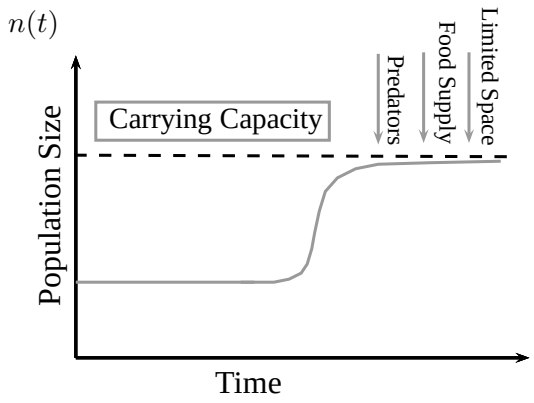

FIGURE 1.4: A number of environmental factors such as predation, availability of space and food determine the number of organisms that can survive in a given space. This is known as the carrying capacity of that area.

rate is positive. Conversely, if the population size is larger than the carrying capacity, the population declines and the population growth rate, becomes negative. When the population size reaches the carrying capacity the population growth stops and a stable equilibrium of the population size is achieved. At the same time, if the population of a species depends on its size, it is expected that this population will grow to reach its carrying capacity.

When the size of the population increases, the per capita birth rate may decline to maintain an equilibrium with the available resources. Equally, as the population size increases, the per capita death rate may also increase due to competition for available resources. The carrying capacity of an ecosystem is reached when the per capita growth rate is equal to the per capita death rate implying that the *effective population growth rate* is equal to zero. This indicates a close relation between the critical patch size and the carrying capacity of the ecosystem given that, if the carrying capacity of a system goes to zero as a function of the system size, the system attains its critical patch size.

As noted by Zollner [21], "real mice aren't blind", and real animals do perceive and interact with their environment developing different behaviour in different type of habitats. The behaviour of animals towards their environment may become very complex since it can include overlapped features such as: learning mechanisms, memory, sexual behaviour, orientation and perception. In this thesis, we do not want to leave this important feature of population dynamics on the side. Therefore, a term representing the

individuals hazard sensitivity to inhospitable regions that we call *dendrotaxis* is studied here.

1.3.4 Metapopulations

The term metapopulation has its origin in 1979 when Levins [22] proposed a model of local populations distributed in an inhomogeneous environment. He proposed a model with a number of habitat patches connected to each other via migration [23]. According to Hanski [23], a leading ecologist in metapopulation studies, there are four conditions to define a set of local populations as a metapopulation. These are,

1. The suitable habitat must occur in discrete patches and be occupied by local reproducing populations.
2. Even the largest populations must have a considerable risk of extinction.
3. The separation between habitat patches should be sufficiently small, in order to admit recolonisation.
4. The individual dynamics of the local populations are not synchronized [16].

However this definition is very restrictive. Some modifications have been performed since its appearance. In the following paragraphs we present a less restrictive definition of metapopulation.

A fragmented ecosystem is constituted by a set of discrete suitable habitat patches and a set of patches unsuitable for population persistence in the same geographical area. The habitat patches occupied by populations of the same species will be called *resources-rich* patches. The regions between suitable habitat, where population persistence is not possible, will be called *scarce-resource* patches. The populations inhabiting the high-quality patches, are either isolated from each other, or can be connected by a limited exchange of individuals through migration, dispersal or human-mediated movement. Such a collection of relatively isolated, but locally interacting populations of the same species is called a *metapopulation*. This definition is based on work by Akçakaya *et. al.*, and Smith *et. al.* [16, 24]). Figure 1.5 shows how metapopulations interact.

In this sense, the systems we study along Chapters 4 and 5 constitute examples of metapopulation systems.

Metapopulations operate on two different scales. On the local scale individuals move and interact with each other. On the global scale the dynamics is driven by the interactions of the local populations. These interactions occur when colonisation and dispersal take place. *Dispersal* arises when a certain number of individuals move from a patch, across habitat types, and settle in another suitable habitat patch. *Colonisation* on the other hand, is the process where the individuals move from occupied patches, to unoccupied ones, to form new local populations. As all the local populations have a probability of extinction, the long-term persistence of the metapopulation depends on the recolonisation. Dispersal and colonisation of single population species are extensively studied concepts in this thesis and will be used subsequently.

One example of a natural metapopulation is a species inhabiting a confined fresh water ecosystem; such as a pond or a lake. One may think that these types of habitat are isolated. However, plant and invertebrate populations belonging to these ecosystem may be extensively interconnected. Birds that travel from a confined freshwater ecosystem to another may transport invertebrates and/or plants which may flourish in the new habitat [24]. Examples of induced metapopulation includes large neo-tropical cats such as the jaguar (*Panthera onca*) and puma (*Puma concolor*). These species live in areas of tropical rainforest which are frequently transformed into farm land. This results in the fragmentation of the ecosystem and the creation of discrete patches of habitat. The areas converted into farm land transform into *scarce-resources* patches. Nevertheless connectivity between the high quality patches is kept.

Another example of metapopulation is the recently introduced Asiatic red-bellied beautiful squirrel *Callosciurus erythraeus* into the Argentinian Pampas. This species will be our reference species along the thesis and therefore is investigated in more detail in further chapters.

The general focus in this thesis is based on the population of a single species. Therefore the concepts of a patch, critical patch size, carrying capacity, directed movement and metapopulation will be applied to single species populations. The aim is to discover

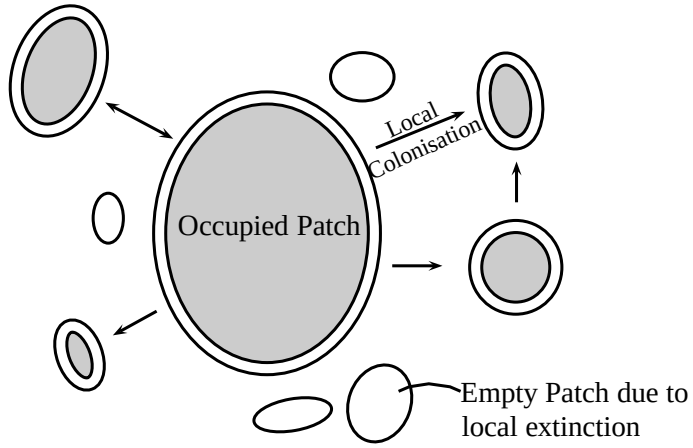

FIGURE 1.5: A schematic of a metapopulation where populations of each patch are connected by migration from patch to patch is shown. The filled ellipses indicate occupied patches and the empty ellipses indicate unoccupied patches. The arrows show the migration from one patch to another.

expressions to measure and quantify some of the parameters defined above. These parameters will be used to model local extinction, dispersal and colonisation of habitat fragments and global extinction in fragmented ecosystems.

1.4 Summary

This thesis focuses on population dynamics in fragmented ecosystem. It contains an introduction to fragmented population ecology and one and two-dimensional systems are investigated through analytic and numerical analyses.

We divide this report into 6 chapters as follows: Chapter 1 provides an introduction with a summary of the contents of the thesis and explains the objectives and motivation. It also contains a biological background explaining important concepts about ecosystems and fragmented ecosystems. Concepts such as critical patch size, carrying capacity, metapopulation, population growth rate, population death rate, diffusion coefficients and dendrotaxis are defined. In Chapter 2 relevant population models studied in the literature are discussed and analysed. We focus on the logistic model and modified versions of it which are used throughout this thesis to explain the basic characteristics of fragmented ecosystems. A relevant literature review that summarizes different models developed for various subjects such as population models in inhomogeneous environ-

ments, reaction-diffusion population models, and the spread of invading organisms is treated in this chapter. A comparison between the research presented in the literature and our findings is included.

Chapter 3 deals with the analysis and solutions of one-dimensional problems. Among them a semi-infinite problem for an almost homogeneous ecosystem with specific boundary conditions is solved. Single one-dimensional patch systems with specific boundary conditions are also solved in this chapter. In chapter 4 we discuss a modified logistic model with diffusion and dendrotaxis in one dimension. The model is analysed both numerically and analytically. The results of this model are compared with experimental models analysed by Guichón *et. al.* [15]. In chapter 5 the modified logistic model with diffusion and dendrotaxis discussed in Chapter 4 is analysed in two dimensions. The model is mainly analysed numerically and analytical solutions for the system are outlined.

The key results of the thesis are contained in Chapters 3, 4 and 5. In Chapter 3 the study of carrying capacities and currents in single one-dimensional patches is an important contribution for these type of systems because its study is fundamental for the study of more complex system constituted by two or more patches. Once the carrying capacity and individual flux in the length scale of a single patch are obtained, methods such as homogenisation [10, 25] can be used to find the effective dynamics of more complex systems; however, these methods and calculations are not discussed in this thesis. In Chapters 4 and 5 the main contribution is the development of a new model for the study of certain type of populations. In this model a term that accounts for the individual sensitivity to hazardous areas is considered. The analysis of these systems provide a different type of dynamics of the population that is examined in different situations, giving very interesting results on velocities, diffusion and growth population rates that depend on the spatial structure of the systems. These results suggest generic control strategies for the spread of these type of populations.

Chapter 6 provides a summary of the work accomplished in this thesis, and presents challenges for the future. In this chapter we discuss the results obtained and outline the conclusions of this research. Finally, in Appendix I we provide the outline of a model for

analytical studies and solutions for two-dimensional systems of corridors, which presents alternative mathematical methods of solutions in these type of systems.

Chapter 2

Standard continuous population models

In this chapter I introduce key concepts regarding the formulation, analysis and interpretation of mathematical population modelling. A number of models used throughout the years to mathematically explain the growth and dispersal of populations are considered here. Firstly a model with constant growth rate introduced by Malthus is considered [26]. We then add density dependence to the population growth to obtain and describe the so called logistic model [27]. Thereafter, the logistic model is enhanced by introducing spatial diffusion yielding a reaction-diffusion model widely used in population ecology literature [5, 8, 28, 29]. Characteristics such as the attraction or repulsion to some areas of the system, generally called *taxis*, are also introduced [5, 29]. Finally, we non-dimensionalise.

2.1 Constant population growth

The simplest population dynamics model to be considered is a model with constant *net per capita growth rate* r. Let b be the per capita reproduction rate and d the per capita mortality rate, then

$$r = b - d. \tag{2.1.1}$$

Considering linear growth, the population variation with time can be expressed by

$$\frac{dn}{dt} = rn. \tag{2.1.2}$$

In equation (2.1.2) n represents the population and t the time. No density-dependent effects are considered. Therefore, b, d and r are constant. The solution for this equation is

$$n(t) = n_0 e^{rt}, \tag{2.1.3}$$

where n_0 is the population at $t = 0$. This solution implies that, if $r > 0$, the population grows exponentially without limit. Conversely, if $r < 0$, the population shrinks until it disappears.

This type of population growth is called *Malthusian growth*, and (2.1.2) is called the *Malthusian equation* in continuous time [26, 30], constituting the simplest minimal reproducing population model. This model is fundamental to all population ecology. Unfortunately, this model ignores the fact that resources cannot keep pace with population growth. Therefore, a better description of the population dynamics is required.

2.2 Logistic equation

In 1845 Verhulst modelled a self-limiting process now generally known as the continuous logistic model [27, 31]. This model operates when a population becomes limited by its environmental resources. It is the simplest model for population growth with density dependence and it is written as follows;

$$\frac{dn}{dt} = \alpha n \left(1 - \frac{n}{\chi}\right), \tag{2.2.1}$$

n represent the population per unit area, t is the time and χ the carrying capacity per unit area (if the problem is solved for one-dimensional systems the carrying capacity

and the population are measured in units of length instead of area). The modelling assumption is that the per capita birth rate $b(n)$ depends on the density of the population (due to competition for resources), and becomes negative above some population threshold, but there is no specific time dependence. If the net per capita reproduction rate depends only on the population then

$$r(n) = b(n) - d(n). \tag{2.2.2}$$

In this framework the birth rate $b(n)$ and the death rate $d(n)$ are functions of the population number. It is expected that as the population increase, the density population will decrease. This means that the birth rate decrease because of a lack of resources. Equally, it is expected that the death rate increases because of competition for these resources. The simplest way to find the function $r(n)$ is to expand $b(n)$ and $d(n)$ in a Taylor expansion around zero. Therefore,

$$b(n) = b_0 - k_b n, \tag{2.2.3}$$

and

$$d(n) = d_0 + k_d n. \tag{2.2.4}$$

As the birth rate cannot go negative, the threshold χ at which the net birth rate becomes negative is defined as the *carrying capacity* of the environment in question [32].

Using the expressions for the functions $b(n)$ and $d(n)$, the complete expression for the growth rate of the logistic population model can be written,

$$\frac{dn}{dt} = r(n)n = (b(n) - d(n))n = [(b_0 - k_b n) - (d_0 + k_d n)]n, \tag{2.2.5}$$

which simplified gives

$$\frac{dn}{dt} = (b_0 - d_0)n - (k_b + k_d)n^2. \tag{2.2.6}$$

Defining

$$\alpha = b_0 - d_0, \tag{2.2.7}$$

where $b_0 \geq d_0$, and

$$\chi = \frac{b_0 - d_0}{k_b + k_d}, \tag{2.2.8}$$

the resulting equation for the population dynamics is written:

$$\frac{dn}{dt} = \alpha n \left(1 - \frac{n}{\chi}\right). \tag{2.2.9}$$

This is the *continuous logistic equation* that describes the dynamics where, if the population density increases, the death rate increases until the threshold χ is reached. Here χ represents the carrying capacity of the system, α is the net rate of increase per capita (*i. e.*, before competition), so αn is the rate of population increase before competition. This term governs the dynamics of the system at early times. The second term $\frac{\alpha n^2}{\chi}$ represents the rate of population growth proportional to the amount of available resources in the presence of intra-species interference. It models the exploitation and competition of the individuals of population n for limited resources. This term becomes important at later time, when the population has grown enough for the individuals to start interfering with each other.

2.3 Reaction-diffusion equations

Reaction-diffusion equations arise in many fields of physics, engineering, chemistry, biology and ecology. These equations can be used to model a series of different types of phenomena. For example, in the case of dispersive behaviour of populations it is simple to think of the distribution of a population in terms of density functions.

Let us consider diffusion in space. If we have any surface S enclosing a volume V, the general conservation equation says that the rate of change of mass or amount of material in the volume V is equal to the mass or individual flux c through the surface S that

encloses the volume V, plus the generated mass inside the volume [31],

$$\frac{\partial}{\partial t}\int_V n(\mathbf{x},t)dv = -\int_S \mathbf{J}\cdot\mathbf{ds} + \int_V f dv. \tag{2.3.1}$$

Here, $\mathbf{J}$ is the flux of mass and f is the source of mass. Applying the divergence theorem to equation (2.3.1),

$$\int_V \left[\frac{\partial n}{\partial t} + \nabla\cdot\mathbf{J} - f(n,\mathbf{x},t)\right] dv = 0. \tag{2.3.2}$$

Since V is an arbitrary volume, the integrand in equation (2.3.2) must be zero. This results in the continuity equation

$$\frac{\partial n}{\partial t} + \nabla\cdot\mathbf{J} = f(n,\mathbf{x},t). \tag{2.3.3}$$

For a given model we must specify $f(n,\mathbf{x},t)$ and $\mathbf{J}$. The form we choose for the terms f and J, dictates the dynamics of the system.

The way a source function f is represented mathematically depends on the intrinsic characteristics of each population. In particular in this thesis, we explore a couple of mass source functions f, representing population growth or decay functions depending on the reproduction and death rate of the population itself, as well as on environmental factors.

The mass flux given by J in equation (2.3.3), is also investigated in the form of the population individual flux in a given domain.

According to *Fick's law* of diffusion, the amount of transport of matter n, or in this thesis individuals of a population, in the $\mathbf{x}$ direction, perpendicular to a unit normal area of the volume V, in a unit time, (*i. e.*, the flux $\mathbf{J}$) is proportional to the gradient of the density of matter. Hence, $\mathbf{J} = -D\nabla n$. The minus sign indicates that the matter is transported from high to low densities [33]. In general, the diffusion coefficients may depend on the spatial coordinates and the density of matter. Therefore,

$$D = D(n,\mathbf{x}) \tag{2.3.4}$$

and the flux is given by,

$$\mathbf{J} = -D(n, r)\nabla n(x, t) \tag{2.3.5}$$

However, if D is taken to be a constant, independent of matter density and space then, the term $\nabla \cdot (D\nabla n) = D\nabla^2 n$ and equation 2.3.3 is rewritten as,

$$\frac{\partial n}{\partial t} = f + \nabla \cdot (D\nabla n) = f + D\nabla^2 n. \tag{2.3.6}$$

This type of diffusion is commonly referred as Fickian diffusion. If f represent for example, the birth-death process given by a logistic growth and n represents the population density we obtain the *Fisher-Kolmogorov equation*,

$$\frac{\partial n}{\partial t} = \alpha n \left(1 - \frac{n}{\chi}\right) + D\nabla^2 n, \tag{2.3.7}$$

sometimes also called the *Fisher-Skellam equation* [2, 34]. This equation is the starting point to explain the dynamics of many population models based on differential equations. It describes a population that reproduces logistically and disperses randomly. Here n represents the population per unit length, area or volume (depending on the system dimension), α is the linear reproduction rate, and χ is the carrying capacity per unit length, area or volume.

If f, on the other hand, only represents a death process, like for example, when a population confronts adverse environmental conditions, we obtain a decaying population in time that diffuses randomly,

$$\frac{\partial n}{\partial t} = -\alpha' n + D\nabla^2 n. \tag{2.3.8}$$

Until now, we had only mentioned fluxes including diffusion exclusively. However, the flux term $\mathbf{J}$ may vary with respect to the population spatial behaviour. For example, if we consider that individuals movement take place in response to stimuli or *taxis* to its environment the flux term $\mathbf{J}$, changes accordingly [35–37]. In this thesis a directional movement called *dendrotaxis* in response to spatial location of areas of plentiful resources is considered for the modelling in the population flux $\mathbf{J}$ in Chapters 4 and 5 where it

will be described extensively.

2.4 Spatially structured models

In Chapter 1 we established that the main focus of this work is to model, analyse and interpret population dynamics in fragmented environments. This means that the systems that we consider are heterogeneous. Different parts of the whole system obey different equations of types (2.3.7),(2.3.8). The dynamics of the whole system depends sensitively on the dynamics in the individual parts, and on the boundary conditions at the interfaces between them. In the following chapters we analyse equations of this type and the resulting global dynamics.

2.5 Interface conditions

In order to analyse the dynamics in a fragmented environment where different parts of a system follow different type of behaviour, the interface conditions between different regions are crucial for the understanding of the system dynamics. Here we shall always require the continuity of the normal flux $\mathbf{J} \cdot \mathbf{n}$ between patches, *i.e.*, that the number of individuals leaving a certain type of region is equal to the number of individuals entering a different contiguous region. To formulate the correct boundary conditions for the population density, we consider various possibilities that will be addressed at the right moment, according to the system under analysis.

2.6 Taxis and dendrotaxis

In Chapter 4, we introduce a term representing the individuals hazard sensitivity when outside resource-rich regions called *dendrotaxis*. This sensitivity can be compared with the measurement of the tendency of a group of particles, or in this case individuals, to diffuse as a function of position as it occurs for example, in the chemotaxis, phototaxis and thermotaxis [38]. The term taxis refers to the innate response on the behaviour

of an organism due to a directional stimulus. Therefore the term dendrotaxis refers to individuals that direct their movements towards patches of plentiful resources, avoiding areas of scarce ones. This behaviour generates a gradient of the population dispersal, affecting the way individuals disperse in a heterogeneous environment. A more detailed description of how this term affects the dynamics of a system undergoing dendrotaxis is provided in Chapter 4.

2.7 Transient, stationary state and linearisation analyses of the general problem

The model equations we deal with in this thesis are non-linear partial differential equations (PDEs) based on reaction-diffusion systems. Non-linear PDEs are in general hard to solve and their solution sets are difficult to analyse. This is the reason why non-linear PDEs are often approximated with linear PDEs, and linear and non-linear ODEs (like in the case of stationary state analyses). Sometimes the general solution of a PDE can be discovered. However, for most of the problems of interest it is usually not necessary to obtain it since the aim of the equation is to describe the dynamics of a model [39].

In this thesis, different methods to analyse and describe the dynamics of these equations are introduced including the linearisation of the equations, the analysis of stationary states and the numerical analysis of the full evolution of the PDEs.

2.7.1 Transient analysis

The transient analysis of a PDE takes place when the dynamics of the problem under analysis is studied over time. In this thesis, this means that the dynamics of the population change over space given by equations (2.3.7) and (2.3.8) is analysed over time.

Since equation (2.3.7) is a non-linear PDE, the transient analysis of the models presented in this thesis is done numerically. Through numerical analysis of the transient problem we study different characteristics of the dynamics of our system evolution over

time. These characteristics include the solution and analysis of waves of advance, the population movement across patches with different dynamical functions, the spatial effect over the population movement over time and the evolution of populations over time in different habitat patches.

2.7.2 Stationary state

When the evolution over time of the population reaches an equilibrium, making the changes of population over time negligible, then we can say that the population has reached a stationary state where

$$\frac{dn}{dt} = 0. \tag{2.7.1}$$

In this case, the partial differential equations (2.3.7) and (2.3.8) transform into a non-linear and a linear ODE respectively (in the one-dimensional case), making their analysis more accessible. The stationary state equations analyses will allow us to study the population behaviour at long times, once an equilibrium has been reached and the population distribution over space is constant.

2.7.3 Linearisation

Partial differential equations that model the dynamics of biological systems are often non-linear. However, the study of linear PDEs becomes important because many times the solutions to non-linear systems, can be approximated by the solutions to associated linear problems. Linearisation involves creating a linear approximation of a nonlinear system that is valid about a given solution. We use this type of analysis to investigate what is the evolution of a population close to a point in a given domain and time.

For example, assuming that the initial conditions for equation (2.3.7) are such that $n(x,t)$ is initially close to $n(x,t) = 0$ by supposing that $n(x,t) = 0 + \epsilon n_0(x,t)$, where ϵ is an arbitrarily small positive quantity. We can substitute this into (2.3.7) to obtain

$$\frac{\partial n_0}{\partial t} = \alpha n_0 - \epsilon \frac{n_0^2}{\chi} + D\nabla^2 n_0. \tag{2.7.2}$$

Taking the limit $\epsilon \to 0$ we obtain the linearisation of (2.3.7) at $n(x,t) = 0$,

$$\frac{\partial n_0}{\partial t} = \alpha n_0 + D\nabla^2 n_0. \tag{2.7.3}$$

Since $n(x,t) = \epsilon n_0(x,t)$, n_0 satisfies the same boundary conditions as n and we can solve the linearised problem, as we will see in the following chapters.

2.8 Literature review

In this section we present a review of the literature related to the study area of this thesis: fragmented ecosystems. The review is divided in several subsections as follows: Firstly, we present a number of approaches taken to model these type of ecosystems including biological comparison and analysis of different mathematical modelling. Then, we examine the literature on reaction-diffusion models, and also look at some models that generalise this approach. Lastly, we make a link between the models studied in the literature and those which we shall present in this thesis, emphasising both relevant similarities and differences. The focus of this thesis is to describe single population models. Therefore, we shall focus on single population models, and exclude the rather larger literature involving interacting models of two or more species that is discussed for example in [31].

2.8.1 General review

The dynamics of a population subject to movement in fragmented ecosystems can be analysed in many different ways. The focus of the study of a particular aspect of the dynamics then, gives birth to different models. These models can be either experimental, based on the acquisition of biological data and its interpretation, or theoretical, based on the general dynamics of the ecosystem with the aim of reproducing its behaviour.

2.8.1.1 Biological models

In discussing ecological models, we note the importance of reconciling observation with theory. Mathematically, plausible ecological models are relatively easy to formulate, but do not always pass basic observational tests. For example, Delgado and Penteriani [40], showed via radio-tracking data, that random walk models, that imply dispersal driven by Fickian diffusion, do not predict accurately the spatial spread of the eagle owl *Bubo bubo*, inhabiting heterogeneous systems. They discovered that random walk models, compared with the radio-tracking data, severely underestimate the spatial spread of this species.

On the other hand, Andow *et. al.* [41], described how reaction-diffusion models, applied to a pair of populations inhabiting homogeneous environments predicted their velocity of spread very accurately. They proved that the velocity of spread of the muskrat (*Ondatra zibethicus*) and the small cabbage white butterfly (*Pieris rapae*) could be accurately predicted using a logistic population growth and Fickian diffusion as a dispersal strategy.

These two examples show that different modelling strategies are neccesary to reproduce the dynamics of different populations, building paths to focus modellers attention on different aspects of the different types of biological systems. In the case of the study of Delgado and Penteriani, for instance, they propose to integrate behavioural traits in the population dispersal modelling. The inclusion of behavioural effects on population dispersal, has recently received much more attention, as we will see in §2.8.5. Some examples of behavioural studies are presented in the work of Zollner and Lima, on dispersal dynamics of the white-footed mice, (*Peromyscus leucopus*) [21, 42], the dispersal of eastern chipmunks (*Tamias striatus*), grey squirrels (*Sciurus carolinensis*), and fox squirrels (*Sciurus niger*) [43] in fragmented agricultural landscapes. They focus on the measurement of perceptual range, that is the maximum distance from which an animal can perceive the presence of remote patches of habitat, noticing that the ability of dispersal of a population depends on this factor. Their results emphasise the need to introduce behavioural factors in the modelling of movement of these type of species individuals across fragmented landscapes, like they do in [44]. Selonen and Hanski [45] on the other hand, investigated by statistical sampling of radio-collared individuals, how

the elements of a fragmented landscape, such as patches and corridor linking patches, have different roles in the dispersal of individuals. They studied the role of connecting woodland strips between woodland patches as possible dispersal corridors for the Siberian flying squirrel. They also investigated the movement of the squirrels across open areas. By data collection statistics, their results show that flying squirrels used corridors and sometimes open areas for inter-patch movement. They also found that individuals moved faster and more directly in open areas than in woodland regions, and that the type of connection that a patch would have with other patches, such as open areas or corridors, did not affect the will of the individuals to leave a patch.

These biological examples are presented here for two reasons: The first one is that, the models studied in Chapter 4 and 5 have their biological basis on a squirrel species. These papers then, provide some behavioural context to model the movement and dispersal of these type of species in fragmented landscapes. The second one is that these models, provide the justification to add behavioural factors in the continuous equation models provided in this thesis. These factors are added in Chapter 4 in form of a term that models the individuals attraction towards better environments.

The use of mathematical models, in particular models based on continuum partial differential equations, can provide important insights and predictions for the dynamics of ecosystems in general and fragmented environments in particular. Some times, simple diffusion is sufficient to model the dispersal of certain populations, as it happens for the muskrat *Ondatra zibethicus* and the small cabbage white butterfly *Pieris rapae et. al.* [41]. However, to model the population dynamics of other species, it is necessary to add other factors, such as the individuals behaviour towards their environment, as shown in the examples provided in this section. In this thesis we try to incorporate a set of different factors in the modelling of population dispersal in fragmented systems. In our basic models we include key biological features (birth, death, diffusion) that are modelled mathematically by reaction-diffusion equations introduced in Chapter 3. In Chapters 4 and 5 we introduce some behavioural factors. In particular we study the propensity to drift towards a good environment by including an extra term to the equations.

2.8.1.2 Theoretical models

In this section we present a set of mathematical models that describe different features of population dynamics in fragmented ecosystems. Continuum models may describe some aspects of the populations dynamics very well, but other characteristics are better treated with a discrete description. The difficulty in analysing a certain population may also determine the type of method taken to study it, and sometimes, not only one, but several approaches are needed. This results in a diversity of ways to study population dynamics in fragmented environments. Here, we outline a few approaches based on discrete and stochastic models, lattices and integro-differential equations, while we postpone the analysis of continuum reaction-diffusion models for the following section.

A key development occurred in 1953, when Kimura [46] developed the so-called the "stepping stone model". This model assumes that the individuals of a population over an area are more or less distributed discretely forming clusters of colonies. This model has been used in the field of population ecology as a reference. For instance, Durret and Levin [47] described a couple of models based on discrete particle system models, in which the space is represented by a grid of sites with a finite number of states where a state might correspond to the presence or absence of an individual on a site, for example. Their results obtained from studying single populations models indicate that, when the probabilities of reproduction are small enough, the system always die out. However, if the reproduction probabilities are large enough, an equilibrium state that avoids extinction, appears.

Bevers and Flather [48], developed a probabilistic model based on reaction-diffusion equations to describe the dispersal of a population in a fragmented system. They proposed a map lattice for the population domain and assumed different growth functions depending on the spatial variables and used it to determine relationships between shape and persistence of population under Fickian diffusion.

Roques and Stoica [49] used nonlinear reaction and diffusion models applied to heterogeneous environments generated via stochastic processes to investigate species persistence in fragmented environments. Subsequently, Roques and Chekroun [11], using

reaction-diffusion equations, eigenvalue equations, and stochastic models, simulated the phenomenon of harvesting in a population over a two-dimensional habitat. They investigated the consequences of fragmentation over harvesting populations. They discovered that the harvesting allowance that a species can sustain maintaining a constant harvesting rate over time, results larger for aggregated regions than for dispersed ones.

In other approaches, Kot *et. al.* [7] used detailed dispersal data and population growth dynamics to construct integro-differential equations describing population dynamics of animal and plant populations, resulting on explicit formulas for the speed of invasion of populations dependent on their distribution.

Fagan *et. al.* [50] analysed how the size of a patch in a fragmented landscape affects the dynamics of a forager population using integro-differential equations. They discovered that, the way that populations make use of their habitat is crucial to determine the stability of the populations, and established critical patch sizes for population persistence and stable equilibria. Latore *et. al.* [20] also developed an integro-differential model to predict critical patch size for seasonal plant population living in a finite homogeneous habitat. Using previous models [4, 51] as the basis of their model, they found that the critical patch size of seasonal plant populations depends on the population growth rate and on dispersal characteristics.

Much of this thesis addresses problems raised by Guichón and Doncaster [15]. These authors used spatial explicit stochastic models to predict control strategies for the spread of an invasive species: the Asiatic red-bellied beautiful squirrel *Callosciurus erythraeus*. Their model is based on empirical data extracted from the squirrel location in Argentina, as well as from other published sources [52–57]. They found that a good control strategy for this invasive species, consists on the extraction of individuals from the now established habitat, in order to stop their reproduction and spread.

Other authors have also investigated fragmentation effects over populations by use of observational methods [58], lattices and stochastic approaches [59–61], integro-differential equations [62–64] and other statistical methods [65–69]. Here however, we restrict the review to continuum reaction-diffusion approaches, that is the main direction of this thesis.

2.8.2 Continuum models using pde's

In order to model accurately a population growth and dispersal over a fragmented environment, the main biological features that need to be accounted for are: population reproduction and death rates, dispersal, intra-species and inter-species competition, carrying capacities, habitat fragmentation, and directed movement. Reaction-diffusion models in general take account of some of these features by formulating partial differential equations that depend on the location of the individuals over space and time. For example, the dynamics of a single population system can be modelled by the presence of a population density ($n(x,t)$), and its interaction with the environment in space and time. The rate of change of population density can be described by

$$\frac{\partial n}{\partial t} = births - deaths + migration \tag{2.8.1}$$

This simple conservation equation underlies mathematical modelling of populations using partial differential equations. In the following we discuss examples of such models including: a non-diffusive model, early reaction-diffusion models, reaction-diffusion models in single domains, reaction-diffusion models in heterogeneous domains, and generalised reaction-diffusion models.

2.8.2.1 A non-diffusive model

In 1971, Levins [70] built a model for coexistence and exclusion of different species in a fragmented environment. In this model, Levins assumes a logistic growth function in the inhabitable regions, with a linear extinction rate outside the good habitat. Based only on these assumptions, Levins finds that the competition among species is directly related to their local extinction and migration rates. The model lacks diffusive terms describing individual migration. However, it provides a basis for models of higher complexity, like those we use in Chapters 3-5. For instance, in these models we assume, following Levins model, the existence of logistic growth functions in the resource-rich regions and linear decay in resource-scarce regions. In addition to these terms, our models will include

factors related to the dispersal of individuals, boundary conditions and behavioural features.

2.8.2.2 Early models

The origins of the study of population growth and dispersal dates back to the 1930s. The first mathematical paper describing the population spread in a homogeneous one-dimensional domain is due to Fisher, Kolmogorov *et. al.* and Skellman [2, 34, 51]. Fisher discussed the problem of a population distributed in a line where a mutant gene grows following a logistic law. The population disperses with a fixed diffusion constant in a one dimensional domain. For this problem Fisher proposed a one dimensional equation given by:

$$\frac{\partial u}{\partial t} = \frac{\partial^2 u}{\partial x^2} + u(1-u). \tag{2.8.2}$$

Equation (2.8.2) describes the nonlinear evolution of a population in a one-dimensional habitat. Around the same time period Kolmogorov *et. al* [34] studied a more general problem using parabolic partial differential equations describing simultaneously the growth and diffusion processes.

Fisher and Kolmogorov independently discovered that equation (2.8.2) has an infinite number of travelling wave solutions. Since then, equation (2.8.2) have been the basis of many population models including those we shall use. Equation (2.8.2) is studied in Chapters 3, and is the basis of the model studied in Chapters 4 and 5.

Later on, Skellam [51] developed a model for the dispersal of living organisms using random-walk theory. He discovered that the survival of a population that moves within its habitat is related to their habitat size. As a result, he proposed that if the area of an isolated terrestrial habitat is smaller that a certain critical size, the population cannot survive. This study initiated the research on critical patch size. In this context, Kierstead and Slobodkin [4] developed a model based on planktonic patchiness studying a population model with diffusion and linear growth. In their model they assume a population inhabiting a region of fixed size with lethal surrounding areas. In this work, Kierstead and Slobodkin found a measure for the critical patch size of populations in one

dimension given by $L_c = 2.4048\sqrt{\frac{D}{\alpha}}$ where D is the diffusivity constant and α is the net growth rate in the patch. From their discovery, these type of models received the name of KISS models, where KISS is an acronym for the discoverers of it (Kierstead, Slobodkin and Skellam). The ideas implemented by Kierstead, Slobodkin and Skellam are one of the fundamental pieces needed to construct the theory of fragmented populations and they are examined and extended in Chapter 3.

2.8.2.3 Single patch models with logistic growth and diffusion

Single patch systems with different type of boundary conditions are the basis required to study fragmented systems, and provide the principal piece of a heterogeneous environment, *i.e.* a fragment. Therefore, many have investigated these apparently simple systems over the years. In Chapter 3 we also investigate single patch dynamics.

In 1994 Holmes *et. al.* [71] summarized a number of ecological models using partial differential equations to discuss dispersal, ecological invasions, the effect of habitat geometry and size, and spatial patterning. Their study is based on reaction-diffusion equations including biased random motion. The purpose of this study was to make pde's models accessible to experimental ecologists, emphasising the importance of pde's in the modelling of a great variety of ecological processes.

Okubo developed a two-dimensional extension to the KISS model [72] that predicts a critical patch area given by

$$A = c_0 \pi \sqrt{\frac{D}{f'(0)}}. \tag{2.8.3}$$

Here, c_0 is a constant determined by the geometry of the patch, D is the diffusion coefficient and $f'(0)$ (the first derivative of the population growth function), represents the population growth rate at very low population density.

Cantrell and Cosner have extensively studied of models for heterogeneous ecological systems using reaction-diffusion equations. Their results include measures of critical patch size [3] and dispersal changes due to predator incursions that also affect critical patch size [73]. They have also formulated interface conditions relating population density directly inside and directly outside a patch [74]. In these papers they mainly explore

single patch, or closed domain systems, by investigating their eigenvalue solutions and relating them to biological quantities. The mathematical technique they usually follow to study these systems is the analysis of eigenvalue equations. In chapter 3 we touch on the subject of eigenvalue problems using them to study critical patch size in closed domains. However, later on, our approach focus on the study of individual fluxes across different domains, either in semi-infinite domains and finite ones.

2.8.3 Travelling waves

The interest of knowing what happens in regions that are large enough to reach constant velocities in time, either homogeneous or heterogeneous, and how the dispersal of populations can be related to mathematical structures is not a new subject and here the study of travelling waves as a form of dispersal is treated.

As mentioned in §2.8.2.2, in 1937 Kolmogorov, Petrovski and Piskunov [34] found that for the logistic equation with diffusion,

$$\frac{\partial u}{\partial t} - \nabla^2 u = u(1-u) \tag{2.8.4}$$

there is a family of planar travelling waves that for a given set of initial conditions travel at constant speed c with minimum speed $c_{min} = 2$ and such that no fronts exist with $c < c_{min}$.

Kolmogorov *et. al.* indicated that the population would have an infinite speed of propagation, unless a threshold level, below which a population cannot be detected, existed. Giving conditions for this threshold existence, Kolmogorovs' *et. al.* model predicted that the population would propagate as a wave front with velocity

$$c_{min} = 2. \tag{2.8.5}$$

for asymptotically large times.

Andow *et. al.* [41], studied the success of single population invasions, taking place in different habitats, for three independent experimental cases. In this study, the theoretical

predictions, previously described by Kolmogorov *et. al.* were corroborated experimentally by Andow *et. al.* for two out of three study cases. The velocity of spread of populations is a very important measure in biological populations since it helps predicting the fate of populations in time. In the following section, we present a more complete review of propagating waves in populations, since this is one of the key features we analyse in Chapter 5.

In general, the velocity of a wave of advance c for the Fisher equation in a one-dimensional infinite homogeneous space has received great attention [2, 5, 28–31]. However, no analytic solutions of this equation for general velocities c [75] exist except for some exceptions. Ablowitz and Zeppetella, [76] obtained a particular solution for the velocity of the wave of advance given by $c = 5/\sqrt{6}$ for the population distribution

$$n(x,t) = \frac{1}{(1+e^{(x-ct)/\sqrt{6}})^2}. \tag{2.8.6}$$

In two-dimensional systems, travelling wave solutions for the Fisher-Kolmogorov equation have received much less attention [14, 75, 77, 78] and so far, no analytic travelling wave solutions for general velocities have been found [77]. However, some results for travelling waves solutions in two dimensions can be found. Brazhnik and Tyson [77] study different travelling wave solutions in two dimensions for the Fisher equation. Some of these solutions are explicit and some other numerical.

In this thesis, we study numerically travelling waves in corridor geometries to investigate the velocity of the wave of advance, rather than the structure of the wave itself. This velocity will help us to calculate the speed of propagation of populations subject to the Fisher-Kolmogorov equation.

2.8.3.1 Periodic environments with travelling waves

In 1976 Levin, [79] produced a paper in which he uses a reaction-diffusion equations to model an heterogeneous system with n different species distributed over an interconnected network of m patches. In this study he discussed how the spatial configuration of the environment may influence species diversity depending on the heterogeneity of the

environment. Levin's model constitutes a seminal approach to the study of many patch systems using reaction-diffusion equations.

Kinezaki *et. al.* [6] modelled biological invasions in the context of periodically fragmented environments. They consider a two-dimensional striped environment consisting of favorable and unfavorable habitats with the respective widths L_1 and L_2. These are alternately arranged along the x-axis. For the dynamics of the system they use an extended Fisher equation in which they suppose different diffusion constants and different per capita growth rates for the favorable and unfavorable habitats. The results of this model show different forms of travelling wave solutions that depend on a set of parameter values determining the level of the domain fragmentation. In this work they also determine that, as the fragmentation scale increases, the rate at which the population expands their habitat, increases as well. Kinezaki, Kawasaki and Shigesada [80] then constructed a two-dimensional model based on a modified Fisher model. In this work, the growth rates and diffusion coefficients were varied sinusoidally on a two-dimensional domain. They show that the velocity of the wave of advance depended on the amplitude and the wave length of the diffusion coefficient and the intrinsic growth rate. Many other models based on these two models have emerged since then [14, 81–83]. These models typically express environmental heterogeneity by assuming periodic or a-periodic variable diffusion coefficients and intrinsic growth rates in the partial differential equation. Their solution and investigation usually involves the use of statistical and stochastic tools, and their applications are diverse. These include mathematical applications like the demonstration of existence and uniqueness theorems on travelling waves [14, 82] and biological applications such as, how to maximise the chances of survival of certain populations [83] and how to prevent biological invasions [84].

In particular, the model by Fagan *et. al.* [85] resembles the model studied in Chapter 3. In [85] a one-dimensional a-periodic system is analysed using reaction-diffusion equations with spatially variable growth and decay functions. While the population dynamics is completely deterministic, the heterogeneity over space is stochastic. This stochasticity, together with the growth and decay coefficients, critical patch sizes and maximum gap lengths, determines how far a population can disperse. The results of Fagan *et. al.*

suggest that a close relationship between the population biological traits (growth, decay, critical patch area and maximum gap cross ability) and the occupancy and spread of populations exist.

The equations and boundary conditions used in this study are similar to those which we use in the analysis of the model proposed in Chapter 3. However, the approach taken to analyse the system is completely different. We focus on the dynamics of a single patch surrounded by unfavorable regions and then, we study it in detail. Our results show how the individual flux depends on the biological traits such as growth and decay rates, as well as diffusion coefficients. We then relate these results to the biological traits such as carrying capacity and critical patch size. We believe that once the correct dynamics for a single patch are obtained, a general model can be developed for either a periodic or a-periodic system. Therefore, the study of local systems is a priority in this thesis.

In chapters 4 and 5 we also analyse equations similar to the ones analysed by Fagan *et. al.*, but we introduce a behavioral term and study in detail much smaller systems constituted by two patches and a gap, corridors and single patch dynamics including also density dependent factors such as the Allee effect, described in the following section.

2.8.4 Models with Allee effect

The Allee effect owes its name to the pioneering work of of W.C. Allee [86], who noticed firstly that goldfish had better chances to survive in waters inhabited previously by goldfish than in waters that did not have goldfish populations before [87]. Then, he also noticed that larger groups in populations enhanced reproduction and survival rates [88]. Nowadays, the Allee effect is a widely studied topic in spatial ecology and is believed to be an important factor in dispersal and colonisation. McCarthy [89] defines it as an inverse density dependence in the population, occurring when the population growth rate is reduced at low population size. This may, for example, occur when the reproductive success is very poor due to external factors such as the difficulty to find mates. In this thesis, the influence of the Allee effect on the colonisation of an initially empty patch is studied in Chapters 4 and 5.

The Allee effect applied to reaction-diffusion equations, has been applied in different models [7, 71, 90, 91]. For example, Keitt *et. al.* [92] studied spatially continuous and discrete reaction-diffusion models where Allee effects cause invasions to fail under different circumstances. Their results indicate that species habitat ranges may be limited by Allee effects. On the other hand, Cantrell and Cosner [93] investigated the consequences of an Allee effect over an island that is being colonised from a source population on a continent in a one-dimensional system. They discovered that the colonising species have to be close enough to the island being colonised and have sufficiently rapid dispersal as well as sufficiently low mortality rates in transit for colonisation. In this study no special boundary conditions or spatial heterogeneity is incorporated. The models we analyse in Chapter 4 and 5 are similar to this model, and they also predict a dependence between distance to the patch to colonise and the colonisation success. However, our models also include certain types of boundary conditions that will account for behavioural factors and explicit heterogeneity over the landscape. In contrast with Cantrell and Cosner [93] model, we also perform an extensive study on the relationship between gap length and the ability to establish a population in the initially empty patch and we numerically investigate two-dimensional systems.

2.8.5 Models with generalised flux terms

In different areas of science such as medicine, engineering, materials, among others, terms modelling transport and fluxes are many times determined by terms which go beyond simple Fickian diffusion. These generalised flow models can model for example the response of an agent or individual to a directional stimulus. This is the case of chemotaxis, phototaxis and thermotaxis [38]. In bio-medicine for example, these modelling taxis terms, play a very important role in phenomena such as fracture-healing [94] or tumor growth [95]. Another example is the modelling of very fast invasions of human populations. In this case, these taxis terms are based on the assumption of directed movements as methods of resource exploration, and the existence of resources that depend on the population density [96].

In terms of ecological fragmentation, the implementation of terms related to directed

movement in spatially explicit reaction-diffusive models goes back to the studies by Levin [97] who used aggregation and individual based models to explore the responses of individuals to their environment. His results show that clusters of individuals are formed in a non-uniform way as a consequence of the responses of individuals to their environment and to each other. Later, Grunbaum [98] developed a model based on advection-diffusion equation (advection for the taxis terms) where the magnitude of both, diffusion and advection were governed by an algorithm which modelled the individuals learned response to its local environment. If such learning did not exist, there was no individual taxis.

Cantrell [99] also developed a reaction-diffusion-advection model for two competitors with different dispersal strategies, inhabiting a spatially heterogeneous environment, using eigenvalue analysis. One of the species dispersed by simple diffusion, while the other had a term accounting for directed movement towards better environments, beside the normal Fickian diffusion one. This paper shows that the species with directed movement terms, moves faster than ones without it. Moreover, he showed that a species with directed movement has a competitive advantage over one without it, this is in contrast to species subject to simple diffusion only, where the slower diffusing species always has the competitive advantage.

One of the latest models including movement behaviour is a model attributed to Fagan *et. al.* [100]. In this model they use an individual-based approach assuming resource availability as the biggest driver of movement decisions. Using evolutionary programming and artificial intelligence techniques they showed qualitatively how to integrate different behaviours (orientation, perception and memory) in individual dispersal, according to the existing surrounding environment.

Our model includes this behavioural trait in the boundary conditions as it is explained in Chapter 4. As the individuals approach the boundary of a habitat patch, they feel threatened by their surrounding. This is modelled by constructing a dendrotaxis function which adds an extra term to the flux. This function will produce a discontinuity in the population density at the boundary (the individuals have a strong preference for resource rich regions over scarce-resource regions) and continuity on the flux (the number of individuals leaving a regions is the same number arriving to the next region). The

model we propose in Chapters 4 and 5 is then based on reaction-diffusion equations with boundary conditions that account for the individuals sense of danger. We explore extensively the model of two patches separated by a dangerous region in one- and two-dimensions, while we also analyse different structures in two-dimensions.

2.8.6 Summary

In this section we summarise the key results of this literature review applied to the development of different models in this thesis. As stated in §2.8.2, continuum population models can typically be formulated as a conservation equation of the type,

$$\frac{\partial n}{\partial t} = births - deaths + migration \tag{2.8.7}$$

where each factor is modeled by a mathematical function. In Chapter 3, we investigate single patch models based on an equation with logistic growth and diffusion

$$\frac{\partial n}{\partial t} = n(1-n) + \nabla^2 n \tag{2.8.8}$$

that was first developed by Fisher, Kolmogorov et. al. and Skellman [2, 34, 51]. We investigate properties such as critical patch size, previously investigated by Kierstead and Slobodkin [4], Cantrell and Cosner [3, 73], Holmes *et. al.* [71] among others. We also look at dispersal rates previously investigated in [41], at growth rates studied in [4, 7, 48, 51, 70, 85, 101]. We study carrying capacities also analysed in [85] and boundary effects as seen in [34, 74]. However, the focus of Chapter 3 is to understand the population dynamics in single patch systems, and explore their density and currents, finding new solutions and to investigate novel phenomena.

In chapters 4 and 5, we expand the model given by equation (2.8.8) assuming environments of the form previously studied by Kinezaki *et. al.* [6] and [14, 81–83]. However, this previous work is predominantly based upon stochastic models, that insert the heterogeneity in the growth function. We, on the other hand, assume different growth functions in each region as in [85], and use interface conditions to model the individuals

preference for one domain over another. These boundary conditions help us to model a directed movement type term. To our knowledge, this approach is new in the area of fragmented ecosystems.

We also study the consequences of Allee effects on these type of systems. Such studies have been carried out in [7, 71, 90, 91, 93] for different systems, but, due to the interface conditions applied in Chapters 4 and 5, the consequences of the Allee effect on population dispersal are different and very interesting, as we will see later in this thesis.

2.8.7 Other reviews

The literature review presented here is a review based on single population models related to the models studied in this thesis. However, a number of interesting reviews on the area of spatial ecology can be found in [5, 102–105].

2.9 Summary

In this chapter, we gave an overview of the basic models and concepts used to study and analyse populations in fragmented environments.We also presented a literature review of theoretical work related to the work performed in this thesis.

Chapter 3

One-dimensional population models

In chapter 2 we discussed the most standard population models used in mathematical ecology, commonly employed as a starting point for the analysis and study of spatially structured population systems. Using these models as groundwork for our analysis, in this chapter we study one-dimensional problems in fragmented environments.

One of the advantages of solving one-dimensional problems is that they are usually simpler to solve, the results are more accurate and some are even exact. However, the study of one-dimensional systems have also some disadvantages. For example, one-dimensional systems do not provide the whole information relevant for real two-dimensional systems analysis, and important features of the dynamics may be lost. Another disadvantage is that some one-dimensional mathematical methods, cannot be extended to two dimensions and there are no exact solutions. Therefore, other methods, mainly numerical, must be used. In this chapter, we analyse one-dimensional systems that, even with the disadvantages mentioned above, provide essential information about the dynamics of more complex systems in two and more dimensions. In Chapter 4 we expand the analysis to include some other characteristics of these type populations while in Chapter 5 two-dimensional systems are analysed.

3.1 Semi-infinite domain with absorbing boundaries

Here, we analyse the dynamics of a one-dimensional single population system inhabiting a semi-infinite patch with plentiful resources available for the population individuals, subject to logistic growth and diffusion in the presence of absorbing boundaries and lethal surroundings. In applied probability theory as well as in theoretical physics, the term *absorbing boundaries* refers to the fact that the quantity under study (in this case n is zero at the boundary [106]. Here we will adopt this term to refer to this type of boundary condition.

An exact solution by means of a first integral for model equation in the stationary state is found, followed by an approximate analysis for the same system. Finally, these two methods are compared.

In homogeneous environments it is a sensible assumption to say that over long time scales, the species population does not change with time. However, if the ecosystem presents inhomogeneities, the situation changes. When the ecosystem presents a certain level of fragmentation where regions of plentiful and scarce-resources co-exist, the individuals start diffusing along them. This diffusion corresponds to a current of individuals moving between regions. Based on this idea we divide the semi-infinite system into three regions: One region represents a homogeneous habitable region which will be called *high-quality patch*. Another region represents a disturbed habitat. This habitat results in such a danger for the population, that no individual can survive in it. This region is called a *lethal region*. The interface located exactly between the two patches is the *boundary*.

Figure 3.1 shows a homogeneous environment and a system composed by a high quality patch surrounded by a lethal region. Some individuals diffuse out of the patch generating a flux of individuals towards the lethal region.

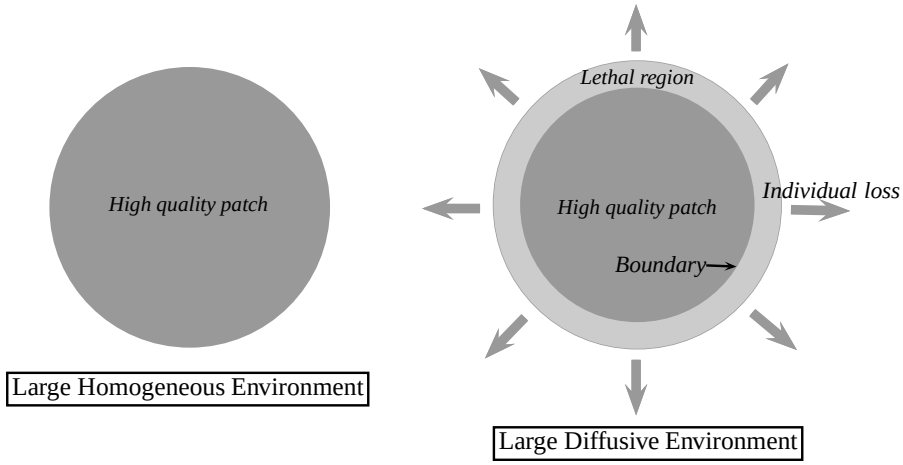

FIGURE 3.1: The figure on the left is a homogeneous environment. At steady state this system has a constant population over time. The figure on the right shows a system composed by a high quality patch surrounded by a lethal region. Some individuals diffuse out of the patch, towards the lethal region. This situation generates a loss or flux of individuals towards the lethal region.

3.1.1 Model

When a population inhabits an homogeneous region, individuals of the population tend to diffuse homogeneously over the entire region, spreading according to the intrinsic characteristics of the population. However, if this region is surrounded by a completely different environment, like for example, an island surrounded by sea, the individual behaviour will change. There are two possibilities: either the individuals avoid going towards these regions, or they simply diffuse towards them.

Here we examine the case where a single population system distributes almost homogeneously along a semi-infinite patch, diffusing along it, and carelessly diffusing towards the absorbing boundary and lethal surroundings. Later we consider the case where the individuals perceive the danger of going away from the region with plentiful resources, thus, avoiding the dangerous or lethal areas.

Assuming that the population in a semi-infinite patch follows the dynamics in time represented by a source function plus diffusion, like the one described by equation (2.3.6), we can write,

$$\frac{\partial n}{\partial t} + \nabla \cdot \mathbf{J} = f(n, \mathbf{x}), \tag{3.1.1}$$

where n is the population per unit area, f represents the population growth function, $\mathbf{J}$

is the individuals flux, x is the spatial variable and t is the time. If the population obeys a logistic growth, diffusing at the same time along the high quality patch and towards the lethal region, f is then written as,

$$f(n,\mathbf{x}) = \begin{cases} \alpha n\left(1-\dfrac{n}{\chi}\right) & \text{in the resource-rich patch} \end{cases} \tag{3.1.2}$$

while

$$n = 0 \quad \text{in the lethal region} \tag{3.1.3}$$

χ represents the total carrying capacity and α is the population growth rate. $\mathbf{J}$ corresponds to the flux of individuals diffusing from the high quality patch to the lethal region and it is given by,

$$\mathbf{J} = -D\nabla n. \tag{3.1.4}$$

According to this model the population grows logistically in the high quality patch, the individuals die in the lethal region, and the individuals diffuse in the patch. Outside the patch, as we assumed lethal surroundings, the population and the flux are zero. An extensive analysis of a similar system consisting of a population following logistic growth in a finite region can be found in [28]. However, we would like to focus in the analysis of a semi-infinite region that is not so widely studied.

3.1.2 Model non-dimensionalisation

To simplify the model described by equations (3.1.1) - (3.1.4) we non-dimensionalise the equations and parameters of this one-dimensional system. The units of equation (3.1.1) are: $[n] = [L^{-1}]$, $[D] = [L^2T^{-1}]$, $[\alpha] = [T^{-1}]$, $[\chi] = [L^{-1}]$ and $[x] = [L]$, where L represent length units and T time units. Defining the dimensionless quantities: $t^* = \alpha t$, $n^* = \dfrac{n}{\chi}$ and $x^* = \dfrac{x}{\xi}$, where $\xi = \sqrt{\dfrac{D}{\alpha}}$, we can now rewrite the system in the new starred variables to obtain,

$$\frac{\partial n^*}{\partial t^*} = n^*(1-n^*) + \frac{\partial^2 n^*}{\partial x^{*2}} \quad \text{in the resource-rich patch,} \tag{3.1.5}$$

and

$$n^* = 0 \quad \text{in the lethal region.} \tag{3.1.6}$$

In this context n^* is the *normalised population* which represents the population existent in the patch over the carrying capacity per unit length χ. t^* is the *relative time* with respect to the population growth rate α, and ξ is defined as the *diffusion length*. This length describes the diffusion of a population in space, given a constant diffusion coefficient and the per capita population growth rate. Finally, x^* is the *length scale* x divided by ξ.

The initial conditions in this system imply a completely full patch at $t = 0$ *i.e.*

$$n^* = 1 \quad \text{at } t^* = 0, \tag{3.1.7}$$

everywhere. At the same time, the boundary conditions of this system are given by,

$$n^* = 0 \quad \text{at } x^* = 0, \tag{3.1.8}$$

$$n^* \to 1 \quad \text{as } x^* \to \infty. \tag{3.1.9}$$

These initial and boundary conditions are key to determine the system dynamics. $n^* = 0$ at $x^* = 0$, implies that at the patch boundary the population goes to zero and no population exist beyond it. On the other side, $n^* = 1$ as $x^* \to \infty$ implies that as we move away from the boundary, the population grows and saturates reaching the value of $n^* = 1$ at distances where the environment becomes practically homogeneous away from the boundary. We also consider that the change of population in space as $x^* \to \infty$ reaches a constant value resulting in the boundary condition,

$$\frac{\partial n*}{\partial x^*} = 0 \quad \text{as } x^* \to \infty. \tag{3.1.10}$$

This behaviour is shown in figure (3.2).

FIGURE 3.2: Semi-infinite domain ($x^* \to \infty$) where the population tends to one as x^* increases.

Equation (3.1.5) is a second order non-linear partial differential equation which is difficult to solve, and its solution is hard to analyse. In general, this equation does not have an exact solution [39], and its approximate or semi-analytic solutions, involve the treatment of elliptic functions.

Fortunately for us, an exact solution for the stationary state of this system, with the boundary conditions imposed by equations (3.1.8), (3.1.9) and (3.1.10) does exist as we will show in §3.1.3. In §3.1.3 and §3.1.4 we find an exact and an approximate solution for equations (3.1.5) and (3.1.6) in the following way. Firstly, we obtain the solution to the exact integral of the model. Later, the system is analysed using a patching method, which will be explained in §3.1.4. Finally, the results of these two methods are compared and the accuracy of the approximated method with respect to the exact solution. A good approximation from the patching method to the exact result is expected to be reached. A good approximation will permit the use of this method in the analysis of other one-dimensional systems with the certainty of obtaining reasonable results.

3.1.3 Analytic solution for the stationary state

Equation (3.1.5) has no general analytic solution [5] and the solution to the system presented cannot be formulated analytically. However, an explicit analytic solution for the stationary state may be obtained. Due to the lack of analytic solutions for the vast majority of this type of systems, the existence of an analytic solution allow us to measure the accuracy of the approximate system solutions with the exact solution in order to validate our analysis. This is of great importance since most of the results found in this

thesis are either approximate semi-analytic, or numerical.

In a completely homogeneous system, the population is such that their individuals fill up the system completely. However, the system we are analysing, is not completely homogeneous. There is a current of individuals diffusing towards the lethal region throughout the boundary. If we consider an initial population that fills up the whole of the semi-infinite patch, then we can write after dropping the stars from equations (3.1.5) - (3.1.9),

$$n(x,t) = 1 \tag{3.1.11}$$

After some time, there will be a flux of individuals towards the lethal region. Since the size of the patch is semi-infinite, the individual flux towards the lethal region is very small with respect to the patch size, and constant after some time. The change of the population over time is therefore negligible, and we can consider the system to be in a stationary state. The population flux eventually becomes constant, and consequently produces a stationary state for the population,

$$n \to n_s(x) \quad \text{as } t \to \infty. \tag{3.1.12}$$

where n_s stands for the population in stationary state. In the stationary state, equation (3.1.5) becomes a non-linear second order ODE. In general, the solution to this equation involves performing elliptic integrals. Fortunately, the case studied here has an exact solution and this solution is analysed by analytically solving the equation (3.1.5) with the boundary conditions given by equations (3.1.8), (3.1.9) and (3.1.10).

3.1.3.1 Stationary state analysis

Rewriting equation (3.1.5) for the stationary state and dropping the subindex s of the population we obtain,

$$0 = n(1-n) + \frac{d^2n}{dx^2}. \tag{3.1.13}$$

Defining

$$u = \frac{dn}{dx} \tag{3.1.14}$$

we obtain

$$\frac{du}{dx} = -n(1-n), \tag{3.1.15}$$

that substituted into equation (3.1.13) gives

$$u\frac{du}{dn} = -n(1-n), \tag{3.1.16}$$

Equation (3.1.16) can now be integrated to obtain

$$\int u du = \int -n(1-n)dn, \tag{3.1.17}$$

equivalent to,

$$\frac{u^2}{2} = -\frac{n^2}{2} + \frac{n^3}{3} + C, \tag{3.1.18}$$

To find the value of the constant C we use the boundary conditions provided in equations (3.1.9) and (3.1.10) to obtain,

$$C = \frac{1}{6} \quad \text{given that as } x \to \infty,\ u = 0 \text{ and } n = 1 \tag{3.1.19}$$

Rearranging terms and substituting the value of C in equation (3.1.18), we apply the boundary condition stated in equation (3.1.8) to obtain,

$$\int_0^{\bar{n}} \frac{dn}{\sqrt{(1-n^2) - \frac{2}{3}(1-n^3)}} = \int_0^{\bar{x}} dx. \tag{3.1.20}$$

Luckily, equation (3.1.20) has a repeated root $n = 1$, so the solution of the integral can be written in terms of elementary functions. When a repeated root is found in the denominator of the integrand of a polynomial function of degree 3 or 4, the repeated factor can be taken out of the radical to leave a polynomial of degree of 1 or 2 inside the square root and express the integral in terms of elementary functions [107]. If equation (3.1.20) lacked the repeated root mentioned above, it would become an integral equation, preventing us from finding an analytic solution in terms of elementary functions.

Factorizing and arranging terms, equation (3.1.20) becomes

$$\sqrt{3}\int_0^{\bar{n}} \frac{dn}{\sqrt{(1-n)^2(2n+1)}} = \int_0^{\bar{x}} dx. \tag{3.1.21}$$

Taking $v = \sqrt{2n+1}$ and $\dfrac{dv}{dn} = \dfrac{1}{\sqrt{2n+1}}\dfrac{dn}{dx}$ then

$$\frac{dv}{dx}\sqrt{2n+1} = \pm\frac{1}{\sqrt{3}}(1-n) = \pm\frac{1}{2\sqrt{3}}(3-v^2). \tag{3.1.22}$$

Notice that for $n = 0$, $v = 1$. With this change of variable equation (3.1.21) transforms into

$$2\sqrt{3}\int_1^{\bar{v}} \frac{dv}{3-v^2} = \int_0^{\bar{x}} dx. \tag{3.1.23}$$

where $\bar{v} = \sqrt{2\bar{n}+1}$. The solution of the integral given by equation (3.1.23) is

$$\ln\left(\frac{\sqrt{3}+\bar{v}}{\sqrt{3}-\bar{v}}\right) - \ln\left(\frac{\sqrt{3}+1}{\sqrt{3}-1}\right) = \bar{x} \tag{3.1.24}$$

that can be simplified to

$$\ln(2-\sqrt{3}) + \ln\left(\frac{\sqrt{3}+\bar{v}}{\sqrt{3}-\bar{v}}\right) = \bar{x}. \tag{3.1.25}$$

Taking exponentials in both sides of equation (3.1.25) we obtain

$$e^{\bar{x}} = (2-\sqrt{3})\left(\frac{\sqrt{3}+\bar{v}}{\sqrt{3}-\bar{v}}\right) \tag{3.1.26}$$

that in terms of $\bar{v}$ can be written as

$$v = \sqrt{3}\left(\frac{e^{\bar{x}} - (2-\sqrt{3})}{e^{\bar{x}} + (2-\sqrt{3})}\right) \tag{3.1.27}$$

Substituting $\bar{v} = \sqrt{2\bar{n}+1}$ in equation (3.1.27) and rearranging terms, we can now express the population $\bar{n}$ with respect to the distance $\bar{x}$. Dropping the bar from the variables in equation (3.1.25) we obtain,

$$n(x) = \frac{1}{2}\left[3\left(\frac{1-(2-\sqrt{3})e^{-x}}{1+(2-\sqrt{3})e^{-x}}\right)^2 - 1\right]. \tag{3.1.28}$$

Equation (3.1.28) gives the dependence of n on x for a semi-infinite domain, where n is population in space at stationary state and x is the spatial variable.

In figure 3.3 the expression given by equation (3.1.28) is presented graphically. Later we compare these results with the results obtained in §3.1.4 in §3.1.5.

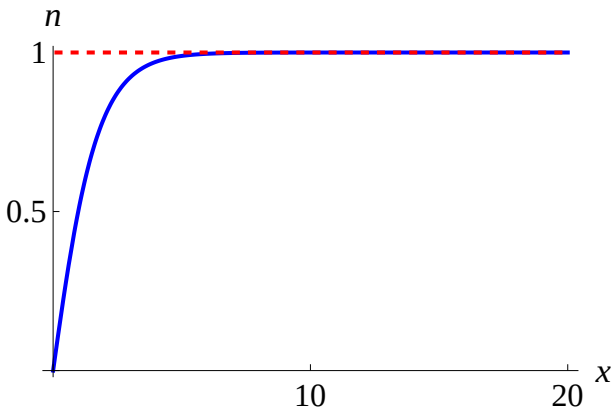

FIGURE 3.3: Analytic dependence of the population n against spatial variable x for a semi-infinite system. As $x \to \infty$, $n \to 1$ whereas for $x \lesssim 1$, $n(x)$ is linear.

3.1.4 Approximate analysis

As we mentioned in §3.1.3, the analytic general solution of equation 3.1.5 does not exist. However, the existence of an analytic solution for specific boundary conditions gives us the possibility to compare this results with other approximate solutions of similar systems. Here we compare this analytic solution with an approximate solution of the same system using the patching method [108]. This analysis will allow us to test the accuracy of approximate solutions with analytic ones in order to validate our models.

3.1.4.1 Model

The patching method is a technique to solve boundary-value problems used when the differential equations can be solved in closed form for special types of forcing terms [108]. By approximating the original forcing term by one of these special types in various regions, a closed form solution in separate parts, can be found over the whole domain. The solutions in the various regions as well as their derivatives, are patched

at the points joining each separated region of the domain, obtaining an approximate solution for the whole domain.

In this case we consider a two regions system where the region $x \lesssim 1$ is governed by a population that grows linearly while in the region where $x \to \infty$, the population approaches one, $n \to 1$. These two regions are matched at the point δ where the solution and their derivatives of both solutions are equal, as shown in figure 3.4.

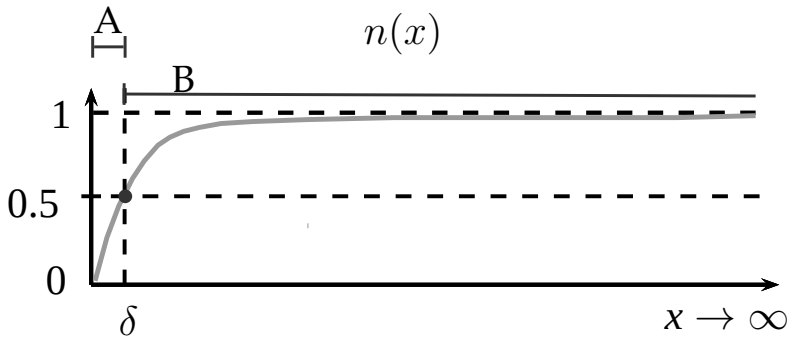

FIGURE 3.4: The patching method is used to match the solutions of two regions in a semi-infinite single patch system, n grows linearly when $x \lesssim 1$ and $n \approx 1$ as $x \to \infty$. The domain is divided in two regions A and B to describe the system through the patching method. The patching point in the figure is $x = \delta$

Consider now, a semi-infinite system in the stationary state with absorbing boundaries, where the the population at $x = 0$ is zero and at infinity is one. From figure (3.4) we can see that the domain can be split in two regions. Without loss of generality, we suppose that in region A the population grows from $n(x = 0) = 0$ to the value $n = 0.5$ as x increases. In region B the population grows from $n = 0.5$ to $n = 1$. Without loss of generality, the point $n = 0.5$ is chosen as matching point, although other matching points can be chosen, as we will see in §3.1.7.

In region A the system dynamics is governed by the equation

$$n \cdot (1 - n) + \frac{d^2(n)}{dx^2} = 0. \tag{3.1.29}$$

Because in this region n is close to the boundary and at the boundary $n = 0$, we can

linearise equation (3.1.29) to obtain

$$n = -\frac{d^2 n}{dx^2}, \tag{3.1.30}$$

that has the solution

$$n = n_0 \sin(x) \tag{3.1.31}$$

using the initial condition $n(0) = 0$, where $x \in [0, \delta]$. As we move away from $x = \delta$, the value of n becomes close to 1. Assuming then that in region B,

$$n = 1 - m \tag{3.1.32}$$

where $m << 1$, equation (3.1.29) can be written as

$$(1 - m) \cdot (1 - (1 - m)) + \frac{d^2(1 - m)}{dx^2} = 0. \tag{3.1.33}$$

Linearising and rearranging terms we obtain,

$$m = \frac{d^2 m}{dx^2}. \tag{3.1.34}$$

that has the general solution

$$m = m_1 \sinh(x - \delta) + m_0 \cosh(x - \delta). \tag{3.1.35}$$

As the boundary conditions of the system require that as $x \to \infty$, $n \to 1$ the solution transforms into

$$m = \frac{1}{2} m_0 e^{-(x-\delta)}. \tag{3.1.36}$$

where δ is the point where $n = 0.5$, the point where both solutions are matched.

3.1.4.2 Solution matching

If we assume that inside region A, $n < 0.5$, while in region B, $n > 0.5$ we find that the solution in A equates the solution in B, at $n = 0.5$, for some $x = \delta$.

Recalling that $n = 1 - m$ in region A, equations (3.1.36) and (3.1.31) are matched at $n = 0.5$ to obtain

$$n = 1 - m_0 e^{-(x-\delta)} = 0.5 \tag{3.1.37}$$

and

$$n = n_0 \sin(x) = 0.5 \tag{3.1.38}$$

In this example, we also assume that the population, as well as the current, is continuous. This implies that the solution must be continuous with continuous derivative, therefore,

$$n_0 \cos(x) = m_0 e^{-(x-\delta)}. \tag{3.1.39}$$

Rearranging terms and matching solutions at $x = \delta$ we find that,

$$n_0 \cos(\delta) = 0.5. \tag{3.1.40}$$

Dividing equation (3.1.38) by equation (3.1.40), the value of δ where the two solutions match is

$$\cot \delta = 1 \Rightarrow \delta = \pi/4. \tag{3.1.41}$$

Substituting the value of δ in equation (3.1.38) the value of n_0 is obtained, such that,

$$n_0 \sin(\pi/4) = 0.5 \Rightarrow n_0 = 1/\sqrt{2}, \tag{3.1.42}$$

and from equation (3.1.37), m_0 is found to be,

$$m_0 = \frac{1}{2} \exp(\pi/4 - \pi/4) = \frac{1}{2}. \tag{3.1.43}$$

Once m_0 and n_0 have been obtained, the general solution for the system can be written as,

$$n = \frac{1}{\sqrt{2}} \sin(x) \quad \text{for } |x| < \pi/4, \tag{3.1.44}$$

and

$$n = 1 - \frac{1}{2} e^{\pi/4 - x} \quad \text{for } |x| > \pi/4. \tag{3.1.45}$$

The solution for the patching approximation solution is shown in figure 3.5 where the black dot represents the matching point of the solution.

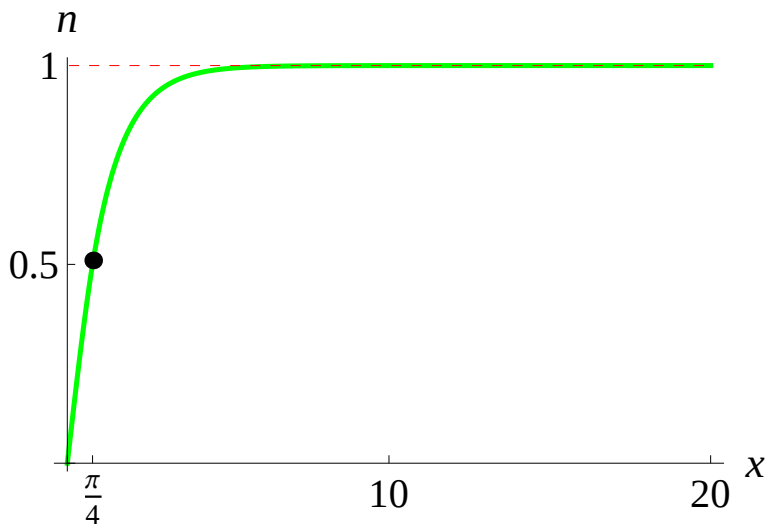

FIGURE 3.5: A patching solution shows the dependence of the rescaled population n with respect to the distance x from the boundary in a semi-infinite domain. The black dot at $x = \pi/4$, $n = 0.5$, indicates the matching point of the solutions between region A and B.

3.1.5 Comparison between exact and approximate solutions

Figure 3.6 shows the solutions for the patching method and the exact method. The solid line shows the exact solution, while the dashed line shows the approximate solution. Notice that when $x >> 1$ the solutions are practically the same. For x close to the boundary however, these solutions slightly differ from each other. To see how important the difference between the exact method and the patching method is, an analytical comparison of the two solutions is given in §(3.1.5.1) and §(3.1.5.2).

3.1.5.1 Approximations for x close to zero

To compare the solutions given in equations (3.1.28) and (3.1.44) we first expand them using a Taylor series, for x close to zero obtaining,

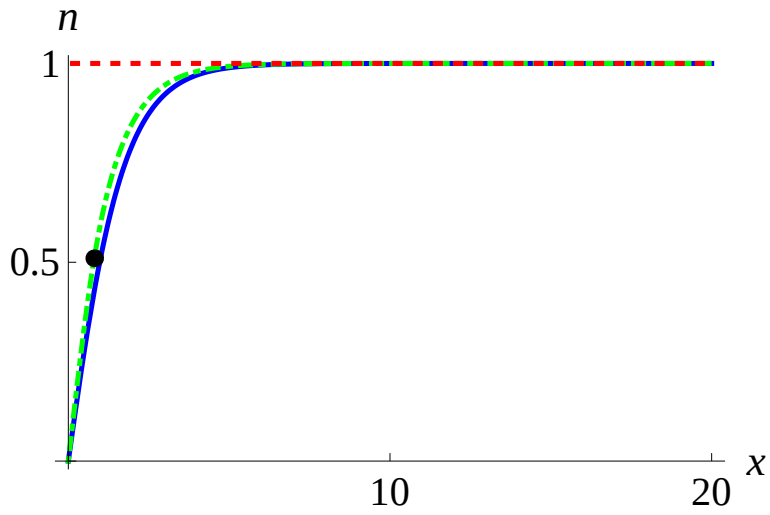

FIGURE 3.6: A comparison between exact and approximate solutions of $n(x)$ in a semi-infinite domain is shown. The solid line corresponds to the exact solution while the dashed line shows the patching solution. The black dot represents the matching point.

$$n(x << 1) = \frac{1}{2}\left[3\left(\frac{1-(2-\sqrt{3})(1-x)}{1+(2-\sqrt{3})(1-x)}\right)^2 - 1\right]$$
$$\approx \frac{x}{\sqrt{3}} \approx 0.58x \tag{3.1.46}$$

for equation (3.1.28). This solution shows a linear growth in e^{-x} when x is close to zero.

In the case of the patching method the solution for $x < \pi/4$ is given by equation (3.1.44). Again performing a Taylor expansion for x close to zero, we obtain

$$\sin(x) = x - \frac{x^3}{3!} + ... \tag{3.1.47}$$

then, keeping linear terms, equation (3.1.44) is approximated to,

$$\frac{x}{\sqrt{2}} \approx 0.71x. \tag{3.1.48}$$

This solutions show that there is some discrepancy between the exact solution and the approximate solution that has to be taken into account. The effect of this discrepancy

on the system dynamics will depend on the size of the patch. If the patch is very large (*i.e.* if its' size tends to infinity) the difference between results is negligible, while if the patch size is close to the critical patch size, the difference becomes important.

3.1.5.2 Approximations for $x >> 1$

For values of $x >> 1$, *i.e.* for values of x where e^{-x^2} becomes negligible, the solution of the exact method gives

$$n = \frac{1}{2}\left[3\left(\frac{1-(2-\sqrt{3})e^{-x}}{1+(2-\sqrt{3})e^{-x}}\right)^2 - 1\right]. \tag{3.1.49}$$

Expanding and keeping only linear terms in the exponential, the equation (3.1.49) can be simplified to give

$$n \approx \frac{1}{2}\left[\frac{3-6(2-\sqrt{3})e^{-x}-1-2(2-\sqrt{3})e^{-x}}{1+2(2-\sqrt{3})e^{-x}}\right]. \tag{3.1.50}$$

Rearranging equation (3.1.50) gives,

$$n \approx 1 - 1.072e^{-x}. \tag{3.1.51}$$

In the case of the patching approximation we have that for $x > \pi/4$

$$n \approx 1 - 1.097e^{-x}. \tag{3.1.52}$$

which is indeed, very close to the result obtained by the exact solution.

3.1.6 Organism current

Here, we study the individuals current within the system. This current measures the number of individuals moving from the resource-rich patch into the lethal region. We expect that in the interior far from the boundary the current will be approximately zero $J = 0$ since the population will be evenly distributed in these regions. As we get closer to the boundaries, the individuals leaving the resources rich patch create a gradient in the

population distribution resulting in a current of individuals that reaches its maximum $J = J_{max}$ at the boundary.

Assuming that the current is given by Fick's law and using the rescaled units, the flux is given by

$$J(x) = -\frac{dn}{dx}. \tag{3.1.53}$$

From equation (3.1.28) we have that the exact solution for the semi-infinite patch is given by

$$n = \frac{1}{2}\left[3\left(\frac{1-(2-\sqrt{3})e^{-x}}{1+(2-\sqrt{3}e^{-x})}\right)^2 - 1\right]. \tag{3.1.54}$$

The flux is given by the derivative $-\dfrac{dn}{dx}$, hence,

$$\frac{dn}{dx} = -\frac{(6e^x(7-4\sqrt{3}+(-2+\sqrt{3})e^x))}{(-2+\sqrt{3}-e^x)^3}. \tag{3.1.55}$$

In the case of the patching method, we use the matching point $\delta = \pi/4$ where the solution for n is given by equations (3.1.44) and (3.1.45). Taking the derivative $-\dfrac{dn}{dx}$ of these two equations the flux for the patching method is given by,

$$-\frac{dn}{dx} = -\frac{1}{\sqrt{2}}\cos(x) \quad \text{for } |x| < \pi/4 \tag{3.1.56}$$

and

$$-\frac{dn}{dx} = -\frac{1}{2}e^{\pi/4-x} \quad \text{for } |x| > \pi/4 \tag{3.1.57}$$

The figure 3.7 shows the flux of individuals in a semi-infinite domain for the patching and the exact methods. In both cases the figures show the absolute value of the flux in direction of the positive axes starting from the boundary. The flux shows how the population changes in space, reaching a maximum in the boundary of the patch. Observe in figure 3.7 that as $x \to \infty$ the flux goes to zero, whilst if x is very close to zero the flux increases. Notice also that, for x close to the boundary, the exact solution differ from the approximate one. Differences between exact and approximate solutions always exist, however, in the following section we investigate an alternative to reduce this difference

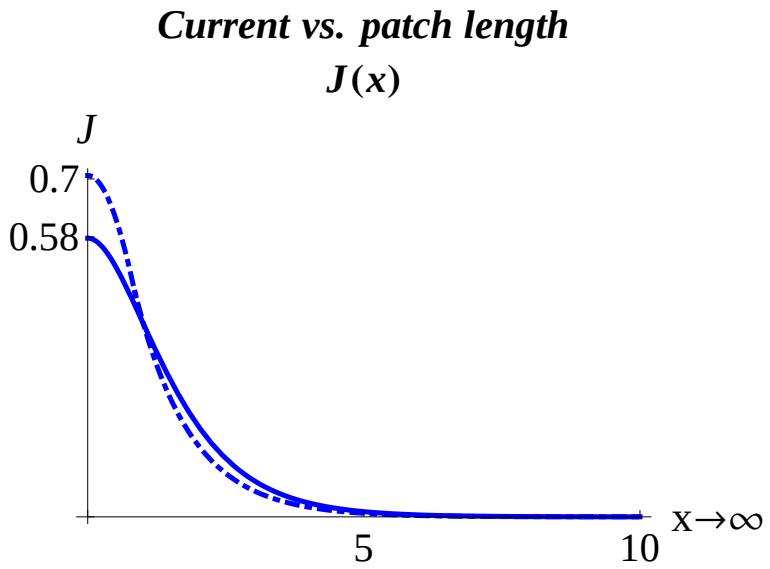

FIGURE 3.7: Flux of individuals in a semi-infinite domain. The solid line shows the exact solution while the dashed line shows the patching solution. It can be seen that for x close to the boundary there is a considerable flux. However as $x \to \infty$ the flux tends to zero.

between the solutions.

3.1.7 Different matching points

Due to the existing difference between the exact and the approximate solution, particularly in the region where $x \lesssim 1$, here we explore different patching points to see if the location of the chosen matching point affects the results obtained.

Patching point	Solution for $x << 1$	Solution for $x >> 1$
$n = 0.25$, $\delta = 0.32175$	$n \approx 0.79x$	$n \approx 1 - 0.689e^{-x}$
$n = 0.5$, $\delta = \pi/4$	$n \approx 0.71x$	$n \approx 1 - 1.097e^{-x}$
$n = 0.75$, $\delta = 1.24905$	$n \approx 0.79x$	$n \approx 1 - 1.7435e^{-x}$

TABLE 3.1: Semi-infinite domain comparison for different patching points.

Table 3.1 show the patching solution for different solution matching points, while figures 3.8 and 3.9 show the different solutions at different matching points for the population and the flux of individuals respectively compared with the exact solution.

Equations 3.1.46 and 3.1.51 provide the information of the exact solution for $x < \pi/4$,

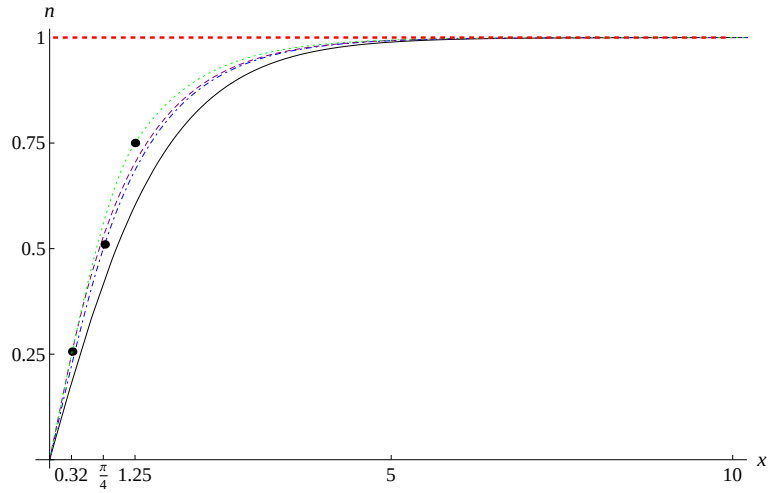

FIGURE 3.8: Comparison between exact and approximate solutions of $n(x)$ in a semi-infinite domain. The black solid line corresponds to the exact solution while the dashed lines show different patching solutions. The black dot represents the matching points at $n = 0.25$, $n = 0.5$ and $n = 0.75$.

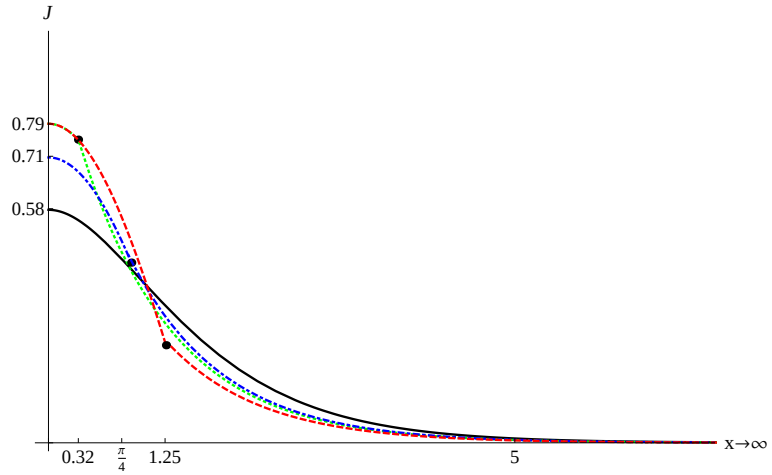

FIGURE 3.9: Comparison between exact and approximate solutions of $J(x)$ in a semi-infinite domain. The black solid line corresponds to the exact solution while the dashed lines show different patching solutions. The black dot represents the matching points at $n = 0.25$, $n = 0.5$ and $n = 0.75$.

and $x >> \pi/4$ respectively. These results compared with the results found in Table 3.1 tell us that the best approximate solution is provided by our first analysis where the patching point was located at $\delta = \pi/4$.

We notice that trying different matching points for the system analysed in this chapter does not improve our first approximation. Therefore, the solutions found in §3.1.4.2 and §3.1.6 are the ones we keep for the rest of this analysis. Even if there is some difference

between the solutions, the approximation is qualitatively similar to the exact solution within the whole domain, and for distances large enough ((*i.e.* for distances where the change of population in space is negligible), the solution is practically the same for both, the exact and the approximate solution.

The discrepancy between solutions influences the analysis of approximate solutions for domains sizes close to the critical patch size $x = \pi$, and suggests the exploration of different approximation methods in future analyses to increase the precision of the results found in this chapter.

3.1.8 Individual loss

In this section we measure the reduction of the total population in the stationary state due to the flux of individuals through the boundary.

By studying figure 3.6 we can qualitatively observe that the available space left by the population size lost due to diffusion and death, through the boundary is larger when using the exact method than when the approximate method is used. The quantitative measure of this feature of the system is important, since it gives us an idea of how important the nature of the boundary conditions and the patch length are for the preservation of individuals. Mathematically speaking, the size of the population lost $\mathcal{L}$ due to the presence of the boundary is given by

$$\mathcal{L} = \int_0^\infty (1 - n)dx. \tag{3.1.58}$$

where $n = 1$ would represent a completely filled homogeneous patch and n is the density of individuals in the patch.

In the case of the exact solution, we have that, according to equation (3.1.21), the change of population in space is given by

$$\frac{dn}{dx} = \frac{1}{\sqrt{3}}\sqrt{(1-n)^2(2n+1)}, \tag{3.1.59}$$

therefore,

$$\int_0^1 (1-n)\frac{dn}{dn/dx} = \int_0^1 \frac{\sqrt{3}dn}{(2n+1)^{1/2}}. \tag{3.1.60}$$

Assuming that $u = 2n + 1$, equation (3.1.60) can be expressed as

$$\frac{\sqrt{3}}{2}\int_1^{\sqrt{3}} \frac{du}{\sqrt{u}} = \sqrt{3u}\,\Big|_1^{\sqrt{3}} = \sqrt{3(2n+1)}\,\Big|_0^{\sqrt{1}} = \sqrt{3}(\sqrt{3}-1) \approx 1.268. \tag{3.1.61}$$

In the case of the approximate solution we have use the matching point $\delta = \pi/4$. As equation (3.1.58) has to be divided into two regions we write,

$$\int_0^\infty (1-n)dx = \int_0^{\pi/4} (1-n)dx + \int_{\pi/4}^\infty (1-n)dx. \tag{3.1.62}$$

From equations (3.1.44) and (3.1.45), the individual loss through the boundaries for the approximate solution is given by

$$\begin{aligned}\int_0^\infty (1-n)dx &= \int_0^{\pi/4}\left(1-\frac{1}{\sqrt{2}}\sin(x)dx\right) + \int_{\pi/4}^\infty \left(1-\left(1-\frac{1}{2}e^{\pi/4-x}\right)\right)dx = \\ &= \frac{1}{2}\left(1+\frac{\pi}{2}\right) + \frac{1}{\sqrt{2}}\left(\cos(\frac{\pi}{4}-1)\right) \approx 1.078.\end{aligned} \tag{3.1.63}$$

This is equivalent to the number of individuals lost divided by the carrying capacity per unit length $\left(\frac{n}{\chi}\right)$. In both cases, exact and approximate, we observe that the number of individuals lost is of the order of one correlation length scale. This can be interpreted as if the patch length was decreased in length by one correlation length because of the number of individual lost through the boundary.

Let us also observe that the loss of individuals is larger in the case of the exact solution than in the approximate solution. However, both solutions are in the same correlation length scale range.

3.1.9 Summary

Table 3.2 shows a comparison of the results obtained for the semi-infinite system using the two different methods: the exact solution method and the patching method with the matching point at $n = 0.5$, $\delta = \pi/4$.

	Exact method	Patching method
$x << 1$	$x/\sqrt{3}$	$x/\sqrt{2}$
$x >> 1$	$1 - 1.072e^{-x}$	$1 - 1.097e^{-x}$

TABLE 3.2: Semi-infinite domain comparison for the patching method and the exact method.

These results show that the comparison of the patching method with the exact method is a good approximation. These solutions do not perfectly match for patch sizes of the order of the CPS, however, both solutions describe the same type of dynamics. This comparison gives assurance on the results obtained (and to be obtained) using these types of methods. We know that an approximate solution using the patching method, for example, will not be exactly the same to an exact solution. However, we can be confident on having good approximations, that can explain accurately the dynamics of the systems analysed.

In §3.1.6 we analysed the flux of individuals in a semi-infinite patch as shown in figure (3.7). We observe that as we move away from the boundary the individual flux decreases. On the other hand, the closer we are to the boundary the higher the flux becomes. Notice also that the flux is always leaving the occupied area.

Finally, in this section, we found that the reduction of the total population close to the boundary can be summarised in terms of a loss of population, equivalent to a length of approximate one correlation, or effective patch length.

3.2 A single finite patch with absorbing boundaries

In this section we study the analytic solution for a one-dimensional, *absorbing boundaries*, single patch problem. This type of system has been widely studied through different methods and by different authors due to its relevance in the study of fragmented ecosystems.

For instance, Grindrod [33] and Murray [31] discuss this problem in terms of waves and pattern formation and Murray also discusses the construction of the problem in detail.

Okubo [5] uses reaction-diffusion models, and Kot [28] solves the linearised problem. A more mathematical approach is given by Cantrell and Cosner [8] who study features like critical patch size and population persistence by means of reaction-diffusion equations. Other authors [29, 30, 101] also study this same problem with different perspectives and goals.

The relevance of this problem lies in the fact that this system provides the basis of the analysis of fragmented ecosystems by analysing the most basic fragmented environment: a patch with plentiful resources embedded in a larger domain composed of areas of scarce-resources with decaying growth functions that depend on the spatial coordinates.

Our goal by analysing this system, is to provide a deep understanding of the basis of fragmented ecosystems by studying and re-discovering some results previously found. At the same time, we aim to add new results and interpretations of the system, in order to expand the understanding of this, and other systems analysed in this thesis. This analysis includes the study of diffusion coefficients, carrying capacity, growth rate, fluxes, and some corrections to results found by other authors. These corrections are important in the analysis of models that aim to describe more accurately biological phenomena.

Using firstly, eigenvalue equations, we perform a Fourier series expansion to the system, and finally we apply, the patching method to obtain an approximate solution. Using the results produced on this analysis, we discuss the carrying capacity of the system, the effective growth rate of the population and the current due to the diffusion of individuals outside the patch.

3.2.1 Model

In §3.1 we studied a single semi-infinite patch with an absorbing boundary. In this section, the equations governing the dynamic of the systems analysed are similar, but the boundary conditions change since the patch is finite. The system under analysis here is centered at $x = L/2$, has length L, initial conditions given by

$$n(t = 0) = 0 \tag{3.2.1}$$

and boundary conditions given by,

$$n = 0 \quad \text{at } x = 0 \text{ and } x = L, \tag{3.2.2}$$

and

$$\frac{\partial n}{\partial x} = 0 \quad \text{at } x = L/2 \tag{3.2.3}$$

as shown in figure 3.10. Assuming that the population inside a finite patch with absorbing boundaries follows the dynamics given by equation (3.1.5) then,

$$\frac{\partial n}{\partial t} = n(1-n) + \frac{\partial^2 n}{\partial x^2} \quad \text{for } 0 < x < L, \tag{3.2.4}$$

in a patch of finite non-dimensional length L with plentiful resources. Outside this region we have that,

$$n = 0 \quad \text{for } x < 0 \text{ and } x > L. \tag{3.2.5}$$

Here, as in §3.1.2, n is the relative population, t is the relative time and x is the length scale. The population grows logistically and diffuses in the plentiful resources patch, while in the lethal regions the individuals die.

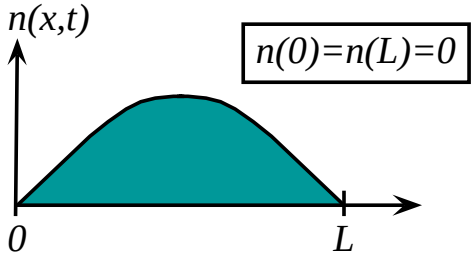

FIGURE 3.10: Population of a one-dimensional patch of length L centered at $x = L/2$ with absorbing boundaries.

3.2.2 Early time analysis

In this section we consider that at early times $n(t \approx 0)$ is close to zero. As n is small we can neglect the quadratic term of the logistic equation and linearise equation (3.2.4) to write,

$$\frac{\partial n}{\partial t} = n + \frac{\partial^2 n}{\partial x^2}, \tag{3.2.6}$$

subject to the boundary conditions $n(0) = n(L) = 0$ and $\dfrac{\partial n}{\partial x}(L/2) = 0$.

Using the method of separation of variables [39, 109] we solve equation (3.2.6). Assuming that $n(x,t) = n(x)T(t)$ we rewrite equation (3.2.6) as

$$\frac{1}{T}\frac{\partial T}{\partial t} = \frac{1}{n}\left(n + \frac{\partial^2 n}{\partial x^2}\right). \tag{3.2.7}$$

As both sides of equation (3.2.7) have to be satisfied simultaneously, then

$$\frac{\partial T}{\partial t} = \tilde{\alpha}T, \tag{3.2.8}$$

and

$$\left(n + \frac{\partial^2 n}{\partial x^2}\right) = \tilde{\alpha}n. \tag{3.2.9}$$

The solution of equation (3.2.8) is simply

$$T(t) = e^{\tilde{\alpha}t}. \tag{3.2.10}$$

and $\tilde{\alpha}$ is a constant to be found. To solve equation (3.2.9), we note that equation (3.2.9) together with the boundary conditions (3.2.2) are an eigenvalue problem.

An eigenvalue problem is a boundary value problem of the type

$$\mathcal{A}f = \lambda f \tag{3.2.11}$$

where any non-zero function that returns from the operator exactly as it is, except for the multiplicative scaling factor λ (its eigenvalue), is called the eigenfunction of the operator $\mathcal{A}$. The solution of the differential eigenvalue problem will also depend on the boundary conditions of f where each eigenvalue λ_i admits a corresponding solution for f_i when combined with the boundary conditions [108].

Notice that in equations (3.2.8) and (3.2.9) $\tilde{\alpha}$ is a constant because both equations, must be satisfied simultaneously. This happens only when $\tilde{\alpha}$ do not depend on x or on t, i.e. when $\tilde{\alpha}$ is a constant. Equation (3.2.9) then represents an eigenvalue equation where $\tilde{\alpha}$

represents the eigenvalue and $n(x)$ is the eigenfunction. This equation admits an infinite number of solutions given by an infinite sequence of eigenvalues

$$\tilde{\alpha}_1 \geq \tilde{\alpha}_2 \geq \tilde{\alpha}_3 ... \geq \tilde{\alpha}_k \geq ... \quad \text{with } \tilde{\alpha}_k \to -\infty \tag{3.2.12}$$

as $k \to \infty$ [8, 109]. From equation (3.2.12) we can see that the principal eigenvalue of equation (3.2.9) is the largest eigenvalue $\tilde{\alpha_1}$.

On the other hand, it can be shown that the eigenfunction associated to the principal eigenvalue of a function [8] can be taken to be positive inside the domain. We emphasise this particular aspect of the eigenvalue equation because this means that the solution of equation (3.2.9) represents a possible population and will grow exponentially if $\tilde{\alpha_1} > 0$ and decay exponentially if $\tilde{\alpha_1} < 0$. This problem also predicts that when $\tilde{\alpha_1} = 0$ the critical patch size is reached, as shown for instance by Grindrod [33], and Cantrell [8].

To find the solution of equation (3.2.9) we rewrite it as

$$-\kappa^2 n = \frac{\partial^2 n}{\partial x^2}, \tag{3.2.13}$$

where

$$-\kappa^2 = \tilde{\alpha} - 1. \tag{3.2.14}$$

The sign of the eigenvalue $-\kappa^2$ give us the behaviour of the solution. Given the boundary conditions (3.2.2), and (3.2.3), the only possible set of eigenvalue solutions are given by values where $-\kappa^2 > 0$. The solution of this equation is,

$$n(x) = n_0 \sin(\kappa x) + m_0 \cos(\kappa x), \tag{3.2.15}$$

where n_0 and m_0, are determined using the boundary conditions. The boundary conditions imply that $m_0 = 0$, since $n(0) = 0$ and equation (3.2.15) reduces to,

$$n(x) = n_0 \sin(\kappa x). \tag{3.2.16}$$

The boundary conditions imply that,

$$n(0) = n(L) = 0, \tag{3.2.17}$$

resulting in

$$\sin(0) = \sin(L) = 0, \tag{3.2.18}$$

that happens only when,

$$\kappa L = n\pi. \tag{3.2.19}$$

obtaining as a final solution for $n(x)$

$$n(x) = n_0 \sin\left(\frac{n\pi x}{L}\right). \tag{3.2.20}$$

Equation 3.2.20 explicitly shows how the principal eigenvalue $n\pi/L$ is the one found for the solution $n(x)$ in order to satisfy the boundary conditions.

From equations (3.2.10), and (3.2.20) the general solution of equation (3.2.6) can be written,

$$n(x,t) = \sum_{0}^{\infty} A_n \exp\left[1 - \frac{n^2\pi^2}{L^2}t\right] \sin\left(\frac{n\pi}{L}x\right). \tag{3.2.21}$$

The coefficients A_n can be obtained using the Fourier sine series as it is shown in standard literature [109, 110]. Here we restrict ourselves to show the solution of equation (3.2.21) for $n = 0, 1$ in figure 3.11 since our analysis is focused in more specific parameters ($\tilde{\alpha}$).

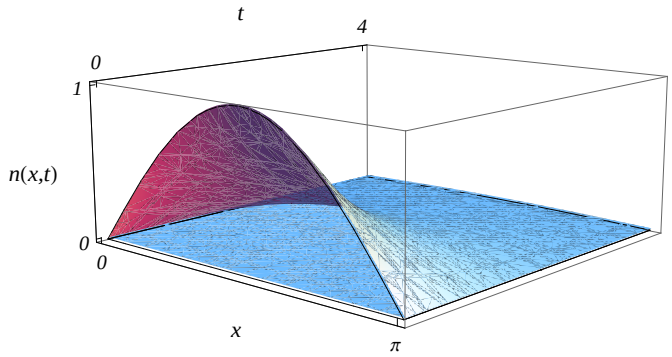

FIGURE 3.11: Population density solution of a single patch with absorbing boundaries.

Equation (3.2.9) allows us to take the maximum positive eigenvalue of the equation

to obtain the maximum effective growth rate of the population in the patch. This eigenvalue is associated with the effective population growth in a patch. Taking $\kappa L = \pi$, we substitute $1 - \tilde{\alpha} = \kappa^2$ in equation (3.2.19) to obtain,

$$\tilde{\alpha} = 1 - \frac{\pi^2}{L^2} \tag{3.2.22}$$

Equation (3.2.22) gives us a relationship between the effective growth rate and the patch size L. Notice also that the largest value that the effective population growth can take is $\tilde{\alpha} = 1$. These factors provide important information about the system dynamics that can be summarised as:

1. If $L < \pi$, $\tilde{\alpha} < 0$ and the population declines. In patches with effective patch size smaller than π the individual loss rate due to dispersal through the boundary overcomes the local growth rate inside the patch.

2. If L is fixed and bigger than π then $\tilde{\alpha} > 0$, this means that the local population growth rate is larger than the loss rate of individuals from dispersal. The population grows until it reaches the carrying capacity of the system which is directly related with the size of the patch.

3. If L grows to infinity, equation (3.2.22) reaches its maximum value $\tilde{\alpha}_{max} = 1$. This means that as we increase the size of the system, the boundary conditions become less important and the system looks more like an homogeneous system.

One key reason for studying the linearised problem analysed in this section is that this system gives predictions on the persistence of decay of a population depending on the sign of the eigenvalue $\tilde{\alpha_1}$. It also predicts that when $\tilde{\alpha_1} = 0$ the critical patch size is reached as shown for instance by Grindrod and Cantrell [8, 33].

3.2.3 Critical patch size

In this section we analyse what happens at the critical patch size, $L = \pi$. If $L = \pi$, $\tilde{\alpha} = 0$ and $\frac{\pi^2}{L^2} = 1$ gives us the *critical patch size*:

$$L = L_c = \pi \tag{3.2.23}$$

The importance of this quantity relies on the fact that it provides a measure of the minimum size required for an ecosystem to sustain a population. In terms of ecological conservation this is of great importance because it gives us an idea of how much a fragmented ecosystem can be sustainable depending on its level of fragmentation and the size of each fragment.

Although the analyses provided here are one-dimensional, and most biological systems are at least two-dimensional, one-dimensional model can provide qualitative insight of the model dynamics, other models can be used as a reference, and in other cases (like in the CPS measurement) they can be extended to two dimensional results.

The result given by equation (3.2.23) indicates that when the critical patch size is reached, the individual loss due to dispersal balances the local population growth rate resulting in an effective growth rate of $\tilde{\alpha} = 0$. This means that the effective increment on the number of individuals in the system is zero reaching a steady state where the change of population in time remains constant.

Figure 3.12 shows the behaviour of $\tilde{\alpha}$ against L. It can be seen from figure 3.12 that $\tilde{\alpha}$ approximates 1 when L tends to infinity. It also shows that $\tilde{\alpha} = 0$ when $L = \pi$ and becomes negative when $L < \pi$.

The concept of critical patch sizes for heterogeneous systems have been studied before. Many of the results given in this whole section can also be found in books such as those written by Murray [31], Kot [28], Cantrell and Cosner [8] and Okubo [5]. The original paper where the critical patch size was studied for the first time was written by Kierstead and Slobodkin [4]. All these authors find a critical patch size for the one-dimensional linearised system given by equation (3.2.23).

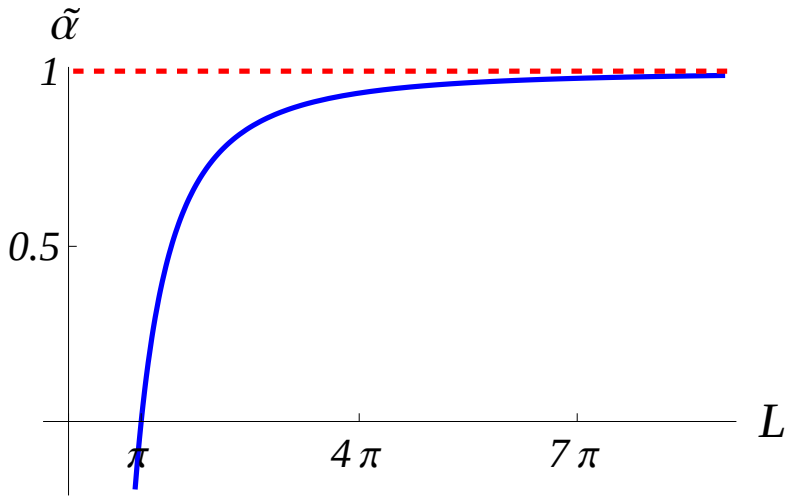

FIGURE 3.12: Effective growth rate $\tilde{\alpha}$ against effective patch size. Notice that $\tilde{\alpha}$ is negative for effective patch sizes smaller that π, zero for effective patch size equal to π and positive for effective patch sizes larger than π. The maximum value of $\tilde{\alpha}$ is one.

The measurement and understanding of relevant biological quantities is the main purpose of this thesis. Therefore, the study of all these fragmented systems is focused on finding relations and links of known and unknown results to biological parameters and features of these type of systems. For example, in this chapter we emphasize the relevance of what we call the *effective growth rate* and its relation with the *critical patch size* and the *diffusion length scale* or *correlation length* which becomes important in the study of other systems.

3.2.4 Stationary state analyses for a patch with absorbing boundaries

In this section we analyse the stationary state of a system constituted by a single one-dimensional patch with absorbing boundaries and surrounded by lethal regions. The dynamics of the problem are provided by equations (3.2.2) – (3.2.5) while its stationary state is given by

$$n(1-n)+\frac{\partial^2 n}{\partial x^2}=0 \quad \text{for } 0<x<L, \tag{3.2.24}$$

$$n=0 \quad \text{for } x<0 \text{ and } x>L, \tag{3.2.25}$$

The boundary conditions are again specified by

$$n = 0 \quad \text{at } x = 0 \text{ and } x = L, \tag{3.2.26}$$

and

$$\frac{\partial n}{\partial x} = 0 \quad \text{at } x = L/2 \tag{3.2.27}$$

3.2.4.1 Patch limit close to the CPS

In this section we examine the problem of the stationary state of a single patch of size close to π (the CPS) with absorbing boundaries in terms of Fourier series approximations.

Applying equation (3.2.17) to equation (3.1.13) in its stationary state we obtain a solution for the linearised system given by

$$n(x) = n_0 \sin\left(\frac{\pi x}{L}\right). \tag{3.2.28}$$

in the domain $[0, L]$, for L close to π. The objective now is to obtain the value of n_0 by finding the Fourier series approximation to the solution of this equation and obtain a general solution for the problem. Taking equation (3.2.28) and substituting it in the stationary state equation (3.2.24), we get

$$0 = n_0 \sin\left(\frac{\pi x}{L}\right) - n_0^2 \sin^2\left(\frac{\pi x}{L}\right) - n_0 \frac{\pi^2}{L^2} \sin\left(\frac{\pi x}{L}\right), \quad \text{for } 0 < x < L, \tag{3.2.29}$$

and $n = 0$ elsewhere. Now we expand the quadratic term in the Fourier series to find the value of n_0 in terms of the patch length. Thus,

$$\sin^2\left(\frac{\pi x}{L}\right) = \sum_{\ell} A_\ell \sin\left(\frac{\pi x \ell}{L}\right) + B_m \cos\left(\frac{\pi r m}{L}\right). \tag{3.2.30}$$

Now we have to find the values of the coefficients A_ℓ and B_m. The formula to find these coefficients is,

$$A_\ell = \frac{2}{L} \int_0^L f(x) \sin\left(\frac{\ell \pi x}{L}\right) \quad \text{for } \ell = 1, 2, 3... \tag{3.2.31}$$

and

$$B_m = \frac{2}{L}\int_0^L f(x)\cos\left(\frac{m\pi x}{L}\right) \quad \text{for } m = 0, 1, 2... \tag{3.2.32}$$

Fortunately, the function we are dealing with ($\sin^2(x)$) has the following properties which simplify the calculations,

$$B_m = \frac{2}{L}\int_0^L \sin^2\left(\frac{m\pi x}{L}\right)\cos\left(\frac{m\pi x}{L}\right) = 0, \tag{3.2.33}$$

due to orthogonality between the functions [109, 110].

$A_0 = 0$ by definition. Therefore, we find A_1 as a first approximation.

$$A_1 = \frac{2}{L}\int_0^L \sin^2\left(\frac{\pi x}{L}\right)\sin\left(\frac{\pi x}{L}\right) = \frac{2}{L}\int_0^L \sin^3\left(\frac{\pi x}{L}\right) \tag{3.2.34}$$

Making the change of variable $\theta = \dfrac{\pi x}{L}$ and $u = \cos(\theta)$, this integral becomes

$$A_1 = \frac{2}{\pi}\int_0^\pi \sin^3\left(\frac{\pi x}{L}\right) = \frac{2}{\pi}\int_0^\pi \frac{(1-u^2)\sin(\theta)du}{-sin(\theta)}. \tag{3.2.35}$$

that has the solution

$$A_1 = \frac{8}{3\pi}. \tag{3.2.36}$$

It is possible to derive the rest of the coefficients, however we are only interested in the first terms as these have the largest effect on the system dynamics. With this result equation (3.2.29) develops into,

$$0 = n_0\sin\left(\frac{\pi x}{L}\right) - \frac{8}{3\pi}n_0^2\sin\left(\frac{\pi x}{L}\right) - \frac{\pi^2}{L^2}n_0\sin\left(\frac{\pi x}{L}\right), \tag{3.2.37}$$

dividing by $n_0\sin(\frac{\pi x}{L})$ equation (3.2.37) reduces to

$$0 = 1 - \frac{8}{3\pi}n_0 - \frac{\pi^2}{L^2}. \tag{3.2.38}$$

Rearranging terms in equation (3.2.38)we obtain

$$n_0 = \frac{3\pi}{8}\left(1 - \frac{\pi^2}{L^2}\right). \tag{3.2.39}$$

From eqn. (3.2.39) is clear to see that n_0 is positive only when $L > L_c = \pi$. The equilibrium solution for this system is then

$$n = n_0 \sin\left(\frac{\pi x}{L}\right) = \frac{3\pi}{8}\left(1 - \frac{\pi^2}{L^2}\right)\sin\left(\frac{\pi x}{L}\right). \tag{3.2.40}$$

This equation describes the stationary state of a population reproducing on a one-dimensional patch of length L larger than, but close to π. This approximation is valid only for patch lengths close to the critical patch size where the steady-state solution keeps its sinusoidal form. For larger patch lengths, the solution given by equation (3.2.40) changes loosing its sinusoidal form. To analyse systems of larger size we use the patching method used in §3.1.4.

In Figure 3.13 we observe that the total population n is larger than zero when $L > L_c$. For $L \approx L_c$ the steady state of the population n presents a population close to zero, but still positive. As the patch length is increased, the total population in stationary state increases.

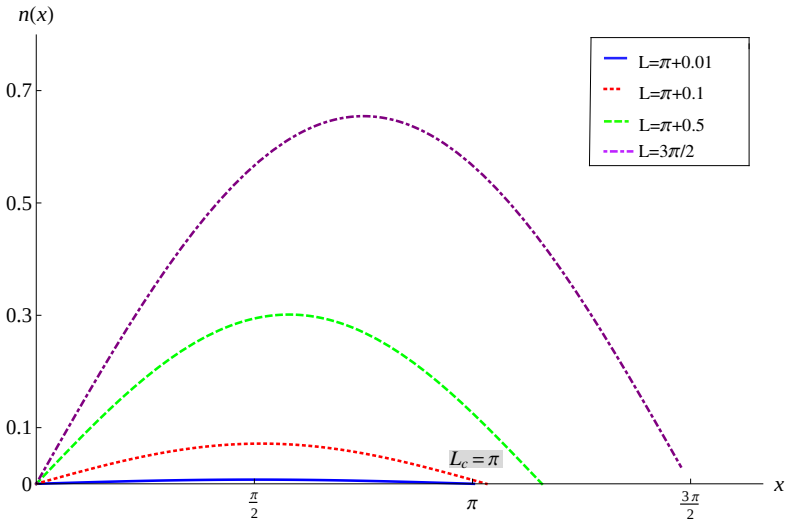

FIGURE 3.13: Stationary state for the population density given by $n = n_0 \sin(\pi x/L)$ against the patch length L. Notice that the patch length L must be larger than the critical patch size $L_c = \pi$ in order to obtain a positive stationary state.

3.2.5 Limit for patches much larger than the CPS

In this section we analyse a finite one-dimensional single patch of length L with absorbing boundaries. The problem is analysed for the stationary state of the system. The patch is considered to be centered at $x = 0$ and is solved using the patching method. Here we assume that the patch length is large $L >> 1$, but not infinite. Therefore, suitable boundary conditions for the system are $n(x = 0) \approx 1$ and $n(x = |L/2|) = 0$.

Assuming that the system is in a stationary state ($\frac{\partial n}{\partial t} = 0$), we divide the patch into two regions A and B as shown in figure (3.14). In region A we suppose that the total

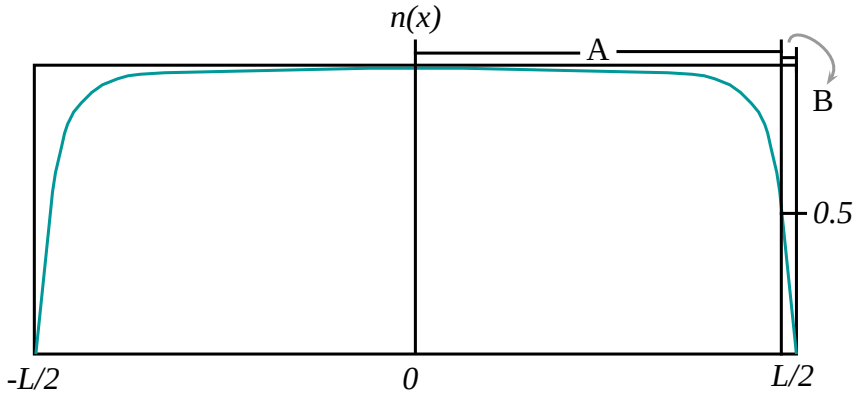

FIGURE 3.14: One-dimensional system with absorbing boundaries in which $n \approx 1$ in the center while $n = 0$ at the boundary.

population is close to one, hence

$$n = 1 - m \tag{3.2.41}$$

with $m << 1$. In particular we assume that $n \geq 0.5$ in region A. In region B we assume that $n < 0.5$. If the whole system has a solution, the solutions of regions A and B match at some point which will be found in the following sections.

3.2.5.1 Solution for region *A*

Assuming that in region A, $n = 1 - m$ and $(n > 0.5)$, equation (3.1.13), can be rewritten as

$$(1 - m)(1 - (1 - m)) + \frac{d^2(1 - n)}{dx^2} = 0, \tag{3.2.42}$$

which can be linearised and rearranged to obtain

$$m = \frac{d^2m}{dx^2}. \tag{3.2.43}$$

The general solution of this equation is

$$m = m_0 \cosh(x). \tag{3.2.44}$$

Therefore, in region A the solution for the population dependent on the length of the patch is

$$n = 1 - m_0 \cosh(x). \tag{3.2.45}$$

3.2.5.2 Solution for region *B*

In region B we assume that $n < 0.5$, therefore, equation (3.1.13) is reduced to

$$n \cdot (1 - n) + \frac{\partial^2(n)}{\partial x^2} = 0, \tag{3.2.46}$$

which can be linearised to obtain

$$n = -\frac{d^2n}{dx^2}. \tag{3.2.47}$$

to obtain the general solution

$$n = n_0 \sin(L/2 - x). \tag{3.2.48}$$

3.2.5.3 Solution Matching

To find the values of m_0, n_0 we apply the boundary conditions assuming that the solution as well as its derivative are continuous. Then we match the solutions at the point $L/2-\delta_1$ where the population value is assumed to be $n = 1/2$. Therefore,

$$n = 1 - m_0 \cosh(L/2 - \delta_1) = 1/2, \tag{3.2.49}$$

and

$$n = n_0 \sin(\delta_1) = 1/2. \tag{3.2.50}$$

Since we assume that the solution and its derivative are continuous, we obtain for the derivative,

$$n_0 \cos(\delta_1) = m_0 \sinh(L/2 - \delta_1). \tag{3.2.51}$$

From equations (3.2.49),(3.2.50) and (3.2.51) the values of m_0, n_0 and δ_1 are found. Equating equations (3.2.49), (3.2.50) and dividing them by equation (3.2.50)we obtain,

$$\cot(\delta_1) = \tanh(L/2 - \delta_1), \tag{3.2.52}$$

that is an equation dependent only on δ_1. However, this is a *transcendental equation* which cannot be expressed in terms of a finite sequence of algebraic operations, hence we approximate it by assuming that $L >> 1$. In the case of the semi-infinite domain the value of δ given by equation (3.1.41) was $\delta = \pi/4$. In this case we assume that δ_1 is slightly larger than $\pi/4$ due to the finiteness of the domain. Hence,

$$\delta_1 = \frac{\pi}{4} + \beta, \tag{3.2.53}$$

applying trigonometric identities to equation (3.2.52), we obtain

$$\tanh(L/2 - \delta_1) = \frac{1 - e^{-(2(L/2-\delta_1))}}{1 + e^{-(2(L/2-\delta_1))}}, \tag{3.2.54}$$

and

$$\cot(\delta_1) = \frac{1 - \tan(\beta)}{1 + \tan(\beta)}, \tag{3.2.55}$$

these solutions imply that,

$$\tan(\beta) = e^{-2(L/2-\pi/4)} e^{2\beta}. \tag{3.2.56}$$

This equation now can be expanded in Taylor series close to the point $x = \beta$, to obtain

$$\beta = e^{-2(L/2-\pi/4)}(1 + 2\beta), \tag{3.2.57}$$

equivalent to

$$\beta = \frac{e^{-(L-\pi/2)}}{1-2e^{-(L-\pi/2)}}. \tag{3.2.58}$$

Equation (3.2.58) gives us the explicit solution to δ_1 written as,

$$\delta_1 = \frac{\pi}{4} + \frac{e^{-(L-\pi/2)}}{1-2e^{-(L-\pi/2)}}. \tag{3.2.59}$$

From equation (3.2.59) we can conclude that for relatively small patches (*i.e.* for patches closer to the CPS) the size of δ_1 increases, while as the patch size tends to infinity, we recover the semi-infinite result for δ *i.e.* $\delta_1 = \pi/4$. The explicit form of (3.2.59) allows us to obtain the values of m_0 and n_0. Using equations (3.2.49), (3.2.50), (3.2.51) and (3.2.59) we find m_0 and n_0,

$$m_0 = \frac{-\cos(\delta_1)}{-\cos(\delta_1)\cosh(\delta_1 - L/2) + \sin(\delta_1)\sinh(\delta_1 - L/2)} \tag{3.2.60}$$

and

$$n_0 = \frac{\sinh(\delta_1 - L/2)}{-\cos(\delta_1)\cosh(\delta_1 - L/2) + \sin(\delta_1)\sinh(\delta_1 - L/2)}. \tag{3.2.61}$$

m_0, n_0 and δ_1 are substituted in the general solutions given by equations (3.2.45) and (3.2.48) to obtain the general system solution given by

$$n = 1 - m_0\cosh(x), \quad \text{if } x \in [-L/2 + \delta_1, L/2 - \delta_1] \tag{3.2.62a}$$

$$n = n_0\sin(L/2 - x), \quad \text{if } x \in [-L/2, -L/2 + \delta_1] \wedge [L/2 - \delta_1, \leq L/2] \tag{3.2.62b}$$

shown in figure (3.15)

3.2.6 Carrying Capacity

Equations (3.2.40), (3.2.62a) and (3.2.62b) provide a solution for $n(x)$ in patches with domain sizes of the order of the CPS and larger. Making use of these results, here we obtain the solution for the carrying capacity in patch systems with lengths of sizes $L \geq L_c$. The carrying capacity can be thought as the total population that a patch can sustain and it is obtained by integrating $n(x)$ over the patch domain $[0, L]$. To obtain

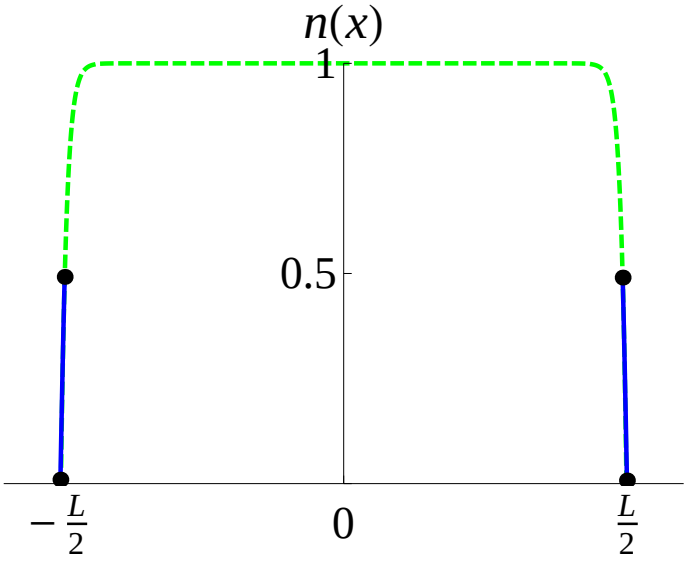

FIGURE 3.15: Solution for a single patch of size $L >> \pi$ with absorbing boundaries. A solution is found for each region A and B, and matched at the points $L/2 - \delta$ and $-L/2 + \delta$.

the carrying capacity dependent on the patch length, for any patch length L, we obtain a solution for patches with size of the CPS order and patches with sizes much larger than the CPS separately. Then we join both solutions and obtain the total carrying capacity Γ.

3.2.6.1 Carrying capacity for $L \approx L_c$

For patch domains of length $L \approx L_c$ the total carrying capacity Γ is given by the integral of $n(x)$ along the one-dimensional domain $[0, L]$ with $L \geq L_c$. The value of $n(x)$ for domains of length close to the critical patch size was found in §3.2.4.1 and it is given by

$$n(x) = \frac{3\pi}{8}\left(1 - \frac{\pi^2}{L^2}\right)\sin\left(\frac{\pi x}{L}\right). \tag{3.2.63}$$

Then, the carrying capacity Γ for a domain of size L is

$$\Gamma = \int_0^L n(x)dx = \int_0^L \frac{3\pi}{8}\left(1 - \frac{\pi^2}{L^2}\right)\cos\left(\frac{\pi x}{L}\right)dx = \frac{3(L^2 - \pi^2)}{4L} \tag{3.2.64}$$

3.2.6.2 Carrying capacity for $L >> L_c$

To find the total carrying capacity per unit length in patches of sizes $L >> L_c$ we use the patching approximation. The carrying capacity of the system corresponds to the integral of the population n over the domain $[-L/2, L/2]$. In this case, the integral over the whole domain is split in two regions corresponding to the solutions of each region. From equations (3.2.62a) and (3.2.62b) the total population integral in space is given by

$$\Gamma = \int_{-L/2}^{L/2} n(x)dx = 2\int_{0}^{\delta_1} n_0 \sin(x) + \int_{-L/2+\delta_1}^{L/2-\delta_1} (1 - m_0 \cosh(x)) \tag{3.2.65}$$

This system is solved changing the origin of the system to $x = -L/2$. We also consider that the solution of the population distribution over x is symmetric. Therefore the integral from $-L/2$ to $-L/2 + \delta_1$ is equal to the integral from $L/2 - \delta_1$ to $L/2$. Using the values of m_0, n_0, and δ_1 found in §3.2.5.3 the carrying capacity for a domain of length $L >> L_c$ is given by

$$\Gamma = 2n_0 \int_{0}^{\delta_1} \sin(x)dx + \int_{-L/2+\delta_1}^{L/2-\delta_1} 1 - m_0 \cosh(x)dx. \tag{3.2.66}$$

The solution of this integral is

$$\Gamma = -2n_0(\cos(\delta_1) - 1) + L - 2m_0 \sinh(L/2 - \delta_1). \tag{3.2.67}$$

Substituting the values of m_0, n_0 and δ_1 this is rewritten as

$$\begin{aligned}\Gamma = {} & \frac{-2\sinh(\delta_1 - L/2)}{\sin(\delta_1)\sinh(\delta_1 - L/2) - \cos(\delta_1)\cosh(\delta_1 - L/2)}(\cos(\delta_1 - 1)) + L + \\ & + \frac{2\cos(\delta_1)}{\sin(\delta_1)\sinh(\delta_1 - L/2) - \cos(\delta_1)\cosh(\delta_1 - L/2)}(\sinh(L/2 - \delta_1))\end{aligned} \tag{3.2.68}$$

In the case where $L >> L_c$, the carrying capacity depends only on the length of the patch and it grows linearly with it.

3.2.6.3 Total carrying capacity

Figure 3.16 shows the dependence of the carrying capacity per unit length on the patch size. Notice that for $L \leq L_c$ the carrying capacity per unit length is zero, then it grows linearly for $L >> L_c$.

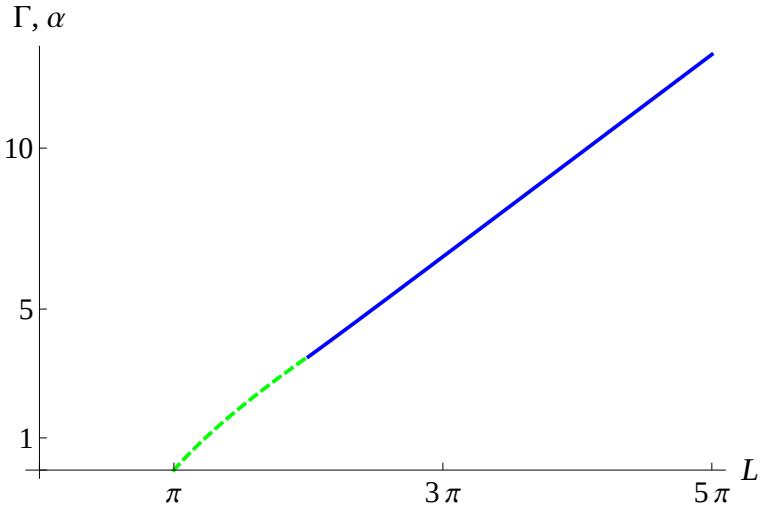

FIGURE 3.16: Carrying capacity Γ dependence on the patch length L.

This result is also compared with the results found on §3.2.3 as shown in figure 3.17. Here we compare the effective carrying capacity per unit length Γ/L with the growth rate $\tilde{\alpha}$ in terms of patch length. The results indicate that the effective growth rate is a monotonically increasing function starting with negative values for $L < \pi$ where the population always decline and therefore the carrying capacity of the patch is zero. At $L = \pi$ the effective growth rate is zero as well as the carrying capacity and the critical patch size is obtained. For $L > \pi$ the effective growth rate $\tilde{\alpha}$ as well as the effective carrying capacity Γ/L start increasing. Both quantities $\tilde{\alpha}$ and Γ/L tend to one as the patch size increases as it would be expected for an homogeneous environment. This indicates that the larger the patch, the less influence the absorbing boundaries have on the population dynamics. Notice that both quantities reach the value 1 only when the system becomes homogeneous.

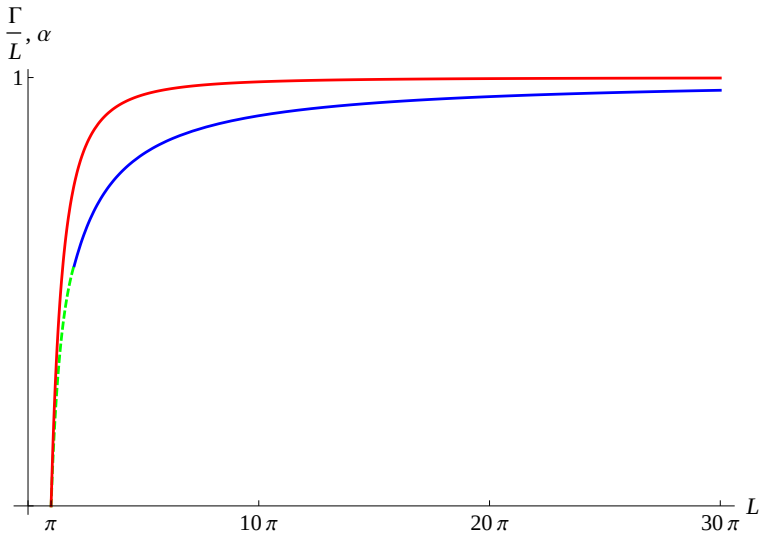

FIGURE 3.17: Comparison of the effective carrying capacity Γ/L and the effective growth rate $\tilde{\alpha}$ against the patch length L.

3.2.7 Current

In this final section we study the outflow of individuals from an absorbing one- dimensional domain patch towards the lethal regions that surrounds it. This current is produced by individual diffusion inside the patch. We expect that the largest current occurs close to the boundary and becomes smaller as we move away from the patch due to the individuals dying outside it.

3.2.7.1 Current for a patch of size $L \approx L_c$

When L is slightly larger than the critical patch size the population distribution is given by equation (3.2.40). The current can be found from this equation given that

$$J(x) = -\frac{dn}{dx}. \tag{3.2.69}$$

in non-dimensional units. As $n(x) = \frac{3\pi}{8}\left(1 - \frac{\pi^2}{L^2}\right)\sin\left(\frac{\pi x}{L}\right)$, the current is

$$J(x) = -\frac{dn}{dx} = -\frac{3\pi}{8}\left(1 - \frac{\pi^2}{L^2}\right)\cos\left(\frac{\pi x}{L}\right) \tag{3.2.70}$$

as shown in figure 3.18. Here it is shown how the current behaves with respect to the population. The solid line represents the population density with respect to the length, while the dashed line shows the current with respect to the patch length. In this figure the patch is centered at $x = 0$ and has a length $L = \pi + 1$. At $x = 0$ the population is maximum and the current is practically zero. As we approach the boundary the current grows and it reaches a maximum exactly at the boundary $x = L/2$.

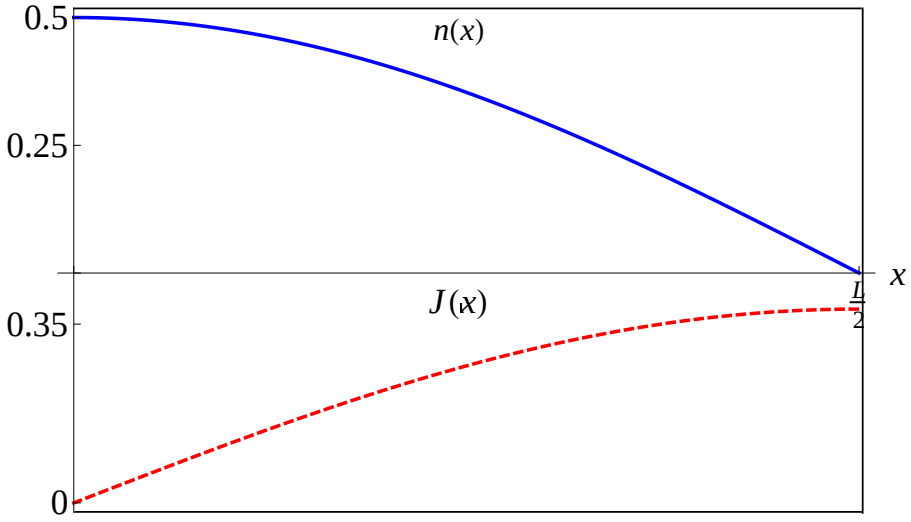

FIGURE 3.18: Comparison between the population population distribution and the current dependent on the patch length. The patch size for this system is $L \approx L_c$.

3.2.7.2 Current for a patch with $L >> L_c$

Figure 3.19 shows the current for $L >> L_c$. As previously in this section the patch is centered at $x = 0$. We observe that along most of the patch length the current is zero, however, as soon as we get close to the boundary it increases abruptly reaching a maximum at the boundary due to the absorbing boundary condition.

3.2.8 Current comparison for differently sized patches

In figure 3.20 three different currents are compared. A current for a domain of size $L \approx L_c$, another for a domain of size $L >> L_c$ and the current for a semi-infinite patch. The figure shows that the larger the patch, the larger the current is. We also found that, the current for a patch with size much larger than L_c is practically the same than

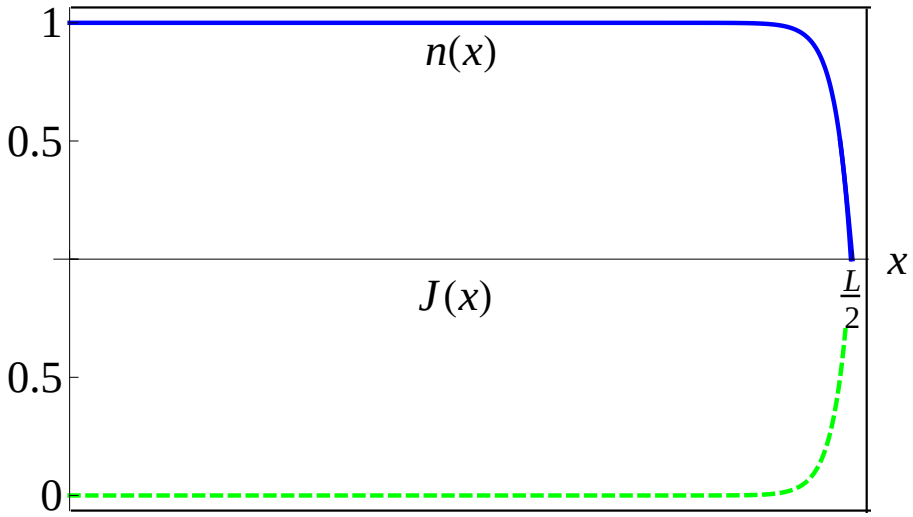

FIGURE 3.19: Population density and current with respect to the patch length. The current in this figure is evaluated for a patch of size $L >> L_c$.

the current found for a semi-infinite patch since the population distribution is similar in both cases. When the patch size tends to infinity, the population is almost homogeneous along the patch. This gives a population distribution close to $n = 1$ almost everywhere, except very close to the boundaries.

Notice also that, although quantitatively the currents for patches of sizes of the order of the CPS and patches of sizes where $L \to \infty$ are different; quantitatively the currents are similar close to the boundary since both have the same sinusoidal form. In all the cases, the current reaches its maximum value at the boundary and it decays with the distance as we move away from the patch boundary, into the patch. This is due to the population diffusion close to the boundary, where the gradient of the population respect to the space coordinate is the largest.

When studying systems of many patches the measure of currents is crucial to determine the sustainability of a system. If the current of individuals is such that they can manage to cross poor resources regions between patches of good habitat, then, the chances for these individuals to establish sustainable reproducing populations in new patches increase. More detailed studies of currents and patches systems are introduced in Chapters 4 and 5 where the ability of crossing a gap between two patches is studied.

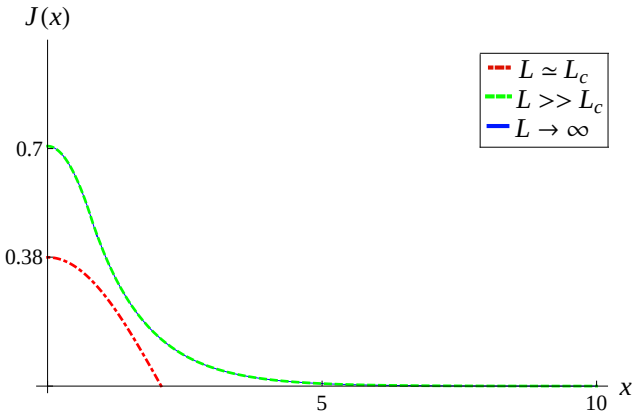

FIGURE 3.20: Comparison of the current for three different patch sizes. If the patch size is of the critical patch size L_c order, the current is small with respect to the current in patch of sizes where $L >> L_c$. If the patch size is much larger than the critical patch size, but still finite, the current found is comparable with the current found for a semi infinite patch.

3.3 A single finite patch with permeable boundaries

In this final section we analyse one-dimensional patch systems with *permeable boundaries*. In theoretical physics and earth science fields, the term *permeable* can usually be related to a flow of matter through a surface [111]. In this sense, we define as a permeable boundary a boundary that allows a flux of individuals through it while keeping the population at the boundary positive.

The idea behind the modelling of a single patch with permeable boundaries, is to think of a resource-rich patch habitat where individuals reproduce and live, surrounded by scarce-resources regions where populations decay, as shown schematically in figure 3.21. In contrast with the systems analysed previously, these systems allow a flow of individuals into the dangerous areas, where the individuals can diffuse and wander around, but always decay and die over time. The probability of death for individuals outside the patch, will depend on different causes such as the time spent in the scarce-resources areas, the distance they travel outside the patch, the level of danger outside the patch, and their resistance to the environment hostility.

The number of individuals that move out of the patch can be characterized by a flux or current which will have a diffusion constant dependent on the hostility of the patch surroundings and the individual resistance to adverse conditions. This diffusion constant

outside the patch, will have a different value from the one inside it.

If we assume that individuals cannot differentiate between different types of habitat, they will diffuse over different types of regions indistinctively, without seeking areas advantageous for them. In this section, we assume that the individuals diffuse in this way. This assumption does not apply very well for populations highly dependent on the spatial availability of resources, but it can model some type of populations. For example, many semi-aquatic species depend on both, aquatic and terrestrial habitats to maintain viable populations [112]. Another type of example, covers some terrestrial migrating species such as elephants, that, even though they do seek for environments with plentiful resources for the herd sustain, they can travel very long distances across different type of environments to reach a suitable habitat [113, 114].

Here, we use these type of analysis as a step-stone model to analyse species highly dependent on their environment.

3.3.1 Model

Let us consider the problem of a one-dimensional patch of length d where the population reproduces and live in the patch but decreases with distance from the boundary.

Taking the model described by equations (3.1.1) – (3.1.4) we write down a conservation equation for $n(x,t)$, where the probability density per unit area of finding an organism in the surroundings of the point x takes the form

$$\frac{\partial n}{\partial t} + \nabla \cdot \mathbf{J} = f(n,x) \tag{3.3.1}$$

where t is the time, n is the population per unit length, $\mathbf{J}$ is the probability flux of individuals and f is the population growth or decay function; Here, the growth function in the resource-rich regions $[-L/2, L/2]$ is modelled by a standard term used in literature [2, 28, 115, 116]: the logistic function. Outside, in the resource scarce regions $[-L/2, L/2]^{\complement}$, a linear decay rate is introduced. For the analysis of equations in this section, we locate the origin of the resource-rich patch at $x = -L/2$ in order to make it

symmetric from the x-axis origin and simplify the calculations. Then,

$$f(n,x,t) = \begin{cases} \alpha(x,n(x)\left(1-\dfrac{n(x)}{\chi(x)}\right) & \text{in } [-L/2,L/2] \\ -\alpha'(x)n(x) & \text{in } [-L/2,L/2]^{\complement} \end{cases} \tag{3.3.2}$$

where, $\chi(x)$ represents the carrying capacity, $\alpha(x)$ is the rate of population growth and $\alpha^{'}(x)$ the decay rate.

From equation (3.3.1) $\mathbf{J}$ is the flux of organisms modelled by a diffusive term of the form,

$$\mathbf{J} = -\mathcal{D}(\mathbf{x})\nabla n \tag{3.3.3}$$

where $\mathcal{D}(\mathbf{x})$ represents Fickian diffusion and its value depends on the location of the individuals, *i.e.* on the type of environment. This term provides a measure of the individuals diffusivity around their environment. Here, we consider that $\mathcal{D}(x)$ is a constant in each region, such that

$$\mathcal{D}(x) = \begin{cases} D & \text{in } [-L/2,L/2] \\ D' & \text{in } [-L/2,L/2]^{\complement} \end{cases} \tag{3.3.4}$$

With these considerations the time dependent problem over the whole x-axis can be written as

$$\frac{\partial n}{\partial t} = \alpha n\left(1-\frac{n}{\chi}\right) + D\frac{\partial^2 n}{\partial x^2} \quad \text{in } [-L/2,L/2], \tag{3.3.5a}$$

$$\frac{\partial n}{\partial t} = -\alpha' n + D'\frac{\partial^2 n}{\partial x^2} \quad \text{in } [-L/2,L/2]^{\complement}.. \tag{3.3.5b}$$

If we assume that both, the population and its derivative are continuous at the boundary, then, the boundary conditions are defined as,

$$n|_{-L/2^+} = n|_{-L/2^-} \quad \text{and } n|_{L/2^-} = n|_{L/2^+}, \tag{3.3.6}$$

for the population, and

$$D\frac{\partial n}{\partial x}\bigg|_{-L/2^+} = D'\frac{\partial n}{\partial x}\bigg|_{-L/2^-} \quad \text{and} \quad D\frac{\partial n}{\partial x}\bigg|_{L/2^-} = D'\frac{\partial n}{\partial x}\bigg|_{L/2^+}. \tag{3.3.7}$$

for the current.

Inside the patch the system dynamics is given by equation (3.3.5a) introduced in §3.1.1 for the non-leaking patch. Outside the patch the dynamics is given by equation (3.3.5b). The negative sign of α' represents a death population rate and D' represents the diffusion constant outside the patch. The population at $t = 0$ is $n = n_0(x)$ which sets our initial conditions, while the boundary conditions that the system has to satisfy as $x \to \pm\infty$ are that $n = 0$ as well.

The model system is shown schematically in figure 3.21 .

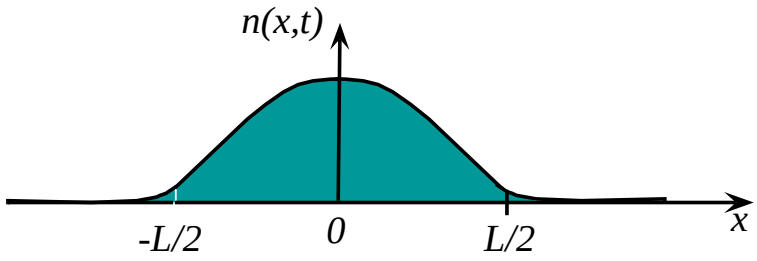

FIGURE 3.21: One-dimensional patch of length L centered at $x = 0$ with permeable boundaries. Inside the patch the population breed normally while outside the patch it decreases exponentially.

3.3.2 Non-dimensionalisation

Using an analogous procedure to the one used in §3.1.2 the terms of equation (3.3.5b) are written in non-dimensional units. The terms of equation (3.3.5a) keep the form obtained in §3.1.2, using the parameters

$$t^* = \alpha t, \quad n^* = \frac{n}{\chi}, \quad x^* = \frac{x}{\xi}, \quad L^* = \frac{L}{\xi} \tag{3.3.8}$$

whereas outside the patch the following parameters are defined:

$$s = \frac{\alpha'}{\alpha} \tag{3.3.9}$$

and

$$\lambda = \sqrt{\frac{D'\alpha}{D\alpha'}}. \tag{3.3.10}$$

D' and α' denote the diffusion constant and the decay rate in the resource-scarce regions. Taking these considerations, the system takes the form,

$$\frac{\partial n^*}{\partial t^*} = n^*(1-n^*) + \frac{\partial^2 n^*}{\partial x^{*2}} \quad \text{in } [-L^*/2, L^*/2] \tag{3.3.11a}$$

$$\frac{\partial n^*}{\partial t^*} = -sn^* + s\lambda^2 \frac{\partial^2 n^*}{\partial x^{*2}} \quad \text{in } [-L^*/2, L^*/2]^{\complement}. \tag{3.3.11b}$$

while its boundary conditions become,

$$n^*|_{-L^*/2^+} = n^*|_{-L^*/2^-} \quad \text{and } n^*|_{L^*/2^-} = n^*|_{L^*/2^+}, \tag{3.3.12a}$$

$$\left.\frac{\partial n^*}{\partial x^*}\right|_{-L^*/2^+} = s\lambda^2 \left.\frac{\partial n^*}{\partial x^*}\right|_{-L^*/2^-} \quad \text{and } \left.\frac{\partial n^*}{\partial x^*}\right|_{L^*/2^-} = s\lambda^2 \left.\frac{\partial n^*}{\partial x^*}\right|_{L^*/2^+}. \tag{3.3.12b}$$

Dropping the starred terms in equations (3.3.11a) – (3.3.11b) the non-dimensional equations of the system become,

$$\frac{\partial n}{\partial t} = n(1-n) + \frac{\partial^2 n}{\partial x^2} \quad \text{in } [-L/2, L/2], \tag{3.3.13}$$

$$\frac{\partial n}{\partial t} = -sn + s\lambda^2 \frac{\partial^2 n}{\partial x^2} \quad \text{in } [-L/2, L/2]^{\complement}, \tag{3.3.14}$$

while the boundary conditions transform into,

$$n|_{-L/2^+} = n|_{-L/2^-} \quad \text{and } n|_{L/2^-} = n|_{L/2^+}, \tag{3.3.15}$$

for the population, and

$$\left.\frac{\partial n}{\partial x}\right|_{-L/2^+} = s\lambda^2 \left.\frac{\partial n}{\partial x}\right|_{-L/2^-} \quad \text{and } \left.\frac{\partial n}{\partial x}\right|_{L/2^-} = s\lambda^2 \left.\frac{\partial n}{\partial x}\right|_{L/2^+}. \tag{3.3.16}$$

for its current.

3.3.3 Eigenvalue problem solution

Following the same type of arguments used to construct equations the governing (3.2.13) and (3.2.14) in §3.2.2 we analyse the problem of a leaking boundary patch of length L centered at $x = 0$. In this case the solution for the leaking patch differs from the solution of the non-leaking due to the differential equation leading the population dynamics in each region, the initial conditions and the boundary conditions at $x = \pm L/2$ for the patch and the boundary conditions at $x = \pm\infty$ for the surrounding region.

Equations (3.3.11a) and (3.3.11b) are linearised to obtain the eigenvalue equations:

$$\tilde{\alpha} n = n + \frac{\partial^2 n}{\partial x^2} \quad \text{for } x \in [-L/2, L/2], \tag{3.3.17}$$

and

$$\tilde{\alpha} n = -sn + s\lambda^2 \frac{\partial^2 n}{\partial x^2} \quad \text{for } x \in [-L/2, L/2]^{\complement}, \tag{3.3.18}$$

which can be rewritten as

$$-\kappa^2 n = \frac{\partial^2 n}{\partial x^2} \quad \text{for } x \in [-L/2, L/2], \tag{3.3.19}$$

and

$$\mathrm{K}^2 n = \frac{\partial^2 n}{\partial x^2} \quad \text{for } x \in [-L/2, L/2]^{\complement}, \tag{3.3.20}$$

with

$$-\kappa^2 = (\tilde{\alpha} - 1)\,, \tag{3.3.21}$$

and

$$\mathrm{K}^2 = \left(\frac{1 + \tilde{\alpha}/s}{\lambda^2}\right). \tag{3.3.22}$$

.

The boundary conditions at $x = \pm L/2$ are given by equations (3.3.6) and (3.3.7) in non-dimensional units,

$$n|_{-L/2^+} = n|_{-L/2^-} \quad \text{and } n|_{L/2^-} = n|_{L/2^+}, \tag{3.3.23}$$

for the population, and

$$D\frac{\partial n}{\partial x}\bigg|_{-L/2^+} = D'\frac{\partial n}{\partial x}\bigg|_{-L/2^-} \quad \text{and} \quad D\frac{\partial n}{\partial x}\bigg|_{L/2^-} = D'\frac{\partial n}{\partial x}\bigg|_{L/2^+}. \tag{3.3.24}$$

for the current. The boundary conditions of the system also have to satisfy that $n = 0$ as $x \to \pm\infty$ since we assume that the population decreases in the resources-scarce region. With these boundary conditions, and the initial conditions given by $n(x, t = 0) = n_0$, the solution of equations (3.3.19) and (3.3.20) is given by

$$n(x) = n_0 \cos(\kappa x) \quad \text{for } x \in [-L/2, L/2], \tag{3.3.25}$$

and

$$n(x) = n_1 e^{-\mathrm{K}x} \quad \text{for } x \in [-L/2, L/2]^{\complement}. \tag{3.3.26}$$

As we have assumed continuity at the boundary for the population and the current, we can extract a set relations in the system that provide interesting information about the dynamics of the system. In the following section, we analyse the stationary state of equations (3.3.25) and (3.3.26) to obtain information with respect to the critical patch size and propagation velocities in these type of systems.

3.3.4 Stationary state

Recalling that the system is governed by Fickian diffusion, *i.e.*, $J = -\mathcal{D}(x)\dfrac{dn}{dx}$ the non-dimensional currents inside and outside the resource-rich regions are given by,

$$J(x) = \kappa n_0 \sin(\kappa x) \quad \text{for } x \in [-L/2, L/2], \tag{3.3.27}$$

and

$$J(x) = s\lambda^2 \mathrm{K} n_1 e^{-\mathrm{K}r} \quad \text{for } x \in [-L/2, L/2]^{\complement}. \tag{3.3.28}$$

with

$$\kappa = \sqrt{1 - \tilde{\alpha}} \tag{3.3.29}$$

and

$$\kappa = \sqrt{\left(\frac{1+\tilde{\alpha}/s}{\lambda^2}\right)}. \tag{3.3.30}$$

Matching now the solutions for the populations and the currents at the boundary $x = L/2$, we obtain,

$$n_0 \cos\left(\frac{\kappa L}{2}\right) = n_1 e^{-\kappa L/2}, \tag{3.3.31}$$

and

$$\kappa N_0 \sin\left(\frac{\kappa l}{2}\right) = s\lambda^2 \kappa N_1 e^{-\kappa L/2}. \tag{3.3.32}$$

Dividing equation (3.3.32) over equation (3.3.31) and rearranging terms we obtain

$$\tan\left(\frac{\kappa L}{2}\right) = \frac{s\lambda^2 \kappa}{\kappa}, \tag{3.3.33}$$

at the boundary. Then, in the stationary state (*i.e.* at $\tilde{\alpha} = 0$) equation (3.3.33) can be reduced to

$$\tan\left(\frac{L}{2}\right) = s\lambda. \tag{3.3.34}$$

3.3.4.1 Propagation velocities rates

The quantity $s\lambda$ can be interpreted in dimensional units as follows: From §2.8 the velocity of the wave of advance front in homogeneous environments where populations follow logistic growth is given by $v = 2\sqrt{D\alpha}$ [4, 41, 51, 117]. Then, the quantity $s\lambda$ in dimensional units is written as

$$s\lambda = \sqrt{\frac{D'\alpha'}{D\alpha}} = \frac{v_o}{v_i} \tag{3.3.35}$$

where v_o stands for the wave of advance velocity front outside the resource-rich region, and v_i stands for the wave of advance velocity front inside the resource rich region. Therefore, equation (3.3.35) can be seen as the propagation velocities ratio between the wave of advance outside the patch v_o and the propagation velocity of the wave of advance inside the patch v_i. The velocity acquired inside the patch v_i will depend on the value of the diffusion and growth rate parameters inside the patch D and α, while the propagation velocity outside the patch, depends on the value of the diffusion and

decay rates outside the patch D' and α'. This is an interesting result since it tells us how the critical patch size of the resource-rich patch depends on the effective growth and death rates, and the diffusion rates between regions. These two velocities make a huge difference on the dynamics of the system predicting completely different behaviours of the population depending on the velocities rate as it will be detailed in the following section.

3.3.4.2 Critical patch size

From equation (3.3.34) we obtain the minimum size necessary to sustain a population dependent on the velocities outside and inside the patch. This critical patch size L_c for a system of a leaking patch surrounded by dangerous regions is then given by

$$L_c = 2 \arctan\left(\frac{v_o}{v_i}\right) \tag{3.3.36}$$

which is schematically shown in figure 3.22.

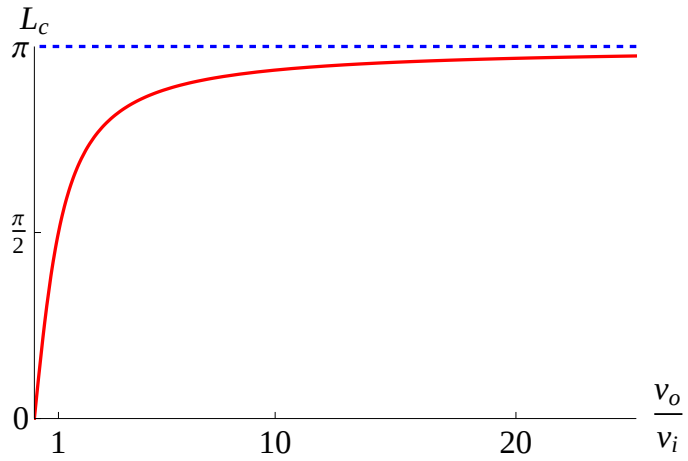

FIGURE 3.22: Critical patch size dependent on the velocity ratio $v = v_o/v_i$ in a patch with permeable boundaries.

Equation (3.3.36) tells us how the parameters D, α, D' and α' influence the system dynamics in the following way:

1. If $v_o \to 0$, then $L_c = 0$. This simply means that α' is zero and there are no deaths outside the patch. Therefore, we have an homogeneous environment and there is

no need of the critical patch size definition.

2. If $v_o = v_i$, then $L_c = \pi/2$. The critical patch size is reduced to half of the size of a patch with absorbing boundaries. Since the surroundings of the resource-rich patch are not lethal, the length where the individuals can diffuse is less restrictive. Less individuals die and the population resist for longer time.

3. If $v_o >> v_i$, then $L_c \to \pi$. This limit agrees with previous results. If the velocity outside the patch v_o increases, the death rate, the diffusion coefficient, or both increase giving place to a system with more dangerous surroundings. In the limit when $v_o \to \infty$, the system becomes a patch with lethal surrounding and we recover the result for the critical patch size where $L_c = \pi$

3.3.5 Population and current for a patch with permeable boundaries

In this section we use some of the results found in §3.3.2 to study the population distribution and its current in a patch of size $L = \pi$ with permeable boundaries in the stationary state. Equation (3.2.40) gives the population distribution for a patch of size L with absorbing boundaries. Here we define a patch of size $L_c = L = \pi$, centered at $x = 0$. Due to the permeable boundaries, the population at the boundary $x = L/2$ is different than zero, therefore we can write,

$$n(x) = n_0 \cos(\frac{\varpi x}{L}) \quad \text{if } x \in [-L/2, L/2]. \tag{3.3.37}$$

where $\varpi = \pi - \beta$ and β is a positive and small quantity to define a resource-rich patch domain slightly smaller than the CPS. Using the initial population, found in equation (3.2.39), $n_0 = \dfrac{3\pi}{8}\left(1 - \dfrac{\pi^2}{L^2}\right)$ we can write for a domain of size $\pi - \beta$

$$n_0 = \frac{3\varpi}{8}\left(1 - \frac{\varpi^2}{L^2}\right). \tag{3.3.38}$$

The system solution outside the patch is given by equation,

$$n(x) = n_1 e^{-\left(\dfrac{x - L/2}{\gamma}\right)} \quad \text{if } x \in [-L/2, L/2]^{\complement}. \tag{3.3.39}$$

On the other hand, the population currents inside and outside the patch are given by,

$$J(x) = -\frac{3\varpi^2}{8L}\left(1 - \frac{\varpi^2}{L^2}\right)\cos\left(\frac{\varpi x}{L}\right) \quad \text{if } x \in [-L/2, L/2] \tag{3.3.40}$$

and

$$J(x) = s\lambda n_1 e^{-\left(\frac{x - L/2}{\lambda}\right)} \quad \text{if } x \in [L/2, L/2]^{\complement}. \tag{3.3.41}$$

From equations (3.3.37) – (3.3.41), we can find the value of n_1. Equating equations (3.3.37) and (3.3.39) as well as their currents (3.3.40) and (3.3.41) at $x = L/2$ we numerically obtain,

$$n_1 = 0.2547 \tag{3.3.42}$$

With n_0 and n_1 given by equations (3.3.38) and (3.3.42) the population and the current dependent on x are given by

$$n(x) = \frac{3\varpi}{8}\left(1 - \frac{\varpi^2}{L^2}\right)\sin(x) \quad \text{if } x \in [-L/2, L/2], \tag{3.3.43}$$

and

$$n(x) = 0.2547e^{-\left(\frac{x - L/2}{\gamma}\right)} \quad \text{if } x \in [-L/2, L/2]^{\complement}, \tag{3.3.44}$$

while,

$$J(x) = -\frac{3\varpi^2}{8L}\left(1 - \frac{\varpi^2}{L^2}\right)\sin\left(\frac{\varpi x}{L}\right) \quad \text{if } x \in [-L/2, L/2] \tag{3.3.45}$$

and

$$J(x) = 0.2547s\gamma e^{-\left(\frac{x - L/2}{\gamma}\right)} \quad \text{if } x \in [-L/2, L/2]^{\complement}. \tag{3.3.46}$$

The population and current for a leaking patch with size $L_c = \pi$ can be plotted now. Figure 3.23 shows the population distribution and the current of a permeable boundaries patch of size $L = \pi$.

The top figure in 3.23 shows the population distribution (solid line) over a patch of size close to $x = \pi$, showing a population maximum at the center of the patch. The population is continuous in space, and decays after $x = L/2$ where individuals diffuse towards the dangerous regions.

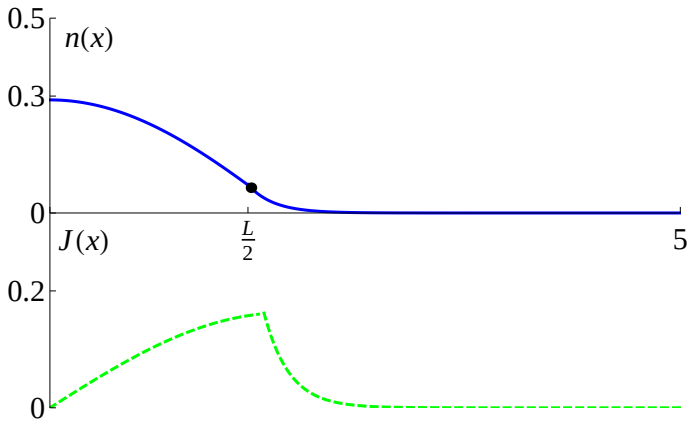

FIGURE 3.23: Population distribution and current for a patch with permeable boundaries of size $L = \pi$ centered at $x = 0$. The parameters used here are $s = 2$ and $\lambda = 0.2$

The current (dashed line) in figure 3.23 is continuous as expected (*i.e.*, the number of individuals coming from the patch to the boundary is the same number of individuals leaving the patch from the boundary). The current is zero at the patch center, reaching a maximum at the boundary. After this point the current decreases exponentially.

3.3.6 Population and current for a patches of size $L \gg L_c$ with permeable boundaries

In this section, we study the stationary state of a patch of size $L \gg L_c$ with permeable boundaries, using the patching method introduced in §3.1.4. For the stationary state the dynamics of the non-dimensional system is given by equations (3.3.13) – (3.3.14) where $\dfrac{\partial n}{\partial t} = 0$, thus

$$0 = n(1-n) + \frac{d^2 n}{dx^2} \quad \text{if } x \in [-L/2, L/2], \tag{3.3.47}$$

and

$$0 = s\left[-n + \lambda^2 \frac{\partial^2 n}{\partial x^2}\right] \quad \text{if } x \in [-L/2, L/2]^{\complement}, \tag{3.3.48}$$

with boundary conditions,

$$n|_{-L/2^+} = n|_{-L/2^-} \quad \text{and } n|_{L/2^-} = n|_{L/2^+}, \tag{3.3.49}$$

and

$$\left.\frac{\partial n}{\partial x}\right|_{-L/2^+} = s\lambda^2 \left.\frac{\partial n}{\partial x}\right|_{-L/2^-} \quad \text{and} \quad \left.\frac{\partial n}{\partial x}\right|_{L/2^-} = s\lambda^2 \left.\frac{\partial n}{\partial x}\right|_{L/2^+}. \tag{3.3.50}$$

If the patch size is very large, (*i.e.* $L >> L_c$ so $n \approx 1$ in most of the patch, except close to the boundary), then, inside the patch we assume that the population distribution takes the form $n \approx 1 - m$ with $m << 1$. Therefore, the solution of equation (3.3.47) is given by

$$n(x) = 1 - m_0 \cosh(x) \quad \text{if } x \in [-L/2, L/2]. \tag{3.3.51}$$

The solution outside the patch is given by,

$$n(x) = n_1 e^{-\left(\frac{x - L/2}{\lambda}\right)} \quad \text{if } x \in [-L/2, L/2]^{\complement}. \tag{3.3.52}$$

The currents for this system are given by

$$J(x) = m_0 \sinh(x) \quad \text{if } x \in [-L/2, L/2], \tag{3.3.53}$$

and

$$J(x) = s\lambda n_1 e^{-\left(\frac{x - L/2}{\lambda}\right)} \quad \text{if } x \in [-L/2, L/2]^{\complement}. \tag{3.3.54}$$

To find the values of m_0 and n_1 we use the boundary conditions (3.3.49) and (3.3.50) to match the solutions at the boundary $x = L/2$. Hence,

$$1 - m_0 \cosh(L/2) = n_1, \tag{3.3.55}$$

and

$$m_0 \sinh(L/2) = s\gamma n_1. \tag{3.3.56}$$

Rearranging terms we obtain,

$$m_0 = \frac{s\gamma}{\lambda(L/2) + s\lambda \cosh(L/2)}, \tag{3.3.57}$$

and

$$n_1 = \frac{\sinh(L/2)}{\sinh(L/2) + s\lambda\cosh(L/2)}. \tag{3.3.58}$$

With these values, we obtain the general solution for the population distribution $n(x)$ and the current $J(x)$ given by

$$n(x) = 1 - \left(\frac{s\lambda}{\sinh(L/2) + s\lambda\cosh(L/2)}\right)\cosh(x) \quad \text{if } x \in [-L/2, L/2], \tag{3.3.59}$$

and

$$n(x) = \left(\frac{\sinh(L/2)}{\sinh(L/2) + s\lambda\cosh(L/2)}\right) e^{-\left(\frac{x - L/2}{\lambda}\right)} \quad \text{if } x \in [-L/2, L/2]^{\complement}. \tag{3.3.60}$$

whereas,

$$J(x) = \left(\frac{s\lambda}{\sinh(L/2) + s\gamma\cosh(L/2)}\right)\sinh(x) \quad \text{if } x \in [-L/2, L/2], \tag{3.3.61}$$

and

$$J(x) = \left(\frac{s\lambda\sinh(L/2)}{\sinh(L/2) + s\lambda\cosh(L/2)}\right) e^{-\left(\frac{x - L/2}{\lambda}\right)} \quad \text{if } x \in [-L/2, L/2]^{\complement}. \tag{3.3.62}$$

Figure 3.24 shows the behaviour of the population n and the current J with respect to spatial coordinate x for a large patch ($L = 24$) with permeable boundaries. We observe that in the solution for the population distribution, the derivative of the population is discontinuous as shown in the box in the top right of figure 3.24. The derivative discontinuity of the solution may be attributed to the system parameters (diffusion and growth/death rates), which are different for both regions. On the other and, we observe that the current distribution, shown in figure 3.24 with dashed line, is continuous.

The population distribution shown in figure 3.24 describes a population that is very close to one, along most of the length of the resources rich patch. However, as we get close to the boundary, the population decays exponentially on the scarce-resources region. The population decay outside the resources rich patch depends on the velocities ratio

$v = v_o/v_i$ described in §3.3.4.1.

Simultaneously, figure 3.24 shows that the current is zero over most of the patch length; however, close to the boundary it increases. The current reaches a maximum at the boundary and decays outside the patch depending on the values of v.

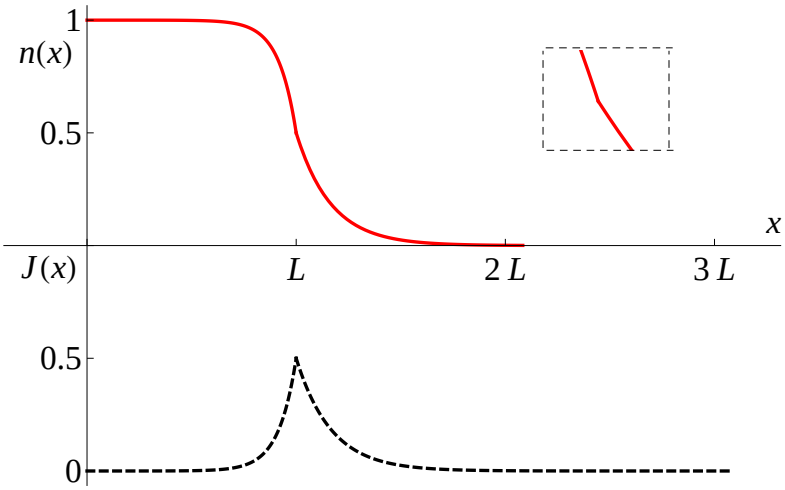

FIGURE 3.24: Population and current for a patch of big length, $L = 24$ with permeable boundaries.

In figures 3.25 and 3.26 the population and current distributions for different ratio velocities $v = v_o/v_i$ are shown. Here we assume that the rate $s = \alpha'/\alpha$ is fixed and equal to 0.5.

Notice that as $v \to 0$ the population as well as the current outside the patch decrease to zero in space recovering the results obtained in the patch with absorbing boundaries, where the population and the current outside the patch are zero.

However, if $v \neq 0$ there is always a current outside the patch. When the propagation velocity inside the resource-rich patch is much larger than the one outside, the individuals do not diffuse much in the scarce-resources region, as if a "fence" existed between both regions. The individuals are kept inside the patch and the ones trying to leave it, struggle to find a way out.

At the same time, if the velocity ratio is bigger than one $v > 1$ the individuals move more freely outside the patch. A larger number of individuals leave the patch and they travel longer distances due to the number of individuals leaving the patch.

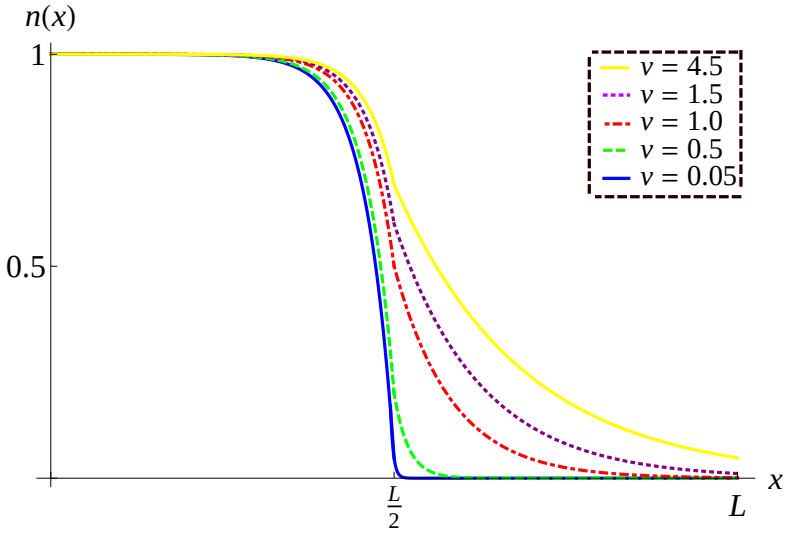

FIGURE 3.25: Population distribution for a large patch of size $L >> L_c$ with permeable boundaries dependent on the propagation velocities ratio $v = v_o/v_i$ outside and inside the patches. As the velocity outside the patch increases, the population decreases restricting the individual diffusion into the dangerous region.

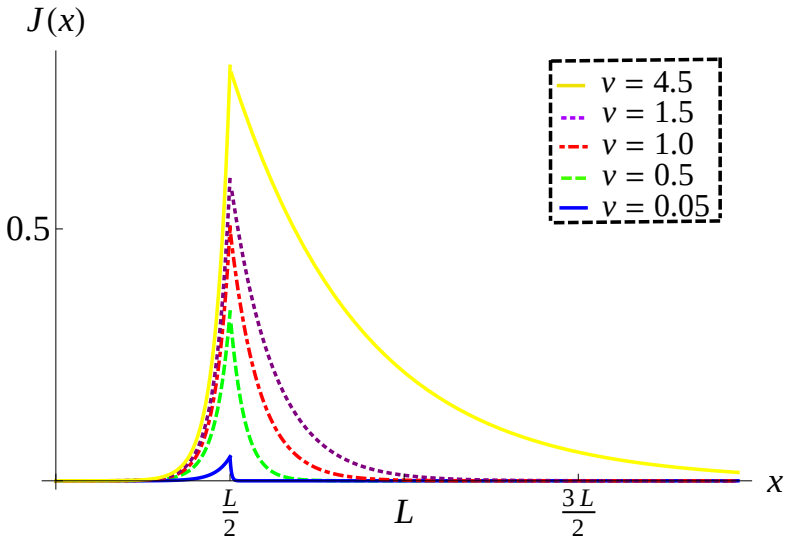

FIGURE 3.26: Current distribution for a large patch of size $L >> L_c$ with permeable boundaries dependent on the propagation velocities ratio, $v = v_o/v_i$ outside and inside the patches. As the velocity outside the patch increases, the current decreases.

3.3.7 Summary

In this section we analysed different characteristics of a one-dimensional patch of size $L >> L_c$ with permeable boundaries. We found that, as expected, most of the population concentrates in the resource-rich patch, declining quickly as individuals enter the scarce-resources area. We also found that, even if the population is continuous along the whole axis domain, its derivative is not. This implies that the different parameters used to describe the system, influence the distribution of the population, hence, affecting its dynamics. As we will see in Chapter 4, some parameters, like the dendrotaxis term, can even make the population distribution to become discontinuous.

We also found that, as expected the size of parameters such as diffusion constants and growth/decay rates influence greatly the system dynamics. We found that the velocity propagation of individuals in these type of systems is governed by the diffusion constants and growth/decay rates inside and outside the resource-rich patch. These velocities determine the population current and distribution over the patch.

The experimental measurement of these type of parameters may help us to reach a better understanding of the dynamics of similarly shaped ecosystems, and provide control population strategies, either for conservation or eradication.

3.4 Summary

In this chapter we studied single one-dimensional patches systems with absorbing and permeable boundaries. We mathematically analysed the systems itself and its different parameters such as effective growth rate, diffusion coefficients and carrying capacity. Different systems were analysed using exact and approximate semi-analytic methods including Fourier series expansion and the patching method. The critical patch size of this type of system was studied and compared with previous results and new ones.

Firstly, we solved exactly and approximately, the system of a semi-infinite system with absorbing boundaries. Both solutions were compared in order to validate the approximate methods used later in this chapter.

We discussed the problem of critical patch size for a single one-dimensional patch with absorbing boundaries as an important biological parameter to obtain, previously studied by other authors. Then, we solved this system for the stationary state of a patch with absorbing boundaries obtaining a solution in agreement with previous solutions through different methods.

The carrying capacity of a single patch with absorbing boundaries was also analysed and compared with the population effective growth rate. We discovered that, as expected, the carrying capacity of a patch with absorbing boundaries makes sense only for patches of sizes larger that the critical patch size. We also found a relation between the patch length and the carrying capacity. As the patch length is increased, the carrying capacity of the system grows as a quadratic function firstly. Then, as the patch length tends to infinity, the carrying capacity grows linearly with it.

The population and current distribution for patches systems with different lengths and boundary conditions was obtained. We compared some results between systems. For example, we found that the currents obtained for large patches with absorbing boundaries, (*i.e.* patches with sizes of over three times the CPS) had practically the same currents found in the case of the semi-infinite patch. This imply that, for the analysis of similar systems, both approximations can be used indistinctively. However, in the case of patches of sizes close to the CPS found in §3.2.3, we found that the current is smaller than the current obtained for the semi-infinite and the patch systems of sizes larger than the CPS, and therefore the differentiation between analyses has to be made.

We analysed some features of a patch with permeable boundaries. We found solutions for population and current distributions for patch sizes close to the critical patch size (CPS) $x = \pi$, and patches much larger than the CPS with permeable boundaries. The analysis provides information about the dynamics of a system with permeable boundaries according to the biological parameters included in these systems (diffusion parameters and growth/decay population rates) which is very important for the understanding of population dispersal.

For patches with permeable boundaries, we found that the critical patch decreases or increases according to rates between propagation velocities inside and outside the patch.

This result gives us an idea of how different populations dispersing at different rates can have very different dynamics. Therefore, different population strategies should be applied for different populations.

We also found that the population currents and distributions in patches with permeable boundaries depends strongly on the propagation velocity of the population inside and outside the patch. The knowledge of these velocities in specific population systems would provide vital information to predict the population dispersal, colonisation or extermination of such population in different environments. It would also help us to anticipate, for example, the invasion of a population, giving us the chance to prevent such an invasion.

The study of these type of systems is also the preamble to Chapter 4 and 5, where other characteristics are added to the population individuals.

Chapter 4

One-dimensional population models with dendrotaxis

4.1 Introduction

The Asiatic red-bellied beautiful squirrel *Callosciurus erythraeus* was introduced into Argentina in 1973 after the release of several individuals into the Argentinian Pampas. This species, benefited from the widespread abundance of introduced trees in the Argentine Pampas has spread from a reduced number of individuals to a population that inhabits over an area exceeding 680 km^2 (Guichón, 2007) [15]. Its abundance results in economic damage and its continuous spread threatens indigenous species in regions such as the Otamendi Natural Reserve [118].

The invasion and spread of *Callosciurus erythraeus* has been studied by Guichón and Doncaster (2008) using spatially explicit stochastic models [15]. This model predicts different situations under alternative scenarios of strategic culling or habitat removal aimed at slowing the spread. These models are based on empirical data extracted from the squirrel location in Argentina as well as from published sources such as Tamura [52–54], Gurnell [55], Yo et al. [56] and Akçacaya [57]. These models make specific predictions on the dynamics of the squirrel; however, these predictions require the use of many biological parameters that are not always easy to measure.

Here, we present a mathematical analysis of potential impacts on spread rates due to squirrel behaviours, particularly in avoiding hazard and seeking mates. Our continuum model describes density-dependent growth and diffusion amongst woodland and grassland patches that have a variable potential for reproductive success. In woodland patches, the population obeys a modified logistic growth. In grassland patches, populations are unable to sustain themselves and decrease exponentially. In all types of patches, diffusion terms that model the dispersal of individuals across the patches are included.

We introduce a novel development for gap analysis, that represents the individuals hazard sensitivity when outside woodland patches. This sensitivity is modelled by a term which has its origin in physical systems. We call this term *dendrotaxis* based on its suitable Greek origin: $\delta\epsilon\nu\delta\rho o$, (dendro=tree), and $\tau\alpha\xi\iota\sigma$, (taxis=arrangement). The term taxis can be defined as the innate response on the behaviour of an organism due to a directional stimulus, like occurs in chemotaxis, phototaxis and thermotaxis [38], hence, the term dendrotaxis indicates that individuals direct their movements towards densely wooded regions, generating a gradient of the population dispersal at the boundary, ensuring a low individual migration from the woodland to the grassland.

Patch geometries are consistent with those found in the pampas, including linear corridors and isolated woodlands. Using numerical methods and semi analytic results we analyse the dependence of the inter-patch length with the flux of individuals from a full woodland patch to an empty woodland patch for one and two-dimensional systems. We find a relation on the inter-patch length and the ability of reproductive success in a previously empty woodland patch. We find that dispersal is slowed by Allee effects, *i.e.*, inverse density-dependent responses to the difficulty of finding mates at low density, when combined with hazard sensitivity. The velocity of spread then depends on inter-patch distances and patch geometries.

4.2 Biological discussion

According to Guichón and Doncaster [15], Tamura [52–54], Gurnell [55], Yo *et. al.* [119], Akçacaya [57] and personal discussions with M.L. Guichón and C.P. Doncaster the red-bellied beautiful squirrel *Callosciurus erythraeus* presents particular behaviours which are summarized in the following paragraphs. The most important factors of the population dispersal will be considered in our mathematical model, while secondary factors will be discarded. These may be added later to the model, depending on its potential importance for the system dynamics.

1. The time scales of movement in the woodland patches are small compared with the time scales in the grassland. In the woodland the squirrels reproduce and inhabit areas for large periods of time (on year length timescales) while in grasslands they always move searching for woodland patches.

2. Squirrels present a hazard sensitivity which has to be considered. In previous models we supposed that individual dispersal was ruled only by Fickian diffusion. In this model we modify the flux term governing equations by introducing a novel term which simulates the individuals hazard sensitivity to open spaces.

3. Individual dispersal may be slowed down due to difficulties of finding mates. We model this by introducing an Allee effect (*i.e.*, an inverse density-dependent response to the difficulty of finding mates at low density) in the numerical simulations. In the previous models we have supposed that populations have a logistic growth function. Another possible growth rate function can be associated with an Allee effect, modelling the difficulty of finding mates. At lower population densities, the squirrels struggle to reproduce to form a sustainable population, which causes a very slow propagation in new habitats with respect to the model without Allee effect. However, slow population spread of invading species may lead to underestimation of the invasion risk posed by them and can also affect the optimal control strategies for these invading species.

4. The general landscape geometry may be summarized into several different types of habitat:

(a) Patches of different sizes represented by forested areas that sustain populations.

(b) Open areas where individuals do not reproduce, with an enhanced death rate that individuals avoid.

(c) Corridors which are represented by long lines of trees where the squirrels can reproduce and sustain populations.

These different types of habitat may or may not be connected between each other and may or may not allow dispersal depending on the configuration of the habitat. For example, if the distance between two good patches of habitat is such that, the probability for individuals to reach a new patch is close to zero, no dispersal will take place; however, if it is short, the individuals may cross the gap between patches. Another example would be the existence of junctions. The population of individuals would spread in different directions which may lead them to different situations. This is shown schematically in fig. 4.1.

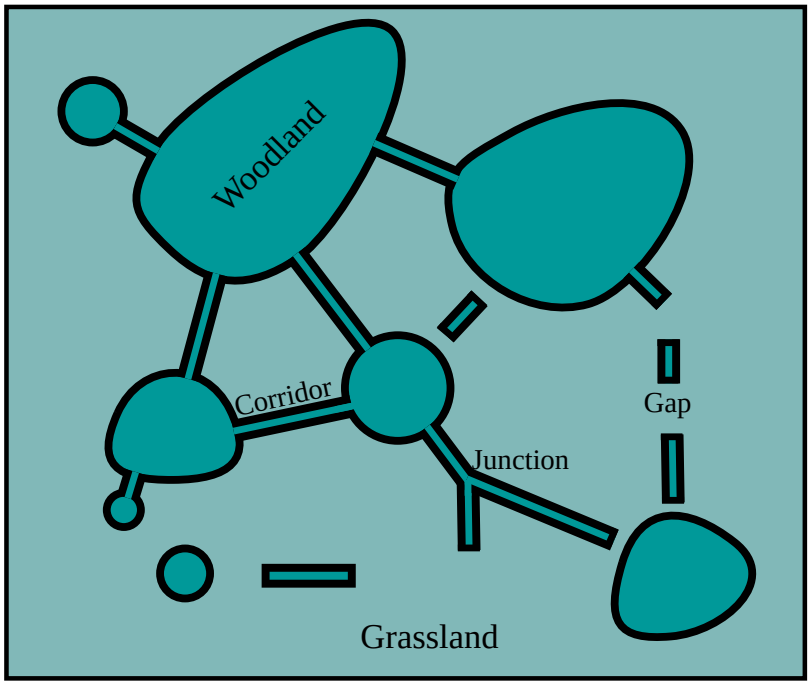

FIGURE 4.1: Individual dispersal in a patchy landscape may follow different dynamics depending on the patch individuals choose to follow

Other factors that can be included in future models are

1. Heterogeneous distributions of food and nest sites affects the squirrel dispersion.

2. The density dependence in terrestrial mammals is more related to fecundity and recruitment of juveniles than to mortality of adults. This may suggest the adoption of a different population growth function in the woodland that can select young individuals over old ones.

3. Squirrels can travel up to several hundred meters per day exploring (for example in a tree corridor) looking for nest sites and/or mates. This implies that the squirrels diffusion length scale is very large.

4. Squirrels are a sociable species and they tend to travel in groups rather than individually. This might be modeled with a term representing surface tension. Qualitatively speaking, the surface tension would model intermolecular attractive forces for the same type of molecules in the surface of a liquid. In this case, the individuals would be "held" together by "cohesive forces" which would be related to the preference of travel in groups. This cohesive force would manifest at the boundary of the woodland patch, creating a "surface tension" like term. Alternatively, this behaviour of population group travel may be modelled with a concentration dependent diffusive flux of the form $-D(n)\nabla n$ where the diffusion coefficient D is a decreasing function of the population n. This would result in the decrease of the diffusion coefficient due to an increase of the number of individuals travelling together.

4.3 Logistic growth model

Based on the biological factors described in §4.2, here we develop a more generic model of population growth and dispersal. This model accounts for the growth and migration of a population of organisms sensitive to landscape fragmentation where regions of plentiful and scarce-resources co-exist. In addition to the spatial variability in resources, we include a term that models the spatial variability of hazardous areas according to the population individuals perception.

In order to follow the steps in the modelling, it is helpful to bear in mind the squirrel migration example introduced in §4.2. There the individuals migrate through a landscape consisting of resources-rich patches where the feeding resources as well as the number of nest sites are plentiful, interspersed with grassland areas where the food resources are scarce, the nest sites are non-existent and the danger of predation is constant.

The model presented here is analogous to the one studied in Chapter 3, with the addition of the hazard sensitivity factor and Allee effects. This factor is the the key modelling challenge in this chapter and Chapter 5.

To introduce this hazard sensitivity factor we provide an analogy from thermodynamics. Here we relate the tendency of molecules to diffuse with the way individuals diffuse in fragmented environments. The chemical potential of molecules acts in a manner similar to the the hazard sensitivity factor. Hence molecules diffuse due to spatial variation in chemical potential and [120] in this case, molecules will naturally tend to go from a higher chemical potential to lower chemical potential.

We start by writing down a conservation equation for $n(\mathbf{r}, t)$, where the probability density per unit area of finding an organism in the surroundings of the point $\mathbf{r}$ takes the form

$$\frac{\partial n}{\partial t} + \nabla \cdot \mathbf{J} = f(n, \mathbf{r}) \tag{4.3.1}$$

where t is the time, n is the population per unit area, $\mathbf{J}$ is the probability flux of individuals and f is the population growth or decay function presented previously in Chapter 3, giving

$$f(n, \mathbf{r}, t) = \begin{cases} \alpha(\mathbf{r}) n(\mathbf{r}) \left(1 - \dfrac{n(\mathbf{r})}{\chi(\mathbf{r})}\right) & \text{in } \Omega \text{ with } \alpha(\mathbf{r}) > 0 \\ \alpha(\mathbf{r}) n(\mathbf{r}) & \text{in } \Omega^{\complement} \text{ with } \alpha(\mathbf{r}) < 0 \end{cases} \tag{4.3.2}$$

where $\chi(\mathbf{r})$ represents the region carrying capacity, $\alpha(\mathbf{r})$ is the rate of population growth (negative in $\Omega^{\complement}$), which varies depending of the region where the individuals are located.

J is again the flux of organisms, previously modelled by Fickian diffusion of the form,

$$\mathbf{J} = -D(\mathbf{r})\nabla n. \tag{4.3.3}$$

However, this type of diffusion makes sense only if individuals are fairly insensitive to environmental factors, resulting in their incapacity to differentiate between advantageous and disadvantageous habitats (see for example [121]). Fickian diffusion do not occur often [18, 28, 122], even in relatively simple organisms that can differentiate between advantageous and disadvantageous habitats, therefore, the flux of organisms is amended here to take the form

$$\mathbf{J} = -D(\mathbf{r})\nabla n + n\mathbf{v}. \tag{4.3.4}$$

In this amendment, beside the Fickian diffusion, a drift velocity **v** towards better environments is included.

This amendment is based on a similar behaviour occurring due to the presence of a chemical potential in molecules. For example, if we have two containers of the same volume with gases at different chemical potentials, diffusion will "push" particles from areas of higher chemical potential towards smaller chemical potential [120].

Here we specify **v** as virtually the simplest form that we can take assuming that it is independent of n and depends on position only, *i.e.* a step function. This assumption is based on the hypothesis that individuals actively seek areas advantageous to them avoiding at the same time, disadvantageous ones.

In summary, we have two type of diffusions in this modelling, one that "pushes" individuals from areas of larger population to areas of lower population, and another produced by the dendrotaxis term that "pushes" individuals from areas of large dendrotaxis to areas of low (or zero) dendrotaxis (since the individuals would be already in the woodlands).

If we consider a scenario in which the growth function f is zero, then the steady state

is given by $\nabla \cdot \mathbf{J} = 0$. Suppose $\mathbf{v}$ takes the form

$$\mathbf{v} = -D(\mathbf{r})\nabla\mu, \tag{4.3.5}$$

for some function $\mu(\mathbf{r})$. The flux term then has a steady state

$$\nabla \cdot [-D(\mathbf{r})\left(\nabla n + n\nabla\mu\right)] = 0 \tag{4.3.6}$$

with an equilibrium solution of the form,

$$\mathbf{n} = Ae^{-\mu(\mathbf{r})} \tag{4.3.7}$$

where A is a constant and has the property $\mathbf{J} \equiv \mathbf{0}$ everywhere as an imposed property. If $\mathbf{v}$ takes another form than (4.3.5), the steady solution does not have $\mathbf{J} \equiv \mathbf{0}$ everywhere and a pointless circulation of individuals occurs due to the fact that with a different function the curl of the flux is different than zero. Assuming that such circulating steady states do not occur, the velocity takes the form $\mathbf{v} = -D(\mathbf{r})\nabla\mu$ and the model proposed in equations (4.3.1) and (4.3.2) is summarised as

$$\frac{\partial n}{\partial t} + \nabla \cdot \mathbf{J} = \alpha(\mathbf{r})n\left(1 - \frac{n}{\chi}\right) \quad \text{in the resource-rich regions } \Omega \tag{4.3.8}$$

and

$$\frac{\partial n}{\partial t} + \nabla \cdot \mathbf{J} = \alpha(\mathbf{r})n \quad \text{in the resource-scarce regions } \Omega^{\complement} \tag{4.3.9}$$

where

$$\mathbf{J} = -D(\mathbf{r})n\nabla(\log n(\mathbf{r}) + \mu(\mathbf{r})), \tag{4.3.10}$$

since equation (4.3.4) depends only on the position. According to equations (4.3.8) and (4.3.9) the population grows logistically in the resource-rich areas while it decays exponentially in the resource-scarce ones. The decay in the resource-scarce areas is the result of lack of resources for feeding, nesting and any activity necessary for reproduction and establishment, besides the high probability of predation. The availability of nesting sites and food in the resource-rich region sets a carrying capacity that also imposes a limit on the total number of individuals in these regions. The dendrotaxis term $-Dn\nabla\mu$

stands for the gradient of sense of danger that the population individuals experience when exploring its surroundings assuming that they are sensitive to advantageous or disadvantageous areas for their survival.

4.3.1 Dendrotaxis function

In order to investigate the qualitative behaviour of the model described in §4.3, we restrict our attention to the case where the population of the resource-rich regions and the resource-scarce regions are both uniform, so that

$$\alpha(r) = \begin{cases} \alpha & \text{in the resource-rich regions} \\ -\alpha' & \text{in the resource-scarce regions} \end{cases} \tag{4.3.11}$$

$$\mu(r) = \begin{cases} 0 & \text{in the resource-rich regions} \\ \mu_0 & \text{in the resource-scarce regions} \end{cases} \tag{4.3.12}$$

and

$$D(r) = \begin{cases} D & \text{in the resource-rich regions} \\ D' & \text{in the resource-scarce regions} \end{cases} \tag{4.3.13}$$

where all the terms, α, α', μ_0, D and D' are assumed to be constants.

The figures 4.2, 4.3 and 4.4 show qualitatively how we expect the dendrotaxis to affect the dynamics of the system. Figure 4.2 shows the population of a system subject to diffusion only. In this case the individuals of the population explore their environment without actively seeking areas that are advantageous to them or moving away from areas that are disadvantageous to them. In figure 4.3 we consider the dendrotaxis term with almost the most simple function that we could take. We specify that μ is constant in the resource-scarce regions and μ is zero in the resource-rich regions. The dendrotaxis function generates a gradient on the population dispersal due to a flow of individuals from higher dendrotaxis areas to lower dendrotaxis region, ensuring a low individual migration from the resource-rich regions to the resource-rich regions as shown in figure 4.4 producing a discontinuity across the boundary between the woodland and the grassland. It works as an effective repulsive field that "pushes" the individuals away

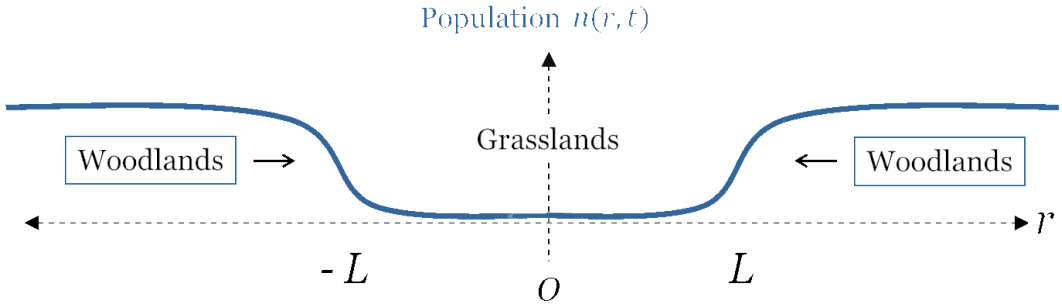

FIGURE 4.2: System subject to diffusive flux only. In the grassland the population grows and diffuses. In the grasslands the population diffuse and decay.

from regions in which μ is larger than zero to those where it is zero.

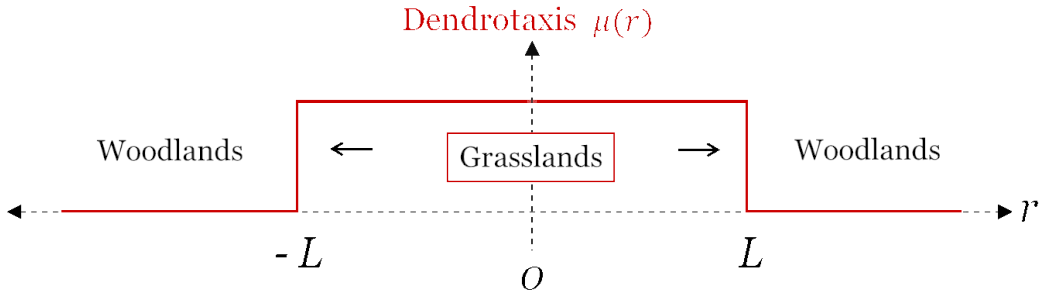

FIGURE 4.3: Dendrotaxis function. This function is a step function where $\mu = 0$ in the resource-rich regions and μ is a positive constant value in the resource-scarce regions.

Figure 4.4 shows how due to the presence of the dentrotaxis term, a discontinuity on the population density at the boundary has to be considered. The boundary discontinuity is modelled imposing jump boundary conditions.

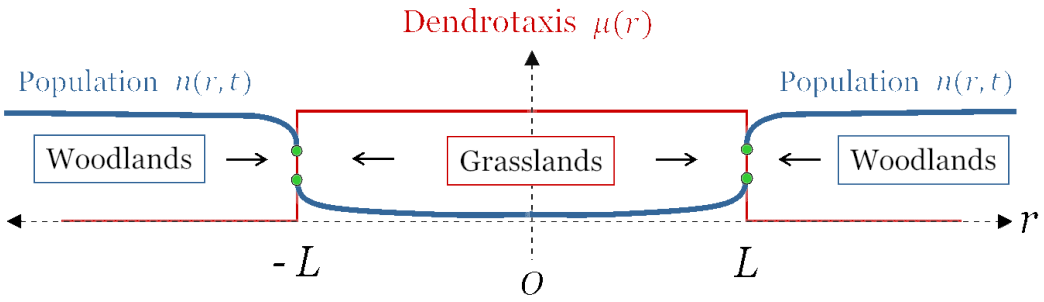

FIGURE 4.4: The presence of the dentrotaxis works as an effective repulsive field that "pushes" the squirrels away from the grassland and into the woodland

The way to explicitly find the jump boundary conditions is by applying a standard "pillbox" argument to equations (4.3.1) and (4.3.10). By doing this we see that the

normal component on the flux density is continuous, that is

$$[\mathbf{J} \cdot \mathbf{N}]_{\delta\Omega} = 0. \tag{4.3.14}$$

where $\mathbf{J}$ represents the flux and $\delta\Omega$ represents the boundary between the resource-rich regions and the resource-scarce regions, while the squared brackets stand for the jump across the boundary on the resource-rich region's side (Ω) and the resource-rich region's side ($\Omega^{\complement}$). This boundary condition maintains the continuity in the flux across the boundary between the two regions. $\mathbf{N}$ is the outward normal to the boundary. In a narrow region on either side of the boundary, where $\Delta x \to 0$, equation (4.3.7) will approximately hold (otherwise the flux becomes very large). It follows then,

$$ne^{\mu(\mathbf{r})}|_{\delta\Omega} = ne^{\mu(\mathbf{r})}|_{\delta\Omega^{\complement}} \quad \text{or} \quad \frac{n|_{\delta\Omega^{\complement}}}{n|_{\delta\Omega}} = \exp(\mu|_{\delta\Omega^{\complement}} - \mu|_{\delta\Omega}). \tag{4.3.15}$$

that based on the dendrotaxis function assumed in equation (4.3.12) becomes

$$n|_{\delta\Omega} = ne^{\mu_0}|_{\delta\Omega^{\complement}} \tag{4.3.16}$$

As it can be seen from equation (4.3.15) the value of n on each side of the boundary are related by a proportionality $\mu|_{\delta\Omega^{\complement}} - \mu|_{\delta\Omega}$ where the function that varies only with the position in the space, and in the case of a step function as the one given by (4.3.12) this proportionality is reduced to μ_0.

Figures 4.5(a) and 4.5(b) show one- and two-dimensional patches with discontinuities in the boundary due tho the presence of a discontinuous dentrotaxis term, solved numerically with COMSOL Multiphysics.

4.3.2 Non-dimensionalisation

Now that the model described by equations (4.3.1)-(4.3.4) has been set-up, we non-dimensionalise the system as in Chapter 3 via

$$t^* = \alpha t, \quad n^* = \frac{n}{\chi}, \quad \mathbf{r}^* = \frac{\mathbf{r}}{\xi}, \tag{4.3.17}$$

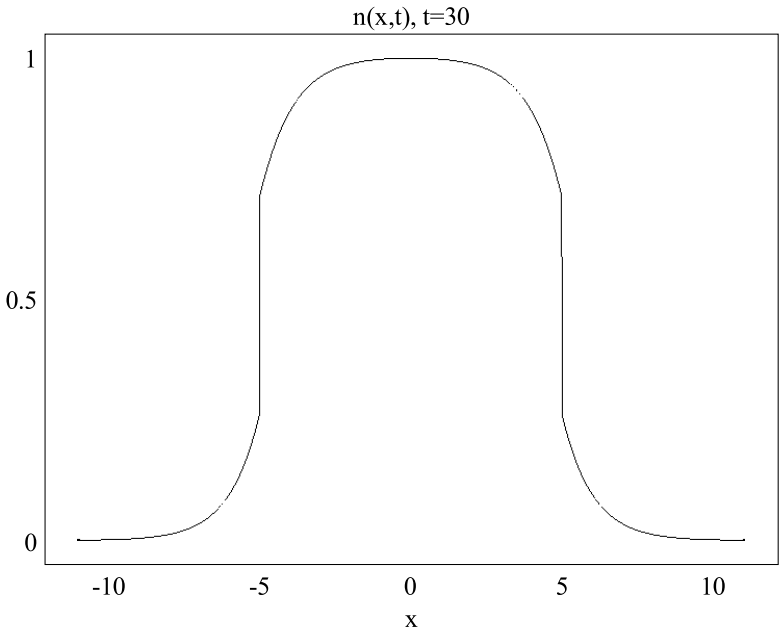

(a) 1D Patch

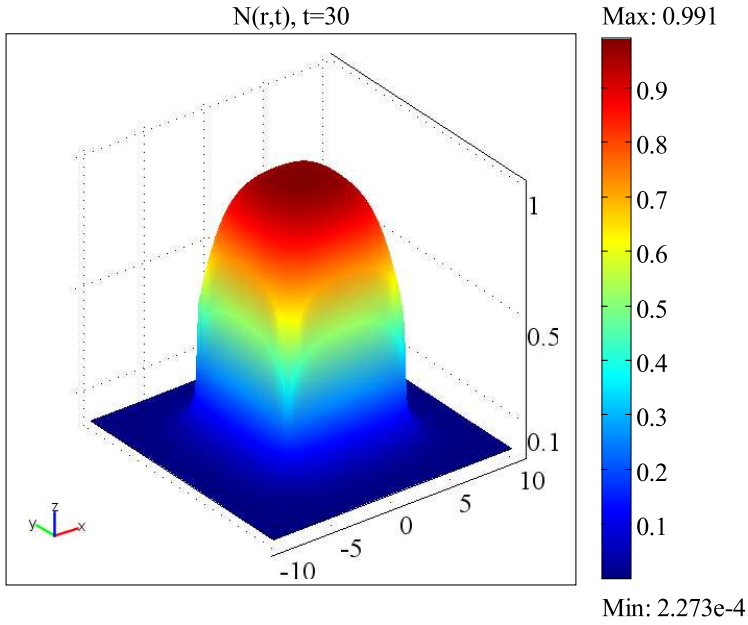

(b) 2D Patch

FIGURE 4.5: One- and two-dimensional patches showing discontinuities in the boundary due to the presence of a discontinuous dentrotaxis term.

where, $\xi = \sqrt{\dfrac{D}{\alpha}}$, α is the growth rate in the resource-rich regions, D is the diffusion coefficient in the resource-rich regions and μ_0 is the constant value of the dendrotaxis function in the resource-scarce regions. By using these parameters we obtain the non-dimensional equations

$$\frac{\partial n^*}{\partial t^*} = n^*(1 - n^*) + \nabla^{*2} n^* \quad \text{in } \Omega, \tag{4.3.18}$$

$$\delta \frac{\partial n^*}{\partial t^*} = -n^* + \lambda^2 \nabla^{*2} n^* \quad \text{in } \Omega^{\complement}, \tag{4.3.19}$$

and jump boundary conditions,

$$n^*|_{\delta\Omega} = n^* e^{\mu_0}|_{\delta\Omega^{\complement}} \tag{4.3.20}$$

and

$$\mathbf{N} \cdot (\nabla^* n^*)|_{\delta\Omega} = \mathbf{N} \cdot \left(\frac{\lambda^2}{\delta}\right) (\nabla^* n^*)\Big|_{\delta\Omega^{\complement}}, \tag{4.3.21}$$

where

$$\delta = \frac{\alpha}{\alpha'} \tag{4.3.22}$$

and

$$\lambda = \sqrt{\frac{D'\alpha}{D\alpha'}}. \tag{4.3.23}$$

The primed constants D' and α' denote the diffusion constant and the decay rate in the resource-scarce regions. In the interest of brevity, we subsecuently drop the star notation in equations (4.3.18) – (4.3.21). The non-dimensional equations of the system then become,

$$\frac{\partial n}{\partial t} = n(1 - n) + \nabla^2 n \quad \text{in } \Omega \tag{4.3.24}$$

$$\delta \frac{\partial n}{\partial t} = -n + \lambda^2 \nabla^2 n \quad \text{in } \Omega^{\complement}, \tag{4.3.25}$$

$$n|_{\delta\Omega} = ne^{\mu_0}|_{\delta\Omega^{\complement}}, \tag{4.3.26}$$

$$\mathbf{N}\cdot\nabla n|_{\delta\Omega} = \frac{\lambda^2}{\delta}\mathbf{N}\cdot\nabla n\Big|_{\delta\Omega^{\complement}}. \tag{4.3.27}$$

These equations are all valid in one and two dimensions.

4.3.3 Parameters analysis

The model presented in §4.3 is a generic description of any population following the behavior given by equations (3.3.8)–(4.3.27), but the parameters found in them will depend on particular aspects of specific populations. Here we examine the example introduced in §4.2 to understand the dynamics of a system formed by squirrels dispersing in a fragmented environment, in the rescaled framework.

To estimate the size of the parameters we assume that $e^{\mu_0} >> 1$ since squirrels strongly prefer to stay in the woodland rather than in the grassland, therefore the drift velocity of the squirrels away from the grassland will be large.

On the other hand, we suppose that $\delta \ll 1$. This assumption implies that the decay rate in the grassland is much larger that the growth rate in the woodland. According to Guichón [15], these squirrels reproduce at a rate of approximately $1.53yr^{-1}$, while the decay rate increases dramatically as soon as they leave the woodlands due to predation and lack of food; implying for example that, it would be extremely unlikely to find a squirrel wandering in the grasslands for anywhere close to 1.53 years.

Finally, we assume that $\dfrac{D'}{D} \gg 1$. This assumption is based on the fact that individual movement, or diffusion in the grasslands is much faster than in woodlands. According to empirical observations described personally by M.L. Guichón and C.P. Doncaster, squirrels move much faster in grasslands than in woodland due to the hazard sensitivity they present. At the same time, we suppose that the diffusion coefficient is small in the woodlands than in the grassland. This assumption is based in the fact that if an

individual establish a nest site with a mate in the woodlands, they will stay around the nest site and not diffuse much.

Notice from equation (4.3.26) that if the drift velocity representing the hazard sensitivity of the individuals is zero, the jump in the boundary goes to zero when $\mu_0 = 0$, recovering the behaviour presented in Chapter 3, governed by Fickian diffusion only, thus canceling the jump in the population density and maintaining the continuity in the individuals flux.

4.4 Numerical solution

Setting up the basis of the model described in §4.3.2, we can study some features of the population dispersal. We start with a numerical analysis of two resources-rich patches separated by a scarce-resources gap shown in figure 4.6. We investigate how the population in a resources-rich patch disperses through it and how the flux of individuals crossing a scarce-resources gap is affected by the scarce-resources gap depending on the size of the parameters discussed in §4.3.3. Finally, we study the dependency of the gap crossing time delay, respect to the gap length. In terms of numerical analysis, we explore the system using COMSOL Multiphysics performing an extensive gap crossing analysis.

4.4.1 Gap crossing

Here we numerically analyse a one-dimensional system constituted by two resources-rich patches (woodland) with a gap of resources-scarce regions (grassland) in between as shown in figure 4.6.

Based on the model built in §4.3.2 we analyse an example of a one-dimensional system constituted by two resources-rich patches as in figure 4.6, and solve equations (3.3.8) – (4.3.27) using COMSOL Multiphysics for different gap sizes.

In the rescaled units, the example we investigate is constructed over the domain $-M < x < M + L$ as shown in the figure 4.7. The resources-rich patches are located at $\Omega = (-M, 0) \cup (L, M + L)$ while the scarce-resources areas are covered by the domain

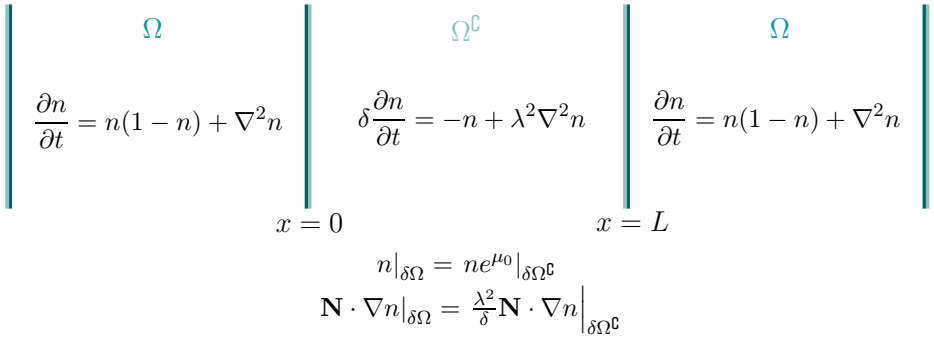

FIGURE 4.6: Two patches of resources-rich separated by a gap of scarce-resources are shown. The equations governing each region are written as well as the boundary conditions in the border between the resources-rich and the scarce-resources regions.

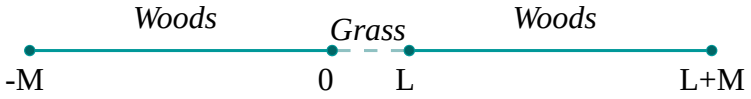

FIGURE 4.7: Geometry of two resources-rich patches surrounded by scarce-resources areas used for the system given in §4.4.1. This system is analysed numerically with COMSOL Multiphysics.

$\Omega^{\complement} = (0, L)$. We assume as initial condition a small population in the domain $(-M, 0)$ occupied by resources-rich with value $n = 0.1$ in the interval $x = (-M, -M + 1)$. For the example developed here $M = 50$ and $L = 10$.

According to equations (3.3.8)–(4.3.27) the parameters that have to be defined are μ_0, λ and δ which, based on the analysis of the parameters done in §4.3.3 we define as $\mu_0 = 3$, $\lambda^2 = 2$ and $\delta = 0.05$. These values may be adjusted according to more accurate biological data, but for simplicity we take these values here. To model the boundary discontinuities resulting from the dendrotaxis term we use Heaviside functions at the boundary of the patches, in this way we obtain the dendrotaxis step function shown in figure 4.3. The introduction of the Heaviside functions is introduced in the flux terms of the general equation at the boundary, instead of being introduced as a boundary conditions due to software limitations.

The results of the example described previously are shown in figure 4.8 for a system with 25666 elements and $0 < t < 100$ time units. Once the left resources-rich patch is filled up some individuals start diffusing to the next patch through the scarce-resources area decaying along the way. In this case the gap between patches is sufficiently small for some individuals to cross it and start reproducing in the new resources-rich patch. Once

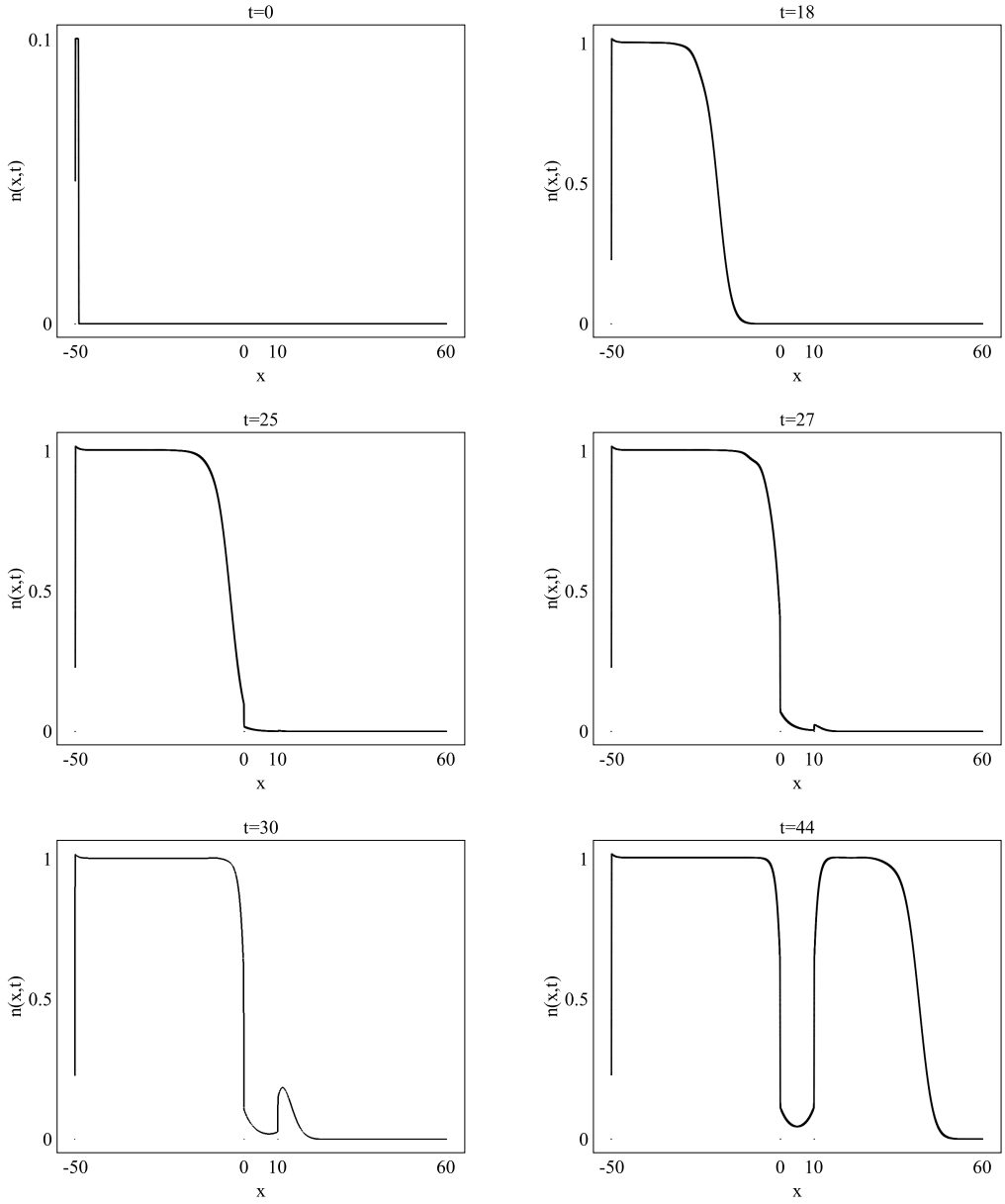

FIGURE 4.8: Individuals dispersal in a one-dimensional two patches system. Each patch has a size of $s = 50$ while the gap, located at $x = 0$ has a length $L = 10$. The parameters used for the solution of this system are $\lambda = \sqrt{2}$, $\delta = 0.05$ and $\mu_0 = 3$. Once the left patch is filled up the individuals start dispersing to the right hand patch filling it up.

the individuals reach the second resources-rich patch they start reproducing logistically once again until they fill up the second patch.

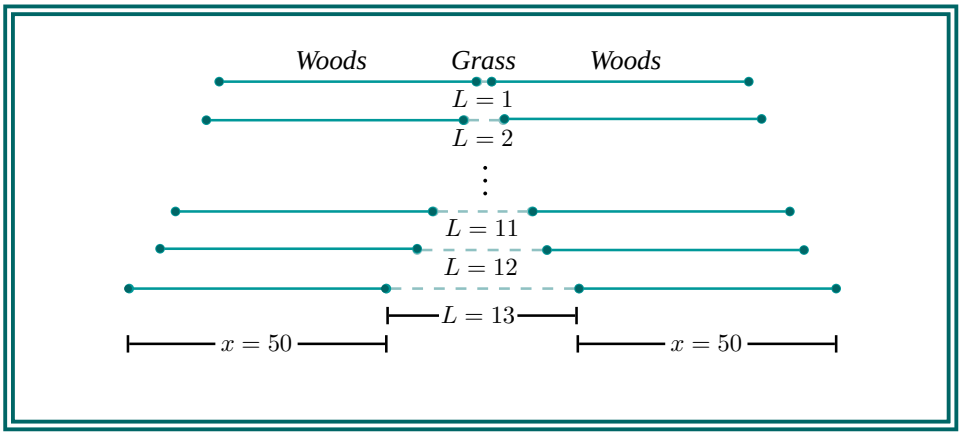

FIGURE 4.9: One-dimensional systems with different gap scarce-resources subdomains.

4.4.2 Time delay dependent on gap length

To analyse the time delay dependence on the gap between patches length, we run the model for a set of systems with different gap lengths, $L = 0, 1, 2, ..., 13$. For each system we measure the time required to fill up the right hand patch up to a fixed population of $n = 0.5$ at $x = L$ starting from the point where the population at $x = 0$, the right hand end of the left hand patch is equal to $n = 0.5$. The relation found tells us how the gap crossing time depends on the gap length.

For the set of systems studied here we assume that each system consist of a pair resources-rich patches of fixed size $x = 50$ separated by a set of different gap lengths $L = 0 - 13$ as exemplified in figure 4.9. For each system, the mesh of every subdomain, has a maximum separation between points of $x = 0.0075$, while the maximum separation between points close to the boundary is $x = .0001$. On the time scale we assume that the solution changes with a time interval of 0.05 ranging from $t = 0$ to $t = 70$ for every single system. By solving this set of systems with COMSOL Multiphysics, using the parameters $\lambda = \sqrt{2}$, $\delta = 0.05$ and $\mu_0 = 3$, we obtain the data provided in Table 4.1

The results for gap crossing time delay provided in Table 4.1 for a number of patch systems with different gap lengths are obtained from systems solutions as the ones shown in figure 4.10.

According to the data obtained from the numerical analysis, the elapsed time to cross a scarce-resources gap grows linearly for sufficiently big gap sizes. However, if the gap

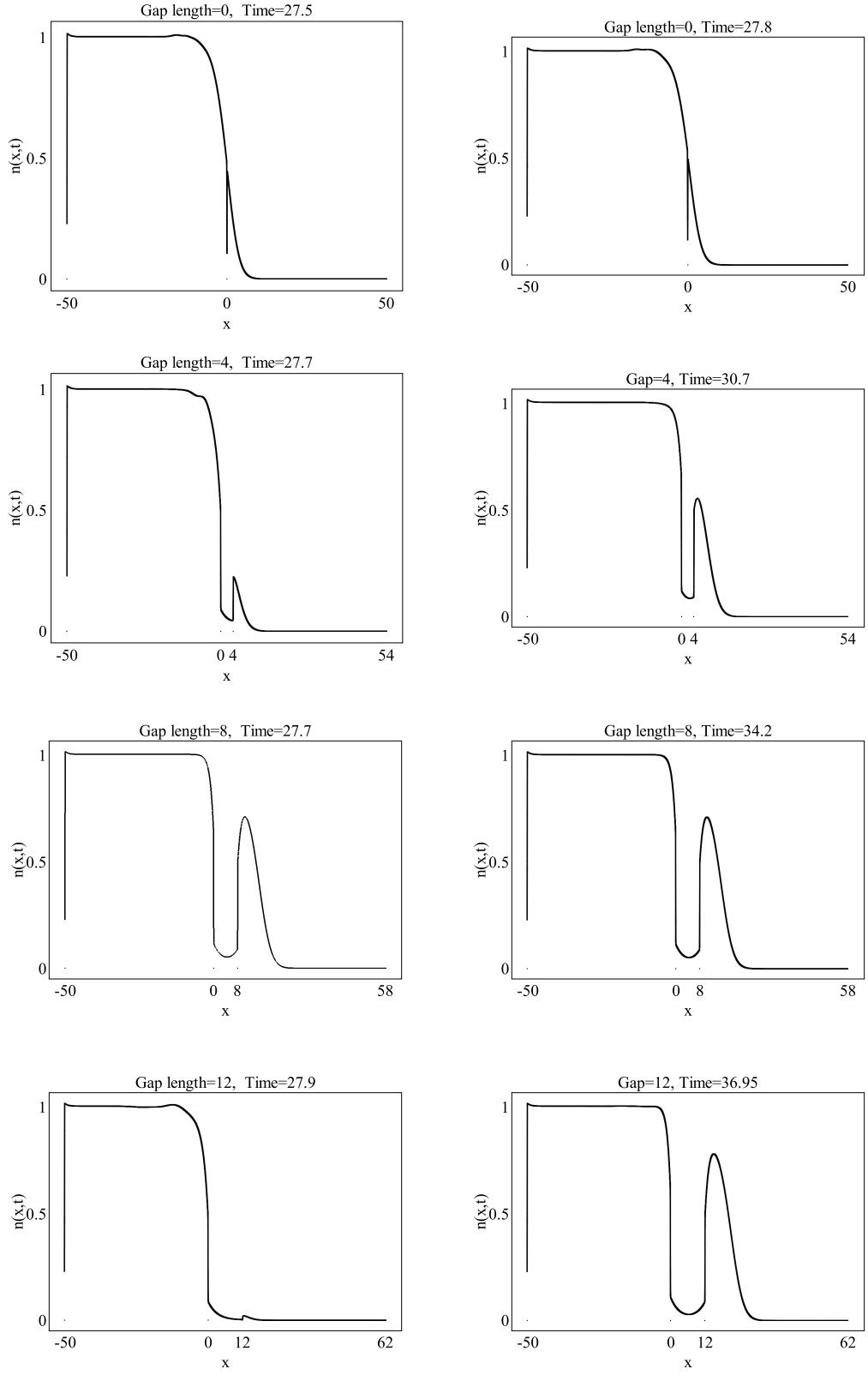

FIGURE 4.10: Population dispersal in a two corridor patches system of length $s = 50$ separated by a gap of variable length, $L = 0-13$. A relationship between the waiting gap crossing time and gap length are found. The left-hand side figures show the population at different times when $n|_{x=0} = 0.5$ and the right-hand side figures of the population at times when $n|_{x=L} = 0.5$ for different gap lengths. The parameters used here are $\lambda = \sqrt{2}$, $\delta = 0.05$ and $\mu_0 = 3$.

Gap size data		
Gap size	Mesh size	Time delay between patches
0	23336	0.3
0.25	23283	0.4
0.5	23401	0.55
0.75	23480	0.6
1	23542	0.7
1.25	23608	0.85
1.5	23686	1.0
1.75	23729	1.15
2	23790	1.3
2.5	23909	1.7
3	24028	2.0
3.5	24146	2.55
4	24263	3.0
4.5	24381	3.4
5	24498	3.8
5.5	24615	4.25
6	24732	4.5
6.5	24849	5.0
7	24966	5.5
7.5	25083	6.0
8	25200	6.5
8.5	25314	6.65
9	25434	7.0
9.5	25551	7.5
10	25666	7.8
10.5	25781	8.35
11	25901	8.6
11.5	26017	8.9
12	26134	9.05
12.5	26251	9.35
13	26368	9.5

TABLE 4.1: Numerical data for different gap sizes with $\lambda = \sqrt{2}$, $delta = 0.05$ and $\mu_0 = 3$.

size grows too much, the data analysis turns complicated because the population flux becomes of the order of the numerical error in the calculations, making the numerical results unreliable. This is the reason why we analyse only up to gap size $L = 10.5$. Figure 4.11 shows the gap crossing time delay against gap length, overlapped with the fitting curve $t = 0.8289L + 0.3586$ for $1.5 \leq L \leq 10.5$.

To evaluate the effectiveness of this curve fitting we use a couple of statistical tools. The *sum of squares due to error* (SSE) measures the deviation of the numerical obtained

data from the fitting function,

$$SSE = \sum_{i=1}^{n} w_i (t_i - f_i)^2 \tag{4.4.1}$$

where t_i corresponds to the obtained numerical data while f_i is the predicted value from the fit. w_i is the weighting applied to each point data, that in this case is assumed as 1. For this measure, a value closer to 0 indicates a small error, making the fit more reliable for prediction.

The other statistical tool we use to evaluate the effectiveness of the fitting function is called *R-square*. This statistic measures how good the fit is to explain the variation of the data defined as,

$$R - Square = 1 - \frac{\sum_{i=1}^{n} w_i (t_i - f_i)^2}{\sum_{i=1}^{n} wi (t_i - t_{av})^2}. \tag{4.4.2}$$

Here t_i represents the numerical data, f_i is the fitted data, t_{av} is the mean of the observed numerical data and $w_i = 1$ is the weighting applied to each point of the observed data. This statistic take values between 0 and 1, and the closer it gets to one, the better the prediction is [123].

For the linear function found in this section we found a $SSE = 0.14$ and a $R-square = 0.998$. These results tell us that the function fit is a good approximation to our obtained data.

The linear dependence of the time with the gap length for gaps with lengths between $1.5 \leq L \leq 10.5$ in 1-dimensional systems is shown in figure 4.12 where the function has 95% of confidence bounds, which means that only the 5% of the data falls out of the predicted fit. The width of the confidence bounds interval indicates how acurate the fit is as well. The wider the interval, the more inaccurate the fitting function is. The linear relation of crossing time with gap length is consistent with a constant velocity of the wave of advance, as seen in many invasions (e.g. Muskrat in Europe).

If the size of the gap L is increased too much, the flux obtained at $x = L$ do not meet the precision required for the numeric calculations to be reliable and the gap length time dependence becomes uncertain. Therefore, in §4.5 we perform an analytic study of how

the population change and disperse in the system studied along §4.4.

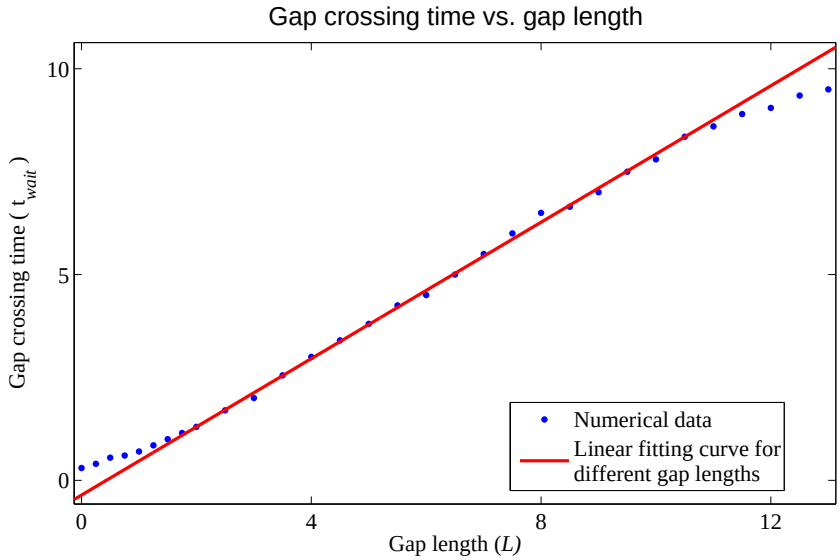

FIGURE 4.11: The blue dots corresponds to the numerical data obtained from the analysis of a series of different systems constituted by two resources-rich patches and different sized gaps in between. It measures the elapsed time to cross a gap depending on the gap length. The red line corresponds to the linear approximation for gap sizes of $L \geq 2.5$. The parameters used here are $\lambda = \sqrt{2}$, $\delta = 0.05$ and $\mu_0 = 3$

4.5 Asymptotic solutions

Analytical results of gap crossing individuals in an inhomogeneous environment are presented in this section. An asymptotic analysis of the model described in §4.3.2, in line with the estimation of the parameters discussed in §4.3.3 is taken for a one-dimensional system.

The system we analyse in this section is shown in figure 4.13. Based on the assumed knowledge of the value of the population on the left hand side resources-rich patch, we investigate how the flux of individuals leaving the full, left hand resources-rich patch, crosses the scarce-resources patch and arrives to the empty resources-rich patch, predicting the dynamics of the right hand resource-rich patch. The dynamics of the empty resources-rich patch may or may not start a new reproducing population depending on variables such as gap length, number of individuals crossing the gap, their ability to disperse and their ability to reproduce. The boundary conditions at the boundary of the empty resources-rich patch $x = L$ will be obtained from the knowledge of the initial

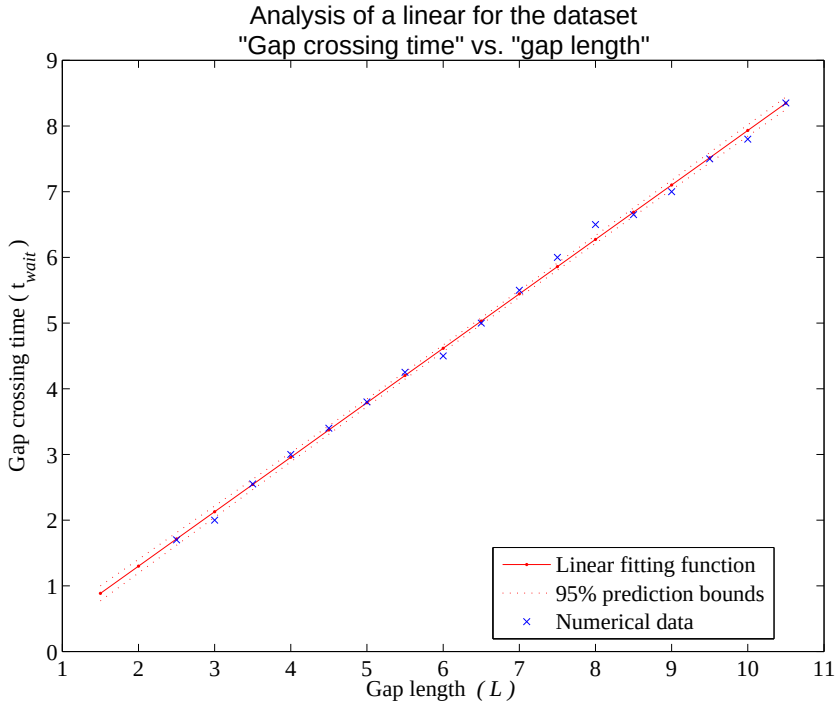

FIGURE 4.12: The dots along the graphic denote obtained data from numerical analyses of different gap sized systems. The solid line is the function fit while the dashed lines show the 95% of confidence bounds for the linear fitting function. As observed in the figure the width of the interval for the confidence bounds is quite thin, that indicates a good data fit. The parameters used here are $\lambda = \sqrt{2}$, $\delta = 0.05$ and $\mu_0 = 3$

population at the boundary of the full patch $x = 0$, and the solution of the system in the scarce-resources region.

In the resource-rich area, Ω the population distributes almost homogeneously in $x = (-\infty, 0)$. The scarce-resources zone $\Omega^{\complement}$ is located in $x = (0, L)$, where the population simply decays. Finally, from $x = L$ to $x = \infty$ another patch appears. We investigate the dynamics of the population located in this last patch based on the information obtained from the first resource-rich patch and the scarce-resource area population behaviour.

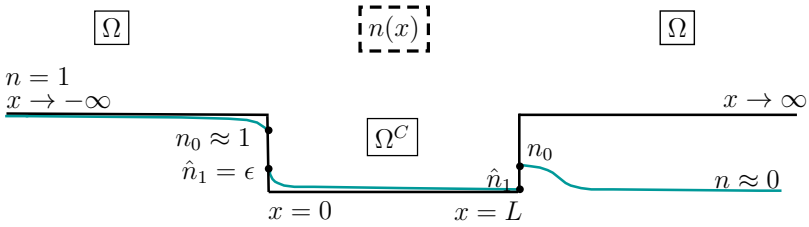

FIGURE 4.13: One-dimensional system of two resources-rich patches with a scarce-resources gap in between. The population at $x = L$ is directly related with the population at $x = 0$ and the boundary conditions.

To analytically describe the system proposed, an asymptotic analysis close to the boundaries is performed we consider the limit

$$e^{-\mu_0} = \epsilon \tag{4.5.1}$$

where $\epsilon \ll 1$ and,

$$\frac{\lambda^2}{\delta} = \frac{\Gamma}{\epsilon}, \tag{4.5.2}$$

where $\Gamma = \mathcal{O}(1)$, $\lambda = \mathcal{O}(1)$ and $\frac{\Gamma}{\epsilon} \gg 1$ as well, so that equations(4.3.24)-(4.3.27) become

$$\frac{\partial n}{\partial t} = n(1-n) + \frac{\partial^2 n}{\partial \mathbf{x}^2} \quad \text{in } x < 0 \text{ and } x > L, \tag{4.5.3}$$

$$\delta \frac{\partial n}{\partial t} = -n + \lambda^2 \frac{\partial^2 n}{\partial \mathbf{x}^2} \quad \text{in } 0 < x < L. \tag{4.5.4}$$

in order to later simplify the system. The boundary conditions become,

$$\epsilon n|_{x=0^-} = n|_{x=0^+} \quad \text{and} \quad n|_{x=L^-} = \epsilon n|_{x=L^+} \tag{4.5.5}$$

and

$$\epsilon \frac{\partial n}{\partial \mathbf{x}}\bigg|_{x=0^-} = \Gamma \frac{\partial n}{\partial \mathbf{x}}\bigg|_{x=0^+} \quad \text{and} \quad \Gamma \frac{\partial n}{\partial \mathbf{x}}\bigg|_{x=L^-} = \epsilon \frac{\partial n}{\partial \mathbf{x}}\bigg|_{x=L^+} \tag{4.5.6}$$

Recalling that $\epsilon \ll 1$ and $\delta \ll 1$, we expand n in powers of ϵ by writing

$$n = n_0 + ... \quad \text{in } (-\infty, 0) \cup (L, \infty) \tag{4.5.7}$$

$$n = \epsilon \hat{n}_1 + ... \quad \text{in } (0, L)\ . \tag{4.5.8}$$

leading to the following set of leading order equations and boundary conditions,

$$\frac{\partial n_0}{\partial t} = n_0(1-n_0) + \frac{\partial^2 n_0}{\partial \mathbf{x}^2} \quad \text{in } (-\infty, 0) \cup (L, \infty), \tag{4.5.9}$$

$$-\hat{n}_1 + \lambda^2 \frac{\partial^2 \hat{n}_1}{\partial \mathbf{x}^2} = 0 \quad \text{in } (0, L) \ , \tag{4.5.10}$$

$$n_0|_{x=0^-} = \hat{n}_1|_{x=0^+} \qquad n_0|_{x=L^+} = \hat{n}_1|_{x=L^-} \tag{4.5.11}$$

$$\left.\frac{\partial n_0}{\partial \mathbf{x}}\right|_{x=0^-} = \Gamma \left.\frac{\partial \hat{n}_1}{\partial \mathbf{x}}\right|_{x=0^+} \qquad \left.\frac{\partial n_0}{\partial \mathbf{x}}\right|_{x=L^+} = \Gamma \left.\frac{\partial \hat{n}_1}{\partial \mathbf{x}}\right|_{x=L^-} \tag{4.5.12}$$

The solution of equation (4.5.10) in $(0, L)$ is given by

$$\hat{n}_1 = A \sinh\left(\frac{x}{\lambda}\right) + B \cosh\left(\frac{x}{\lambda}\right) \tag{4.5.13}$$

while

$$\frac{\partial \hat{n}_1}{\partial x} = \frac{A}{\lambda} \cosh\left(\frac{x}{\lambda}\right) + \frac{B}{\lambda} \sinh\left(\frac{x}{\lambda}\right) \tag{4.5.14}$$

and the boundary conditions are given in equations (4.5.11) and (4.5.12). From equations (4.5.13) and (4.5.14) we find that at $x = 0$

$$\hat{n}_1|_{x=0^+} = B \tag{4.5.15}$$

and

$$\left.\frac{\partial \hat{n}_1}{\partial x}\right|_{x=0^+} = \frac{A}{\lambda} \tag{4.5.16}$$

From equations (4.5.15) and (4.5.16)and the boundary conditions given by (4.5.11) and (4.5.12) we obtain

$$A = \frac{\lambda}{\Gamma} \left.\frac{\partial n_0}{\partial x}\right|_{x=0^-} \quad \text{and } B = n_0|_{0^-}. \tag{4.5.17}$$

Substituting the values of A and B and rearranging terms in equations (4.5.13) and (4.5.14) we obtain the relations

$$n_0|_{x=L^+} = \hat{n}_1|_{x=L^-} = \frac{\lambda}{\Gamma} \left.\frac{\partial n_0}{\partial x}\right|_{x=0^-} \sinh(L/\lambda) + n_0|_{x=0^-} \cosh(L/\lambda), \tag{4.5.18}$$

$$\left.\frac{\partial n_0}{\partial x}\right|_{x=L^+} = \Gamma \left.\frac{\partial \hat{n}_1}{\partial x}\right|_{x=L^-} = \left.\frac{\partial n_0}{\partial x}\right|_{x=0^-} \cosh(L/\lambda) + \frac{\Gamma}{\lambda}\, n_0|_{x=0^-} \sinh(L/\lambda). \tag{4.5.19}$$

hence,

$$n_0|_{x=0^-} = n_0|_{x=L^+} \cosh(L/\lambda) - \frac{\lambda}{\Gamma} \left.\frac{\partial n_0}{\partial x}\right|_{x=L^+} \sinh(L/\lambda), \tag{4.5.20}$$

and

$$\left.\frac{\partial n_0}{\partial x}\right|_{x=0^-} = \left.\frac{\partial n_0}{\partial x}\right|_{x=L^+} \cosh(L/\lambda) - \frac{\Gamma}{\lambda}\, n_0|_{x=L^+} \sinh(L/\lambda). \tag{4.5.21}$$

obtaining a set of relationships between the population at $x = 0$ and the population at $x = L$.

We now seek an approximate solution by making the further approximation that $L >> \lambda$, where λ is a dimensionless quantity related to the the wave of advance velocities rate inside and outside the woodland patch.

We expand equations (4.5.18) – (4.5.21) in Taylor series to find that,

$$n_0|_{x=L^+} \approx e^{L/\lambda} \left(\frac{\lambda}{\Gamma} \left.\frac{\partial n_0}{\partial x}\right|_{x=0^-} + n_0|_{x=0^-} \right), \tag{4.5.22}$$

$$\left.\frac{\partial n_0}{\partial x}\right|_{x=L^+} \approx e^{L/\lambda} \left(\left.\frac{\partial n_0}{\partial x}\right|_{x=0^-} + \frac{\Gamma}{\lambda}\, n_0|_{x=0^-} \right), \tag{4.5.23}$$

$$\left(n_0|_{x=L^+} - \frac{\lambda}{\Gamma} \left.\frac{\partial n_0}{\partial x}\right|_{x=L^+} \right) \approx n_0|_{x=0^-}\, e^{(-L/\lambda)}, \tag{4.5.24}$$

and

$$\left(\left.\frac{\partial n_0}{\partial x}\right|_{x=L^+} - \frac{\Gamma}{\lambda}\, n_0|_{x=L^+} \right) \approx \left.\frac{\partial n_0}{\partial x}\right|_{x=0^-} e^{(-L/\lambda)}. \tag{4.5.25}$$

If we know the value of the population at $n_0|_{x=0^-}$, equation (4.5.24) give us a set of mixed boundary conditions for the scarce-resource region in terms of the gap length. We can then find the boundary condition for the population at $x = L^+$ since we know

both, the governing equation for the population in the resource scarce region and the boundary conditions.

The value of $n_0|_{x=0^-}$ is obtained from equation (4.5.22). The approximate boundary condition at $x = 0^-$ is then given by

$$\frac{\lambda}{\Gamma}\frac{\partial n_0}{\partial x}\bigg|_{x=0^-} + n_0|_{x=0^-} \approx 0. \tag{4.5.26}$$

since we are assuming that $L >> 0$.

Now we look for the steady state solution of the problem for $x < 0$. Assuming that the extension of the resource-rich patch $x < 0$ is infinite, we can make use of the results found in Chapter 3. In §3.1.3 we analysed the stationary state of a semi-infinite patch following the equation

$$0 = n(1-n) + \frac{d^2n}{dx^2}. \tag{4.5.27}$$

with the boundary conditions given by

$$n = 1 \quad \text{as } x \to \infty. \tag{4.5.28}$$

with solutions for the population and its derivative given by

$$n(x) = \frac{1}{2}\left[3\left(\frac{1-(2-\sqrt{3})e^{-(x-x_0)}}{1+(2-\sqrt{3})e^{-(x-x_0)}}\right)^2 - 1\right]. \tag{4.5.29}$$

and

$$\frac{dn}{dx} = \frac{(6e^{(x-x_0)}(7-4\sqrt{3}+(-2+\sqrt{3})e^{(x-x_0)}))}{(-2+\sqrt{3}-e^{(x-x_0)})^3}. \tag{4.5.30}$$

In the case we are studying here, the resource-rich patch is located over the interval $(-\infty, 0)$, therefore, the solutions given by (4.5.29) and (4.5.30) take negative values of x. The boundary condition applied in §3.1.3 was $n|_{x=0} = 0$ (and therefore $x_0 = 0$). Here we use the boundary condition provided by equation (4.5.26).

The solutions for the population and its derivative, occupying a semi-infinite patch

located in $(-\infty, 0)$ are then given by

$$n(x) = \frac{1}{2}\left[3\left(\frac{1-(2-\sqrt{3})e^{(x-x_0)}}{1+(2-\sqrt{3})e^{(x-x_0)}}\right)^2 - 1\right] \quad \text{for } x < 0 \tag{4.5.31}$$

and

$$\frac{dn}{dx} = \frac{6e^{(x-x_0)}((2-\sqrt{3}) + (7-4\sqrt{3})e^{(x-x_0)})}{((-2+\sqrt{3})e^{x-x_0} - 1)^3} \quad \text{for } x < 0. \tag{4.5.32}$$

Applying now the boundary condition (4.5.26) at $x = 0^-$, we obtain,

$$\frac{1}{2}\left[3\left(\frac{1-(2-\sqrt{3})e^{(-x_0)}}{1+(2-\sqrt{3})e^{(-x_0)}}\right)^2 - 1\right] + \sqrt{2}\frac{6e^{(-x_0)}((2-\sqrt{3}) + (7-4\sqrt{3})e^{(-x_0)})}{((-2+\sqrt{3})e^{-x_0} - 1)^3} = 0, \tag{4.5.33}$$

from where we can find the value of n at $x = 0^-$. Assuming that $\lambda/\Gamma = \sqrt{2}$, we take the only real positive solution obtained for x_0 given by $x_0 = 1.75$ finding that,

$$n_0|_{x=0^-} \approx 0.745. \tag{4.5.34}$$

Figure 4.14 shows the solution for the population in a stationary state for $x < 0$ with the boundary condition given by equation (4.5.26) with $\lambda/\Gamma = \sqrt{2}$ so that $x_0 = 1.75$.

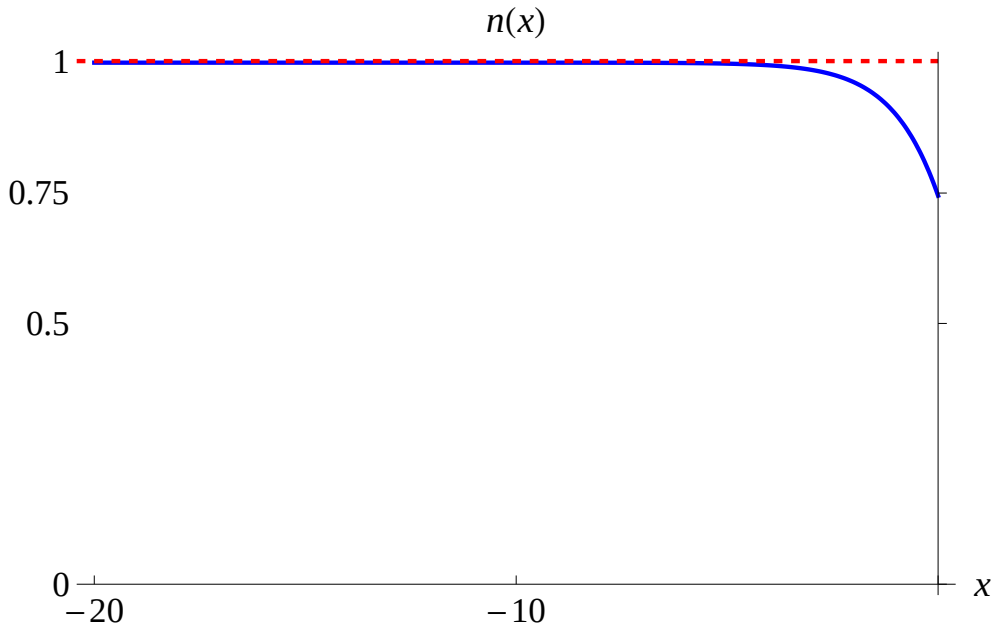

FIGURE 4.14: Population for $x < 0$ in a semi-infinite patch. As $x \to -\infty$, $n \to 1$. At $x = 0$ it is found that $n = 0.745$. We assumed that $\lambda/\Gamma \approx 0.7$.

Once the value of $n_0|_{x=0} = 0.745$ is found, we can substitute it in equation (4.5.24) obtaining,

$$\left(n_0|_{x=L^+} - \frac{\lambda}{\Gamma} \left. \frac{\partial n_0}{\partial x} \right|_{x=L^+} \right) \approx 0.745 e^{(-L/\lambda)}. \tag{4.5.35}$$

Equation (4.5.35) give us a set of mixed boundary conditions for the right hand resources-rich patch shown in figure 4.13. If we also suppose that the second patch is infinite, we can assume that the population at $x = \infty$ will be zero. With this assumptions and the results found in this section, we can now investigate the dynamics of the second patch.

4.5.1 Population dynamics after crossing a gap

In this section we investigate the dynamics of an initially empty patch with plentiful resources, where the boundary conditions are taken from equation (4.5.35) and from the assumption of having a very large patch ($x \to \infty$). As in previous analysis, the population in the initially empty patch takes the dynamics given by equation (3.3.8),

$$\frac{\partial n}{\partial t} = n(1-n) + \nabla^2 n \tag{4.5.36}$$

in a one-dimensional space.

With the initial conditions (4.5.35) plus the assumption that at $t = 0$, $n_0 = 0$ and as $x \to \infty$ the population tends to zero,

$$n|_{t=0} = 0, \tag{4.5.37}$$

and

$$n|_{x\to\infty} = 0, \tag{4.5.38}$$

we analyse the population dynamics in the new patch close to its boundary. Figure 4.15 shows the system we analyse in this section.

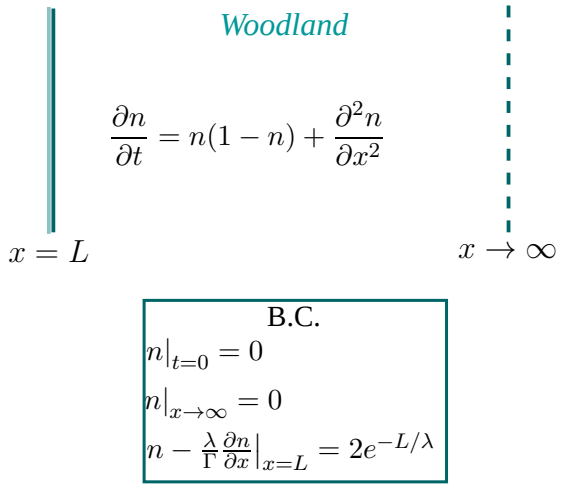

FIGURE 4.15: The dynamics of a gap with the boundary conditions stated is studied. These boundary conditions emerge after a number of individuals coming from a plentiful resource area cross a scarce-resources gap in a one-dimensional system. The population at $x = L$ is directly related, and predicted by with the population at $x = 0$ and the boundary conditions.

Assuming that $e^{-L/\lambda} \to 0$ we can write,

$$e^{-L/\lambda} = \vartheta \ll 1. \tag{4.5.39}$$

Expanding n in powers of ϑ,

$$n = \vartheta n^{(0)} + ... \tag{4.5.40}$$

the set of leading order equations (4.5.36) and boundary conditions (4.5.35), (4.5.37) and (4.5.38) to order ϑ is,

$$\frac{\partial n^{(0)}}{\partial t} = n^{(0)} + \frac{\partial^2 n^{(0)}}{\partial x^2} \tag{4.5.41}$$

$$n^{(0)}\Big|_{x=L} - \frac{\lambda}{\Gamma}\left.\frac{\partial n^{(0)}}{\partial x}\right|_{x=L} = 1, \tag{4.5.42}$$

$$n^{(0)}\Big|_{x\to\infty} = 0 \tag{4.5.43}$$

and

$$n^{(0)}\Big|_{t=0} = 0. \tag{4.5.44}$$

This set of equations is linear, therefore, we can solve it using Laplace transforms.

Defining

$$\bar{n}^{(0)}(x,s) = \int_0^\infty e^{-st} n^{(0)}(x,t)dt, \tag{4.5.45}$$

equations (4.5.41) – (4.5.44) transforms into

$$s\bar{n}^{(0)} = \bar{n}^{(0)} + \frac{\partial^2 \bar{n}^{(0)}}{\partial \mathbf{x}^2}, \tag{4.5.46}$$

$$\left(\bar{n}^{(0)}\Big|_{x=L} - \frac{\lambda}{\Gamma} \frac{\partial n^{(0)}}{\partial x}\Big|_{x=L} \right) = \frac{1}{s}, \tag{4.5.47}$$

and

$$\bar{n}^{(0)}\Big|_{x\to\infty} = 0. \tag{4.5.48}$$

The solution of equation (4.5.46) in the frequency domain is then

$$\bar{n}^{(0)} = Ce^{\sqrt{s-1}(x-L)} + De^{-\sqrt{s-1}(x-L)}. \tag{4.5.49}$$

From equation 4.5.48 we obtain $C = 0$ since $\bar{n}^{(0)} = 0$ as $x \to \infty$, therefore,

$$\bar{n}^{(0)} = De^{-\sqrt{s-1}(x-L)}. \tag{4.5.50}$$

and

$$\frac{\partial \bar{n}^{(0)}}{\partial x} = -\sqrt{s-1}De^{-\sqrt{s-1}(x-L)}. \tag{4.5.51}$$

The value of D is obtained by evaluating equations (4.5.50) – (4.5.51) at $x = L$, and applying the boundary condition from equation 4.5.47,

$$D = \frac{1}{s\left(1 + \frac{\lambda}{\Gamma}\sqrt{s-1}\right)} \equiv \frac{\frac{\Gamma}{\lambda}}{s\frac{\Gamma}{\lambda} + s\sqrt{s-1}} \tag{4.5.52}$$

therefore,

$$\bar{n}^{(0)}(s,t) = \frac{\frac{\Gamma}{\lambda}}{s\left(\frac{\Gamma}{\lambda} + \sqrt{s-1}\right)} e^{-\sqrt{s-1}(x-L)}. \tag{4.5.53}$$

Defining

$$\mathcal{F}(s) = e^{-\sqrt{s-1}(x-L)}, \tag{4.5.54}$$

$$\mathcal{G}(s) = \frac{\frac{\Gamma}{\lambda}}{s\left(\frac{\Gamma}{\lambda} + \sqrt{s-1}\right)} \tag{4.5.55}$$

and using the convolution theorem,

$$\mathcal{L}^{-1}(\mathcal{F}(s)\cdot\mathcal{G}(s)) = \int_0^t f(u)\cdot g(t-u)du \tag{4.5.56}$$

where $f(t)$ and $g(t)$ are the inverse Laplace transforms of $\mathcal{F}(s)$ and $\mathcal{G}(s)$,

$$f(t) = \frac{(x-L)e^{\frac{-(x-L)^2}{4t}+t}}{2\sqrt{\pi t^3}}, \tag{4.5.57}$$

$$g(t) = \frac{\left(\frac{\Gamma}{\lambda}\right)^2\left(1 - e^{\left(\left(\frac{\Gamma}{\lambda}\right)^2+1\right)t}\operatorname{erfc}\left(\frac{\Gamma}{\lambda}\sqrt{t}\right)\right) + \frac{\Gamma}{\lambda}\operatorname{erfi}(\sqrt{t})}{1+\left(\frac{\Gamma}{\lambda}\right)^2}, \tag{4.5.58}$$

where erfc is the complementary error function and erfi is the imaginary error function. The solution in the time domain for equation (4.5.53) is then,

$$n^{(0)}(x,t) = \int_0^t \frac{\left(\frac{\Gamma}{\lambda}\right)^2\left(1 - e^{\left(\left(\frac{\Gamma}{\lambda}\right)^2+1\right)(t-u)}\operatorname{erfc}(\frac{\Gamma}{\lambda}\sqrt{t-u})\right) + \frac{\Gamma}{\lambda}\operatorname{erfi}(\sqrt{t-u})}{1+\left(\frac{\Gamma}{\lambda}\right)^2}\cdot \frac{(x-L)e^{\frac{-(x-L)^2}{4u}+u}}{2\sqrt{\pi u^3}}du. \tag{4.5.59}$$

Assuming that $\dfrac{\Gamma}{\lambda} = 0.7$, the solution of equation (4.5.59) can be plotted. This solution is shown in figure 4.16, where it is observed how the population grows exponentially for $x \approx L$, decaying later as $x \to \infty$. At the same time, the figure shows how the population grows with time, presenting the solution of the equation at 5 different times.

4.5.2 Gap crossing time analysis

To finish the study of this one-dimensional type of systems, here we use some asymptotic analysis to investigate how the elapsed time to cross an asymptotically large gap varies with the size of the gap. According to equation (4.5.59), the population close to the

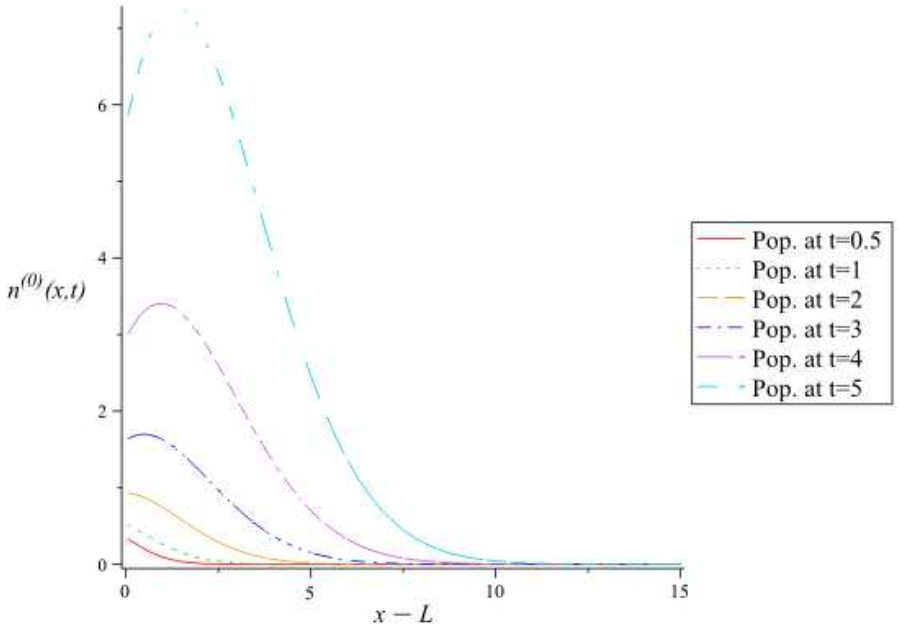

FIGURE 4.16: Semi-analytical results of the population growth in the second patch after the population flux start reaching the second patch with $\Gamma/\lambda = 0.7$.

boundary is given by,

$$n^{(0)}(x,t) = \int_0^t \frac{\left(\frac{\Gamma}{\lambda}\right)^2 \left(1 - e^{\left(\left(\frac{\Gamma}{\lambda}\right)^2+1\right)(t-u)} \operatorname{erfc}(\frac{\Gamma}{\lambda}\sqrt{t-u})\right) + \frac{\Gamma}{\lambda}\operatorname{erfi}(\sqrt{t-u})}{1+\left(\frac{\Gamma}{\lambda}\right)^2} \cdot \frac{(x-L)e^{\frac{-(x-L)^2}{4u}+u}}{2\sqrt{\pi u^3}} du. \quad (4.5.60)$$

To find an approximation to the gap crossing time, we look for the values of t where n first becomes of $\mathcal{O}(1)$. We know from (4.5.39) that

$$n = \vartheta n^{(0)} + ... \quad (4.5.61)$$

where

$$\vartheta = e^{-L/\lambda} \quad (4.5.62)$$

therefore n becomes of size one

$$n^{(0)} \approx e^{L/\lambda} \quad (4.5.63)$$

from where we can find a relationship for the gap length L dependent on the gap crossing time t given by

$$e^{L/\lambda} = \int_0^t \frac{\left(\frac{\Gamma}{\lambda}\right)^2 \left(1 - e^{\left(\left(\frac{\Gamma}{\lambda}\right)^2+1\right)(t-u)} \operatorname{erfc}(\frac{\Gamma}{\lambda}\sqrt{t-u})\right) + \frac{\Gamma}{\lambda}\operatorname{erfi}(\sqrt{t-u})}{1+\left(\frac{\Gamma}{\lambda}\right)^2} \cdot \frac{(x-L)e^{\frac{-(x-L)^2}{4u}+u}}{2\sqrt{\pi u^3}} du \quad (4.5.64)$$

Taking natural logarithms on both sides we obtain

$$\frac{L}{\lambda} \approx \log\left(\int_0^t \frac{\left(\frac{\Gamma}{\lambda}\right)^2 \left(1 - e^{\left(\left(\frac{\Gamma}{\lambda}\right)^2+1\right)(t-u)} \operatorname{erfc}(\frac{\Gamma}{\lambda}\sqrt{t-u})\right) + \frac{\Gamma}{\lambda}\operatorname{erfi}(\sqrt{t-u})}{1+\left(\frac{\Gamma}{\lambda}\right)^2} \cdot \frac{(x-L)e^{\frac{-(x-L)^2}{4u}+u}}{2\sqrt{\pi u^3}} du\right) \quad (4.5.65)$$

that once evaluated and plotted at $x \approx L$, results in a linear dependence of t over L. The slope of this relationship is $\log(f(t)) \approx L/\lambda = 0.8440t - 2.41$, result in agreement with the data found in the numerical analysis where we had found that $t = 0.8289L + 0.3586$, that in terms of L/λ is $L/\lambda = 0.8530t - 0.3059$ with $\lambda = \sqrt{2}$. This result is valid for large L (*i.e.* for values where $e^{L/\lambda} \approx 0$), where we can observe that the slope of the curves match almost perfectly. Let us note also that the slope of the curve depends on the value of the parameter λ which varies according to the species under study and the spatial structure.

In figure 4.17 we show the linear dependence of L/λ over t for $\Gamma = 1$, $\lambda = \sqrt{2}$, and $L = 10$, while figure 4.18 shows the comparison between the numerical results and the semi-analytical ones.

We can conclude from this section that both results show that the gap crossing time shows a linear relationship with the gap length, which, as expected, tell us that the longer the gap between patches, the longer the time the individuals take to cross the gap.

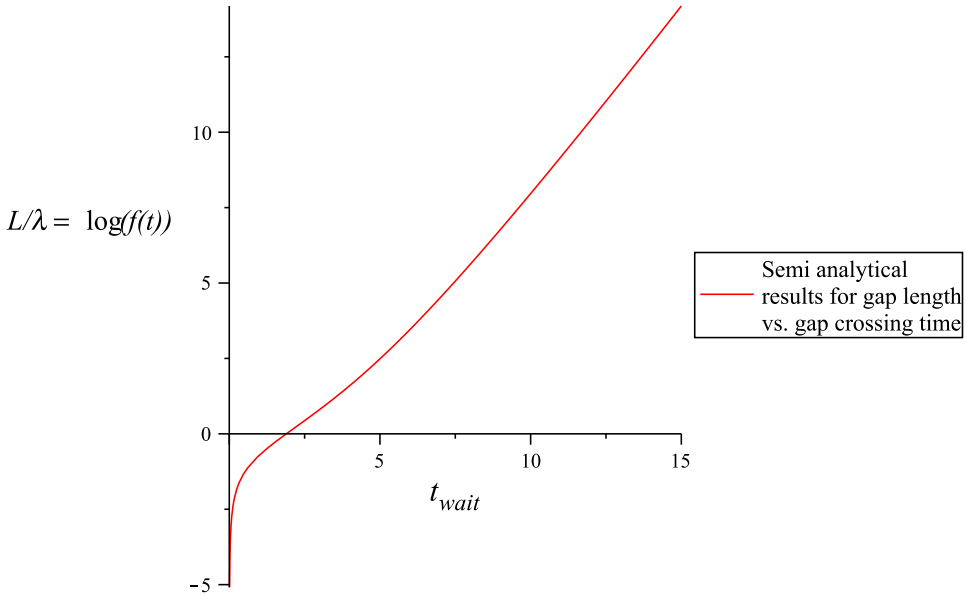

FIGURE 4.17: Semi-analytic results found for the dependence of the gap length where $L/\lambda \approx \log(n^{(0)}(t))$ versus the gap crossing time t. The parameters used here are given by $\lambda = \sqrt{(2)}$ and $\Gamma = 1$.

In the following section we analyse another factors that can contribute to the slowing of the spread of individuals in a fragmented environment.

4.5.3 Allee effect

Another possible scenario in the analysis of population dispersal in a fragmented environment is to assume the existence of an *Allee effect* in the population growth function among the resource-rich regions. The Allee effect is a negative density dependence in the population and it occurs when population growth rate is reduced at low population size [89]. An Allee effect may occur for example, when the reproductive success is very poor due to factors such as low fecundity or difficulty to find mates.

The spread of an invading species typically starts at very low density populations. This suggest that we should include Allee effects in the model, and we suspect that they may

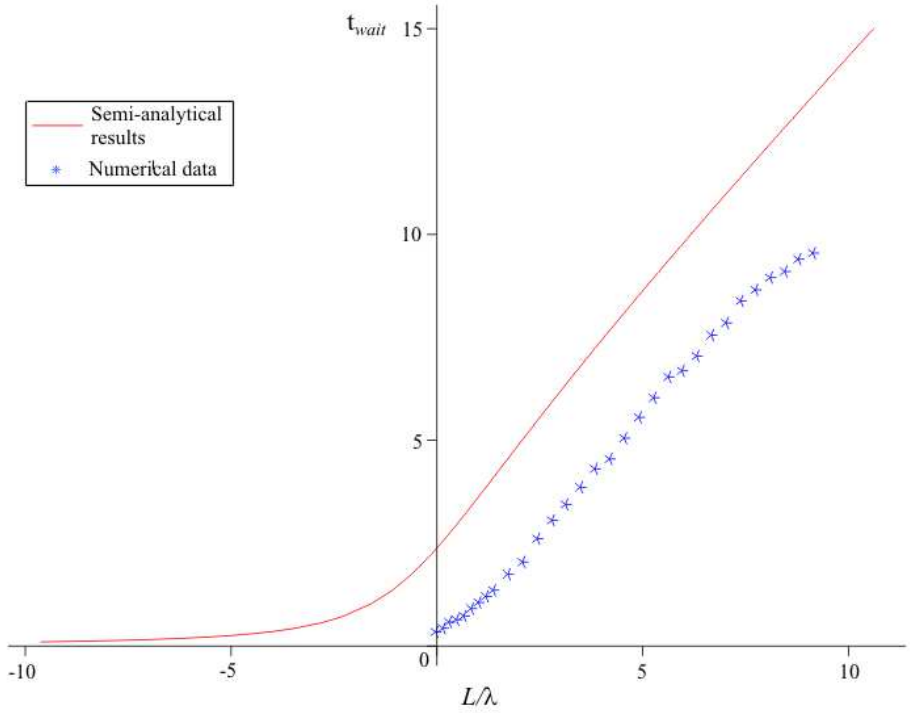

FIGURE 4.18: Numerical and semi-analytic results found for the dependence of the gap length L versus the gap crossing time t. The comparison between results is given for large L where both results have practically the same slope. These results have importance only for $L > 0$. The parameters used here are given by $\lambda = \sqrt{2}$ and $\Gamma/\lambda = 0.7$ where we have assumed that $\Gamma = \mathcal{O}(1)$.

significantly influence the spread. Allee effects are known to affect the strategies for optimal control as well as the determination of individuals spatial ranges, distributions and patterns [103].

The system we analyse in this section is the same we analysed in §4.5 and shown in figure 4.13. Based on knowledge of the value of the population at the boundary of the left hand side resources-rich patch, we investigate the dynamics of the right hand resources-rich patch. In this case the dynamics of the empty right handed resources-rich patch do not follow simple logistic growth, but a function presenting an Allee effect. This effect may results in the possible collapse of the population depending on variables such as Allee effect strength, as well as gap length, number of individuals crossing the gap, their ability to disperse and their ability to reproduce.

To model the Allee effect, we introduce a generic growth function including a negative density dependence factor at low population. Consider a single population system, the

population growth can be described by the equation

$$f(n, \mathbf{r}, t) = \alpha(n) g(n, \mathbf{r}) \quad \text{in the resource-rich regions} \tag{4.5.66}$$

where $\alpha(n)$ denotes a negative density dependent net growth function, where the net growth rate is given by

$$\alpha = b - d \tag{4.5.67}$$

where b is the total number of population births and d, the total number of deaths. We include the Allee effect by assuming that the number population births depends on the population density, so that

$$b \to \frac{\bar{b}\,(n/n_0)}{1 + n/n_0} \tag{4.5.68}$$

where n_0 is related to the critical population where α goes negative. Rewriting equation (4.5.67) in terms of (4.5.68) we obtain,

$$\alpha = \bar{\alpha} - \bar{b}\left(\frac{n_0}{n + n_0}\right) \tag{4.5.69}$$

where $\bar{\alpha} = \bar{b} - d$. Substituting (4.5.69) in (4.3.1) and (4.3.2) we can write

$$\frac{\partial n^*}{\partial t^*} = \left[\bar{\alpha} - \bar{b}\left(\frac{n_0}{n^* + n_0}\right)\right] n^*(1 - \frac{n^*}{\chi}) + D\frac{\partial^2 n^*}{\partial x^{*2}} \tag{4.5.70}$$

where χ, represents the carrying capacity of the system, D is the diffusion coefficient in the resource-rich regions and $\left[\bar{\alpha} - \bar{b}\left(\frac{n_0}{n^* + n_0}\right)\right]$ is the net population growth rate which gives us a density dependent growth function for the areas of rich resources. Here the stars denote dimensional variables.

4.5.3.1 Non-dimensionalisation

In order to simplify equation (4.5.70) we non-dimensionalise the system by,

$$t = \bar{\alpha} t^*, \quad n = \frac{n^*}{\chi}, \quad \mathbf{x} = \frac{\mathbf{x}^*}{\xi}, \tag{4.5.71}$$

where, $\xi = \sqrt{\frac{D}{\bar{\alpha}}}$. χ represents the carrying capacity of the system and $\bar{\alpha}$ is the density dependent population growth rate and D is the diffusion coefficient in the resource-rich regions. This gives the non-dimensional equation

$$\frac{\partial n}{\partial t} = \left[1 - \frac{\varsigma\nu}{\varsigma + n}\right] n(1-n) + \frac{\partial^2 n}{\partial x^2} \quad \text{in the resource-rich regions.} \tag{4.5.72}$$

where,

$$\varsigma = n_0/\chi, \quad \text{and } \nu = \bar{b}/\bar{\alpha}\ . \tag{4.5.73}$$

Figure 4.19 shows how the Allee effect influences the population growth function. Hereafter we shall assume that $\varsigma << 1$.

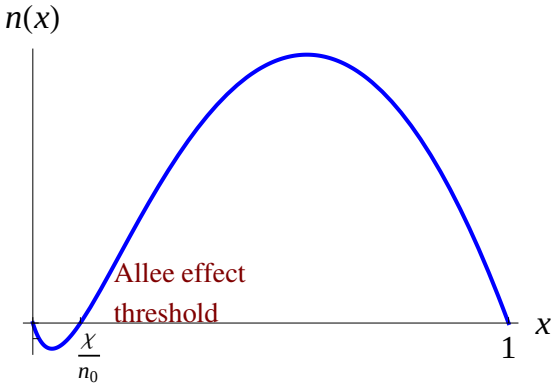

FIGURE 4.19: Allee effect influence on the population growth in a empty resources-rich patch. The growth rate is negative below some threshold and it becomes positive after this threshold indicating that at values of $n \approx 0$, the reproductive success is unlikely.

4.5.3.2 Steady state analysis

We now would like to investigate what happens in the initially empty patch located at $x > L$ under the presence of an Allee effect. Our hypothesis is that migration from $x < 0$ results in either (I) a steady solution for a small decreasing population in $x > L$, or (II) a growing population solution in $x > L$ that eventually develops into a travelling wave. Here, we investigate the possibility of non-growing forms due to the presence of Allee effects in form of steady state solutions.

Writing the set of governing equations and boundary conditions for the initially empty

patch and assuming that $n = \mathcal{O}(\varsigma)$, since the population flux arriving to the patch is close to zero at the boundary we write $n \approx \varsigma N$ in $x > L$. To a leading order approximation, equation (4.5.72) becomes,

$$\frac{\partial N}{\partial t} = \left[1 - \frac{\nu}{1+N}\right] N + \frac{\partial^2 N}{\partial x^2}. \tag{4.5.74}$$

The boundary conditions for this system come from the asymptotic relationships we found in §4.5 between the population at $x = 0$ and $x = L$. At $x = L^+$ equation (4.5.24) gives,

$$\left(N|_{x=L^+} - \frac{\lambda}{\Gamma} \frac{\partial N}{\partial x}\bigg|_{x=L^+} \right) \approx \frac{n|_{x=0^-}}{\varsigma} e^{(-L/\lambda)}. \tag{4.5.75}$$

to order ς. The boundary conditions at $x \to \infty$ are given by

$$N \to 0 \quad \text{and} \quad \frac{\partial N}{\partial x} \to 0 \quad \text{as } x \to \infty \tag{4.5.76}$$

Hence, the interesting limit happens when $\dfrac{e^{(-L/\lambda)}}{\varsigma}$ is of $\mathcal{O}(1)$. Once the governing equation and boundary conditions are set, we look for a steady state solution to equation (4.5.74) satisfying,

$$0 = \left[1 - \frac{\nu}{1+N}\right] N + \frac{\partial^2 N}{\partial x^2}. \tag{4.5.77}$$

Writing $\dfrac{\partial N}{\partial x} = u$, we can rewrite equation (4.5.77) as

$$u du = -\left[1 - \frac{\nu}{1+N}\right] N dN. \tag{4.5.78}$$

This equation can be integrated on both sides, to obtain an expression for $\dfrac{\partial N}{\partial x}$ in terms of N given by

$$\frac{\partial N}{\partial x} = \pm \left[2\nu(N - \log(N+1)) - N^2\right]^{1/2}, \tag{4.5.79}$$

where the constant factor is equal to zero considering the boundary conditions given by equation (4.5.76). As we are looking for a decaying solution to equation (4.5.79) so $n = 0$ as $x \to \infty$, we substitute the negative solution of (4.5.79) into the boundary condition

(4.5.75) to obtain

$$\left(N|_{x=L^+} + \frac{\lambda}{\Gamma} \left[2\nu(N - \log(N+1)) - N^2 \right]^{1/2} \Big|_{x=L^+} \right) = \frac{n|_{x=0^-}}{\varsigma} e^{(-L/\lambda)}. \qquad (4.5.80)$$

This equation gives us a relationship for $N|_{x=L^+}$ in terms of the gap distance between the two resource-rich patches. If equation (4.5.80) has at least one real root, then equation (4.5.77) is fulfilled and steady solutions to equation (4.5.79) exist. If no root can be found, then there is no stationary state solution to (4.5.79), and our hypothesis is that the population carries on growing, developing into a travelling wave solution over time.

Defining $M = \frac{n|_{x=0^-}}{\varsigma} e^{(-L/\lambda)}$, we can now plot equation (4.5.80) for different values of M and ν. Solutions to the stationary state are possible whenever equation (4.5.80) has a real root, *i.e.* when the solution to equation (4.5.80) crosses the x-axis. Notice that, for each value of ν there is a critical value of M (or L) for which a stationary state solution exist. If not such solution exists, we anticipate that the population will develop into a travelling wave. Notice that the values that M can take range between $0 - 0.745$, since $N|_{x=0^+} = 0.745$ from equation (4.5.35), and $L \geq 0$. The smaller M is, the bigger the gap L is. Therefore, the existence of a stationary state solution increases as M decreases.

From the solutions to equation (4.5.80) shown in figure 4.20 we see that, if $\frac{n|_{x=0^-}}{\varsigma} e^{(-L/\lambda)}$ is large enough, then no steady solutions exist. At the same time, if the Allee effect is close to zero or non-existent, there are no solutions to the stationary state. However, as ν increases, steady solutions start to appear. Finally, if $\nu = 0$, there is no real solution to equation (4.5.80). This is in accordance with what one would expect. Large gaps and large Allee parameters stop the solution from propagating.

Figure 4.20 shows the solution to equation (4.5.80) displaying the dependence of the parameter ν on M. Varying the values of these two parameters $\nu \in [1, 1.35]$ and $M \in [0, 0.7]$ and using the values for the parameters $\Gamma = 1$ and $\lambda = \sqrt{2}$, we discover a family of solutions for the existence of steady state solutions to equation (4.5.80), that occurs when a solution crosses the N-axis. Notice that for each value of M and ν there is only one curve solution which may or may not cross the N-axis. By fixing the value of ν we

can find a critical value of M where the solution for the stationary state exist; using the critical value of M we can also find the critical value of L where stationary state solutions exist.

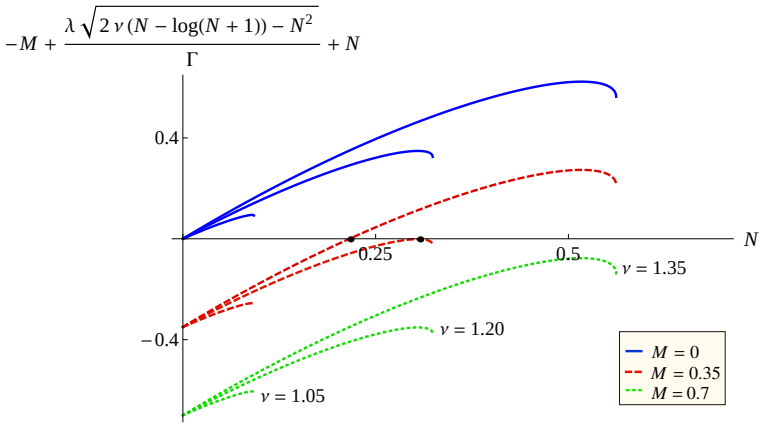

FIGURE 4.20: The Allee effect parameter ν and the gap length parameter M give place to a set of stationary state solutions to equation (4.5.80) for $N = N|_{x=L^+}$. These solutions are found when a curve crosses the x-axis indicating the existence of a real root. These roots are denoted by the black dots in the figure. The parameters range here are $M \in [0, 0.7]$ and $\nu \in [1, 1.35]$ while $\lambda = \sqrt{2}$ and $\Gamma = 1$.

As an example we assume that $\nu = 1.06$ and $M = 0.093$. Using these two values we numerically find the root of equation 4.5.80, given by $N = 0.088$. As the root exist, we now solve numerically equation (4.5.79) with the value of $N|_{x=L^+}$ equal to $N = 0.088$. Figure 4.21 shows the solution for the population close to $x = L$ with the parameters mentioned.

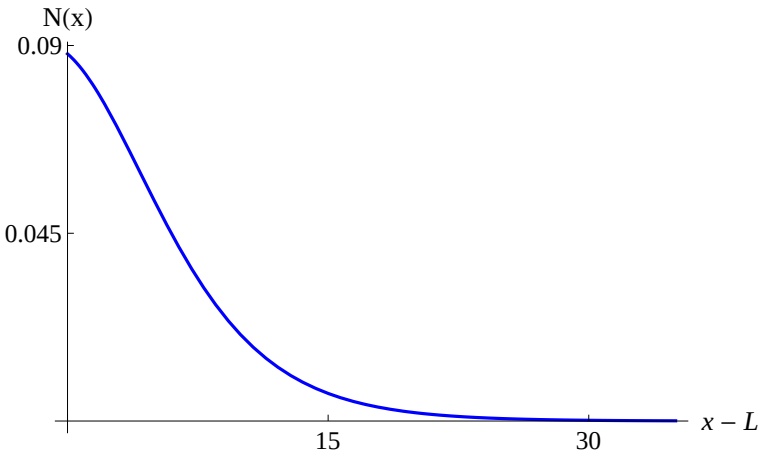

FIGURE 4.21: Solution of equation 4.5.74 for the population dependence on the distance. This population presents an Allee effect and has a steady state solution where a small population decays along the right hand patch. The Allee effect parameters used are $M = 0.093$, and $\nu = 1.06$.

Now, from figure 4.20 we can observe that for each value of ν we can find a critical value of M at which the stationary state solution ceases to exist. Since $M = \frac{n|_{x=0^-}}{\varsigma} e^{(-L/\lambda)}$, the M_{crit} is given by,

$$M_{crit} = \frac{n|_{x=0^-}}{\varsigma} e^{(-L_{crit}/\lambda)}, \tag{4.5.81}$$

and the L_{crit} is then given by

$$L_{crit} = \lambda \log\left(\frac{n|_{x=0^-}}{\varsigma M_{crit}}\right). \tag{4.5.82}$$

Equations (4.5.80), (4.5.81) amd (4.5.82) give us a set of relationship between M_{crit}, L_{crit} and ν from which we can find the maximum distance that a population can cross. According to these relationships, if $L > L_{crit}$, only stationary state solutions exist, and no dispersal takes place. If $L < L_{crit}$ then, we believe that the solution develops into a travelling wave solution. In the following section, we test these results against some numerical simulations.

Figure 4.22 shows how the critical gap length L_{crit} depends on the Allee parameter. As ν grows, the critical length L_{crit} decreases, as expected. The larger the Allee effect is, the smaller distance the individuals are able to cross in order to reproduce and form population travelling waves.

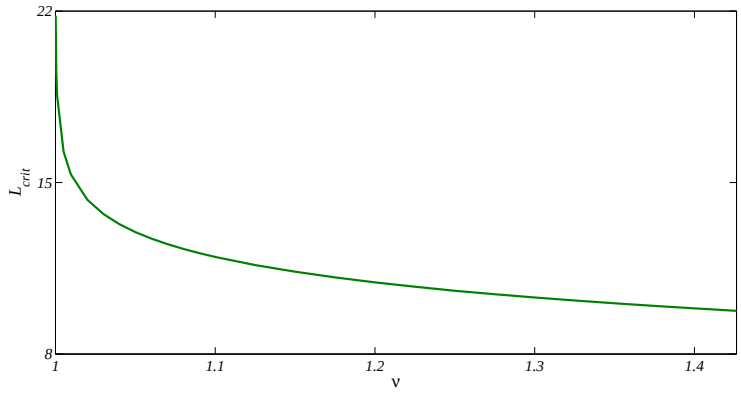

FIGURE 4.22: Dependence of the Allee critical gap length L_{crit} on the Allee parameter ν. The Allee effect parameters ν and critical gap lengths L_{crit} were obtained using equation (4.5.80) to obtain a value of L_{crit} for each value of ν. These parameters used are given by $n|_{x=0^-} = 0.745$ $\Gamma = 1$, $\lambda = \sqrt{2}$ and $\varsigma = 0.001$.

4.5.3.3 Numerical results

Using COMSOL Multiphysics we analyse the system studied in this section with a mesh consisting of 25666 elements, 1000 time units and an Allee effect growth function given by

$$\left(1 - \frac{\nu}{1+N}\right) \tag{4.5.83}$$

where $\nu = 1.4$ in the first analysis, for an Allee parameter slightly larger than the critical Allee parameter $\nu_{crit} \approx 1.35$ for a system with a gap length of $L = 10$. For the second analysis we take $\nu = 1.3$, an Allee parameter value slightly smaller than the critical Allee value.

If the Allee effect is sufficiently large, the numerical results show that the population reaches a stationary state shown in figure 4.23. This figure display the results obtained for the system analysed in §4.4.1 but with the presence of an Allee effect, with value $\nu = 1.4$. The dynamics of the system is driven by equation (4.5.72) and the boundary conditions are given by (4.3.26) and (4.3.27). The parameters of the system are $\mu_0 = 3$, $\delta = 0.05$ and $\dfrac{\Gamma}{\lambda} = 0.7$.

The results obtained for this system show that the individuals current crossing to the right hand patch reaches a stationary state due to the presence of an the Allee effect. This stationary state shows a constant population decay over time, forbidding the population from reproducing along the patch.

On the other hand, if we choose a slightly smaller value for the Allee parameter ($\nu = 1.3$), the numerical results show that, even with the presence of an Allee effect, the individuals reproducing over time, develop into a growing population as presented in figure 4.24. Notice however, that the time scale taken for the individual population to grow, is much longer than the time scale found for a population without an Allee effect (see §4.4.1).In the cases analysed here, we assumed that the gap length was $L = 10$. In this case, as shown in the figure, the population does fill up the patch eventually, forming a travelling wave solution.

Intuitively, these results are congruent with what may happen in reality. If the gap

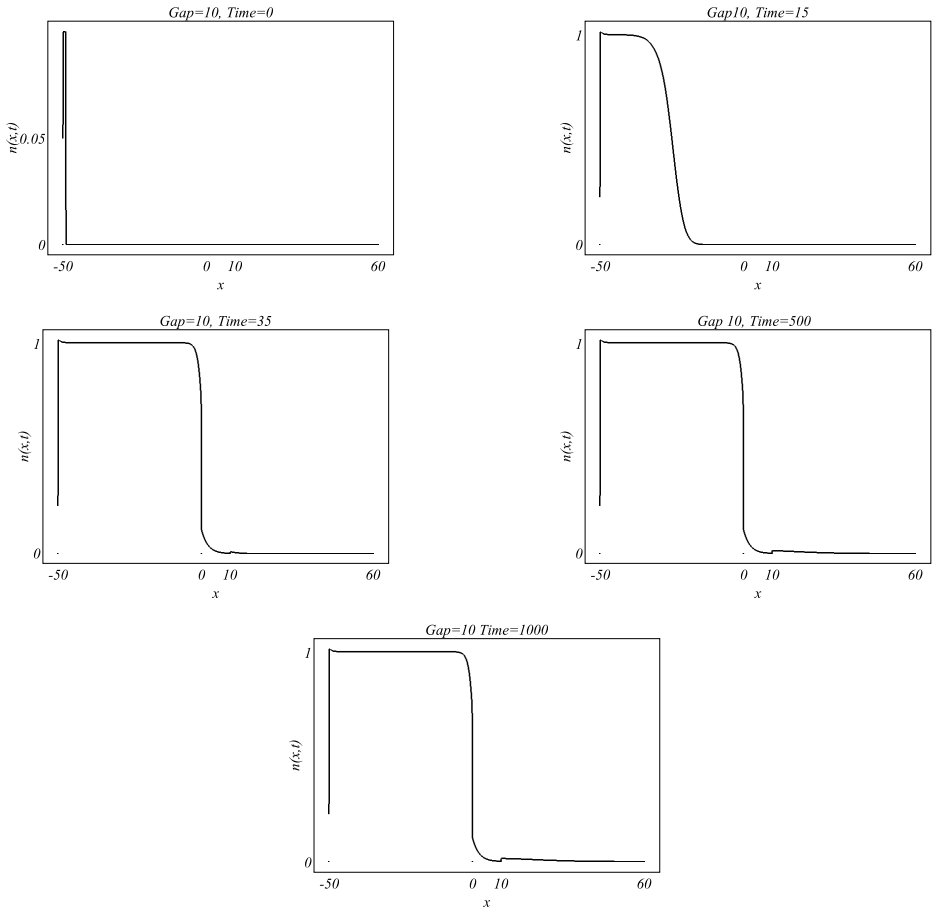

FIGURE 4.23: Individuals dispersal in a two patches system with Allee effect. Once the left patch is filled up the individuals start dispersing to the right hand patch. Due to the presence of an Allee effect the right-hand empty patch do not fill up, although it does present a stationary state of a small decaying population where the maximum population is close to zero. The parameters used in this system are: $\mu_0 = 3$, $\delta = 0.05$, $\frac{\Gamma}{\lambda} = 0.7$ and $\nu = 1.4$

length between patches is larger that the critical gap length, the few individuals that cross it would find very difficult to reproduce, failing to deliver a sustainable population. At the same time, if the gap is smaller than the critical gap length, the individuals will struggle to reproduce, but will eventually find mates. However, the reproduction process will take longer due to the difficulty to find mates.

These results suggest that, the introduction of external factors that can induce or increase an Allee effect on the population, can be used as a population control strategy. The deployment of oral contraceptives could be an option to induce and increase an Allee effect in some populations, like in the control of the population example introduced in Chapter 4: the Asiatic red-bellied beautiful squirrel *Callosciurus erythraeus*. We be-

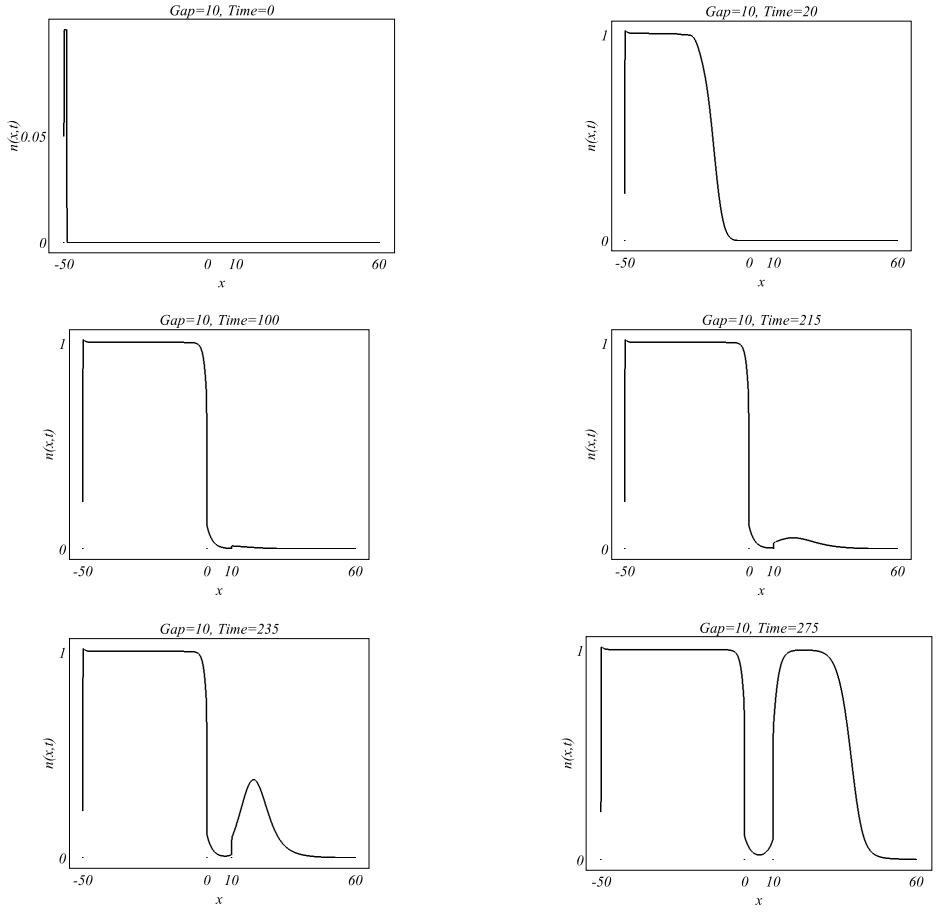

FIGURE 4.24: Individuals dispersal in a two patches system with Allee effect. Once the left patch is filled up the individuals start dispersing to the right hand patch. Since the Allee effect parameter $\nu = 1.3$ applied to this system is below the critical Allee parameter $\nu_{crit} \approx 1.35$ for a gap size $L = 10$, the right-hand empty patch fills up. The population forms a travelling wave solution, but in a longer period of time. The parameters used in this system are: $\mu_0 = 3$, $\delta = 0.05$, $\dfrac{\Gamma}{\lambda} = 0.7$, and $\nu = 1.3$

lieve this is a feasible strategy, since a very small increment on the Allee parameter ν makes a big difference in terms of population spread success as it is shown in figure 4.22. It also suggest that an early strategy of population control in populations presenting Allee effect, can be very effective in order to eradicate an invasive population, since the population reproduction rate at small populations is close to zero.

4.6 Summary

In this chapter we analysed one-dimensional systems presenting variable reproduction potential dependent on the spatial position. Additionally, we modelled a term for indi-

viduals attraction towards certain type of environments (rich resource regions) named dendrotaxis. In these regions the individuals of a given species population would reproduce and diffuse.

The model proposed in this chapter presents the novelty of including not widely studied factors in population modelling, that is, the explicitly spatial preference of individuals over some regions against others. We found interesting results regarding individual dispersal in heterogeneous regions. In particular we study the dispersal of individuals in a system composed by two regions where populations are reproductively successful, separated by a region characterised by terms denoting threat for the population survival. Relationships between gap lengths and success of population dispersal are encountered, showing that if the gap between resource-rich regions is increased, the probability of success for a population diminishes. We also found a set of relationships that allow us to predict the dynamics of a population entering a plentiful resource region, after crossing a scarce-resource region. We discovered a population relationship between the time it takes to cross a gap between regions and the gap length, both, analytically and numerically. Comparisons between asymptotic solutions, as well as numerical ones are developed along the whole chapter matching both results to a very good accuracy.

In §4.5.3 we study the impact of an introduced Allee effect over this type of population. As expected, when population is subject to Allee effects, the individual dispersal success has enormous consequences. Depending on the strength of the Allee effect, we found that either populations diffuse much slower than in the case of simple logistic growth, or the reproduction success in the initially empty patch fails. These results suggest that different population control strategies may be applied. Among those strategies we can propose an early elimination or extraction of invading individuals in new patches, or administration of oral contraceptives to enhance the Allee effect.

In this context, we found a relationship that gives us the dependence of the Allee parameter ν, on the gap length between patches L. We found that, the larger the Allee effect is, the smaller the gap should be in order for the population to become successfully reproductive. We obtain critical gap lengths L_{crit} for fixed values of ν that show the maximum distance that a current of individuals can cross, before it develops into a

decaying stationary state.

In the following chapter we develop similar studies for this type of systems in two-dimensional regions.

Chapter 5

Two-dimensional population models with dendrotaxis

5.1 Introduction

In this chapter the dynamics of a two-dimensional single population systems in a fragmented environment is studied. We extend the approach taken in Chapter 4, to a two-dimensional analysis and investigate some aspects of dispersal movement in corridor networks.

Our reference biological system in this thesis has been represented by the dispersal of the population of *Callosciurus erythraeus* in the Argentinian pampas, introduced in §4.1-4.2. However, all the systems studied here can model any biological population subject to logistic growth in plentiful resource patches that, due to saturation, have to disperse towards new habitats. The way these individuals disperse is achieved by crossing areas of threat for their survival. In these models we assume that individuals distinguish between hazardous areas and areas of abundant resources.

In this chapter we examine features of the population dynamics in two-dimensional fragmented areas such as individual dispersal rates, individual gap crossing dynamics and invasion success, dependent on the geometry of the system and the intrinsic characteristics of the system.

We numerically study the gap crossing dynamics of a population. In analogy to the systems studied in Chapter 4 we analyse the dynamics of two long thin corridors of suitable habitat separated by a gap embedded in a hazardous area. By thin we mean that the width compared with the length of the corridors is much smaller (by at least two orders of magnitude).In Appendix A we formulate the mathematical problem that we need to solve in order to perform a semi-analytic analysis of gap crossing dynamics.

5.2 Corridor habitats

We define habitat corridor as a linear habitat embedded in a larger area of disconnected regions of habitat. Differing from other definitions [124], this definition includes connected and disconnected linear habitats that support both, breeding populations and transient individuals.

Recently, the study of corridors in conservation ecology has played an important role in the study of population dispersal and population viability increase [124–128] with different opinions about their success relative to landscape connectivity improvement. There is empirical evidence that for specific species corridors improve the connectivity of the landscape and enhance animal dispersal. There are some example of this, like the case of the eastern chipmunk *Tamias striatus*, that make use of different width sized fence row corridors, of different habitat composition, to disperse live and reproduce [129]. Other study cases of rodent dispersal in fragmented environments with corridors are studied in [43, 130–133].

In this chapter our reference species is again the Asiatic red-bellied beautiful squirrel *Callosciurus erythraeus*, and its introduction and spread over the Argentinian pampas across an area exceeding 680 km^2 [15].

The way individuals make use of corridors can be divided in two types: transient corridor users and corridor inhabitants. The transient users simply travel along corridor without establishing in them. The inhabitants breed and reproduce in the corridors. The possibility of establishment of an individual in a corridor will depend for example, on the width, size and resources availability in the corridor with respect to the species.

Corridors become the species dwelling only if they cover all the species needs such as: nest or habitat space, food and availability of reproductive partners [134].

Guichon *et. al.*, [15], analysed a geographical population distribution located in the area of Jauregui, Argentina shown in figure 5.1. From figure 5.1, we observe a complex spatial distribution of different types of habitat where the squirrels live and reproduce. In the following sections, we focus on a particular type of structure found for the analysed distribution. This structure will be compared with a line corridor network.

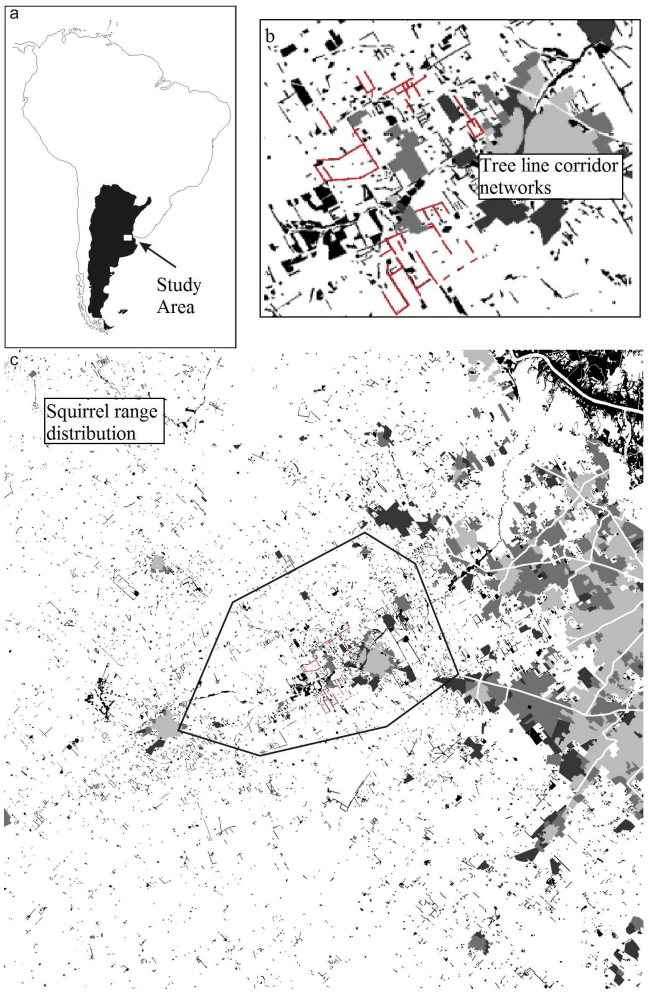

FIGURE 5.1: Geographical distribution of *Callosciurus erythraeus* in the region of Jauregui, Argentina where tree line corridor networks can be observed. The white areas in regions (b) and (c) denote grassland regions, the grey areas correspond to sub-urban areas and the darker areas to woodland. The red lines highlight some tree corridor lines an networks. The image of the squirrel geographical location of the squirrel population was taken from (Guichón, 2007) [15].

According to personal information exchange with M.L. Guichón and C.P. Doncaster the Asiatic red-bellied beautiful squirrel make constant use of tree corridors as a mean of

dispersal and as a nesting resource as well. The tree patches are highly fragmented in these regions and a big part of the region is structured as corridors which may or may not connect areas of woodland. Thus, a considerable proportion of the squirrels habitat is more or less linear.

In the next section, we present a mathematical analysis of wave of advance velocities in 2-dimensions dependent on patch or corridor width and its impact on population dispersal over corridor networks. We make use of continuum models describing density-dependent growth and diffusion amongst resource-rich regions and corridors and areas of scarce-resources with variable potentials for reproductive success.

In corridors and resource-rich regions, populations obeys a modified logistic growth. In scarce-resource areas, populations are unable to sustain themselves and decrease exponentially. In all types of patches, diffusion terms that model the dispersal of individuals across the patches are included. We also analyse, as in the previous chapter, spread rates due to squirrel behaviours, particularly in avoiding hazard and seeking mates.

In the following section we analyse how the velocity of the wave of advance changes with the width of a resource-rich region or corridor. This velocity will allow us to investigate the dispersal of individuals in corridor networks, common in agricultural fragmented landscapes. Later, we will formulate the gap crossing problem for two-dimensional systems.

5.3 Travelling waves in one- and two-dimensional homogeneous environments

If u is a function representing a travelling wave solution, propagating in one direction, the shape of the solution is the same for all time and has a constant speed of propagation c [31], *i.e.*

$$u = u(\mathbf{r}\cdot\hat{\mathbf{m}} - ct) = u(z), \qquad \text{with} \quad z = \mathbf{r}\cdot\hat{\mathbf{m}} - ct, \tag{5.3.1}$$

where $\hat{\mathbf{m}}$ is the direction of propagation, as shown in figure 5.2.

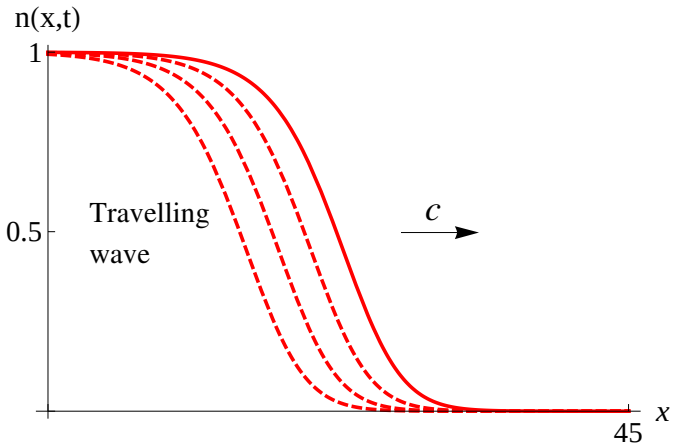

FIGURE 5.2: One-dimensional travelling wavefront with velocity c along the x axis.

The study of travelling waves has been widely investigated in biological phenomena processes due to its recurrent appearance. These phenomena range from chemical reactions to mechanical waves in many vertebrate eggs and population dispersal [31]. In the following sections, we investigate the dynamics of a plane wave travelling in a two-dimensional space. Firstly, we introduce some analytical results for travelling waves in homogeneous regions. Numerical results of how a population of individuals confined to move along a linear region spreads over it are also shown.

5.3.1 Analytic analysis

In general, determining the velocity of a wave of advance c in a one-dimensional infinite homogeneous space following the dynamics of Fisher equation in non-dimensional units,

$$\frac{\partial n}{\partial t} = n(1-n) + \frac{\partial^2 n}{\partial x^2} \tag{5.3.2}$$

is a problem that has been extensively studied [2, 5, 28, 30, 31].

Equation (5.3.2) is the simplest reaction-diffusion equation that admits travelling wave solutions [31]. If the travelling wave is moving from left to right with the boundary conditions $n(-\infty, t) = 1$ and $n(\infty, t) = 0$, then, the velocity of these travelling wave solutions, has the limit

$$c \geq c_{min} = 2 \tag{5.3.3}$$

Kolmogorov *et. al.*, also proved that if the population $n(x,0)$ also has compact support, of the form

$$n(x,0) = n_0(x) \geq 0, \qquad \text{with} \quad n_0(x) = \begin{cases} 1 & \text{if } x \leq x_1 \\ 0 & \text{if } x \geq x_2 \end{cases} \tag{5.3.4}$$

where $x_1 < x_2$ and u_0 is continuous in $x_1 < x < x_2$, then the solution of equation (5.3.2) evolves into a travelling wave solution of the form $u(z)$ with $z = x - 2t$. This means that it always evolves to a travelling wave solution with the minimum velocity $c_{min} = 2$ [31]. If the initial conditions do not have compact support, then the solution depends on the behaviour of $u(x,0)$ as $x \to \pm\infty$. This marked dependence of the velocity of the wave of advance on the initial conditions at infinity is explained in Murray's book [31] following an analysis done by Mollison [135] as shown below.

If we first consider the leading edge of an evolving wave where the population density in the equation (5.3.2) is close to zero so we can neglect the quadratic term, we obtain a linearised equation given by

$$\frac{\partial n}{\partial t} = n + \frac{\partial^2 n}{\partial x^2}. \tag{5.3.5}$$

Considering that as $x \to \infty$, $n(x,0) \approx Ae^{-ax}$, for $A > 0$ and $a > 0$, and that there is a travelling wave solution of the form

$$n(x,t) = Ae^{(x-ct)}, \tag{5.3.6}$$

we can substitute equation (5.3.6) into (5.3.5) to obtain a relationship between a and c given by

$$ac = 1 + a^2 \quad \Rightarrow c = a + \frac{1}{a}. \tag{5.3.7}$$

Notice from figure 5.3 that the minimum velocity for the relationship given by equation (5.3.7) is $c_{min} = 2$ for $a = 1$ while for any other value of $a > 0$ the velocity is larger than $c = 2$. If we now consider $min[e^{-ax}, e^{-x}]$ for $x >> 0$ (given that we assumed $n^2 \ll n$ for the Fisher linearised equation), then

$$a < 1 \Rightarrow e^{-ax} > e^{-x} \tag{5.3.8}$$

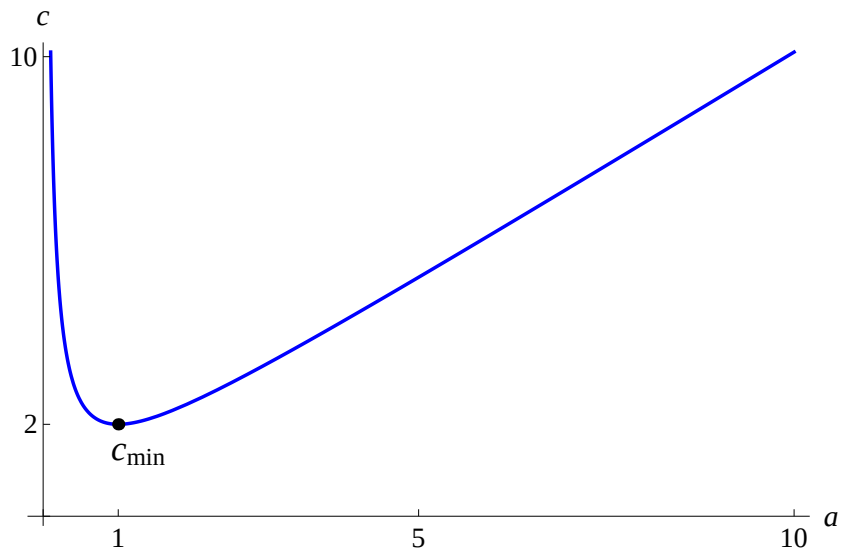

FIGURE 5.3: The velocity c dependent on a shows a minimum at $a = 1$ for which $c_{min} = 2$. For any other value of $a > 0$, $c > 2$.

which tell us that the velocity of propagation with the asymptotic initial condition given by $n(x, 0) \approx Ae^{-ax}$ depends on the leading edge of the wave, and the velocity of the wave of advance is given by equation (5.3.7). On the other hand, if $a > 1$ then e^{-ax} is bounded above by e^{-x}, (where $a = 1$) giving an asymptotic wave front velocity of $c = 2$. Therefore, if the initial conditions are given by $n(x, 0) \approx Ae^{-ax}$, then the asymptotic wave speed of the travelling wave solution of equation (5.3.2) is

$$c = a + \frac{1}{a}, \quad 0 < a \leq 1, \quad c = 2, a \geq 1. \tag{5.3.9}$$

In two-dimensional systems, propagating wave fronts for the Fisher-Kolmogorov equation have received much less attention [14, 75, 77, 78] and so far, analytic travelling wave solutions for general velocities c have not yet been found [77]. However, some results for travelling waves solutions in two dimensions can be found.

The non-dimensional Fisher equation in a two-dimensional space is written as,

$$\frac{\partial n}{\partial t} = n(1 - n) + \frac{\partial^2 n}{\partial x^2} + \frac{\partial^2 n}{\partial y^2}. \tag{5.3.10}$$

If we assume that a two-dimensional travelling wave moves in the direction of the x-axis,

we can write $c = c(y, z)$ where $z = x - ct$ and,

$$-c\frac{\partial n}{\partial z} = n(1-n) + \frac{\partial^2 n}{\partial z^2} + \frac{\partial^2 n}{\partial y^2}. \tag{5.3.11}$$

If we assume an infinite homogeneous environment, then, n does not depend on the variable y and the wave propagating in the two-dimensional space in the x-axis direction recovers the form it had in the one-dimensions, namely that discussed in this section.

The system analysed in the following sections, is again, inhomogeneous. The properties of the solutions become a difficult task since they depend on the spatial variables, for instance, on the width of the spatial component y. This factor complicates the search for an analytical solutions [136] and numerical results have to be investigated. In the following section, we numerically analyse the velocity of the wave of advance in corridors of different widths. We expect that these velocities also satisfy equation (5.3.3), and that for infinitely wide systems, the travelling waves solutions approach the solutions found in the one-dimensional systems $c \to 2$.

5.4 Numerical solution for travelling waves in corridors

In the following sections we study the numerical behaviour of a population following logistic growth over a set of long corridors with variable widths. Here we investigate a corridor of uniform width and determine how the speed of the wave of advance depends on the width of the corridor.

Later, we analyse the effect of junctions on corridor networks, focusing on the effect of junctions on the propagation velocity. Finally, we analyse numerically the gap crossing time dependence on the gap length between two corridors.

These analyses are used to infer the approximate behaviour of the spreading dynamics over a corridor network.

5.4.1 Mathematical problem

The model set-up of the two-dimensional system provided here is based on the one provided in Chapters 3 and 4. Here we recall equations (4.3.24) – (4.3.27) to describe the dynamics of a general ecosystem constituted by a single population dispersing in a fragmented environment over a two-dimensional space as shown in figure 5.4. The population dynamics in non-dimensional variables (see §4.3.2 for more details) is given by,

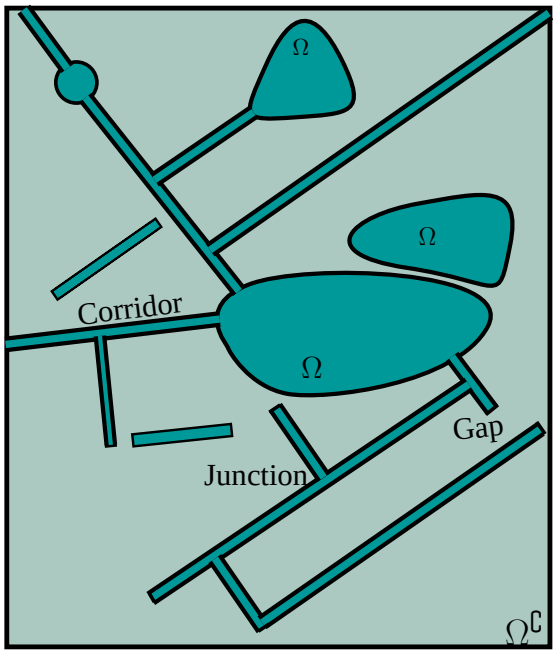

FIGURE 5.4: Two-dimensional geometry for an arbitrary two-dimensional system with corridor networks.

$$\frac{\partial n}{\partial t} = n(1-n) + \nabla^2 n \quad \text{in } \Omega \tag{5.4.1}$$

$$\delta \frac{\partial n}{\partial t} = -n + \lambda^2 \nabla^2 n \quad \text{in } \Omega^{\complement}, \tag{5.4.2}$$

where Ω represents areas of plentiful resources and $\Omega^{\complement}$ areas of scarce-resources. The jump conditions are given by,

$$\epsilon n|_{\delta\Omega} = n|_{\delta\Omega^{\complement}}, \tag{5.4.3}$$

$$\mathbf{N} \cdot \nabla n|_{\delta\Omega} = \frac{\lambda^2}{\delta} \mathbf{N} \cdot \nabla n \Big|_{\delta\Omega^{\complement}} \tag{5.4.4}$$

where $\epsilon = e^{-\mu_0}$, $\delta = \dfrac{\alpha}{\alpha'}$ and $\lambda = \sqrt{\dfrac{D'\alpha}{D\alpha'}}$.

As in Chapter 4, the parameters D, D', α, α' represent the diffusion coefficients inside and outside the plentiful resources regions, the growth rate in the plentiful resources areas and the decay rate in the scarce-resource regions respectively. Meanwhile, μ_0 represents the constant value of the dendrotaxis function in resource-scarce regions,

$$\mu(r) = \begin{cases} 0 & \text{in the resource-rich regions} \\ \mu_0 & \text{in the resource-scarce regions} \end{cases} \tag{5.4.5}$$

5.4.2 Corridors

In this section, we attempt to find a numerical approximation for the speed of propagation of a population system, over an infinite corridor of uniform width, traversing an infinite region of scarce-resources. In order to do this we consider the geometry shown in figure 5.5. From this figure we assume that the corridor is represented by the region Ω, and the scarce-resource regions are represented by the region $\Omega^{\complement}$. We also suppose, that the length of the corridor is $2Q \gg 1$ and that the width of the domain is much larger than the width of the corridor $P \gg R$ which will enable us to discard boundary effects from the scarce resources regions.

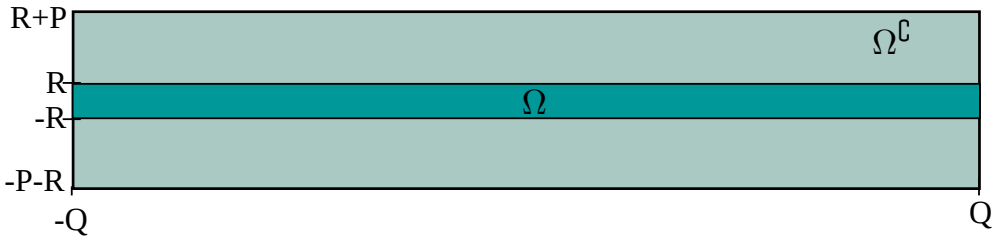

FIGURE 5.5: Two-dimensional geometry used in the numerical analysis of the dispersal of individuals between along a single tree line corridor of variable width $2R$.

In the plentiful resources areas we assume as usual, logistic population growth plus diffusion (equation (5.4.1)), in grasslands, the population decays exponentially and diffuses (equation (5.4.2)). Finally, the boundary conditions around the woodland regions are constructed by using a step dendrotaxis function. In rescaled units the example investigated here and shown in figure 5.5 we take: $2Q = 100$, while the domain width is given

Velocities for different corridor widths		
Corridor width	Mesh size	Approx. velocity
1	13630	No travelling wave
1.5	19022	No travelling wave
1.8	19862	2.857142
2	19823	2.898550
2.5	20703	2.941176
3	21411	3.030303
3.5	22015	3.125000
4	22354	3.333333
4.5	22691	3.225806
5	22992	3.200000
5.5	22869	3.125000
6	23630	3.125000
7	25024	3.030303
8	25282	2.941176
10	29862	2.857142
12.5	31816	2.777777
15	26388	2.777777
20	27017	2.500000
30	37198	2.380952
40	43849	2.272727
50	41988	2.083333
80	42067	2.000000

TABLE 5.1: Numerical data for corridors of same length but with different widths. The parameters used in this system are $\lambda = \sqrt{2}$, $\delta = 0.05$ and $\mu_0 = 3$.

by $2P = 20$. The quantity $2R$ indicates the corridor width.The initial conditions are given by,

$$n|_{t=0} = \begin{cases} 0.1 & x \in \{-Q, -Q+1\},\ y \in \{-R, R\} \\ 0 & \text{elsewhere} \end{cases} \tag{5.4.6}$$

Based on the analysis of the parameters done in §4.3.3 here, the parameters μ_0, λ and δ are defined as, $\mu_0 = 3$, $\delta = 0.05$ and $\dfrac{\Gamma}{\lambda} \approx 0.7$ matching the values taken in equations (5.4.1)–(5.4.3).

We vary the width of the corridors, by changing the value of R. We take different values of R shown in Table 5.1 to obtain the velocity of the wave of advance in corridors of widths $2R = 0 - 50$. For corridors of widths larger than $2R = 10$, we also expand the width of the domain P to assure that the system is not influenced by the domain boundaries. These numerical results are shown in Table 5.1.

To obtain the velocity, we measure the position and time of the cross section of the two-dimensional wave of advance at $y = 0$ as shown in figure 5.6. Then, we register the positions x_i by determining $x(t_i)$ so that $n(x(t_i), t_i) = 0.5$ at different times t_i. We finally record the positions and times x_i, t_i to obtain a set of values for the velocity $v_w = \frac{\Delta x}{\Delta t}$. Taking several measures of time for each system, we obtain the velocity of the travelling wave, when the velocity v_w becomes constant, so $v_w = c$. The velocity of the travelling wave depends on the width of the system $2R$ and it is denoted as c_{2R}, that appears once the changes of position respect to fixed intervals of time become constant.

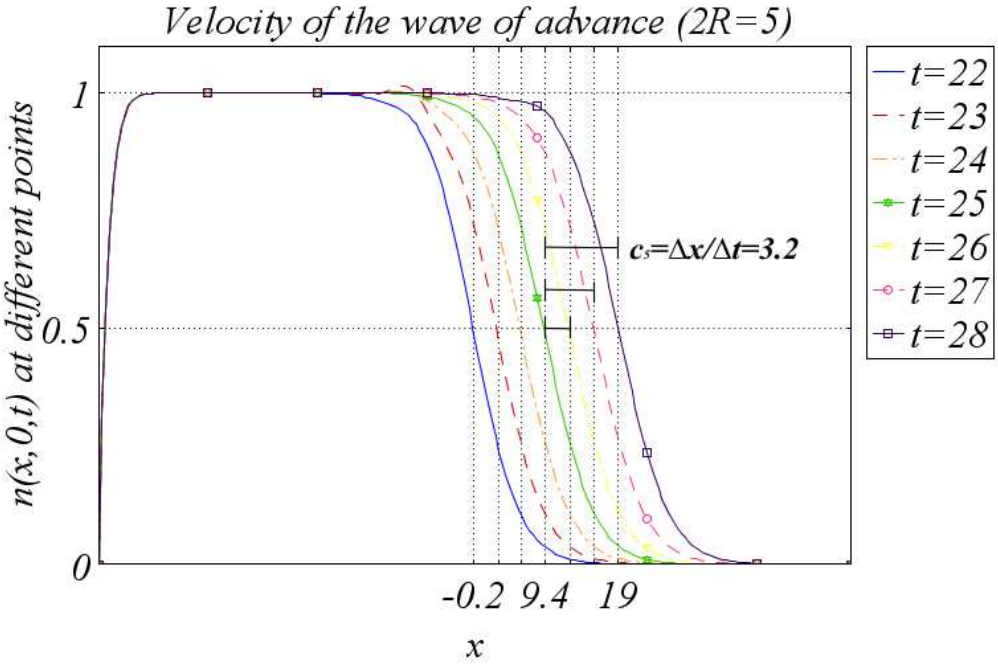

FIGURE 5.6: Position of the wave of advance over the x-axis at different times for a corridor with width $2R = 5$. Once the wave starts travelling fixed distance over fixed intervals of time the velocity of the wave of advance $c_5 = 3.2$ is measured.

The data recorded is obtained for meshes that are robust under changes of size and time, *i.e.* for smaller number of mesh elements, the results do not change. According to the data acquired from the numerical analysis, the wave of advance velocities for the different corridor widths range between $c = 2.0 - 3.3333$. These results allow us to assume in the following sections that, the individuals spread at more or less the same width-dependent velocity over long corridors. We also observe that, as the corridor

gets wider, the velocity decreases approaching the one-dimensional velocity in a Fisher-Kolmogorov system $c_{min} = 2$. The dependence of the velocity with respect to corridor width is shown in figure 5.7 where we observe how the velocity increases from $c_{1.8} = 2.85$ in a corridor of width $2R = 1.8$, to a maximum value of $c_4 = 3.333$ in a corridor of width $2R = 4$ decreasing later with the corridor width, and approaching the minimum velocity $c_{80} = 2.0$, found in one-dimensional systems.

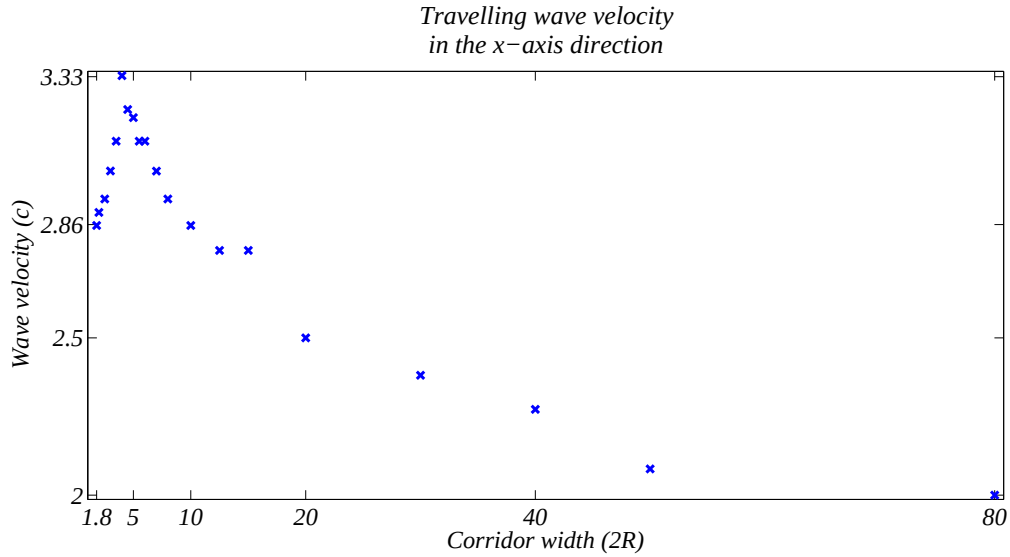

FIGURE 5.7: Dependence of the velocity of the wave of advance with respect to the corridor width. The velocity varies from a maximum velocity of $c_4 = 3.333$ to $c_{80} = 2.0$ where the system behaves as a one-dimensional travelling wave in the x-axis direction.

Figure 5.7 shows the velocity of the wave of advance dependence on the corridor width. The results show that for corridor widths between $R = 1.8 - -4$, the velocity increases along the corridor and for $R > 4$ it decreases tending to the minimum velocity $c_{min} = 2$. The nature of this velocity variation is not clear to us, and needs further investigation. However, an explanation of the velocity increase for narrow corridors could be associated to the fact that individuals leave the corridor from the sides, diffuse rapidly outside the corridor and come back in further ahead of the wave, thereby increasing the velocity of the wave of advance. For corridor widths larger than 4 the velocity of wave of advance decreases approaching the minimum velocity found in one-dimensional systems. Another explanation for this velocities variation may be attributed to corridor boundary effects,

although a conclusive interpretation for the behaviour of the population wave of advance velocity dependent on the corridor width results difficult at this point.

Nevertheless, these numerical results give us an idea of how population individuals would spread along a whole network of corridors, assuming that they spread at more or less the same velocity for sufficiently wide corridors, *i.e.* for corridors with $5 \precapprox R \precapprox 10$. In the following analyses, we will assume that the velocity of spread is close to $c = 3$ for corridors of relatively small width ($5 \precapprox R \precapprox 10$), in agreement with our numerical results. In order for a habitat to support a breeding population, it is necessary for it to have the minimum food and resources needed for the population to establish there. Therefore, if the width of the corridor is very small, it may not support any population, as obtained in the numerical solutions for corridors of widths $R = 0 - 1.2$.

Figure 5.8 shows the cross section of the population at $t = 50$ for different corridor widths. This figure shows that for each corridor the population has a maximum that depends on the corridor width as observed. Once the population maximum is obtained at some point over the x-axis x_0, the population travels in the form of a wave of advance, again, in the direction of the x-axis. For corridors with width $1.3 < 2R < 1.8$ no travelling wave solutions are found. In this case, the population do reproduce over time, filling the patch over long periods of time. However, no travelling wave solution appears in these systems. For corridors with width $0 < 2R < 1.2$ no population is sustainable according to the numerical results obtained. In these type of corridors, the population diffuses a little, but the width is so small that the population cannot reproduce. Therefore, the population decays and collapse after long periods of time.

Another point that has to be considered in this analysis is that, the diffusion length $\xi = \sqrt{\frac{D}{\alpha}}$ (the thickness of the wave of advance) has to be much smaller than the corridor domain length $2Q$. This is in order to maintain the form of the travelling wave. This means that the solutions obtained here are applicable only over corridors of lengths $2Q >> \xi$. According to Guichón *et. al.*, the parameter estimates for the beautiful red-bellied squirrel population rate of increase and mean dispersal distances (or diffusion coefficient) over woodland areas are $\alpha = 1.53yr^{-1}$ and $D = pi \cdot 1km^2/yr$ which gives a value of $\xi \approx 654m$ in. As we require $2Q$ to be much larger than ξ, the length scale

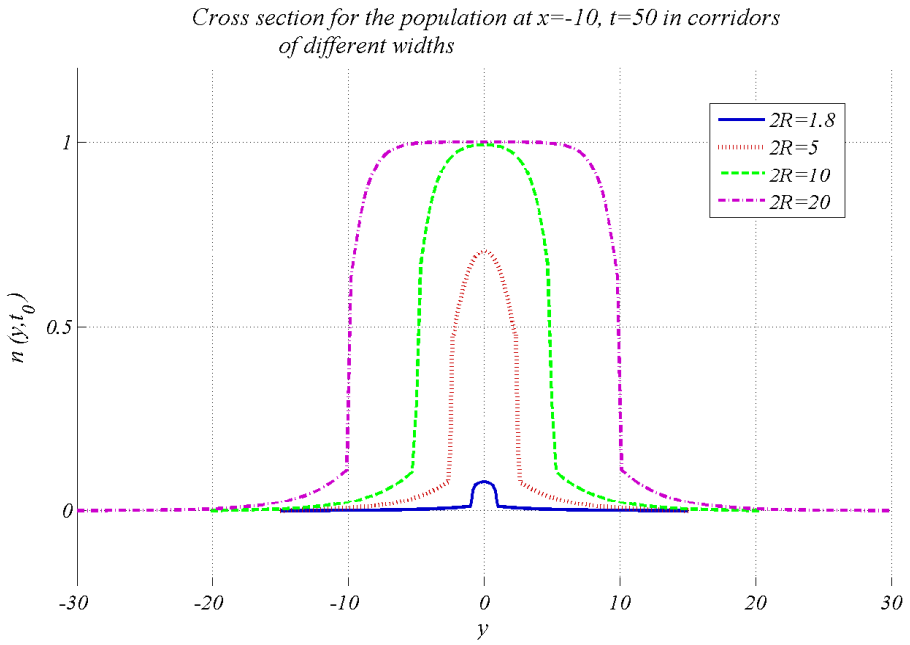

FIGURE 5.8: Individuals disperse in a set of corridor systems of widths $2R = 1.8, 5, 10, 20$. The cross section of the population at $t = 50$ in each system is plotted. Observe that each system has a maximum in the population where the carrying capacity of the system that depends on the corridor width is reached . If the corridor width is smaller than $2R = 1.2$ the population does not reproduce successfully due to lack of minimal habitat area for the population survival. The parameters in these systems are $\lambda = \sqrt{2}$, $\delta = 0.05$ and $\mu_0 = 3$.

of the corridors has to be probably measured in kilometers. For shorter corridors other strategies would have to be applied.

In the next section we analyse the effect of junctions on dispersal velocity to then be able to do an overview of a whole corridors network.

5.4.3 Junctions

In this section we analyse the effect that junctions have over the individual dispersal of a populations in corridor type geometries.

Intuitively, we anticipate that the contribution to the woodland areas that a junction has, will have little impact over the spread of the population along the whole corridor network. However, we expect the population to have a little more available space to diffuse at the junction, influencing the dynamics of the population close to the junction. The velocity of spread will have more or less the same value away from the junction, and

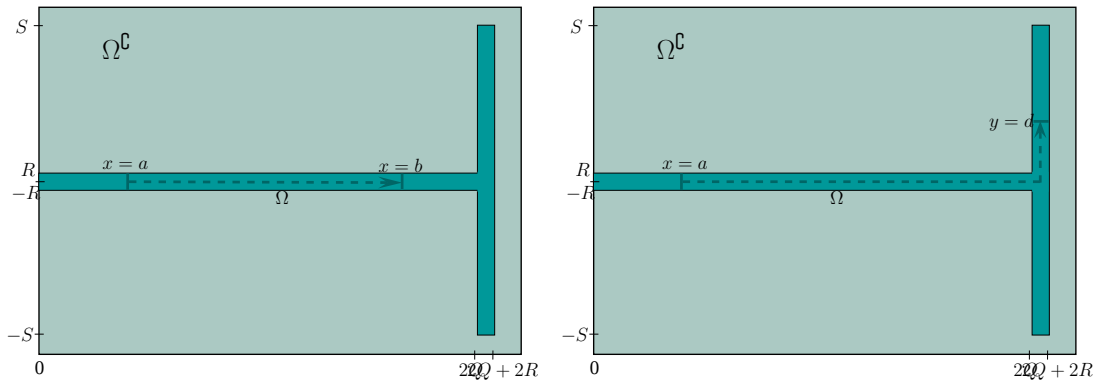

FIGURE 5.9: Individuals disperse in a corridor of width $2R$ with a long junction at the right end. The plot shows the distance taken to measure the velocities of the population before and after getting to the junction.

the population will continue reproducing until it finds an obstacle, such as gaps between woodlands.

Figure 5.10 shows the contour plot of the population at $n = 0.5$ along a corridor connected by a junction at uniformly spaced times $\Delta t = 10$. The domain mesh is constituted by 21789 elements and the numerical solutions are recorded over 150 units of time. As the population arrives to the junction, the individuals start reproducing and dispersing equally in both directions filling eventually both sides of the corridor.

The velocity in the corridor of width $2R = 5$ before the junction $P_1 = \{(x, y) = (\{0, 100\}, \{-2.5, 2.5\})\}$ is found to be approximately $c = 3.2$ for sufficiently large times, while the average velocity after crossing the junction, from $P_2 = (x = 202.5, y = 0)$ to $(x = 202.5, y = 40)$ (see figure 5.9), is about $c = 3.7$, noticing a relatively small increment on the velocity due to the presence of the junction. This increment was noticed in all the systems analysed numerically.

As predicted previously, we find that the presence of junctions in a corridor network has little effect on the overall velocity of population dispersal.

5.5 Gap crossing numerical analysis in 2D

In this section a two-dimensional gap crossing analysis analogous to the one done in §4.4 is performed. We carry numerical studies for the solutions of equations (5.4.1) –

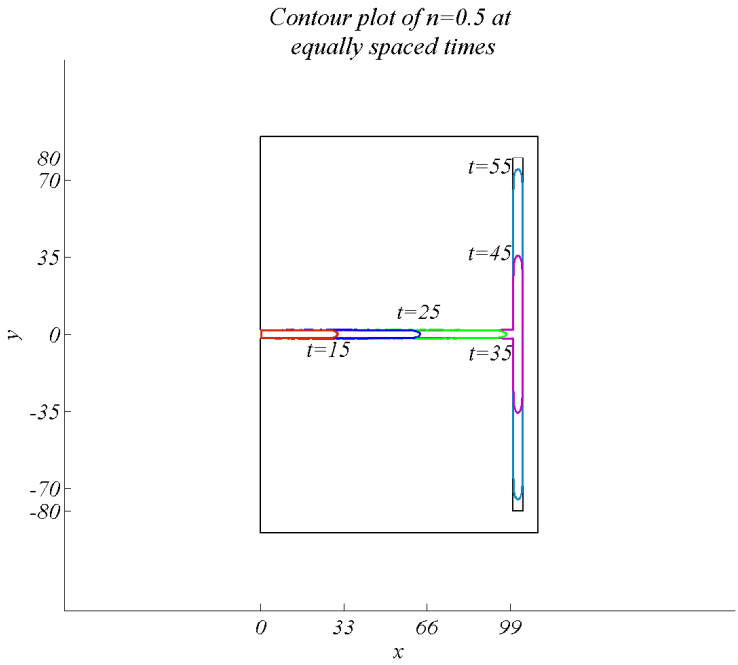

FIGURE 5.10: Individuals disperse over a corridor of width $2R = 5$ joint by another corridor through a junction. The contour plot of the population is shown at equally spaced times, showing the effect of the junction over the population dynamics. The parameters used in this system are $\lambda = \sqrt{2}$, $\delta = 0.05$ and $\mu_0 = 3$.

(5.4.4) in two woodland patches separated by a grassland gap with the geometry shown in figure 5.11. Here, we numerically investigate the population dispersal from a full woodland patch, across a grassland gap and towards a second empty woodland patch using COMSOL Multiphysics. We discuss the effects of the size of the grassland gap, the diffusion coefficients and the growth and decay rate parameters discussed in §4.3.3 on the dispersal of individuals.

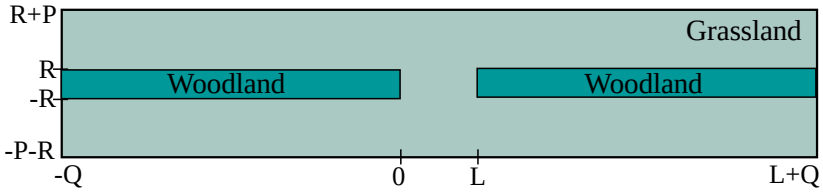

FIGURE 5.11: Two-dimensional geometry used in the numerical analysis of the dispersal of individuals between two tree line corridors across a grassland area.

In the resource-rich regions the population diffuses and grows logistically (equation (5.4.1)). In the scarce-resources regions the population diffuses and decays (equation (5.4.2)). In rescaled units, the example we investigate is built over the geometry presented in figure 5.11. In this case we assume that $R = 2$, $P = 8$, $Q = 100$ and $L = 10$.

The initial condition is again given by

$$n|_{t=0} = \begin{cases} 0.1 & x \in \{-Q, -Q+1\},\ y \in \{-R, R\} \\ 0 & \text{elsewhere} \end{cases} \tag{5.5.1}$$

According to equations (5.4.1)–(5.4.3) the parameters μ_0, λ and δ, based on the analysis of the parameters done in §4.3.3 are defined as, $\mu_0 = 3$, $\delta = 0.05$ and $\dfrac{\Gamma}{\lambda} \approx 0.7$. These are generic values that can be adjusted according to biological data, but for simplicity we take again these values.

The results of the example described previously are shown in figure 5.12 for a system with 34514 elements and 100 time units. These numbers are taken once we have confirmed that the numerical results are robust under changes to the mesh and time sizes. This figure describes the dynamics of a two-dimensional system constituted by two woodland patches and grassland surroundings. Once the left woodland patch is filled up some individuals start diffusing to the next patch through the grassland decaying along the way. Even if the number of individuals leaving the first patch is very small compared with the total population, the diffusion taking place in grasslands allows some individuals to reach the second patch. At the same time, the gap between patches is small enough to permit the gap crossing for some individuals. Once the gap obstacle is overcome the individuals start reproducing logistically in the new woodland patch, until they fill it up.

As in the one-dimensional systems, if the gap is large enough, the numerical results for the population flux become of the order of the numerical error in the calculations, making the numerical results unreliable.

5.5.1 Gap crossing time

In this section we investigate the time it takes for a population to cross a gap of given length L from a resource-rich region to another. We investigate the dependence of the crossing time upon the gap length. We expect to obtain a linear relationship on the crossing time as we did in the one-dimensional case. Here we consider the system

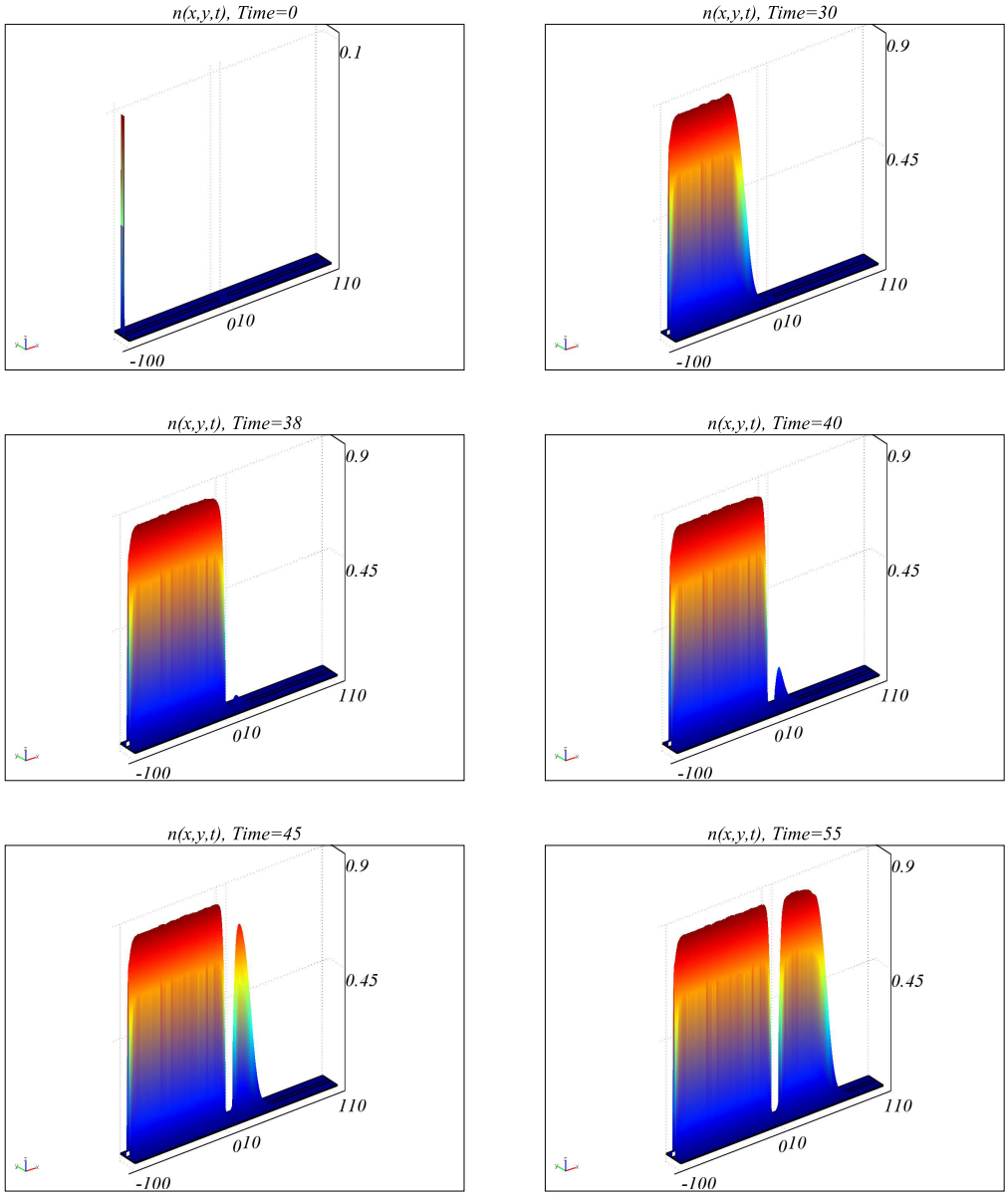

FIGURE 5.12: Individuals dispersal in a two-dimensional two patches system. Once the left patch is full the individuals start dispersing to the right hand patch crossing the gap, reproducing and eventually filling it up. The parameters used for this numerical simulation are $\mu_0 = 3$, $\delta = 0.05$ and $\dfrac{\Gamma}{\lambda} \approx 0.7$

analysed in §5.5 for gap lengths varying from $L = 0$ to $L = 12$.

The way we measure the gap crossing time in this case is similar to the one performed in the one-dimensional case. For each system of fixed gap length, we measure the time τ it takes for the population density to go from a value of $n = 0.5$ from the point $x = 0$, to a population value of $n = 0.5$ at the point $x = L$ starting from the point where the population at $x = 0$, the right hand end of the left hand patch is equal to $n = 0.5$. This procedure is repeated for each gap length $L = 1 - 12$, and the relationship between waiting time and gap length is found.

For each system, the mesh of every sub-domain, has a maximum separation between points close to the boundary of $x = 0.35$. On the time scale we assume that the solution changes with a time interval of 0.1 ranging from $t = 0$ to $t = 100$ for every system. The meshing for the two-dimensional system is coarser than the one-dimensional one due to the limited computational resources available. However, we made sure that the results obtained by solving this set of systems are robust under changes in mesh and time, so the results obtained are the same than the results obtained with even coarser meshes. These systems were solved using COMSOL Multiphysics, with the parameters $\lambda = \sqrt{2}$, $\delta = 0.05$ and $\mu_0 = 3$ and the results obtained are presented in Table 5.2.

The results for gap crossing time delay provided in Table 5.2 for a number of patch systems with different gap lengths are obtained from systems solutions as the one shown in figure 5.12.

According to the data obtained from the numerical analysis in two-dimensional systems, the elapsed time to cross a grassland gap also grows linearly. As the gap gets larger, the population current becomes of the order of the numerical error, making the analysis inaccurate. Therefore, we analyse only systems with gaps of size $L < 12$. Figure 4.11 shows the gap crossing time delay against gap length, overlapped with the fitting curve $t = 1.115L - 0.5307$ for $2 \leq L \leq 10$. This relationship corresponds to a velocity of the population spread over the resources-scarce regions since it gives a relationship of distance travelled over time. Hence, this velocity has the constant value $c_{2D} = 0.8968(= 1/1.115)$. This velocity is smaller than the velocity found for the one-dimensional case, which makes sense, since the movement is in two dimensions. In the one-dimensional case

Gap size data		
Gap size	Mesh size	Time delay between patches
0	21422	0.15
0.25	21411	0.40
0.5	21181	0.55
0.75	21249	0.70
1	21542	1.00
1.25	21355	1.15
1.5	21577	1.55
1.75	21621	1.40
2	21459	2.00
2.5	21429	2.25
3	21683	2.85
3.5	21611	3.50
4	21579	4.00
4.5	21859	4.25
5	21715	4.95
5.5	21667	5.40
6	21725	5.95
6.5	21910	6.50
7	21930	7.10
7.5	21912	8.00
8	21608	8.50
8.5	21834	9.20
9	21916	9.60
9.5	21870	9.50
10	22132	9.90
10.5	21878	10.05
11	21700	10.75
11.5	21922	11.20
12	21906	11.75

TABLE 5.2: Numerical data for different gap sizes in a two-dimensional system with $\lambda = \sqrt{2}$, $\delta = 0.05$ and $\mu_0 = 3$.

we found that the relationship between waiting time and gap length was $t = 0.8289L + 0.3586$, and therefore, the velocity was given by $c_{1D} = 1.2064 (= 1/0.8289)$

To evaluate the effectiveness of this curve fitting we use the statistical tools used in the analysis for the one-dimensional system. The sum of squares due to error (SSE) given by equation (4.4.1) is obtained as well as the R-Square, defined in equation (4.4.2). These two values are given by a $SSE = 0.4543$ and a $R - Square = 0.9956$. These results tell us that, even if the SSE is relatively large in comparison to the one obtained for the one-dimensional system, the fitting function is a good approximation to the numerical

data.

The linear dependence of the time with the gap length for gaps with lengths between $2 \leq L \leq 10$ in the two-dimensional system is shown in figure 5.14 where the function has 95% of confidence bounds.

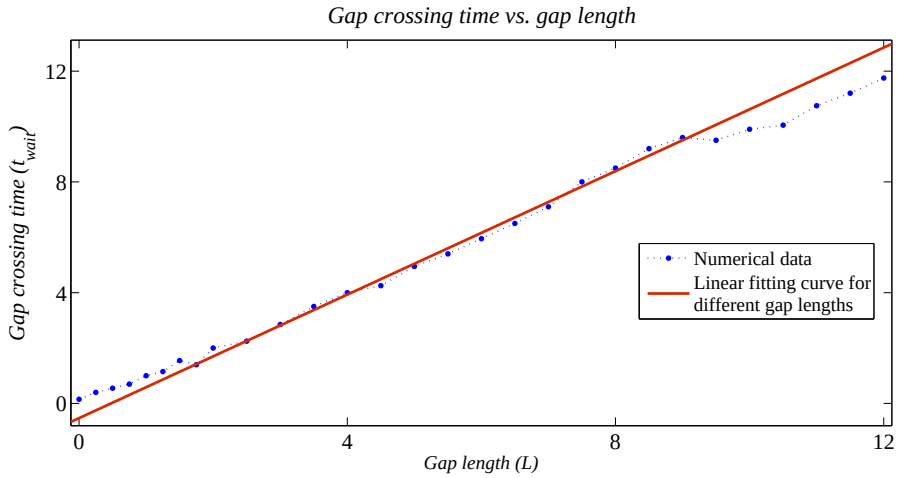

FIGURE 5.13: The blue dots corresponds to the numerical data obtained from the analysis of a series of different systems constituted by two woodland patches and different sized gaps in between. It measures the elapsed time to cross a gap depending on the gap length. The red line corresponds to the linear approximation for gap sizes of $L \geq 2.5$. The parameters used here are $\lambda = \sqrt{2}$, $\delta = 0.05$ and $\mu_0 = 3$

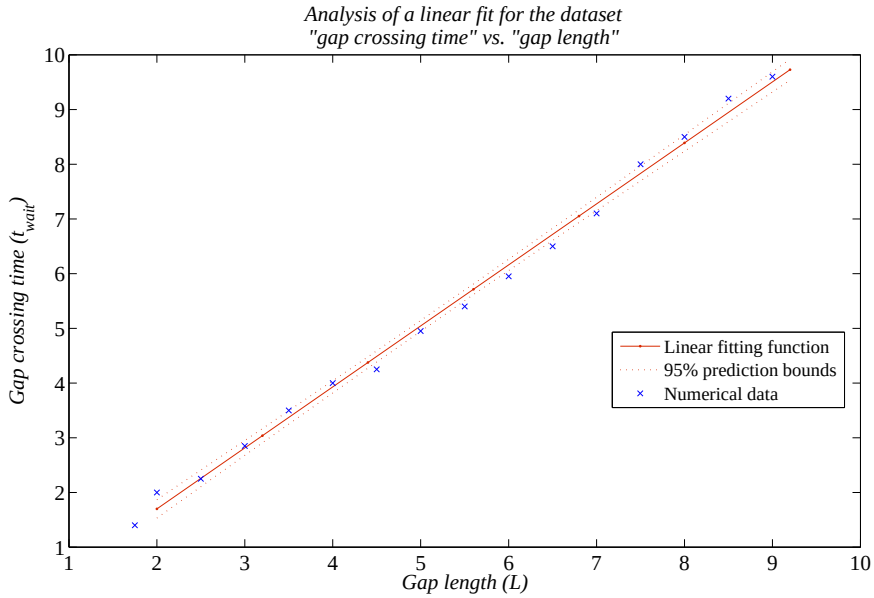

FIGURE 5.14: The dots along the graphic denote obtained data from numerical analyses of different gap sized systems. The solid line is the function fit while the dashed lines show the 95% of confidence bounds for the linear fitting function. As observed in the figure the width of the interval for the confidence bounds indicates a good data fit. The parameters used here are $\lambda = \sqrt{2}$, $\delta = 0.05$ and $\mu_0 = 3$

As found in the one-dimensional system, we found that the gap crossing time between patches follows a linear relationship for sufficiently large gaps. This is a very interesting discovery since with the knowledge of the velocity of the wave of advance over resource-rich regions and corridors, it can help us predicting the way individuals disperse in networks of heterogeneous habitats, providing information necessary to develop control strategies with anticipation.

5.6 Allee effect

The last aspect we study in this chapter, is the effect of an Allee effect on the population growth function over the resource-rich regions. We expect that, as in the case of the one-dimensional systems, the Allee effect will affect the dispersal of the populations, either by decreasing the individual flux between patches or by stopping it.

We would also expect the existence of a critical gap crossing distance for each set of Allee parameters, as we found in the one-dimensional case. We model the Allee effect as in Chapter 4 to model Allee effect by writing,

$$\frac{\partial n}{\partial t} = \left[1 - \frac{\varsigma\nu}{\delta + n}\right] n(1-n) + \nabla^2 n \quad \text{in the resource-rich regions,} \tag{5.6.1}$$

in non-dimensional units, where the dimensionless parameters are given by,

$$\varsigma = n_0/\chi, \quad \text{and } \nu = \bar{b}/\bar{\alpha}\ . \tag{5.6.2}$$

To solve the model including the Allee effect we apply the growth function in the resource-rich regions given by equation (5.6.1). Using COMSOL Multiphysics we analyse a system of 45410 elements and 1000 time units for a set of corridors with a gap of length $L = 10$ between them.

The numerical results obtained are shown in figures 5.15 and 5.16.

In figure 5.15 we observe that, if the proposed Allee effect over the domain is sufficiently small, the current of individuals eventually start reproducing over the new initially empty

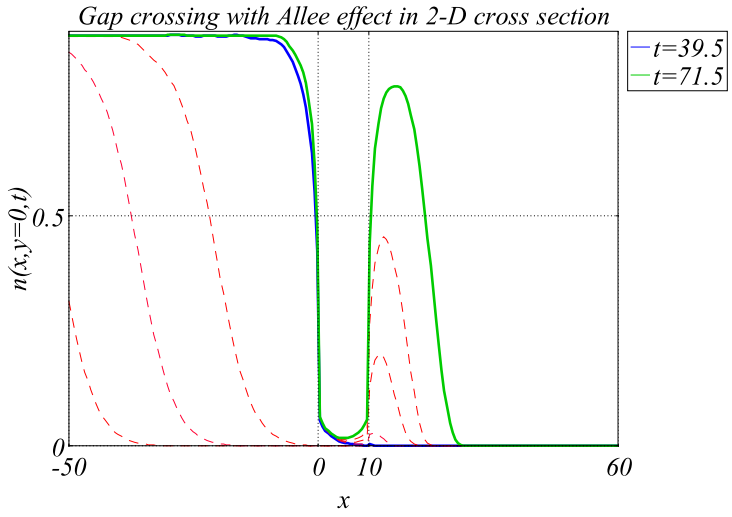

FIGURE 5.15: Cross section for the population dispersal in a two patches two-dimensional system with Allee effect at different times. Once the left patch is filled up the individuals start dispersing to the right hand patch. Due to the presence of a weak Allee effect the right-hand empty patch fills up, but in a longer period of time. The blue solid line shows a population reaching the value $n = 0.5$ at $x = 0$ and $t = 39.5$. The green solid line shows the time $t = 71.5$ when the population reaches the value $n = 0.5$ at $x = 10$. The parameters used in this system are: $\mu_0 = 3$, $\delta = 0.05$, $\frac{\Gamma}{\lambda} \approx 0.7$, $\varsigma = 0.00125$ and $\nu = 5$

patch. However, the waiting time taken for them to reach a population of $n = 0.5$ at $x = L$ starting from a population of $n = 0.5$ at $x = 0$ increases. For instance, the crossing time obtained for the patch without Allee effect was $t = 9.9$, while the gap crossing time obtained for this Allee effect increases to $t = 32$.

On the other hand, if we increase the Allee effect assuming values of $\varsigma = 0.0075$ and $\nu = 5$, we notice that, the flux of individuals reaching the second patch, never manages to reproduce successfully as shown in figure 5.16. These results are obtained for a system with a gap of length $L = 10$, that in all the previous studies, had presented a reproductive success in the new patch. Notice however, that, as in the one-dimensional case, a stationary state for a constantly decaying population in the new patch, does exist. This result is shown in figure 5.17.

These results suggest for example, that the introduction of external factors that can induce or enhance an Allee effect on the population can be used as a control strategy. The deployment of oral contraceptives could be an option to induce an Allee effect in some populations, like in the control of the population example introduced in Chapter

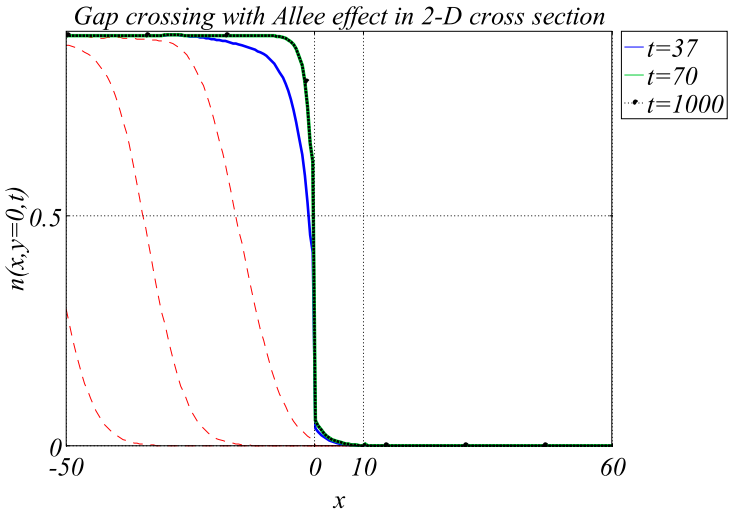

FIGURE 5.16: Cross section for the population dispersal in a two patches system with Allee effect at different times. Once the left patch is filled up the individuals start dispersing to the right hand patch. Due to the presence of an Allee effect the right-hand empty patch do not fill up, although it does present a stationary state of a small decaying population, as in the one-dimensional case. The blue solid line shows the population at $t = 37$, the green line shows when the population reaches a stationary state at $t = 70$. Finally the black dotted line shows how the population stationary state is kept over time. It shows the population at $t = 1000$. The parameters used in this system are: $\mu_0 = 3$, $\delta = 0.05$, $\frac{\Gamma}{\lambda} \approx 0.7$, $M = 0.01$, $\varsigma = 0.0075$ and $\nu = 5$

4, Asiatic red-bellied beautiful squirrel *Callosciurus erythraeus*.

5.7 Networks of corridors

Once the main structures that compose a network of corridors have been studied, we can make a summary of how a population would disperse over a corridor network, composed of long corridors where, the lengthscale of the wave of advance in the corridor is much shorter than the length of the corridor itself. Let us take the example of figure 5.18 as an example.

Assuming that the velocity over a corridor is $c = 3$ and that junctions do not have a major effect on the velocity dispersal we can find the time it takes for a population to move from a to b through a corridor network. If we also assume that the slope of the waiting time against gap length is $m = 1$, then we can also find the waiting time for the population to cross gaps of different length. Here we assume that there is no Allee

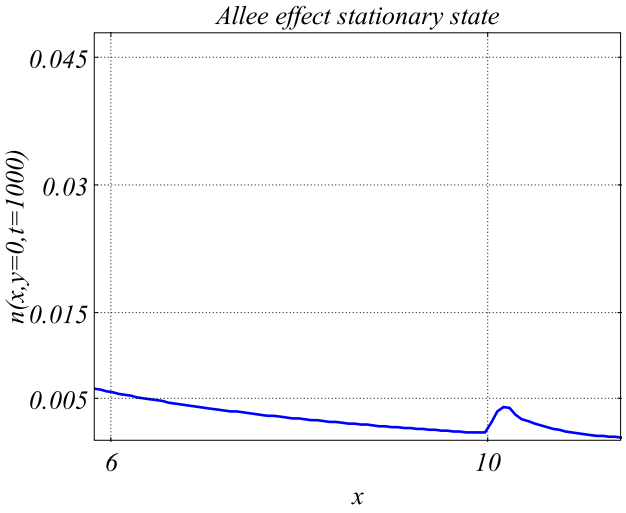

FIGURE 5.17: Cross section for the population dispersal in a two patches system with Allee effect. A close up of the stationary state of a decaying population in the second patch at $t = 1000$ is shown. The parameters used in this system are: $\mu_0 = 3$, $\delta = 0.05$, $\frac{\Gamma}{\lambda} \approx 0.7$, $M = 0.01$, $\varsigma = 0.0075$ and $\nu = 5$

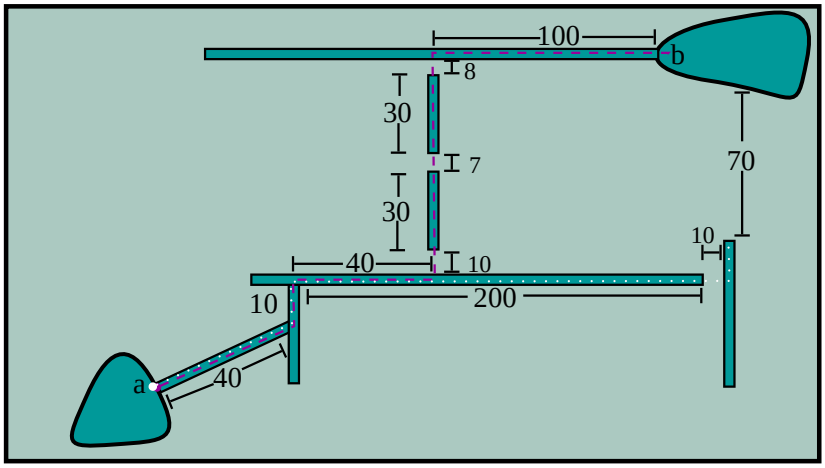

FIGURE 5.18: Example of a two-dimensional corridor network used to illustrate the results found in §5.4.2 5.4.3 and 5.5. The darker areas represent suitable habitat, while the clearer ones are hazardous regions for the population. The population disperse along the corridor network from (a) to (b) through two different paths: the dashed one and the dotted one.

effect.

In figure 5.18, we propose a number of arbitrary values for the corridor lengths and gaps as shown. From these values we can find the time it takes to go from the point a to the point b through different paths. If we take the purple dashed path, we can add the values of the corridor lengths the population travels to obtain a total of 250 length units.

In the case of gaps, we obtain a total of 25 length units. Assuming that the velocity over the corridors is $c = 3$ and that for the gap lengths $\Delta x = \Delta t$ we obtain a total travelling time of $t = 3(250) + 25 = 805$ units of time.

If we take the white dotted path, we reach a point where the gap reaches a length that makes the numerical analysis unreliable. In this case our hypothesis is that without the presence of an Allee efect, the population flux eventually reaches the next patch, producing a dispersing population that eventually reproduces. If an Allee effect is assumed in the population dynamics, no dispersal would take place, resulting in the failure of population dispersal from point c to b.

This is an extremely simplified example, with arbitrarily taken values for the corridor lengths and gaps. However, with the right biological parameters, and better accuracy in each segment of network, the results found along this chapter can help us describe the population dispersal over real landscapes, similar to the one described in this section. This is of importance in landscape ecology, since these type of models, provide an alternative type of strategy, that could be used in conjunction with the standard methods of data collection and statistical analysis [15, 41, 65, 105].

5.7.1 Short corridors

In the case where the corridors are much shorter than the lengthscale of the wave of advance, another simplification becomes appropriate in which the population within a segment of corridor, grows at the same rate at all points within the corridor. In other words, the spatial derivative along the corridor are negligible in (5.4.1).

5.8 Summary

In this chapter we investigated two-dimensional systems numerically presenting variable reproduction potentials dependent on the spatial location. We include the dendrotaxis term modelling in this way the individuals attraction towards environments with plentiful resources. In these regions individuals of a given species population reproduce

and diffuse. In particular we analyse regions with corridor type structures, which are one of the spatial configurations in which our reference biological example, *Callosciurus erythraeus*, live and reproduce.

We found a set of results regarding individual dispersal in these type of regions. We provide results to population moving along corridors, investigating the effect of corridor width and corridor junctions over the individual dispersal. We discover that for corridor widths large enough $2R > 1.8$ waves of advance with velocities in the range $2 \leq c \leq 3.2$ exist. We also find that the existence of junctions do not have a considerable effect on the population dispersal velocities.

We also study the dispersal of individuals in a system composed of two corridors of favourable habitat, separated by a region of scarce-resources. As in Chapter 4, we found relationships between gap lengths and success of population dispersal. In these two-dimensional systems we find that the larger the gap between corridors, the reproduction success in a new corridor decreases. We also investigated the dependence of gap crossing time between corridors on the gap length. As in the case of the one-dimensional analysis, we found the relationship between these two quantities is linear. However, in this chapter, the slope of the waiting time vs. the gap length is larger. We believe that this can be attributed to the system dimension. Since in two dimensions the individuals can move in the x and y direction, the waiting time becomes larger due to the increment on the degrees of freedom of the system.

We made a summary of all the structures studied along this chapter to exemplify how a population would disperse in a corridor network. We conclude that with a small set of biological parameters and more accuracy of the measures for each type of segment of the network, a good prediction of real populations dispersal may be achieved. Hence, these models could present an alternative to predict population dispersal over landscapes with structures similar to the one studied here.

Finally, we investigated the impact of the Allee effect over systems of corridors separated by scarce-resources regions. As expected, when the population is subject to Allee effects, the individual dispersal success decreases. These results may help producing new strategies for population control. Among those strategies we can propose an early

elimination or extraction of invading individuals in new patches, or administration of oral contraceptives to enhance the Allee effect.

In terms of conservation on the other hand, populations may already exist at their carrying capacity. Then, if a land removal takes place, the population may overcome its carrying capacity. This would force a migration into other resources-rich areas. The results presented in this chapter and the previous one can be also applied to the movement and dispersal of conservation targeted populations. The same results presented in Chapter 4 and 5 could be applied to evaluate the possibility for a population to disperse and survive in a purposely modified homogeneous ecosystem. At the same time, these results may help to provide strategies of land conversion, in order to provide the necessary resources for a population to survive in such landscape.

Chapter 6

Discussion, Conclusions and Further Work

6.1 Discussion

In this thesis we focused on the study of the dynamics of populations inhabiting heterogeneous environments. We studied different continuous models based on partial differential equations in one and two dimensions. Using different methods: analytical, semi-analytical and numerical we analysed features that have not previously been explored in existing models.

We then proposed a new model for population dynamics in fragmented environments accounting for the landscape effect on individual behaviour. This model acknowledges the individuals response to hazardous areas by introducing a new term in the reaction-diffusion equation that works as an attractive field towards resource-rich areas.

In Chapter 1 we gave an introduction of the dynamics of fragmented environments in terms of biological concepts. Then in Chapter 2, we introduced and explained the most commonly used continuous population models in population ecology. We also provided a bibliographic review based on the biggest advances around the study of dispersal of populations in fragmented environments.

Later in Chapter 3, we firstly presented a set of analyses based on pre-existent population models. Then, we included new studies and results of three different systems. In the first system we analysed a semi-infinite system with absorbing boundary conditions. We found analytic results for this system, which were compared with approximate results for the same system, in order to validate other approximate results computed for the systems analysed later.

The second analysis was performed for a single one-dimensional system of length of the order of the critical patch size, and the third analysis was done for a single one-dimensional patch of length patches much larger than the CPS but finite ($L \gg L_c$), both systems with absorbing boundaries.

Some of the results found for patches with lengths close to the critical patch size, like the critical patch size limit itself, were previously investigated. However, we presented them as a way to enhance the understanding of these systems and their relationship with the new results found. The results found in this chapter include a relationship between the carrying capacity and the effective population growth rate with the patch length, obtaining a linear relationship between patch size and carrying capacity.

One of the characteristics we analysed in depth in Chapter 3 was the individual flux and its relationship with the patch size and the boundary conditions. We focus our attention on this quantity since its measurement is a key feature to describe population movement and dispersal over different environments. We found that, the current of individuals correspondent to patches with sizes $L \gg L_c$ is almost identical to the one found in semi-infinite systems. This is an interesting result, since the semi-infinite patch system is tractable analytically while large systems are not. Therefore, we found that the possibility of using semi-infinite systems to approximate results of large ones is possible.

We also found that for patches with permeable boundaries, the critical patch size depends on the ratio between the propagation velocity of the population, inside and outside the patch. We discovered that the population distribution and the current of individuals, also depends on these two velocities of propagation. This dependence show us that the way individuals disperse in a system constituted by a resources-rich patch surrounded by resources-scarce regions is similar to a population confined in a patch (the resource-rich

one) surrounded by a fence. When the individuals reach the boundary, even if they are not restricted by any obstacle, our results show that they "struggle" to leave the patch. This conclusion is obtained from the lack of continuity on the population derivative at the patch boundary.

Finally, we observe that in all the single-patch systems analysed in Chapter 3, the current reaches its maximum at the boundary, while the population density tends to zero. Far away from the boundary, the current decays in the patch and in the dangerous or lethal areas. On the other hand the population distribution is constrained mainly to the patch, becoming zero outside it, for the case of lethal boundaries, and decaying exponentially in the case of systems with permeable boundaries.

In Chapter 4 we build up a model based on a biological reference system: the invasion and dispersal of the Asiatic red-bellied beautiful squirrel *Callosciurus erythraeus* in the Argentinian pampas. This model is constructed on the groundwork of the individuals dynamics provided in [15] and by personal communication with Dr. M. L. Guichón and C. P. Doncaster.

In this model we introduce an explicit term that accounts for the spatial preference of individuals for some regions over others in their own environment, that we name dendrotaxis. The way we introduce this environmental preference is through the boundary conditions. Beside this, we associate the population growth or decay function to the spatial location of the individuals. Joining these two factors we develop the system analysed in Chapter 4 and 5 where a population that depends explicitly on their location for their reproductive success, and that accounts for their individuals sensitivity to their surroundings is modelled.

In Chapter 4 we focus the analysis on one-dimensional systems. In particular we study the dispersal of individuals in a system composed by two patches of potentially successful reproductive populations, separated by a region of danger for the population. We find a linear relationship between the time taken to cross such hazardous areas and the hazard area length. In this analysis we include analytic and numerical results, showing that this relationship holds for both analyses, when the hazard area length is big. We also find semi-analytic results for the population distribution, after crossing a gap.

Then we analyse the consequences of the presence of an Allee effect on the dynamics of this system. We find analytic solutions for a stationary state solution, that develops when the Allee effect is such that the population is unsuccessful to reproduce. If such stationary state does not exist, our assumption is that the population eventually reproduce following logistic growth and developing into travelling wave solutions. In this context, we found a relationship between the size of the Allee parameter ν and the gap between patches L. We discovered the existence of a critical gap L_{crit} that, for a given value of ν tells us the maximum length of the gap that a population can cross, before it goes to a decaying stationary state. This relationship shows that, as expected, the bigger the Allee effect is, the smaller the gap has to be for the population to be able to support breeding populations.

The latest mathematical analysis is done in Chapter 5, where we analysed the model constructed in Chapter 4 in a two-dimensional space. The analyses performed in this chapter are mainly numeric, although, there is an outlined semi-analytical analysis of these systems in Appendix 1.

Consistent with the type of geometries where our reference species the "Asiatic red-bellied beautiful squirrel", we studied corridor type structures. We did an analysis of travelling wave solutions finding a dependence between the velocity of the wave of advance and the corridor width. We find that when the corridor is wide enough, and the velocity of spread is in a single direction, the velocity is given by $c_{min} = 2\sqrt{D\alpha}$. This velocity is the minimum velocity [34] found for a travelling wave solution to the Fisher equation in one dimension,

$$\frac{\partial n}{\partial t} - \nabla n = n(1-n). \tag{6.1.1}$$

For corridor widths larger or equal than $2R = 1.8$, we found that the velocity is always larger than the minimum velocity $c > c_{min}$. However as the corridor width increases, the velocity of the wave of advance tends to the minimum velocity $c_{min} = 2$.

We also find critical widths for corridors, for which travelling wave solutions are formed. This width corresponds to $2R = 1.8$ in rescaled units. A relationship between corridor width and velocity of the travelling wave solution was found, and velocity of the wave

of advance over junctions was examined. Finally, we analysed the compatibility of this model with the dynamics of our reference species behaviour. Since the mean dispersal rate of the Asiatic red-bellied beautiful squirrel D, is very large compared with its reproduction rate α, the correlation length, that is proportional to $\xi \propto \sqrt{\frac{D}{\alpha}}$ is of the order of $600m$. In order to conserve the travelling wave form, we need that $L >> \xi$. Therefore, the mathematical model presented in Chapter 5 can be applied only to corridors of length scales of the order of kilometers.

Then, we analysed the dynamics of individuals gap crossing over corridor geometries with gaps, similar to the analysis performed in Chapter 4. We discovered a linear relationship between the waiting time t_{wait} to cross a gap, and the gap length L. This is in agreement with the results found in Chapter 4, although the slope of the linear relationship is larger in the case of the two-dimensional system. We attribute this difference to the dimensionality of the system. In two dimensions the individuals have a one more degree of movement freedom, and therefore the waiting time is larger.

We then explored the consequences of the Allee effect over the patch-gap-patch system. As in the case of the one-dimensional system, the response of the population due to the Allee effect is characterized by either the delay on the reproduction time of the population reaching an initially empty resource-rich patch, or by the developing of a population decaying stationary state. We believe that, as in the case of the one-dimensional system, the existence of critical gap lengths L_{crit} dependent on the applied Allee effect must exist. However this not explored, and we leave it as a future work to develop in the following months.

Finally, we summarised the results found for separated geometry structures to explore a system containing all of them. A calculation of the dispersal of a population over a corridor network through different paths was examined, finding dispersal times dependent on the path taken by the species. The results found as a whole in Chapters 4 and 5, lead us to believe that with the use of a small set of parameters such as the population mean dispersal time, reproduction rates, Allee effect values (if they exist), and decay rates in different environments, can help us to predict the dispersal time from region to region over the same fragmented habitat.

In general, this thesis presents an analysis of spatially fragmented systems where a variety of systems and their dynamics are examined in different situations. These analyses gave very interesting results related to dispersal velocities, reproduction success dependent on the landscape structure, Allee effect consequences dependent on the population ability to disperse and on the landscape configuration, and dispersal effects caused by behavioural features (individuals sense of danger).

6.2 Conclusions

In this thesis we provide a short introduction to spatial population ecology, explaining the basic biological concepts needed to understand and implement mathematical models that resemble the biological systems. An introduction to the standard mathematical models of fragmented ecosystems is also presented and a literature review on the subject is done.

We also present a set of one- and two-dimensional models for fragmented ecosystems, focusing on the dynamics of population dispersal over fragmented environments. Two different approaches are taken: in the first one, the population diffuses without being affected by the structure of their environment. In the second one, the population disperses acknowledging the structure of their landscape, showing a preference for some regions over others.

We find a set of results that explain the population dynamics with respect to relevant biological features for the individual dispersal, such as, dispersal rates, death rates, consequences of Allee effects on the population reproduction, carrying capacities dependent on patch sizes, dispersal velocities, and ability to cross hazardous regions.

Although the models presented here are very simplistic compared with other models such as, the stochastic models presented by Guichón and Doncaster [15], they have some advantages. Their advantage relies on the generality of the results obtained. Even if we used the Asiatic red-bellied beautiful squirrel as a biological reference, these models can be applied to any other population subject to similar conditions and behaviours.

The importance of the models presented in this thesis is that they give a new insight

into the field of spatial population models, presenting alternative ways to understand the population dynamics over systems constituted by one or two patches, that can be generalised to systems with a larger number of patches. Therefore, the analyses provided along this thesis are focused on the discovery of specific results for the population dispersal in systems of one or two patches surrounded by areas of variable danger.

6.3 Further work

In Chapter 3, we detailed the dynamics of the population and current distribution of a population confined to a one-dimensional patch surrounded by regions of variable danger. These results, are very specific to the length scale of the system analysed in this thesis. However, these results could be generalised for a system with a large number of patches, either, by assuming periodicity on the system structure or stochasticity in the patch distribution. This would provide general results for systems with a large number of patches such as effective population growth and decay rates, effective carrying capacities, effective current distribution and effective population distributions. Some ways to perform these generalisation include homogenisation methods and a variety of function distributions.

In Chapter 4, we introduced the idea of dendrotaxis to model individuals behaviour towards their environment. The way we modelled this term was by assuming a sharp attraction, in the form of step functions towards resource-rich regions. This results in the imposition of jump conditions in the boundary. However, a more realistic approach may consider that the level of attraction towards the resource-rich regions depends on the distance to the patch. Therefore, the introduction of, for example, a linear or an exponential function as a dendrotaxis term may model the individual behaviour in a better way.

We also pointed out in Chapter 5, that the analysis performed for corridor structures was only suitable in corridors of lengths much bigger than the diffusive length $L \gg \xi$. An analysis of the population dynamics for short corridors is therefore needed. In short length corridors, we presume that no travelling waves will form, and different means of

dispersal rate may have to be investigated.

A more detailed analysis of the Allee effect over two-dimensional systems, as well as analytical analyses are also needed. Obtaining critical gap lengths L_{crit} for fixed values of Allee parameters is one of most immediate features to analyse, since its accurate measurement may direct the development of population control strategies, such as the implementation of contraception methods for the targeted population.

Analytical results for two-dimensional analyses are outlined in Appendix A. However, the completion of these analyses, and the possible implementation of different methodologies and modelling features to these systems, can be a very interesting area of future research.

Finally, a clear comparison between the results originated from experimental data and stochastic models (as the ones presented in [15]), with the results found through the models presented in this thesis, would be a very interesting topic of study. This comparison would test the validity of the models presented here, pointing out issues and possible strategies to improve the models proposed in this thesis.

Appendix A

Semi-analytic analysis of corridors and gap crossing

In this appendix we perform a semi-analytic analysis of the a two-dimensional system constituted by one-dimensional line corridors that follow a logistic reproduction function immersed in a two-dimensional plane with decaying reproduction functions, shown in figure A.1.

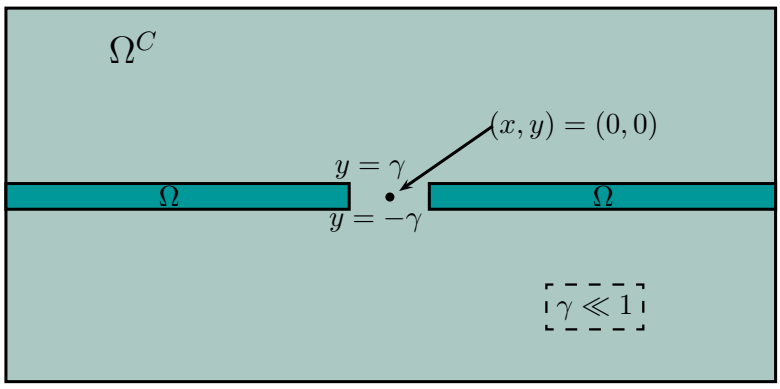

FIGURE A.1: Two-dimensional geometry used in the analysis of the dispersal of individuals between two tree line corridors and through a grassland area.

A.1 Model setup

Going back to the set of equations given by (5.4.1)-(5.4.4), we know that in the resource-rich regions the population grows logistically and in the scarce-resource regions, the population decays linearly. We also know that at the boundary the dendrotaxis term produce a discontinuity on the population number at the boundary, while the flux of individuals from one patch of woodland to another is kept continuous. Keeping this in mind we analyse the geometry given in figure A.1. The darker areas in figure A.1 represent line corridors where the population grows logistically, while the rest of the domain is constituted by scarce-resource regions. If we assume that the line corridors are very thin then we can assume that $\gamma \ll 1$ from figure A.1 and we can write $y = \gamma Y$. With this consideration equations (5.4.1)–(5.4.2) transform into

$$\frac{\partial n}{\partial t} = n(1-n) + \frac{\partial^2 n}{\partial x^2} + \frac{1}{\gamma^2}\frac{\partial^2 n}{\partial Y^2} \quad \text{in } \Omega, \tag{1.1.1}$$

$$\delta\frac{\partial n}{\partial t} = -n + \lambda^2\nabla^2 n \quad \text{in } \Omega^{\complement}. \tag{1.1.2}$$

while the boundary conditions (5.4.3)–(5.4.4) become,

$$n|_{y=\gamma} = n|_{Y=1}, \tag{1.1.3}$$

$$n|_{y=-\gamma} = n|_{Y=-1}, \tag{1.1.4}$$

and

$$\mathbf{N}\cdot\nabla n|_{y=\gamma} = \frac{\Gamma}{\gamma^2}\mathbf{N}\cdot\nabla n\Big|_{Y=1}, \tag{1.1.5}$$

$$\mathbf{N}\cdot\nabla n|_{y=-\gamma} = \frac{\Gamma}{\gamma^2}\mathbf{N}\cdot\nabla n\Big|_{Y=-1}. \tag{1.1.6}$$

Here, as in equations (3.3.10) and (4.5.2), $\lambda = \sqrt{\dfrac{D'\alpha}{D\alpha'}}$ and $\Gamma = \frac{\epsilon\lambda^2}{\delta}$. In Ω we expand n in powers of γ by writing

$$n = n_0(x,t) + \gamma^2 n_1(x,Y,t) + ... \tag{1.1.7}$$

to leading order. Equation (1.1.1) becomes

$$\frac{\partial n_0}{\partial t} = n_0(1-n_0) + \frac{\partial^2 n_0}{\partial x^2} + \frac{\partial^2 n_1}{\partial Y^2} \quad \text{in } \Omega. \tag{1.1.8}$$

Expanding n in $\Omega^{\complement}$ we obtain,

$$n = \epsilon \tilde{n}_0(x,t) + ... \quad \text{in } \Omega^{\complement}. \tag{1.1.9}$$

Observe that the canonical limit is given by $\Gamma = \mathcal{O}(\gamma^2)$, then, defining $\Gamma = \gamma^2\tilde{\Gamma}$, $\tilde{\Gamma} = \mathcal{O}(1)$. Equation (1.1.2) becomes,

$$0 = -\tilde{n}_0 + \lambda^2 \left(\frac{\partial^2 \tilde{n}_0}{\partial x^2} + \frac{\partial^2 \tilde{n}_0}{\partial y^2} \right) \quad \text{in } \Omega^{\complement}. \tag{1.1.10}$$

The one-dimensional boundary conditions given in equations (4.5.11) and (4.5.12) are transformed into the four boundary conditions for the two-dimensional system:

$$\left.\frac{\partial n_1}{\partial Y}\right|_{Y=1} = \tilde{\Gamma} \left.\frac{\partial \tilde{n}_0}{\partial y}\right|_{y=0^+}, \tag{1.1.11}$$

$$\left.\frac{\partial n_1}{\partial Y}\right|_{Y=-1} = \tilde{\Gamma} \left.\frac{\partial \tilde{n}_0}{\partial y}\right|_{y=0^-} \tag{1.1.12}$$

$$n_0(x,t) = \left.\tilde{n}_0\right|_{y=0^+}, \tag{1.1.13}$$

$$n_0(x,t) = \left.\tilde{n}_0\right|_{y=0^-}. \tag{1.1.14}$$

Integrating equation (1.1.8) respect to Y we obtain,

$$\int_{Y=-1}^{Y=1} \frac{\partial n_0}{\partial t} dY = \int_{Y=-1}^{Y=1} n_0(1-n_0) + \frac{\partial^2 n_0}{\partial x^2} + \frac{\partial^2 n_1}{\partial Y^2} dY, \tag{1.1.15}$$

that results in the equation

$$\frac{\partial n_0}{\partial t} = n_0(1-n_0) + \frac{\partial^2 n_0}{\partial x^2} + \frac{1}{2}\left[\left.\frac{\partial n_1}{\partial Y}\right|_{Y=1} - \left.\frac{\partial n_1}{\partial Y}\right|_{Y=-1} \right], \tag{1.1.16}$$

or equivalently,

$$\frac{\partial n_0}{\partial t} = n_0(1-n_0) + \frac{\partial^2 n_0}{\partial x^2} + \frac{\tilde{\Gamma}}{2}\left[\left.\frac{\partial \tilde{n}_0}{\partial y}\right|_{y=0^+} - \left.\frac{\partial \tilde{n}_0}{\partial y}\right|_{y=0^-}\right]. \tag{1.1.17}$$

Due to the symmetry of the system $\left(\left.\frac{\partial \tilde{n}_0}{\partial y}\right|_{y=0^-} = -\left.\frac{\partial \tilde{n}_0}{\partial y}\right|_{y=0^+}\right)$ we have that

$$\frac{\partial n_0}{\partial t} = n_0(1-n_0) + \frac{\partial^2 n_0}{\partial x^2} + \tilde{\Gamma}\left.\frac{\partial \tilde{n}_0}{\partial y}\right|_{y=0^+}. \tag{1.1.18}$$

In summary we have that for a 2 dimensional system composed by two arbitrarily thin corridors and grassland area the equations are sumarised on dropping the subscripts for n_0 and $\tilde{n}_0$ as,

$$\frac{\partial n}{\partial t} = n(1-n) + \frac{\partial^2 n}{\partial x^2} + \tilde{\Gamma}\left.\frac{\partial \tilde{n}}{\partial y}\right|_{y=0^+} \quad \text{in } \Omega, \tag{1.1.19}$$

$$0 = -\tilde{n} + \lambda^2 \nabla^2 \tilde{n} \quad \text{in } \Omega^{\complement}, \tag{1.1.20}$$

$$n(x,t) = \tilde{n}|_{y=0^-} = \tilde{n}|_{y=0^+} \quad \text{for } x > |L|, \tag{1.1.21}$$

$$\left.\frac{\partial \tilde{n}}{\partial y}\right|_{y=0^-} = -\left.\frac{\partial \tilde{n}}{\partial y}\right|_{y=0^+} \quad \text{for } -L < x < L \tag{1.1.22}$$

schematically shown in figure A.2.

With this set of equations we can analyse the problem analytically. By setting the initial conditions $n(x,t)|_{t=0} = n|_{y=0^+}$ we can solve for $\tilde{n}$ (1.1.20), evaluate $\left.\frac{\partial \tilde{n}}{\partial y}\right|_{y=0^+}$ and evolve equation (1.1.19) in time. In the following section we choose to use a boundary integral method to solve this problem, due to the complexity of the problem.

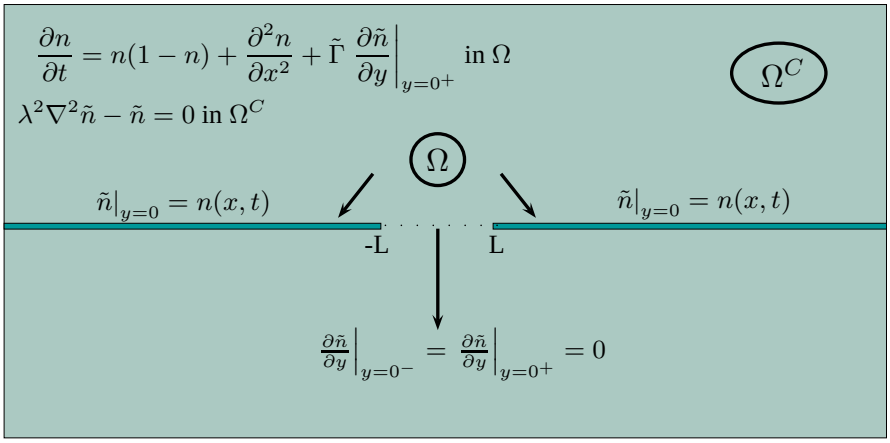

FIGURE A.2: A summarised two- dimensional geometry for the analysis of a two long corridor system is presented. In the corridor the population grows logistically, while in the grassland the individuals die at linear rate. At the boundary the individuals present a "sense of danger" which prevents them from leaving the corridor.

A.2 Boundary integral method analysis

Since the equations in $\Omega^{\complement}$ are independent of time, the population change in time is zero everywhere, except in the lines $\{|x| > L, y = 0; \in \Re^2\}$ where the population follows the dynamics given by equation (1.1.19). Equation (1.1.19) expresses how the population grows logistically and diffuses throughout the corridor. In the region $\{\Re^2 \setminus \{y = 0, |x| > L\}\}$, named $\Omega^{\complement}$, the population obeys a linear death rate with diffusion, modelled by equation (1.1.20).

One way to solve this set of equations is by means of *Green's functions* and *Boundary Integral Methods* [56, 137–139]. These methods involve finding the solution of a partial differential equation in form of an integral equation where the kernel of this integral equation is partially or totally constituted by the Green's function of the problem. Therefore, the solution of a boundary integral problem requires the ability to calculate the Green function of the differential equation under study.

Green's functions can express differential equations in terms of distributions instead of functions. To illustrate this feature of Green's functions we write an ordinary differential equation in terms of linear operators,

$$\mathcal{L}(x)u(x) = f(x) \tag{1.2.1}$$

where L is a linear operator, $f(x)$ is a known function and $u(x)$ is the solution to find. A way of solving this equation is by means of eigenfunction expansions, but another way is through Green's function calculation. In this case, equation (1.2.1) can be written as

$$\mathcal{L}g(x,\rho) = \delta(x-\rho_i) \tag{1.2.2}$$

where ρ_i can be thought as point of excitation or a potential source [140]. The solution $u(x)$ is given by an integral where the kernel of the resulting integral equation is composed, partially or completely, by the Green's function $g(x,\rho)$ associated to the partial differential equation [137].

The essential feature and importance of boundary integral methods, is that often they allow a problem involving the domain of interest to be simplified to one where only its boundary is involved [141]. In this way the dimension of the problem is also reduced by one. This method reduces a boundary value problem of a differential equation in a domain to an integral equation on the boundary. The boundary value problem of the differential equation is exchanged for a singular integral equation in the boundary, where the problem is solved either analytically if possible, or numerically [56].

Then, in terms of boundary integral equations, the solution of equation (1.1.20), $\lambda^2\nabla^2\tilde{n}-\tilde{n}=0$ away from the line $y=0$ can model the effect of the boundary conditions by assuming the presence of a linear source along $y=0$, where the strength of the source is *a priori* unknown.

The method we use is explained as follows. To obtain the field $n(\mathbf{r})$ produced by a distributed source $\rho(\mathbf{r};\mathbf{r}_0)$, the effect of each elementary portion of source $\rho_i(\mathbf{r}_0)$ is calculated and integrated over the source distribution.

As shown in figure A.3, if $G(\mathbf{r};\mathbf{r}_0)$ is the problems' Green's function at the observer's point $\mathbf{r}$ caused by a unit source $\rho_i(r_0)$ at the point $\mathbf{r_0}$, then the field $n(\mathbf{r})$ produced by a source distribution $\rho(\mathbf{r}_0)$ is the integral

$$n(\mathbf{r}) = \int_a^b \rho(\mathbf{r}_0)G(\mathbf{r};\mathbf{r}_0)d\mathbf{r_0} \tag{1.2.3}$$

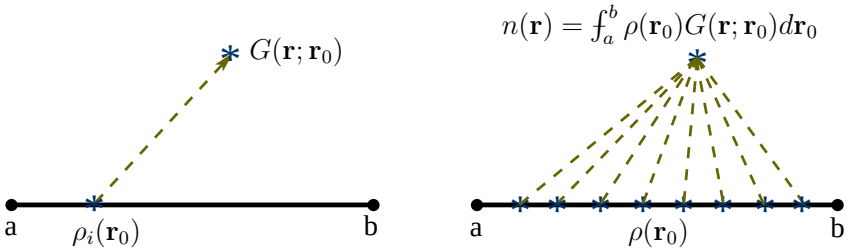

FIGURE A.3: On the left, a field $G(\mathbf{r};\mathbf{r}_0)$ produced at the point $\mathbf{r}$ by a source located at $\mathbf{r}_0$ is shown. On the right, the field $n(\mathbf{r};\mathbf{r}_0)$ produced by the source distribution $\rho(\mathbf{r}_0)$ at the point $\mathbf{r}$ is described. Each source distribution $\rho_i(\mathbf{r}_0)$ contributes to obtain the field $n(\mathbf{r};\mathbf{r}_0)$.

in the whole range of $\mathbf{r_0}$ occupied by the sources [138].

If the equation is homogeneous, but the boundary conditions are not, the problem can be solved by considering the boundary conditions as equivalent to sources using the boundary integral method, see [142]. Inhomogeneous boundary conditions are replaced by homogeneous ones and the sources changed appropriately.

Here we wish to solve for $\tilde{n}_0$ which satisfies the following problem,

$$\lambda^2\nabla^2\tilde{n}_0 - \tilde{n}_0 = 0 \qquad \text{in } \Omega^{\complement}, \tag{1.2.4}$$

$$\tilde{n}_0|_{y=0} = n_0(x,t) \qquad \text{for } |x| > L \tag{1.2.5}$$

$$\left.\frac{\partial\tilde{n}_0}{\partial y}\right|_{y=0} = 0 \qquad \text{for } |x| < L. \tag{1.2.6}$$

$$\tilde{n}_0 \to 0 \qquad \text{as } x, y \to \infty \tag{1.2.7}$$

Firstly, we solve (1.2.4) over the whole space $\Re^2$ and then apply the boundary conditions. To satisfy the boundary conditions, we solve equation (1.2.4), considering that the sources are located in the boundary of the whole plane $\Re^2$, or in this case, in

$\{|x| > L, y = 0; \in \Re^2\}$. The Green function for equation (1.2.4) satisfies,

$$\nabla^2 G - \frac{1}{\lambda^2} G = \delta(x - x_0)\delta(y - y_0), \tag{1.2.8}$$

that is referred sometimes as the *modified Helmholtz equation* and has the solution,

$$G(x, y) = \frac{1}{2\pi} \mathcal{K}_0 \left(\frac{r}{\lambda}\right), \quad r = \sqrt{(x - x_0)^2 + (y - y_0)^2}, \tag{1.2.9}$$

where $\mathcal{K}_0$ is the modified Bessel function of the second kind [139, 143, 144].

The equation $\lambda^2 \nabla^2 \tilde{n}_0 - \tilde{n}_0 = A(x, y)$, with the boundary conditions given by equations (1.2.5) and (1.2.6) has the solution,

$$\tilde{n}_0(x, y) = \int\!\!\!\!\!\!\int_{-\infty}^{\infty} \mathcal{K}_0 \left(\frac{r}{\lambda}\right) A(x_0, y_0) dx_0 dy_0. \tag{1.2.10}$$

This is the solution for a source $A(x, y)$ everywhere in the space. Thus, if $A(x, y) = 0$ everywhere except on $|x| < L, y = 0$, we can write,

$$\tilde{n}_0(x, y) = \left(\int\!\!\!\!\!\!\int_{-\infty}^{-L} + \int\!\!\!\!\!\!\int_{L}^{\infty} \right) \mathcal{K}_0 \left(\frac{1}{\lambda} \sqrt{(x - x_0)^2 + y^2} \right) A(x_0, t) dx_0, \tag{1.2.11}$$

for some function $A(x, t)$. In order to determine this function in terms of $n_0(x, t)$ we apply the boundary conditions (1.2.5) to obtain

$$n_0(x, t) = \left(\int\!\!\!\!\!\!\int_{-\infty}^{-L} + \int\!\!\!\!\!\!\int_{L}^{\infty} \right) \mathcal{K}_0 \left(\frac{1}{\lambda} |x - x_0| \right) A(x_0, t) dx_0, \tag{1.2.12}$$

assuming $n_0(x, t)$ is a known function. Equation (1.2.12) gives an integral equation which can be solved to find $A(x, t)$ for $|x| > L$.

A.2.1 Problem context

The characteristics of the problem specified by equations (1.2.10)–(1.2.12), results in the postulation of an ill-posed problem. The ill-posedness of the problem origins due to the line break over $y = 0$ at $|x| < L, y = 0$. This break determines the solution of the integral equation (1.2.12) not to be well defined. To handle the ill-posedness

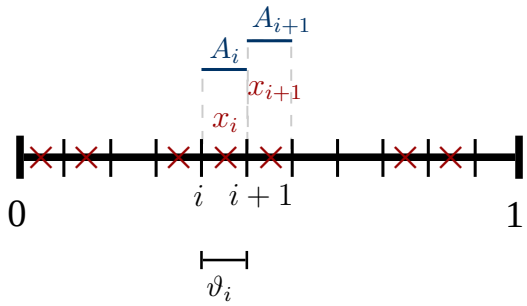

FIGURE A.4: To find the value of the function $A(x_0, t)$ in the domain $x_0 \in [0, 1]$, the whole domain is divided in N sub-intervals. The function $A_i(x_0, t)$, is piecewise constant in each sub-interval ϑ_i where $i = 1, 2, ..., N$. The integral given by equation (1.2.14) is performed for each function $A_i(x_0, t)$. All the integrals are added to find the general solution of the integral equation.

of the problem, different regularisation methods can be used. In §A.2.4 the Tikhonov regularisation method is explored as a choice to find the approximate solution of equation (1.2.12).

A.2.2 Numerical analysis

To find the value of the function $A(x_0, t)$ we solve numerically the integral equation given by equation (1.2.12), supposing that the function $n_0(x, t)$ is a known function. We start firstly by considering the simpler problem,

$$f(x) = \int_0^1 K_0\left(\frac{1}{\lambda}|x - x_0|\right) A(x_0)dx_0 \quad \text{for } 0 \leq x \leq 1 \tag{1.2.13}$$

shown in figure A.4. The interval $x = [0, 1]$ is sub-divided in N intervals of size $\frac{1}{N}$. Each sub-interval is denoted by the variable ϑ. In equation (1.2.13), we approximate the function $f(x)$ as a piecewise linear function for each interval ϑ_i. At the same time, we approximate $A(x_0)$ by a function that is piecewise constant in each sub-interval.

For each sub-interval ϑ_i, we integrate the function $A_i(x_0, t)$ respect to x_0 over the whole domain $[0, 1]$, obtaining for a single sub-interval

$$f(x_i) = \int_i^{i+1} \mathcal{K}_0(\frac{1}{\lambda}|x_i - x_0|)A_i(x_0)dx_0, \tag{1.2.14}$$

that for the domain $[0,1]$ transforms into

$$f(x_i) = \sum_{i=1}^{N} \int_{(i-1)/N}^{i/N} \mathcal{K}_0(\frac{1}{\lambda}\,|x_i - x_0|) A_i(x_0) dx_0. \tag{1.2.15}$$

Equation (1.2.15) defines a row in a matrix equation for every value of x_i that, after evaluating over the whole domain looks like:

$$\begin{pmatrix} f(x_1) \\ f(x_2) \\ \vdots \\ f(x_i) \\ \vdots \\ f(x_N) \end{pmatrix} = \frac{1}{\lambda} \begin{pmatrix} \cdots & \int_{i/N}^{i+1/N} \mathcal{K}_0(\frac{1}{\lambda}\,|x_1 - x_0|) dx_0 & \cdots \\ \cdots & \int_{i/N}^{i+1/N} \mathcal{K}_0(\frac{1}{\lambda}\,|x_2 - x_0|) dx_0 & \cdots \\ \vdots & \ddots & \vdots \\ \cdots & \int_{i/N}^{i+1/N} \mathcal{K}_0(\frac{1}{\lambda}\,|x_i - x_0|) dx_0 & \cdots \\ \vdots & \ddots & \vdots \\ \cdots & \int_{i/N}^{i+1/N} \mathcal{K}_0(\frac{1}{\lambda}\,|x_N - x_0|) dx_0 & \cdots \end{pmatrix} \begin{pmatrix} A_1 \\ A_2 \\ \vdots \\ A_i \\ \vdots \\ A_N \end{pmatrix} \tag{1.2.16}$$

The value of the integral for a sub-interval ϑ_i in the domain $x_0 = [0,1]$ from the point x_j is a single entry of the matrix $\mathbb{M}$ given by,

$$\mathbb{M} = \frac{1}{\lambda} \begin{pmatrix} \cdots & \int_{i/N}^{i+1/N} \mathcal{K}_0(\frac{1}{\lambda}\,|x_1 - x_0|) dx_0 & \cdots \\ \cdots & \int_{i/N}^{i+1/N} \mathcal{K}_0(\frac{1}{\lambda}\,|x_2 - x_0|) dx_0 & \cdots \\ \vdots & \ddots & \vdots \\ \cdots & \int_{i/N}^{i+1/N} \mathcal{K}_0(\frac{1}{\lambda}\,|x_i - x_0|) dx_0 & \cdots \\ \vdots & \ddots & \vdots \\ \cdots & \int_{i/N}^{i+1/N} \mathcal{K}_0(\frac{1}{\lambda}\,|x_N - x_0|) dx_0 & \cdots \end{pmatrix} \tag{1.2.17}$$

where,

$$\begin{aligned} \mathbb{M}(i,j) = \frac{\pi}{N} \Bigg[& (-i+j+1/2) \left[K_0\left(\frac{|-i+j+1/2|}{N}\right) L_{-1}\left(\frac{|-i+j+1/2|}{N}\right) + \right. \\ & \left. + K_1\left(\frac{|-i+j+1/2|}{N}\right) L_0\left(\frac{|-i+j+1/2|}{N}\right) \right] + \\ & + (-j+i+1/2) \left[K_0\left(\frac{|i-j+1/2|}{N}\right) L_{-1}\left(\frac{|i-j+1/2|}{N}\right) + \right. \\ & \left. + K_1\left(\frac{|i-j+1/2|}{N}\right) L_0\left(\frac{|i-j+1/2|}{N}\right) \right] \Bigg]. \end{aligned} \tag{1.2.18}$$

In equation (1.2.18), K_0 and K_1 are the Modified Bessel functions of order 0 and 1

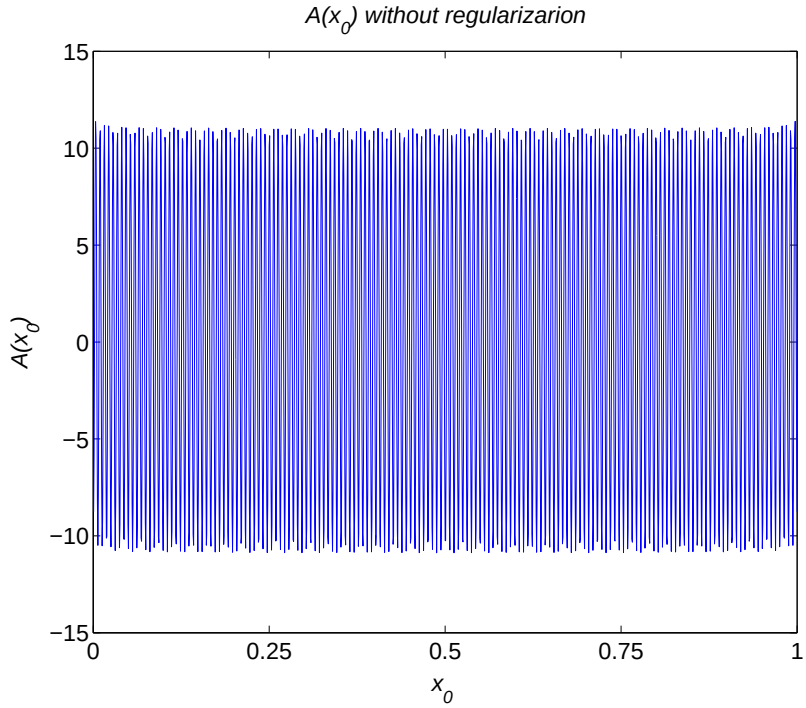

FIGURE A.5: Solution for $A(x_0)$ before regularisation. The regularisation of this function must be done because the integrals performed in each sub-domain are singular. As a consequence the integral equation is ill-posed.

respectively, L_{-1} and L_0 are the Modified Struve functions of order -1 and 0 respectively, N is the total number of sub-intervals the domain is divided in, and the value of the (i, j) entry of the matrix $\mathbb{M}$ is found according to the position on the domain. The matrix equation resulting from this numerical method is then

$$f(x_j) = M_{ij} A_i. \tag{1.2.19}$$

Once the matrix $\mathbb{M}$ is found, we can find the value of the function $A(x_0)$ by inverting the matrix to obtain,

$$A_p = M_{pq} f(x_q). \tag{1.2.20}$$

Figure A.5 shows the solution for $A(x_0)$ calculated using equation (1.2.20). Notice that the solution shown in figure A.5 is not smooth. This is because the matrix $\mathbb{M}$ calculated from such singular integral problems is generally ill-conditioned; therefore, regularisation of the matrix equation given by (1.2.20) is necessary to find the approximate solution to the function $A(x_0)$.

A.2.3 Condition number

The condition number of a matrix measures the sensitivity of the solution of a system of linear equations to errors in the data giving an indication of the accuracy of the results from matrix inversion and the linear equation solution. It is defined as

$$k(\mathbb{A}) = \|\mathbb{A}\| \left\|\mathbb{A}^{-1}\right\| \tag{1.2.21}$$

where A is the matrix defined by the linear equation $\mathbb{A}\mathbf{x} = \mathbf{b}$, and $\|\cdot\|$ stands for the standard Euclidean norm.

If the condition number takes values of $k(\mathbb{A}) = 10^k$ one can expect to loose at least k digits of precision. At the same time, values close to 1 indicate a well-conditioned matrix. In the problem we are examining, the condition number for the non-regularised solution is 753.6305, implying that our solution has lost at least 3 digits of precision.

A.2.4 Tikhonov regularisation

When an ill-posed continuum problem has to be discretised in order to find a numerical solution, the solution of the problem usually involves the incorporation of extra assumptions for its' numerical treatment. A sensible assumption in this case, is to suppose that the solution is smooth. If we assume that the solution of the problem is smooth, then we can use the *Tikhonov regularisation* [145]. This is the most commonly used regularisation method for such ill-posed problems.

The problem

$$\mathbb{A}\mathbf{x} = \mathbf{b}, \tag{1.2.22}$$

analogous to equation (1.2.19), results being ill-posed and the matrix $\mathbb{A}$ happens to be singular, we need to look for a solution with the right properties. The Tikhonov regularisation includes a term that minimizes the condition number giving preference to one solution over the others, producing a smooth solution.

To minimize the error of the matrix equation given by equation (1.2.22) the method we

use consist in optimise the solution using the *linear least squares method* and then add the regularisation term:

$$|\mathbb{A}\mathbf{x} - \mathbf{b}| + \lambda^2 |\mathbb{T}\mathbf{x}| \tag{1.2.23}$$

where $|\cdot|$ represents the Euclidean norm, λ is the regularisation parameter and $|\mathbb{T}|$ is the *Tikhonov matrix*.

If we ignore the regularisation to the solution given by the Tikhonov matrix, the solution is completely dominated by contributions from data errors. By adding regularization we are able to minimize these contributions and maintain the sum given by (1.2.23) of a reasonable size.

The Tikhonov matrix induces a constraint on the solution $\mathbf{x}$ which may be increased or decreased by the value of λ, the regularisation parameter to be chosen [146]. In the example we solve, we assume that the Tikhonov matrix constrains the 4th. derivative of the solution $\mathbf{x}$, making the solution smooth and continuous, whilst the regularisation parameter has the value $\lambda = 1$. The results of the regularisation are shown in §A.2.5

A.2.5 Solution for a line in one dimension

For the problem analysed we suppose that the matrix $\mathbb{T}$ is a difference operator of fourth order which represents the fourth differential operator of the solution. We use this operator to enforce the smoothness of the solution under the assumption that the solution itself is mostly continuous. The function of $\mathbb{T}$ is to ensure that the difference between the forth derivative of the solution and the solution itself tends to zero producing a continuous solution. This regularisation improves the conditioning of the solution enabling a reliable result. The condition number is then reduced to 1.

Figures A.6 and A.7 show the regularised solution for $A(x_0)$ and the error comparison $Err(x_0)$ of the solution, before and after the regularisation respectively. We observe that the solution is greatly improved and smoothed while the error in the solution is decreased substantially.

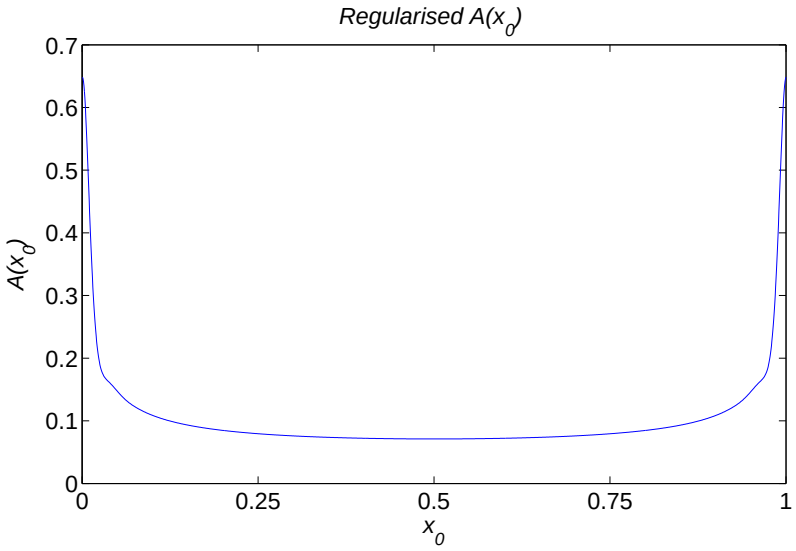

FIGURE A.6: Solution of $A(x_0)$ after regularisation. The regularisation of this function makes the solution smooth and reliable, while the error is also reduced dramatically.

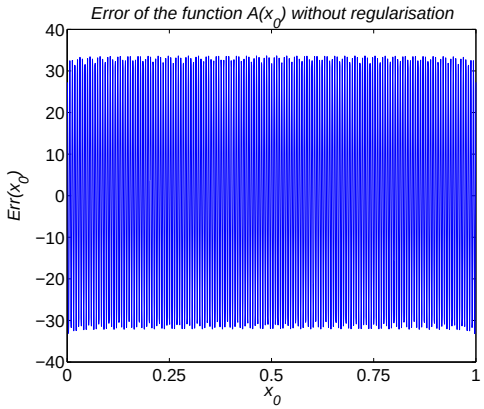

(a) Unregularised Error

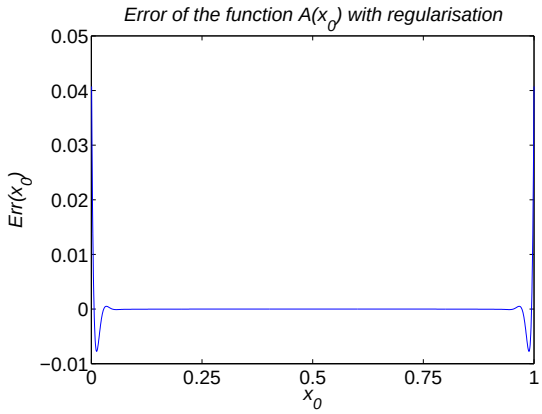

(b) Regularised Error

FIGURE A.7: The figure on the left shows the error $Err(x_0)$ of the function $A(x_0)$ without regularisation. The figure on the right shows the error $Err(x_0)$ with regularisation. After regularising the function $A(x_0)$ the error average, as well as the $Err(x_0)$, decrease substantially.

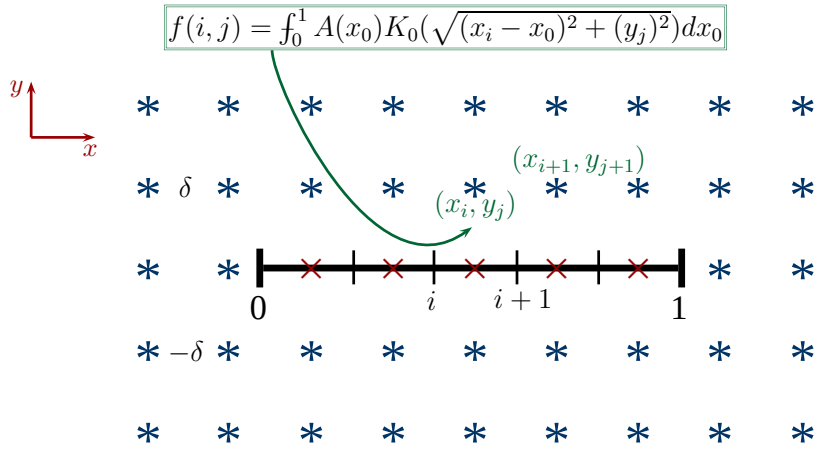

FIGURE A.8: Dependence of the population density on the location in space. Along the line $x \in [0,1], y = 0$ the majority of the population individuals will be located. At the same time, as we move away from this line, the less individuals we will find. The number of individuals located in each point is found by integrating the now known function $A(x_0)$ times the green function $K_0((x - x_0)^2 + y^2)^{1/2}$ over the whole domain in $\Re^2$.

A.3 Two-dimensional analysis of the solution

In §A.2.5 we have found the solution for the function $A(x_0)$ in the domain $[0,1]$. With this solution we investigate how the general solution $n(x,y)$ changes in the plane $\Re^2$. The solution $n(x,y)$ tells us how the population changes in space supposing that the only available woodland area is the line $[0,1]$ and the rest of the plane is grassland. Each point of the line $[0,1]$ will affect the dynamics of the population at the point x_i, y_j as explained in §A.2. To analyse the area around the domain $[0,1]$ we set a domain like the one shown in the figure A.8.

The value of n at the point (x_i, y_i) will be a scalar produced by the integral,

$$n(x_i, y_j) = \int_\Omega A(x_0) K_0((x_i - x_0)^2 + y_j^2)^{1/2} \tag{1.3.1}$$

where (x_i, y_j) is the point where the "population field" $n(x_i, y_j)$ is measured and $A(x_0)$ is the function encountered in §A.2.5.

The function $n(x,y)$, is represented by the integral resultant of the product of the vector $A(x_0)$ and the integral given in (1.3.1). At each point (x_i, y_j) a single value $n(x_i, y_j)$ for the integral (1.3.1) is found, defining the element (i,j) of the matrix $\mathbb{M}$ of size $Q \times R$.

The size of Q is the number of points in x and R is the number of points in y which defines the two-dimensional mesh obtained by calculating the "population field" $n(x, y)$. For the point (x_i, y_j) we have,

$$n(x_i, y_j) = \oint_0^1 (A_1(x_0), ...A_i(x_0), ..., A_N(x_0))K_0((x_i - x_0)^2 + y_j^2)^{1/2} \tag{1.3.2}$$

equivalent to

$$n(x_i, y_j) = \oint_0^1 A_1(x_0)K_0((x_i - x_0)^2 + y_j^2)^{1/2} + ... + \oint_0^1 A_N(x_0)K_0((x_i - x_0)^2 + y_j^2)^{1/2}. \tag{1.3.3}$$

In matrix terms the function $n(x_i, y_j)$ is given by,

$$\mathbf{n} = \begin{pmatrix} n(x_0, y_0) & n(x_1, y_0) & \cdots & n(x_Q, y_0) \\ n(x_0, y_1) & n(x_1, y_1) & \cdots & n(x_Q, y_1) \\ \vdots & \ddots & \vdots & \vdots \\ n(x_0, y_R) & n(x_1, y_R) & \cdots & n(x_Q, y_R) \end{pmatrix} \tag{1.3.4}$$

that gives us the solution of equation 1.2.13 in a two-dimensional domain where all the elements x_i are contained in a domain bigger or equal than $[0, 1] \in x$, and the elements y_j are contained in a domain bigger or equal than $[-\delta, \delta] \in y$.

The solution for a population line located at $x \in (0, 1)$ $y = 0$ in the two-dimensional domain $(x, y \in \{\{0, 1\}, \{-1, 1\})$ is plotted in figure A.9.

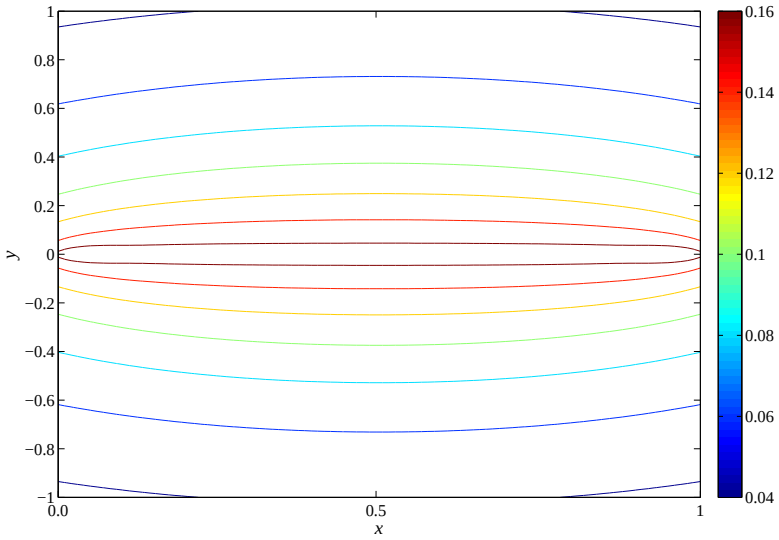

FIGURE A.9: Solution of the population distribution $n(x, y)$ after regularisation. The contour plot indicates how as we move away from the population line $x \in (0, 1), y = 0$ the population disperses and decrease, as expected.

Bibliography

[1] E.P. Odum and G.W. Barrett. *Fundamentals of ecology.* Saunders Philadelphia, 1971.

[2] R.A. Fisher et al. The wave of advance of advantageous genes. *Annals of Eugenics*, 7:355–369, 1937.

[3] R.S. Cantrell and C. Cosner. Spatial heterogeneity and critical patch size: area effects via diffusion in closed environments. *Journal of theoretical Biology*, 209(2): 161–171, 2001.

[4] H. Kierstead and L.B. Slobodkin. The size of water masses containing plankton blooms. *Journal of Marine Research*, 12:141–147, 1953.

[5] A. Ōkubo and S.A. Levin. *Diffusion and ecological problems: modern perspectives.* Springer Verlag, 2001.

[6] N. Kinezaki, K. Kawasaki, F. Takasu, and N. Shigesada. Modeling biological invasions into periodically fragmented environments. *Theoretical population biology*, 64(3):291–302, 2003.

[7] M. Kot, M.A. Lewis, and P. Van Den Driessche. Dispersal data and the spread of invading organisms. *Ecology*, 77.

[8] R.S. Cantrell and C. Cosner. *Spatial ecology via reaction-diffusion equations.* Wiley, 2003.

[9] P. Grinrod. Patterns and Waves: The theory and applications of reaction-diffusion equations. *Bull. Amer. Math. Soc.*, 27(3):320–328, 1992.

[10] M. El Smaily, F. Hamel, and L. Roques. Homogenization and influence of fragmentation in a biological invasion model. *Discrete and Continuous Dynamical Systems, Series A*, 25:321–342, 2009.

[11] L. Roques and M.D. Chekroun. Does reaction-diffusion support the duality of fragmentation effect? *Ecological Complexity*, 7(1):100–106, 2010.

[12] L. Goldwasser, J. Cook, and E.D. Silverman. The effects of variability on metapopulation dynamics and rates of invasion. *Ecology*, 75(1):40–47, 1994.

[13] W.F. Fagan, R.S. Cantrell, and C. Cosner. How habitat edges change species interactions. *American Naturalist*, pages 165–182, 1999.

[14] H. Berestycki, F. Hamel, and L. Roques. Analysis of the periodically fragmented environment model: I–Species persistence. *Journal of mathematical biology*, 51(1): 75–113, 2005.

[15] M.L. Guichón and C.P. Doncaster. Invasion dynamics of an introduced squirrel in Argentina. *Ecography*, 31(2):211–220, 2008.

[16] R.L. Smith and T.M. Smith. *Elements of ecology*. Benjamin Cummings San Francisco, CA, 1998.

[17] E.D. Enger, B.F. Smith, J.W.V. Houton, and C.J. Preston. *Environmental Science: A study of interrelationships*. McGraw-Hill Companies, 2000.

[18] J.H. Brown and M.V. Lomolino. *Biogeography*. Sinauer Associates Sunderland, 1998.

[19] J.R. Krebs and N.B. Davies. *An introduction to behavioural ecology*. Wiley-Blackwell, 1993.

[20] J. Latore, P. Gould, and A.M. Mortimer. Spatial dynamics and critical patch size of annual plant populations. *Journal of Theoretical Biology*, 190(3):277–285, 1998.

[21] P.A. Zollner and S.L. Lima. Orientational data and perceptual range: real mice aren't blind. *Oikos*, 84(1):164–166, 1999.

[22] R. Levins. Coexistence in a variable environment. *American Naturalist*, pages 765–783, 1979.

[23] I. Hanski. *Metapopulation ecology*. Oxford University Press, USA, 1999.

[24] H.R. Akçakaya, G. Mills, and C.P. Doncaster. The role of metapopulations in conservation. *Key topics in conservation biology*, pages 64–84, 2007.

[25] A. Bensoussan, J.L. Lions, and G. Papanicolaou. *Asymptotic analysis for periodic structures*, volume 5. North Holland, 1978.

[26] T.R. Malthus. *An essay on the principle of population, as it affects the future improvement of society. With remarks on the speculations of mr. Godwin, m. Condorcet, and other writers. By TR Malthus*. 1817.

[27] P.F. Verhulst. Notice sur la loi que la population pursuit dans son accroissement. *Correspondance mathematique et physique*, 10:113–121, 1838.

[28] M. Kot. *Elements of mathematical ecology*. Cambridge University Press, 2001.

[29] L. Edelstein-Keshet. *Mathematical models in biology*. McGraw-Hill Companies, 1988.

[30] N.F. Britton. *Essential mathematical biology*. Springer Verlag, 2003.

[31] J.D. Murray. *Mathematical biology: an introduction*. Springer, 2002.

[32] T.J. Sluckin. *Applications of mathematics to biology*. University of Southampton: Lecture notes, 2008.

[33] P. Grindrod. *The theory and applications of reaction-diffusion equations: patterns and waves*. Clarendon Press, 1996.

[34] A.N. Kolmogorov, I.G. Petrovsky, and N.S. Piskunov. Etude de l'"équation de la diffusion avec croissance de la quantité de matiere et son application a un probleme biologique. *Mosc. Univ. Bull. Math*, 1:1–25, 1937.

[35] I.R. Lapidus. Pseudochemotaxis by micro-organisms in an attractant gradient. *J. theor. Biol*, 86:91–103, 1980.

[36] R.T. Tranquillo and W. Alt. Glossary of terms concerning oriented movement. *Biological Motion, Lecture Notes in Biomathematics*, 89:510–417, 1990.

[37] G.S. Fraenkel and D.L. Gunn. *The orientation of animals: Kineses, taxes and compass reactions.* Dover, 1961.

[38] S.C. Kendeigh. *Animal ecology.* Prentice-Hall, 1961.

[39] J.D. Logan. *Applied partial differential equations.* Springer Verlag, 2004. ISBN 0387209352.

[40] M.M. Delgado and V. Penteriani. Behavioral states help translate dispersal movements into spatial distribution patterns of floaters. *The American Naturalist*, pages 475–485, 2008.

[41] D.A. Andow, P.M. Kareiva, S.A. Levin, and A. Okubo. Spread of invading organisms. *Landscape Ecology*, 4(2):177–188, 1990.

[42] P.A. Zollner and S.L. Lima. Illumination and the perception of remote habitat patches by white-footed mice. *Animal Behaviour*, 58(3):489–500, 1999.

[43] P.A. Zollner. Comparing the landscape level perceptual abilities of forest sciurids in fragmented agricultural landscapes*. *Landscape Ecology*, 15(6):523–533, 2000.

[44] P.A. Zollner and S.L. Lima. Behavioral tradeoffs when dispersing across a patchy landscape. *Oikos*, 108(2):219–230, 2005.

[45] V. Selonen and I.K. Hanski. Movements of the flying squirrel pteromys volans in corridors and in matrix habitat. *Ecography*, 26(5):641–651, 2003.

[46] M. Kimura. "stepping stone" model of population. *A. Rep. natn. Inst. Genet. Jap.*, 3(62), 1953.

[47] R. Durrett and S.A. Levin. Stochastic spatial models: a user's guide to ecological applications. *Philosophical Transactions of the Royal Society of London. Series B: Biological Sciences*, 343(1305):329, 1994.

[48] M. Bevers and C.H. Flather. Numerically exploring habitat fragmentation effects on populations using cell-based coupled map lattices* 1. *Theoretical Population Biology*, 55(1):61–76, 1999.

[49] L. Roques and R.S. Stoica. Species persistence decreases with habitat fragmentation: an analysis in periodic stochastic environments. *Journal of Mathematical Biology*, 55(2):189–205, 2007.

[50] W.F. Fagan, F. Lutscher, and K. Schneider. Population and community consequences of spatial subsidies derived from central-place foraging. *American Naturalist*, pages 902–915, 2007.

[51] J.G. Skellam. Random dispersal in theoretical populations. *Biometrika*, 38(1/2): 196–218, 1951.

[52] N. Tamura, F. Hayashi, and K. Miyashita. Dominance hierarchy and mating behavior of the Formosan squirrel, Callosciurus erythraeus thaiwanensis. *Journal of mammalogy*, 69(2):320–331, 1988. ISSN 0022-2372.

[53] N. Tamura, F. Hayashi, and K. Miyashita. Spacing and kinship in the Formosan squirrel living in different habitats. *Oecologia*, 79(3):344–352, 1989. ISSN 0029-8549.

[54] N. Tamura. Seasonal change in reproductive states of the Formosan squirrel on Izo-Oshima Island, Japan. *Mammal Study*, 24:121–124, 1999.

[55] J. Gurnell. *The natural history of squirrels*. Christopher Helm, 1987. ISBN 0747012105.

[56] De hao Yu. *Natural boundary integral method and its applications*. Springer, 2002.

[57] H.R. Akçakaya and W. Root. RAMAS GIS: linking spatial data with population viability analysis (version 4.0). *Applied Biomathematics*, 2002.

[58] G.R. Robinson, R.D. Holt, M.S. Gaines, S.P. Hamburg, M.L. Johnson, H.S. Fitch, and E.A. Martinko. Diverse and contrasting effects of habitat fragmentation. *Science*, 257(5069):524, 1992.

[59] R.S. Cantrell and C. Cosner. Deriving reaction–diffusion models in ecology from interacting particle systems. *Journal of mathematical biology*, 48(2):187–217, 2004.

[60] E.H. van Nes and M. Scheffer. Implications of spatial heterogeneity for catastrophic regime shifts in ecosystems. *Ecology*, 86(7):1797–1807, 2005.

[61] G.P. Boswell, N.F. Britton, and N.R. Franks. Habitat fragmentation, percolation theory and the conservation of a keystone species. *Proceedings of the Royal Society of London. Series B: Biological Sciences*, 265(1409):1921, 1998.

[62] F. Lutscher. Density-dependent dispersal in integrodifference equations. *Journal of Mathematical Biology*, 56(4):499–524, 2008.

[63] R.R. Veit and M.A. Lewis. Dispersal, population growth, and the allee effect: dynamics of the house finch invasion of eastern north america. *American Naturalist*, pages 255–274, 1996.

[64] H.F. Weinberger, K. Kawasaki, and N. Shigesada. Spreading speeds of spatially periodic integro-difference models for populations with nonmonotone recruitment functions. *Journal of Mathematical Biology*, 57(3):387–411, 2008.

[65] E.D. Grosholz. Contrasting rates of spread for introduced species in terrestrial and marine systems. *Ecology*, pages 1680–1686, 1996.

[66] R.S. Cantrell, C. Cosner, and Y. Lou. Approximating the ideal free distribution via reaction-diffusion-advection equations. *Journal of Differential Equations*, 245 (12):3687–3703, 2008.

[67] V. Padrón and M.C. Trevisan. Environmentally induced dispersal under heterogeneous logistic growth. *Mathematical biosciences*, 199(2):160–174, 2006.

[68] D. Olson, C. Cosner, S. Cantrell, and A. Hastings. Persistence of fish populations in time and space as a key to sustainable fisheries. *Bulletin of Marine Science*, 76 (2):213–232, 2005.

[69] L. Roques, M.A. Auger-Rozenberg, and A. Roques. Modelling the impact of an invasive insect via reaction-diffusion. *Mathematical biosciences*, 216(1):47–55, 2008.

[70] R. Levins and D. Culver. Regional coexistence of species and competition between rare species. *Proceedings of the National Academy of Sciences*, 68(6):1246, 1971.

[71] Lewis M.A. Banks J.E. Holmes, E.E. and R.R. Veit. Partial differential equations in ecology: spatial interactions and population dynamics. *Ecology*, pages 17–29, 1994.

[72] A. Okubo. Horizontal dispersion and critical scales for phytoplankton patches. *Spatial pattern in plankton communities*, pages 21–42, 1978.

[73] R.S. Cantrell, C. Cosner, and W.F. Fagan. Habitat edges and predator-prey interactions: effects on critical patch size. *Mathematical biosciences*, 175(1):31–55, 2002.

[74] R.S. Cantrell and C. Cosner. On the effects of nonlinear boundary conditions in diffusive logistic equations on bounded domains. *Journal of Differential Equations*, 231(2):768–804, 2006.

[75] K. Showalter. Quadratic and cubic reaction-diffusion fronts. *Nonlinear Science Today*, 4(4):1–2, 1994.

[76] M.J. Ablowitz and A. Zeppetella. Explicit solutions of fisher's equation for a special wave speed. *Bulletin of Mathematical Biology*, 41(6):835–840, 1979.

[77] P.K. Brazhnik and J.J. Tyson. On traveling wave solutions of fisher's equation in two spatial dimensions. *SIAM Journal on Applied Mathematics*, pages 371–391, 1999.

[78] R. Gardner. Multidimensional Travelling Fronts. *Nonlinear systems of partial differential equations in applied mathematics*, 2:383, 1986.

[79] S.A. Levin. Population dynamic models in heterogeneous environments. *Annual Review of Ecology and Systematics*, 7:287–310, 1976.

[80] N. Kinezaki, K. Kawasaki, and N. Shigesada. Spatial dynamics of invasion in sinusoidally varying environments. *Population Ecology*, 48(4):263–270, 2006.

[81] S. Petrovskii and N. Shigesada. Some exact solutions of a generalized fisher equation related to the problem of biological invasion. *Mathematical biosciences*, 172 (2):73–94, 2001.

[82] H. Berestycki, F. Hamel, and N. Nadirashvili. The speed of propagation for kpp type problems ii: General domains. *American Mathematical Society*, 23(1):1–34, 2010.

[83] L. Roques and F. Hamel. Mathematical analysis of the optimal habitat configurations for species persistence. *Mathematical Biosciences*, 210(1):34–59, 2007.

[84] M. Cristofol and L. Roques. Biological invasions: Deriving the regions at risk from partial measurements. *Mathematical biosciences*, 215(2):158–166, 2008.

[85] W.F. Fagan, R.S. Cantrell, C. Cosner, and S. Ramakrishnan. Interspecific Variation in Critical Patch Size and Gap-Crossing Ability as Determinants of Geographic Range Size Distributions. *The American naturalist*, 173(3):363–375, 2009.

[86] W.C. Allee. *Animal aggregations: a study in general sociology*. AMS Press, 1978.

[87] P.A. Stephens, W.J. Sutherland, and R.P. Freckleton. What is the allee effect? *Oikos*, pages 185–190, 1999.

[88] W.C. Allee. *The social life of animals*. Beacon Press Boston, Massachusetts, USA, 1958.

[89] M.A. McCarthy. The allee effect, finding mates and theoretical models. *Ecological Modelling*, 103(1):99–102, 1997.

[90] J. Shi and R. Shivaji. Persistence in reaction diffusion models with weak allee effect. *Journal of mathematical biology*, 52(6):807–829, 2006.

[91] M.H. Wang, M. Kot, and M.G. Neubert. Integrodifference equations, allee effects, and invasions. *Journal of Mathematical Biology*, 44(2):150–168, 2002.

[92] T.H. Keitt, M.A. Lewis, and R.D. Holt. Allee effects, invasion pinning, and species' borders. *American Naturalist*, 157(2):203–216, 2001.

[93] R.S. Cantrell, C. Cosner, and V. Hutson. Spatially explicit models for the population dynamics of a species colonizing an island. *Mathematical biosciences*, 136 (1):65–107, 1996.

[94] L. Geris, A. Gerisch, C. Maes, G. Carmeliet, R. Weiner, J. Vander Sloten, and H. Van Oosterwyck. Mathematical modeling of fracture healing in mice: comparison between experimental data and numerical simulation results. *Medical and Biological Engineering and Computing*, 44(4):280–289, 2006.

[95] A. Gerisch and M.A.J. Chaplain. Robust numerical methods for taxis-diffusion-reaction systems: Applications to biomedical problems. *Mathematical and computer modelling*, 43(1-2):49–75, 2006.

[96] L. Hazelwood, T. Sluckin, and J. Steele. Very fast demic expansion: numerical models, and applications to human population history. submitted, in revision.

[97] S.A. Levin and M. Whitfield. Patchiness in marine and terrestrial systems: From individuals to populations [and discussion]. *Philosophical Transactions: Biological Sciences*, pages 99–103, 1994.

[98] D. Grunbaum. Using spatially explicit models to characterize foraging performance in heterogeneous landscapes. *American Naturalist*, pages 97–115, 1998.

[99] R.S. Cantrell, C. Cosner, and Y. Lou. Movement toward better environments and the evolution of rapid diffusion. *Mathematical biosciences*, 204(2):199–214, 2006.

[100] T. Mueller, W.F. Fagan, and V. Grimm. Integrating individual search and navigation behaviors in mechanistic movement models. *Theoretical Ecology*, pages 1–15, 2011.

[101] N. Shigesada and K. Kawasaki. *Biological invasions: theory and practice*. Oxford University Press, USA, 1997.

[102] A. Hastings. Models of spatial spread: a synthesis. *Biological Conservation*, 78 (1-2):143–148, 1996.

[103] C.M. Taylor and A. Hastings. Allee effects in biological invasions. *Ecology Letters*, 8(8):895–908, 2005.

[104] D.E. Bowler and T.G. Benton. Causes and consequences of animal dispersal strategies: relating individual behaviour to spatial dynamics. *Biological Reviews*, 80(2): 205–225, 2005.

[105] K.A. With. The landscape ecology of invasive spread. *Conservation biology*, 16 (5):1192–1203, 2002.

[106] S. Redner. *A guide to first-passage processes*. Cambridge Univ Pr, 2001.

[107] M. Abramowitz and I.A. Stegun. *Handbook of mathematical functions with formulas, graphs, and mathematical tables*. Dover publications, 1964.

[108] C.M. Bender and S.A. Orszag. *Advanced mathematical methods for scientists and engineers: Asymptotic methods and perturbation theory*. Springer Verlag, 1999.

[109] W.A. Strauss. *Partial differential equations: An introduction*, volume 3. Wiley New York, 1992.

[110] A.C. King, J. Billingham, and S.R. Otto. *Differential equations: linear, nonlinear, ordinary, partial*. Cambridge Univ Pr, 2003.

[111] J. Comyn. *Polymer permeability*. Springer, 1985.

[112] R.D. Semlitsch. Biological delineation of terrestrial buffer zones for pond-breeding salamanders. *Conservation Biology*, 12(5):1113–1119, 1998.

[113] D. Western and W.K. Lindsay. Seasonal herd dynamics of a savanna elephant population. *African Journal of Ecology*, 22(4):229–244, 1984.

[114] D. Western. Water availability and its influence on the structure and dynamics of a savannah large mammal community. *African Journal of Ecology*, 13(3-4):265–286, 1975.

[115] G.E. Hutchinson. *An introduction to population ecology*, volume 260. Yale University Press New Haven, CT:, 1978.

[116] R.M.C. May and A.R. McLean. *Theoretical ecology: principles and applications*. Oxford University Press, USA, 2007. ISBN 0199209995.

[117] J. Canosa. On a nonlinear diffusion equation describing population growth. *IBM Journal of Research and Development*, 17(4):307–313, 1973.

[118] Compiled by the World Conservation Monitoring Centre. *Protected Areas of the World: A review of national systems. Volume 4: Nearctic and Neotropical*, volume 4. Page Bros. (Norwich) Ltd, UK, 1992.

[119] S.P. Yo, W.E. Howard, and Y.S. Lin. Population-dynamics and regulation of red-bellied tree squirrels (Callosciurus-erythraeus) in Japanese fir plantations. *Bull. Inst. Zool. Acad. Sinica*, 31:89–103, 1992.

[120] R. Baierlein. The elusive chemical potential. *American Journal of Physics*, 69: 423, 2001.

[121] F. Bosch, J.A.J. Metz, and O. Diekmann. The velocity of spatial population expansion. *Journal of Mathematical Biology*, 28(5):529–565, 1990. ISSN 0303-6812.

[122] J. Figuerola and A.J. Green. Dispersal of aquatic organisms by waterbirds: a review of past research and priorities for future studies. *Freshwater Biology*, 47 (3):483–494, 2002.

[123] MathWorks. Curve fitting techniques. `www.mathworks.com/help/toolbox/curvefit`.

[124] P. Beier and R.F. Noss. Do habitat corridors provide connectivity? *Conservation Biology*, 12(6):1241–1252, 1998.

[125] D.K. Rosenberg, B.R. Noon, and E.C. Meslow. Biological corridors: form, function, and efficacy. *BioScience*, 47(10):677–687, 1997.

[126] A.C. Lees and C.A. Peres. Conservation value of remnant riparian forest corridors of varying quality for amazonian birds and mammals. *Conservation Biology*, 22 (2):439–449, 2008.

[127] N.M. Haddad, D.K. Rosenberg, and B.R. Noon. On experimentation and the study of corridors: response to beier and noss. *Conservation Biology*, 14(5):1543–1545, 2000.

[128] N.M. Haddad. Corridor use predicted from behaviors at habitat boundaries. *American Naturalist*, pages 215–227, 1999.

[129] A.F. Bennett, K. Henein, and G. Merriam. Corridor use and the elements of corridor quality: chipmunks and fencerows in a farmland mosaic. *Biological Conservation*, 68(2):155–165, 1994.

[130] V. Selonen and I.K. Hanski. Movements of the flying squirrel pteromys volans in corridors and in matrix habitat. *Ecography*, 26(5):641–651, 2003.

[131] C.D. Fitzgibbon. The distribution of grey squirrel dreys in farm woodland: the influence of wood area, isolation and management. *Journal of Applied Ecology*, pages 736–742, 1993.

[132] R.K. Swihart and T.E. Nupp. Modeling population responses of north american tree squirrels to agriculturally induced fragmentation of forests. *Ecology and evolutionary biology of tree squirrels. Virginia Museum of Natural History Special Publication*, 6:1–19, 1998.

[133] B.F. Sheperd and R.K. Swihart. Spatial dynamics of fox squirrels (*Sciurus niger*) in fragmented landscapes. *Canadian Journal of Zoology*, 73(11):2098–2105, 1995.

[134] P. Beier and S. Loe. In my experience: A checklist for evaluating impacts to wildlife movement corridors. *Wildlife Society Bulletin*, 20(4):434–440, 1992.

[135] D. Mollison. Spatial contact models for ecological and epidemic spread. *Journal of the Royal Statistical Society. Series B (Methodological)*, pages 283–326, 1977.

[136] E.P. Zemskov and A. Loskutov. Exact analytical solutions for nonlinear waves in the inhomogeneous fisher-kolmogorov equation. *The European Physical Journal B-Condensed Matter and Complex Systems*, pages 1–6, 2010.

[137] G. Evans, J. Blackledge, and P. Yardley. *Analytic Methods for Partial Differential Equations*. Springer-Verlag, 1994.

[138] B. Neta. *Partial Differential Equations Lecture Notes*. 2002.

[139] E. Zauderer. *Partial Differential Equations of Applied Mathematics*. John Wiley and Sons, Inc., 2006.

[140] D.G. Duffy. *Green's functions with applications*. Chapman & Hall / CRC, 2001.

[141] A.J. Burton and G.F. Miller. The application of integral equation methods to the numerical solution of some exterior boundary-value problems. *Proceedings of the Royal Society of London. Series A, Mathematical and Physical Sciences*, 323 (1553):201–210, 1971. ISSN 0080-4630.

[142] G.C. Hsiao and W.L. Wendland. *Boundary Integral Equations*. Springer Berlin Heidelberg, 2008.

[143] P.K. Kythe. *Fundamental solutions for differential operators and applications*. Birkhauser, 1996. ISBN 0817638695.

[144] G. Fairweather and A. Karageorghis. The method of fundamental solutions for elliptic boundary value problems. *Advances in Computational Mathematics*, 9(1): 69–95, 1998. ISSN 1019-7168.

[145] A.N. Tikhonov. *Numerical methods for the solution of ill-posed problems*. Springer, 1995. ISBN 079233583X.

[146] L. Marin and D. Lesnic. The method of fundamental solutions for the Cauchy problem associated with two-dimensional Helmholtz-type equations. *Computers & structures*, 83(4-5):267–278, 2005. ISSN 0045-7949.